Mechanisms of Dexamethasone-Induced Hypertension

Sharon Leng Hong Ong

BSc (Med) MBBS FRACP

A thesis submitted for the degree of Doctor of Philosophy
of the Australian National University

May 2010

High Blood Pressure Research Unit
John Curtin School of Medical Research
Australian National University
Canberra, Australia

DECLARATION

The work in this thesis contains no material previously submitted for the award of any degree or diploma in any university or tertiary education institution. The results presented in this thesis are, except where otherwise acknowledged, my own original work.

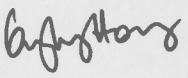

Sharon L H Ong

May 2010

This thesis is dedicated

to the loving memory of my father

Ong Teng Sim

ACKNOWLEDGEMENTS

I am extremely grateful to my supervisor, Professor Judith Whitworth for taking me on and giving me this wonderful opportunity to learn and develop as a researcher. I have learnt very important skills that have helped me significantly in my current roles as a Nephrologist, a lecturer, a researcher and a clinical and research supervisor. I sincerely thank her for her support, encouragement, wisdom and guidance throughout the course of my research studies. I also express my heartfelt gratitude for her continual guidance, beyond her retirement, with finalising this thesis. It was indeed a privilege to be part of her well-organised team.

I am also grateful to my co-supervisor, Dr Yi Zhang, for her assistance, encouragement and support during my PhD research studies.

I would like to thank the staff at the High Blood Pressure Research Unit for their technical assistance- Matthew Sutton, Janine Vickers, Leanne Langton and Kate Mackenzie. I am particularly indebted to Matthew Sutton for his generous assistance with blood pressure measurements (Chapters 4, 6 and 8) and during cull days (Chapters 6 and 8). I am also grateful for the technical assistance provided by Janine Vickers with blood pressure measurements (Chapter 7) and plasma nitrate/nitrite analysis (Chapters 7 and 9). I would also like to thank

Dr Harpreet Vohra for her expert advice and assistance in flow cytometry, and Dr Cheng Wen for his tips on rat surgery.

I also graciously acknowledge the Research and Education Foundation of the Royal Australasian College of Physicians and the National Heart Foundation for generously awarding me the Jacquot Research Entry Scholarship and the Postgraduate Research Scholarship, respectively. This financial support had allowed me pursue this full-time PhD research degree. Part of this research project was funded by an NHMRC Project Grant (Grant number 418026). I am also very grateful for the travel grants from the International Society of Hypertension, the Australia and New Zealand Society of Nephrology and the High Blood Pressure Research Council of Australia that enabled me to attend international and national conferences. I acknowledge the financial support of the High Blood Pressure Research Unit, JCSMR in my travel to the International Society of Hypertension Scientific Meeting in Berlin.

I would also like to thank our collaborators from University of Western Australia, Professor Kevin Croft and Dr Trevor Mori, who performed the plasma F_2-isoprostane assays.

ACT Pathology, The Canberra Hospital had kindly provided pathology services.

I would like to thank my husband, Gary, for his support and encouragement during these years. I thank him for enduring the countless nights and weekends spent in the laboratory.

I would also like to acknowledge my mother and brother for their love and support; and finally, my in-laws for all their help during the busy and hectic times.

ABSTRACT

Adrenocortical steroids with predominant glucocorticoid activity, both naturally-occurring and synthetic, have long been recognised as a cause of hypertension. Models of glucocorticoid-induced hypertension (GC-HT) in the rat such as adrenocorticotrophic hormone-induced hypertension (ACTH-HT) and dexamethasone-induced hypertension (DEX-HT) are well-characterised, although the mechanisms contributing to hypertension are less well-understood. Previous studies have shown that ACTH-HT is associated with increased renal vascular resistance, nitric oxide deficiency and oxidative stress. The latter was shown to be linked to the NAD(P)H oxidase but not the xanthine oxidase pathways. As there were proven differences in the pathogenesis of these two models of GC-HT, mechanisms of ACTH-HT cannot be assumed in DEX-HT.

The main aim of this project was to evaluate the mechanisms of DEX-HT, namely the haemodynamic mechanisms and the role of oxidative stress. The role of β-adrenergic receptor blockade was also evaluated. In some studies, experiments on both dexamethasone (DEX)- and ACTH-HT were conducted for comparison.

DEX (10-20 μg/rat/day) raised blood pressure in rats without significant metabolic side effects such as precipitous weight loss. The haemodynamic experiments showed that DEX-HT in rats was associated with increased total

peripheral resistance and decreased total peripheral conductance, although these were not critical features for the production of DEX-HT.

This project showed that the xanthine oxidase pathway and mitochondria were not the major source of superoxide contributing to oxidative stress in DEX-HT. Mitochondrial superoxide, evaluated using a novel mitochondrial specific fluorogenic probe (mito-hydroethidine) via flow cytometry designed for this purpose, was also shown in this project not to play a major role in ACTH-HT in rats.

The arachidonic acid metabolite 20-hydroxyeicosatetraenoic acid, which is increased by nitric oxide deficiency and known to cause oxidative stress and exacerbate nitric oxide deficiency, also did not play a significant role in the pathogenesis of DEX-HT. Propranolol, both a beta adrenergic receptor blocker and lipid peroxidation inhibitor, was not effective in preventing GC-HT.

In conclusion, an increase in total peripheral resistance and nitric oxide-redox imbalance appear to be features of DEX-HT in the rat although the exact mechanism by which DEX raises blood pressure in human remains incompletely understood. Further studies exploring 1) the differences in mechanisms between naturally-occuring and synthetic glucocorticoids and 2) the relevance of oxidative stress and nitric oxide-redox imbalance in human GC-HT are important in advancing our understanding in this form of hypertension.

CONTENTS

ABBREVIATIONS

20-HETE	20-Hydroxyeicosatetraenoic acid
ACTH	Adrenocorticotrophic hormone
ACTH-HT	Adrenocorticotrophic hormone-induced hypertension
ADH	Antidiuretic hormone
Adr	Adrenaline
ANOVA	Analysis of variance
ANP	Atrial natriuretic peptide
AVP	Arginine vasopressin
BH_4	Tetrahydrobiopterin
C	Control days
cGMP	Cyclic guanosine monophosphate
CI	Cardiac index
CO	Cardiac output
CRH	Corticotrophin releasing hormone
CV	Coefficient of variance
DBP	Diastolic blood pressure
DETC	Diethylthiocarbamate
DEX	Dexamethasone
DEX-HT	Dexamethasone-induced hypertension
$DiIC_1(5)$	1,1',3,3,3',3'-hexamethylindodicarbocyanine iodide
DMSO	Dimethylsulfoxide

DNA	Deoxyribonucleic acid
DOCA	Deoxycorticosterone acetate
EDTA	Ethylenediaminetetraacetic acid
eNOS	Endothelial nitric oxide synthase
ET-1	Endothelin 1
Ex/Em	Excitation/emission
FSC	Forward scatter
GABA	Gamma-aminobutyric acid
GC-HT	Glucocorticoid-induced hypertension
GTP	Guanosine triphosphate
HBF	Hindquarter blood flow
HCAEC	Human coronary artery endothelial cells
HD LA	High dose alpha-lipoic acid
HE	Hydroethidine
HET0016	N-hydroxy-N′-(4-butyl-2 methylphenyl)formamidine
HO-Etd+	2 Hydroxy ethidium
HO-Mito-Etd+	2 Hydroxy-Mito-ethidium
HPMVEC	Human pulmonary micorvascular endothelial cells
HR	Heart rate
HVR	Hindquarter vascular resistance
i.p.	Intraperitoneal
i.v.	Intravenous
iNOS	Inducible nitric oxide synthase
K	Potassium

LA	Alpha-lipoic acid
MAP	Mean arterial pressure
MBF	Mesenteric blood flow
MFI	Mean fluorescence intensity
Mito-HE	MitoSOX Red
mnSOD	Manganese superoxide dismutase
mRNA	Messenger ribonucleic acid
MVR	Mesenteric vascular resistance
MW	Molecular weight
NAC	N-acetylcysteine
NaCl	Saline/ sodium chloride
NAD(P)H	Nicotinamide adenine dinucleotide phosphate
NADH	Nicotinamide adenine dinucleotide
NAdr	Noradrenaline
NO	Nitric oxide
NOS	Nitric oxide synthase
NOx	Nitrate and nitrite
NPY	Neuropeptide Y
ns	Not significant
P	Pre-treatment days
p.o.	Per oral
PBS	Phosphate bufferred saline
PGE_2	Prostaglandin E_2
PGI_2	Prostacyclin

PNMT	Phenylethanolamine *N*-Methyltransferase
RAS	Renin-angiotensin system
RBF	Renal blood flow
ROS	Reactive oxygen species
RVR	Renal vascular resistance
s.c.	Subcutaneous
SBP	Systolic blood pressure
SD	Standard deviation
SEM	Standard error of mean
SHR	Spontaneously hypertensive rat
SI	Stroke index
SOD	Superoxide dismutase
SV	Stroke volume
T	Treatment days
TPC	Total peripheral conductance
TPR	Total peripheral resistance
vs	Versus

PUBLICATIONS AND PRESENTATIONS ARISING FROM THIS THESIS

Publications

Ong SLH, Zhang Y, Sutton M, Whitworth JA. Haemodynamics of dexamethasone-induced hypertension in the rat. *Hypertens Res* 2009; **32**(10): 889-894.

Zhang Y, Wu JHY, Vickers JJ, **Ong SLH**, Temple SEL, Mori TA, Croft KD, Whitworth JA. The role of 20-hydroxyeicosatetraenoic acid in glucocorticoid-induced hypertension. *J Hypertens* 2009; **27**(8): 1609-1616.

Ong SLH, Zhang Y, Whitworth JA. Mechanisms of dexamethasone-induced hypertension. *Curr Hypertens Rev 2009;* **5**(1): 61-74.

Ong SLH, Zhang Y, Whitworth JA. Reactive oxygen species and glucocorticoid-induced hypertension. *Clin Exp Pharmacol Physiol* 2008; **35**(4):477-482.

Ong SLH, Vickers JJ, Zhang Y, McKenzie KUS, Walsh CE, Whitworth JA. Role of xanthine oxidase in dexamethasone-induced hypertension in rats. *Clin Exp Pharmacol Physiol* 2007; **34**(5-6): 522-524.

In Press

Ong SLH, Whitworth JA. How do glucocorticoids cause hypertension: role of nitric oxide deficiency, oxidative stress and eicosanoids. *Clin of North Am* (in press)

In Preparation

Ong SLH, Sutton M, Vohra H, Zhang Y, Mori TA, Croft KD, Whitworth JA. Mitochondrial superoxide production in glucocorticoid-hypertensive rats.

PRESENTATIONS

International Presentations

Ong SLH, Sutton M, Vohra H, Zhang Y, Whitworth JA. Alpha lipoic acid prevents glucocorticoid-induced hypertension in the rat. Oral poster presentation at the International Society of Hypertension Scientific Meeting, Berlin, June 2008.

Ong SLH, Vohra H, Sutton M, Zhang Y, Whitworth JA. Kidney mitochondrial superoxide production in glucocorticoid-induced hypertension in rats. Poster presentation at the International Society of Hypertension Scientific Meeting, Berlin, June 2008.

Zhang Y, Croft KD, Vickers JJ, Ong SLH, Mori TA, Whitworth JA. HET0016, a 20-hydroxyeicosatetraenoic acid inhibitor, prevents and reverses adrenocorticotrophic hormone-induced hypertension. Oral poster presentation at the International Society of Hypertension Scientific Meeting, Berlin, June 2008.

National Presentations

Ong SLH, Sutton M, Zhang Y, Whitworth JA. Haemodynamics of dexamethasone-induced hypertension in the rat. Poster presentation at the Australian and New Zealand Society of Nephrology, Tasmania, September 2009.

Ong SLH, Zhang Y, Whitworth JA. Haemodyamic profile of dexamethasone-induced hypertension in the rat. Poster presentation at the High Blood Pressure Research Council of Australia, Melbourne, December 2008.

Ong SLH, Sutton M, Vohra H, Zhang Y, Whitworth JA. Dexamethasone-induced hypertension in rats is prevented but not reversed by alpha-lipoic acid. Oral poster presentation at the Australian and New Zealand Society of Nephrology, Newcastle, September 2008.

Ong SLH, Sutton M, Vohra H, Zhang Y, Whitworth JA. Alpha-lipoic acid partially prevents adrenocorticotrophin-induced hypertension in the rat. Poster presentation at the High Blood Pressure Research Council Australia Annual Scientific Meeting, Adelaide, December 2007.

Ong SLH, Sutton M, Vohra H, Zhang Y, Whitworth JA. Assessment of mitochondrial superoxide production in kidney cells of glucocorticoid-induced hypertension in the rat. Poster presentation at the High Blood Pressure Research Council of Australia Annual Scientific Meeting, Adelaide, December 2007.

Ong SLH, Vickers JJ, Zhang Y, McKenzie KUS, Whitworth JA. Role of xanthine oxidase in dexamethasone-induced hypertension in the rat. Poster presentation the High Blood Pressure Research Council of Australia Annual Scientific Meeting, Brisbane, December 2006.

Local Presentations

Ong SLH, Sutton M, Vohra H, Zhang Y, Whitworth JA. The antioxidant alpha lipoic acid prevents but does not reverse dexamethasone-induced hypertension in the rat. Oral presentation at the Canberra Region Annual Scientific Meeting, June 2008.

Ong SLH, Sutton M, Vohra H, Zhang Y, Whitworth JA. The antioxidant alpha lipoic acid prevents but does not reverse dexamethasone-induced hypertension in the rat. Poster presentation at the Australian Society of Medical Research, Australian Capital Territory Young Investigator Forum, Canberra, June 2008.

Ong SLH, Vohra H, Zhang Y, Whitworth JA. Fluorogenic assessment of the role of mitochondrial superoxide in dexamethasone-induced hypertension in the rat. Poster presentation at the Australian Society of Medical Research, Australian Capital Territory Young Investigator Forum, Canberra, June 2007.

Ong SLH, Vickers JJ, Zhang Y, McKenzie KUS, Whitworth JA. Role of xanthine oxidase in dexamethasone-induced hypertension in the rat. Poster presentation at the Australian Society of Medical Research, Australian Capital Territory Young Investigator Forum, Canberra, June 2006.

CHAPTER 1

Mechanisms of Dexamethasone-Induced Hypertension

1.1 INTRODUCTION

The involvement of glucocorticoid hormones in hypertension has long been recognised. Cushing's syndrome due to chronic glucocorticoid excess, either endogenous or exogenous, is associated with hypertension. In addition, local cortisol excess due to impaired glucocorticoid metabolism resulting in hypertension has also been implicated in conditions such as apparent mineralocorticoid excess, licorice abuse, renal failure and essential hypertension (Walker, Best *et al.* 1996).

Overproduction of cortisol, the major glucocorticoid hormone in humans, can either be due to primary pathology of the adrenal glands (such as hyperplasia, adenoma or carcinoma) or secondary to pituitary-derived (Cushing's Disease) or ectopic adrenocorticotrophic hormone (ACTH) secretion. Approximately 80% of adults and 47% of children and adoslescents with Cushing's syndrome due to endogenous glucocorticoid overproduction present with hypertension (Magiakou, Smyrnaki *et al.* 2006). Hypertension is a more common problem in patients who develop Cushing's syndrome due to administration of glucocorticoid or ACTH. To date, several forms of synthetic glucocorticoids are available for treatment of a variety of clinical conditions including autoimmune diseases, inflammatory diseases, organ transplantation and cancer. Chronic usage of systemic glucocorticoids at supraphysiological doses, sometimes inevitable for certain medical conditions, often leads to complications such as hypertension, a significant cardiovascular risk factor.

This chapter will review the literature on the proposed pathogenetic mechanisms of hypertension due to a potent synthetic glucocorticoid, dexamethasone (DEX). This chapter also includes a segment featuring the similarities and differences between naturally-occurring and synthetic glucocorticoid hormones.

1.2 GLUCOCORTICOID HORMONES

1.2.1 History

Both glucocorticoid and mineralocorticoid hormones are forms of corticosteroid hormones produced by the adrenal glands. This gland was first described by Eustachius (Eustachius 1564). The vital function of this gland was only recognised in the nineteenth century by Addison who described the syndrome of adrenal insufficiency in his monograph in 1855 (Addison 1937). This finding was further substantiated by Brown-Sequard who found rapidly fatal outcomes from unilateral or bilateral adrenalectomy in animals (Brown-Sequard 1856). These findings had driven the search for a hormone replacement therapy for adrenal insufficiency.

In contrast to the observations by Addison and Brown-Sequard, Harvey Cushing described the syndrome of hypercortism in 1912 but ascribed it to disorders of the adrenal, thyroid and pineal glands, as well as the ovaries and testes (Medvei 1991). It was then realised by Julius Bauer that this syndrome was explained by "sole hyperfunction of the adrenals" (Bauer 1950). The recognition of

hypercortism subsequently led to the establishment of the link between the anterior pituitary and the adrenal gland, the identification and purification of ACTH, the steroid hormones and their synthetic analogues.

Cortisone became available following successful extraction from sheep and cattle adrenal cortices by Kendall and Reichstein (Mason, Myers *et al.* 1936; Reichstein 1962). They both shared the Nobel Prize with Hench, who observed a remarkable remission of rheumatoid arthritis with cortisone injection (Glyn 1998).

The discovery of the therapeutic effects of corticosteroid hormones had revolutionised the treatments of various medical conditions. It also led to the development of many synthetic derivatives of different potencies.

1.2.2 Naturally-occuring glucocorticoids

In humans, cortisol or hydrocortisone is the predominant glucocorticoid produced from cholesterol, the basic precursor of corticosteroid hormones, by the zona fasciculata and reticularis of the adrenal cortex. Its synthesis involves alterations to the cholesterol chemical structure via a series of enzymatic reactions. Due to the lack of adrenal 17-hydroxylase activity in rodents, the predominant glucocorticoid is corticosterone.

The pathway of steroidogenesis in humans is summarised in Figure 1.1. There are 5 important steps in the pathway of cortisol synthesis.

1. Cholesterol is converted to pregnenolone by cholesterol side chain cleavage enzyme (cholesterol desmolase).

2. Pregnenolone is then converted to either progesterone by 3β-hydroxysteroid dehydrogenase or to 17-hydroxypregnenolone by 17α-hydroxylase.

3. 17-Hydroxyprogesterone is then formed from either 17-hydroxypregnenolone by 3β-hydroxysteroid dehydrogenase or by 17α-hydroxylation of progesterone.

4. 21β-Hydroxylation of 17-hydroxyprogesterone results in the formation of 11-deoxycortisol.

5. 11β-Hydroxylation of 11-deoxycortisol leads to the production of cortisol.

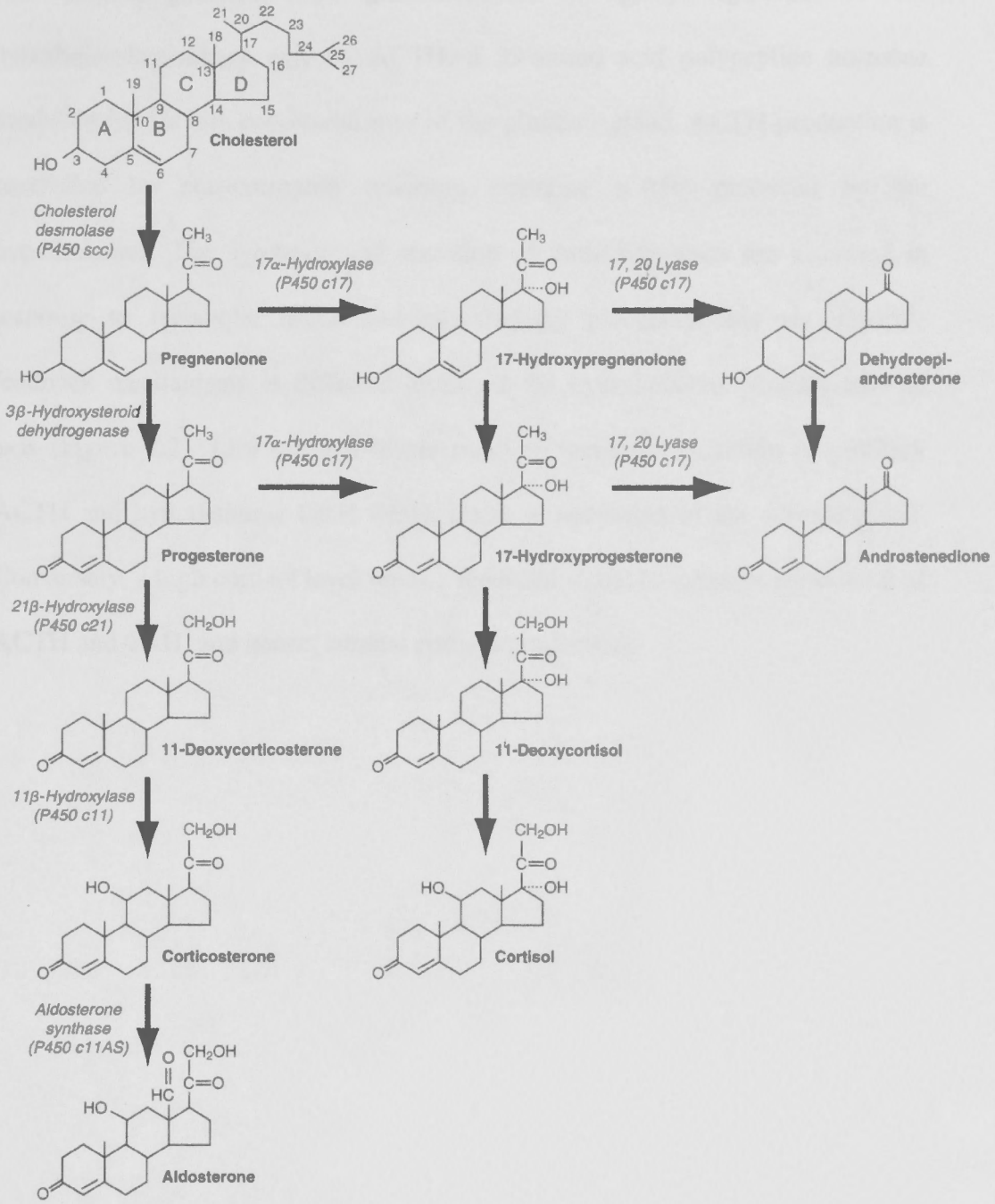

Figure 1.1: Pathways for synthesis of corticosteroids by the adrenal cortex (Guyton and Hall 2000).

The adrenal production of glucocorticoids is tightly regulated via the hypothalamic-pituitary axis by ACTH, a 39-amino acid polypeptide hormone produced by the adrenocorticotropes of the pituitary gland. ACTH production is controlled by corticotrophin releasing hormone (CRH) produced by the hypothalamus. The synthesis and secretion of these hormones are activated in response to metabolic needs and inhibited by glucocorticoids via negative feedback mechanisms at different levels of the hypothalamus-pituitary-adrenal axis (Figure 1.2). Low cortisol levels result in increased secretion of pituitary ACTH and hypothalamic CRH which result in activation of the adrenal gland. Conversely, a high cortisol level sends a feedback signal to suppress the release of ACTH and CRH; and hence, adrenal cortisol production.

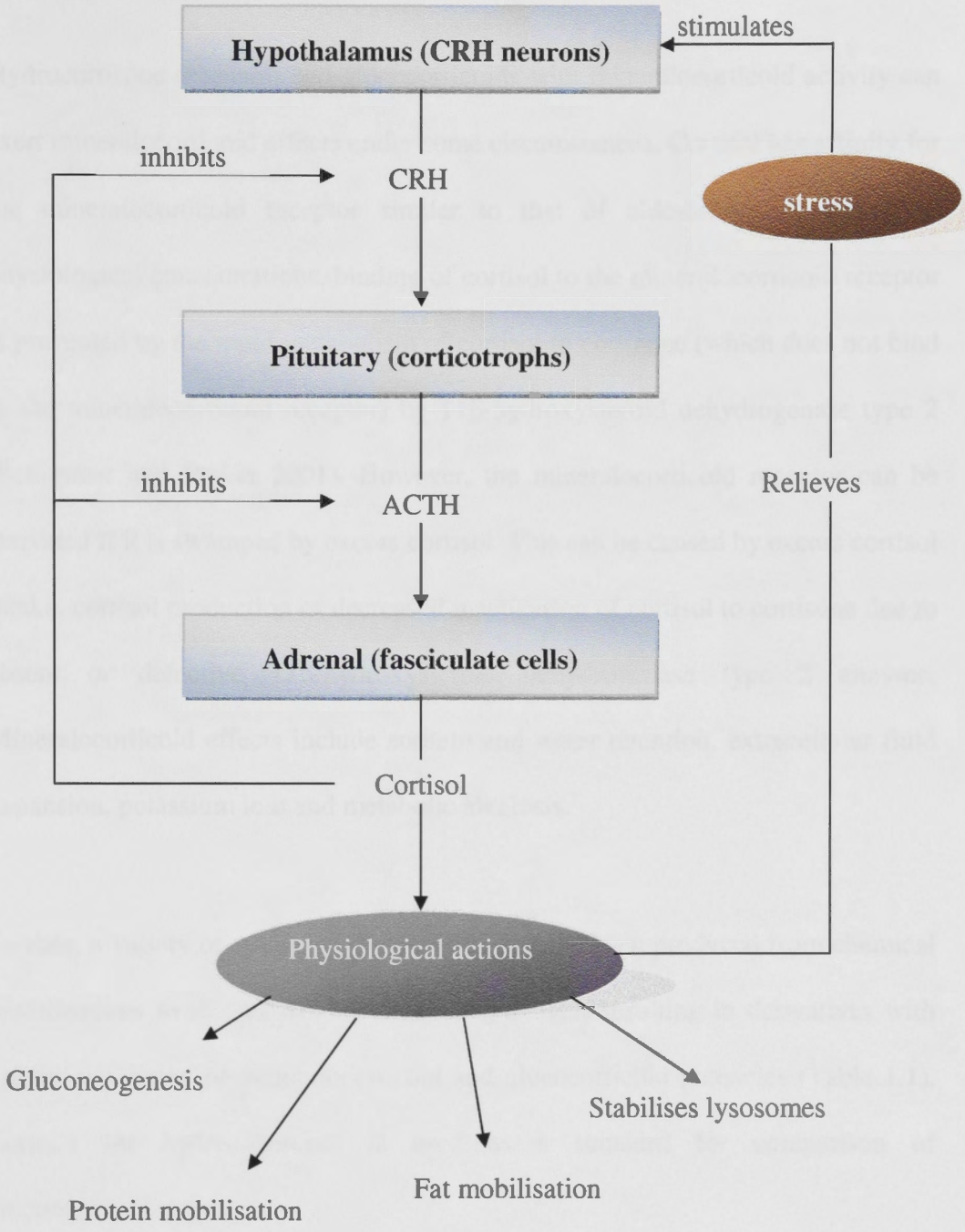

Figure 1.2: Mechanism for regulation of glucocorticoid secretion. ACTH: adrenocorticotrophic hormone, CRH: corticotrophin releasing hormone.

1.2.3 Synthetic glucocorticoids

Hydrocortisone (cortisol) and glucocorticoids with mineralocorticoid activity can exert mineralocorticoid effects under some circumstances. Cortisol has affinity for the mineralocorticoid receptor similar to that of aldosterone. However, at physiological concentrations, binding of cortisol to the minerolocorticoid receptor is prevented by the rapid metabolism of cortisol to cortisone (which does not bind to the mineralocorticoid receptor) by 11β-hydroxysteroid dehydrogenase type 2 (Schimmer and Parker 2001). However, the mineralocorticoid receptor can be activated if it is swamped by excess cortisol. This can be caused by excess cortisol intake, cortisol production or decreased inactivation of cortisol to cortisone due to absent or defective 11β-hydroxysteroid dehydrogenase type 2 enzyme. Mineralocorticoid effects include sodium and water retention, extracellular fluid expansion, potassium loss and metabolic alkalosis.

To date, a variety of synthetic glucocorticoids have been produced from chemical modifications to the cortisol molecule (Figure 1.3) resulting in derivatives with greater separation of mineralocorticoid and glucocorticoid potencies (Table 1.1). Cortisol (or hydrocortisone) is used as a standard for comparison of glucocorticoid potency.

Systemic administration of exogenous glucocorticoids also provides inhibitory feedback signals to suppress CRH, ACTH and adrenal glucocorticoid production.

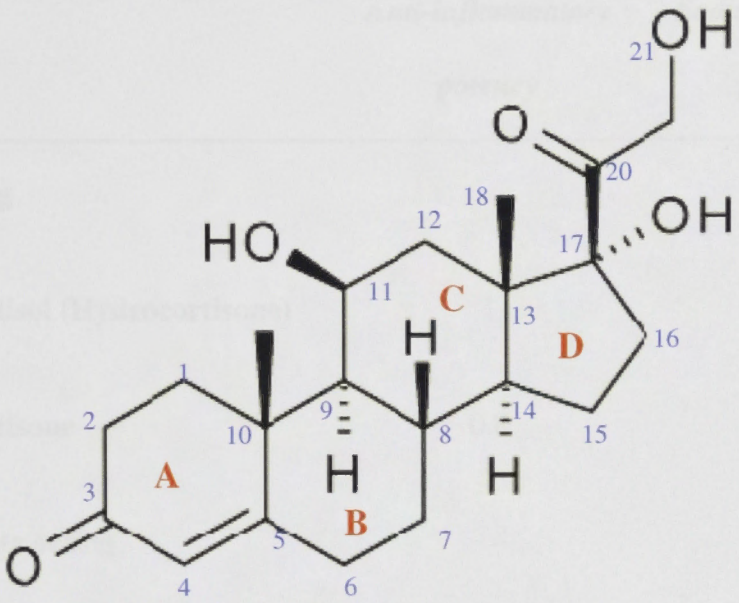

Figure 1.3: Cortisol (Hydrocortisone). The 4,5 double bond and 3-keto group on ring A are both necessary for glucocorticoid and mineralocorticoid effects whereas the 11β-hydroxyl group on ring C is required for glucocorticoid activity only (Schimmer and Parker 2001). The 17α-hydroxyl group on ring D, a substituent for cortisol, is needed for optimal glucocorticoid effect (Schimmer and Parker 2001). The hydroxyl group at C21 on the side chain arising from ring D which is found in all naturally-occuring corticosteroids and most synthetic derivatives is essential for mineralocorticoid function but not glucocorticoid (Schimmer and Parker 2001).

Table 1.1: Relative potencies of representative glucocorticoids (Rang, Dale *et al.* 2007).

Compound	*Anti-inflammatory potency*	*Sodium retaining potency*
Short acting		
Cortisol (Hydrocortisone)	1	1
Cortisone	0.8	0.8
Intermediate acting		
Prednisone	4	0.8
Prednisolone	4	0.8
6α-methylprednisolone	5	minimal
Triamcinolone	5	none
Long acting		
Betamethasone	25	negligible
Dexamethasone	25	minimal

1.3 DEXAMETHASONE

DEX is a synthetic glucocorticoid that is approximately 25 times more potent than cortisol (hydrocortisone). The increased anti-inflammatory and decreased sodium-retaining potencies of DEX relative to cortisol are consequences of chemical modifications that may alter the affinity and intrinsic activity at corticosteroid receptors, absorption, protein binding, rate of metabolic transformation, rate of excretion or membrane permeability (Schimmer and Parker 2001).

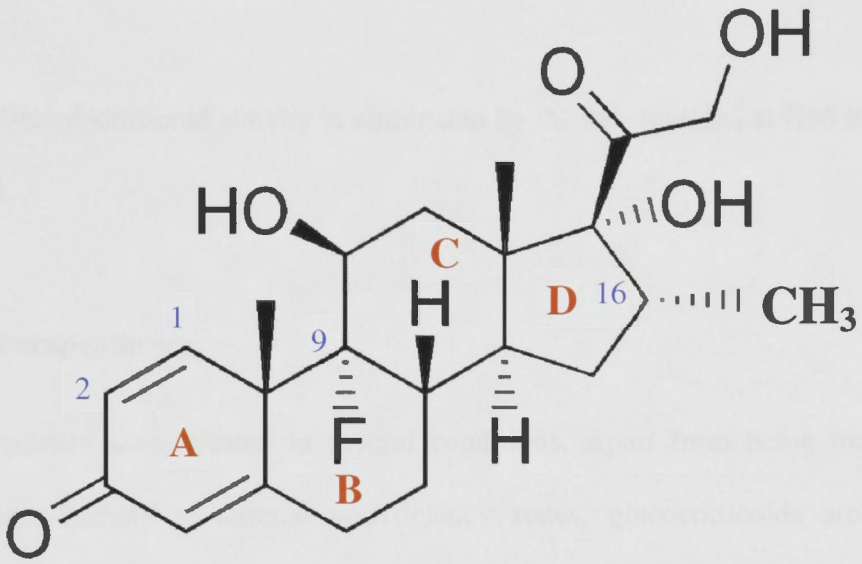

Figure 1.4: Molecular structure of DEX.

Figure 1.4 features the molecular structure of DEX. DEX is synthesised by 3 structural modifications to the basic cortisol structure.

1. The addition of another double bond in the 1,2 position of ring A selectively results in a four fold increase in the glucocorticoid activity compared to hydrocortisone.

2. Fluorination in ring B at the 9α position augments glucocorticoid and mineralocorticoid activity.

3. Mineralocorticoid activity is eliminated by the substitutions at C16 in ring D.

1.3.1 Therapeutic use

Glucocorticoids are indicated in several conditions. Apart from being used as replacement therapy in adrenal insufficiency states, glucocorticoids are also commonly used for non-endocrine conditions such as allergic disease, inflammatory diseases, autoimmune disorders, organ transplantation and malignancies. For most inflammatory and autoimmune diseases, the shorter acting prednisone and methylprednisolone are preferred over the long-acting DEX to facilitate dose tapering. However, DEX is favoured over other glucocorticoids in certain conditions highlighted below.

1.3.1.1 Endocrine uses

DEX may be given to patients with either adrenal insufficiency due to structural or functional adrenal abnormalities, or from structural or functional lesions of the pituitary or hypothalamus.

1.3.1.2 Oncologic uses

DEX is used in multiple myeloma where it is either given alone or in combination with thalidomide (thal-dex protocol) or with Adriamycin (doxorubicin) and vincristine (VAD protocol).

DEX is also given to treat nausea in patients with widespread cancer. This works by the augmentation of the antiemetic effects of $5HT_3$ receptor antagonists, reduction of peritumoral inflammation and prostaglandin production.

DEX can also decrease vasogenic oedema due to central nervous system tumours (intracranial and spinal cord) by stabilising the blood brain barrier. The exact mechanism is poorly elucidated. The upregulation of the blood brain barrier-stabilising factor angiopoietin-1 and downregulation of the blood brain barrier-permeating factor vascular endothelial growth factor due to DEX were thought to be possible mechanisms (Kim, Lee et al. 2008).

1.3.1.3 Obstetrics

DEX, which crosses the placenta (Wintour, Alcorn *et al.* 1994) may be given to women at risk of pre-term delivery to promote fetal lung maturity. It can also be given prenatally to mothers of female fetuses with classical congenital adrenal hyperplasia, diagnosed via prenatal detection of 21-hydroxylase deficiency, to prevent virilisation of external genitalia.

1.3.1.4 Ocular inflammatory diseases

Topical ocular preparations (solution or ointment) are available for use in ocular inflammatory diseases. These include anterior uveitis, external inflammatory eye disease secondary to infections and cicatricial pemphigoid, and post-operative inflammation.

1.3.1.5 Cerebral oedema

Apart from oedema due to neoplastic cerebral lesions, DEX is also used for cerebral oedema due to infections, trauma, intracranial haemorrhage and post cerebral irradiation.

1.3.2 Diagnostic use

The DEX suppression test can be used to diagnose Cushing's syndrome and Cushing's disease.

1.3.2.1 Overnight dexamethasone suppression test

The purpose of this test is to determine if patients with clinical signs suggestive of hypercortisolism demonstrate biochemical evidence of increased cortisol biosynthesis. Suppression of plasma cortisol (measured at 8 am) to less than <140 nmol/L (5 μg/dl) with 1 mg of oral DEX administered the night before (at 11 pm) excludes Cushing's syndrome (Nieman, Biller *et al.* 2008).

1.3.2.2 Formal dexamethasone suppression test

This test is used in the differential diagnosis of biochemically-confirmed Cushing's syndrome. Baseline plasma cortisol levels are documented before administering oral DEX (0.5 mg, every 6 hours for 48 hours) (Stewart 2008). This dose significantly suppresses cortisol production in normal subjects and those with cortisol increases due to obesity and stress, but not in individuals with Cushing's syndrome. This is then followed by a high dose phase where patients are given high dose oral DEX (2 mg, every 6 hours for 48 hours) (Stewart 2008). This dose will suppress plasma cortisol in Cushing's syndrome due to pituitary disease (Cushing's disease) but not from primary adrenal cortical lesions or ectopic ACTH production.

1.3.3 Toxicity

Continued use of systemic DEX at supraphysiological dosages can result in adverse effects common to any other glucocorticoids. These include adrenal suppression with risk of adrenal insufficiency following acute withdrawal,

hypertension, immunosuppression with increased risk of infections, glucose intolerance, diabetes mellitus, osteoporosis, osteonecrosis, myopathy, risk of peptic ulcer disease, cataracts and behavioural changes.

1.3.4 Blood pressure effect of dexamethasone

Hypertension is a common manifestation of DEX use. In normotensive human subjects, hypertension can be induced with oral DEX (1 mg every 8 hours) (Pirpiris, Sudhir *et al.* 1992; Mangos, Walker *et al.* 2006). This blood pressure effect is reproducible in laboratory animals including rats (Zhang, Croft *et al.* 2004; Hu, Zhang *et al.* 2006; Krug, Zhang *et al.* 2008), mice (Wallerath, Witte *et al.* 1999; Wallerath, Godecke *et al.* 2004), sheep (Whitworth, Coghlan *et al.* 1979) and dogs (Nakamoto, Suzuki *et al.* 1991). In rats, DEX dose of as a low as 1 μg (administered via subcutaneous infusion over 4 weeks) (Tonolo, Fraser *et al.* 1988), has been shown to result in a significant increase in SBP.

The exact mechanism of DEX-induced hypertension (DEX-HT) is unknown. Perturbations in the various pathophysiological systems affecting blood pressure such as plasma volume, renin-angiotensin-aldosterone system, sympathetic activity, vasopressor and vasodepressor systems have been proposed as contributing to DEX-HT. Mechanisms of DEX-HT including the role of these factors and the interactions between them will be examined below (Table 1.2).

Table 1.2: Postulated mechanisms of dexamethasone-induced hypertension

1. Sodium retention and volume expansion
2. Hemodynamic changes
3. Increased vascular pressor responsiveness
4. Increased sympathetic nervous system activity
5. Vasopressor hormone excess
    i. renin-angiotensin system
    ii. arginine vasopressin
    iii. endothelin
    iv. cathecholamine
    v. neuropeptide Y
6. Vasodilator hormone deficiency
    i. Atrial natriuretic peptide
    ii. Prostanoids
    iii. Nitric oxide
7. Central stimulation of blood pressure
8. Oxidative stress
    i. NAD(P)H
    ii. oxidase
    iii. Xanthine oxidase
    iv. Uncoupling of eNOS
    v. Mitochondria
    vi. Cyclooxygenase

1.4 MECHANISMS OF DEXAMETHASONE-INDUCED HYPERTENSION

1.4.1 Sodium and water retention

The notion that glucocorticoids induce hypertension through activation of renal mineralocorticoid receptors arises from observations that cortisol produces renal sodium retention and hypertension (Stewart, Walker *et al.* 1995). However, evidence for a causal relationship between sodium retention and glucocorticoid-induced hypertension (GC-HT) is lacking. It is now clear that sodium retention is not the cause of either synthetic or naturally-occuring GC-HT, in humans or rats (Whitworth, Gordon *et al.* 1989; Montrella-Waybill, Clore *et al.* 1991; Williamson, Kelly *et al.* 1996; Li, Wen *et al.* 1999). Experimental cortisol-induced hypertension in humans (Montrella-Waybill, Clore *et al.* 1991; Williamson, Kelly *et al.* 1996) and adrenocorticotrophic hormone-induced hypertension (ACTH-HT) in rats (Li, Wen *et al.* 1999) are not prevented by mineralocorticoid receptor blockade with spironolactone. Synthetic glucocorticoids elevate blood pressure in humans without any sodium retention or plasma volume expansion (Whitworth, Gordon *et al.* 1989). Grunfeld and colleagues have also demonstrated in rats that the mineralocorticoid receptor antagonist RU28318, at a dose that lowered blood pressure in mineralocorticoid hypertension (Moura and Worcel 1981), failed to modify hypertension induced by a glucocorticoid receptor agonist RU26988 (Grunfeld, Eloy *et al.* 1985). They have also found that the glucocorticoid receptor antagonist RU38486 prevented

and improved glucocorticoid receptor agonist RU26988-induced hypertension without altering body weight, urinary water and sodium excretion (Grunfeld, Eloy *et al.* 1985).

DEX has high affinity for glucocorticoid receptors and low affinity for mineralocorticoid receptors. It effectively induces nuclear translocation of both glucocorticoid and mineralocorticoid receptors but stimulates mineralocorticoid receptor-mediated transactivation at a much lower capacity than aldosterone. 11-Ketodexamethasone, the oxidation product of 11β hydroxysteroid dehydrogenase 2, also demonstrated a weak binding affinity for mineralocorticoid receptors and requires a high concentration to achieve nuclear translocation without activating mineralocorticoid receptor-mediated transcription of a reporter gene (Rebuffat, Tam *et al.* 2004) Even though DEX can bind to mineralocorticoid receptors, DEX raises blood pressure in man without mineralocorticoid effects as evidenced by the absence of urinary sodium retention and increase in body weight (Whitworth, Gordon *et al.* 1989). It produces diuresis in preterm infants (Bos, van Asselt *et al.* 2000) and promotes excretion of a water load in adrenal insufficiency in rats (Bengele, McNamara *et al.* 1977; Hayamizu, Kanda *et al.* 1994). DEX-HT in humans was accompanied by natriuresis without any changes in body weight or plasma volume (Whitworth, Gordon *et al.* 1989). In the rat, DEX decreases body weight (Zhang, Croft *et al.* 2004; Hu, Zhang *et al.* 2006) and increases haematocrit by 5% (Hu, Zhang *et al.* 2006).

The increase in blood pressure due to DEX is independent of sodium loading or retention. Okuno *et al.* confirmed that the hypertensive effect of DEX (2.5 mg/L drinking fluids or approximately 30-60 μg/day, given orally) in rats was not influenced by sodium loading with oral 1% NaCl (Okuno, Suzuki *et al.* 1981).

1.4.2 Haemodynamic changes

Haemodynamic studies provide insights into the effects of DEX in the different vascular beds. Hypertension due to a large dose of DEX (0.5 mg/kg/day, given orally) in dogs was accompanied by a reduction in cardiac output and an increase in calculated total peripheral resistance (Nakamoto, Suzuki *et al.* 1991; Nakamoto, Suzuki *et al.* 1992). In humans, DEX (1 mg orally three times daily for 7 days) increased mean arterial pressure from 82 ± 3 to 91 ± 3 mmHg ($p < 0.001$) and calculated total peripheral vascular resistance from 21.9 to 24.3 mmHg/L per minute (± 0.4, $p < 0.01$) without affecting the cardiac output (Pirpiris, Sudhir *et al.* 1992).

Studies of the effect of DEX on the regional haemodynamics are limited. In a study evaluating the effects of DEX (125 μg/kg/hour, intravenous infusion over 24 hours) on the regional haemodynamic responses to lipopolysaccharide in rats, DEX treatment alone (before administration of lipopolysaccharide) increased the mean arterial pressure, hindquarter blood flow and conductance; and decreased renal and mesenteric blood flow and conductance (Gardiner, Kemp *et al.* 1996).

Currently available data indicate that DEX-HT, in both humans and dogs, is characterised by increases in calculated total peripheral resistance. It has been unclear whether this represents a coexisting feature or a pathogenic mechanism of DEX-HT. This issue was addressed in this project and is discussed in Chapters 3 and 4.

1.4.3 Increased vascular pressor responsiveness

Hypertension is associated with structural, mechanical (compliance and distensibility) and functional abnormalities of blood vessels that result in decreased lumen diameter of small arteries and arterioles (Intengan and Schiffrin 2000). Structural impairment of the blood vessel wall is unlikely to play a major role in experimental DEX-HT where the hypertensive action of DEX occurs rapidly within 1-2 days (Nakamoto, Suzuki *et al.* 1991; Pirpiris, Sudhir *et al.* 1992; Zhang, Croft *et al.* 2004; Hu, Zhang *et al.* 2006; Krug, Zhang *et al.* 2008). Furthermore, there are no reports confirming the presence of vascular hypertrophy histologically in DEX-induced hypertensive subjects or animals.

Functional aberrations of the vascular smooth muscle cells, manifesting as increased sensitivity and reactivity to vasoconstrictors (i.e. increased vascular pressor responsiveness) have been described in DEX-HT in humans, rats and dogs (Handa, Kondo *et al.* 1984; Russo, Fraser *et al.* 1989; Russo, Fraser *et al.* 1990; Nakamoto, Suzuki *et al.* 1991; Pirpiris, Sudhir *et al.* 1992). Greater rises in forearm vascular resistance in response to infusions of angiotensin II and

noradrenaline were observed in human subjects with DEX-induced (3mg/day, given orally) hypertension versus controls, consistent with DEX increasing sensitivity to these vasoconstrictors. (Pirpiris, Sudhir *et al.* 1992). Pretreatment with oral DEX (0.3 mg/dL drinking water, approximately 0.1 mg/day or 0.5 mg/kg/day) in rats enhanced blood pressure elevation due to noradrenaline (Handa, Kondo *et al.* 1984). A similarly enhanced pressor response to noradrenaline was observed in DEX-HT (0.5 mg/kg/day, given orally) in dogs but in contrast to the human study (Pirpiris, Sudhir *et al.* 1992), pressor response to angiotensin II was unaltered (Nakamoto, Suzuki *et al.* 1991). *In vitro* perfusion of isolated rat mesenteric vasculatures resulted in a reduced threshold and increased maximal response to noradrenaline in DEX-induced hypertensive rats (2 μg/rat/day, approximately 7-9.5 μg/kg/day, given orally for 28 days) but not in controls (Russo, Fraser *et al.* 1989; Russo, Fraser *et al.* 1990). However, these effects were not reproducible with AVP and potassium chloride infusions (Russo, Fraser *et al.* 1989; Russo, Fraser *et al.* 1990). Ijima and Malik demonstrated that DEX-HT (1.8 mg/kg/week or average of approximately 257 μg/kg/day, for 2 weeks) in rats was associated with increased pressor response to arginine vasopressin but not to noradrenaline or angiotensin II (Iijima and Malik 1988).

These studies, which were undertaken in different species under different experimental conditions, showed some discrepancies in the responses (or lack of response) to vasoconstrictors including angiotensin II, noradrenaline and arginine vasopressin (Handa, Kondo *et al.* 1984; Russo, Fraser *et al.* 1989; Russo, Fraser *et al.* 1990; Nakamoto, Suzuki *et al.* 1991; Pirpiris, Sudhir *et al.* 1992).

Nevertheless, these results suggested a role for DEX in increasing the sensitivity of vascular smooth muscle cells to vasoconstrictors, and vasoconstriction and potentiation of the effects of vasoconstrictors may contribute to DEX-HT.

The mechanisms underlying this heightened response to vasoconstrictors induced by DEX have not been fully elucidated. Sato *et al.* demonstrated a DEX-induced decrease in threshold for the production of inositol triphosphate by cultured vascular smooth muscle cells in response to angiotensin II and arginine vasopressin. This effect was thought to be mediated by the glucocorticoid receptor as it was completely blocked by a specific glucocorticoid antagonist RU38486 (Sato, Suzuki *et al.* 1992). This group later identified that DEX (30 mg/L drinking water, approximately 0.1 mg/rat/day or 0.5 mg/kg/day) in rats stimulated vascular angiotensin II type 1A receptor mRNA even prior to the onset of hypertension (Sato, Suzuki *et al.* 1994).

Another possible mechanism for DEX-induced increased vascular pressor reactivity is alteration in sodium/potassium pump activity (Pamnani, Clough *et al.* 1978; Stern, Palant *et al.* 1994). In an *in vitro* study, direct stimulation of sodium/potassium-pump-mediated cation transport in cultured rat aortic smooth mucle cells was demonstrated after 18-24 hour incubation with 10^{-9} M DEX (Stern, Palant *et al.* 1994). Sodium/potassium pump activity in the tail artery of DEX-induced hypertensive (initial DEX dose of 12.5 mg followed by 6.5 mg weekly, subcutaneous injections) uninephrectomised rats was significantly increased (Pamnani, Clough *et al.* 1978).

Whilst increased vascular sensitivity or reactivity to vasoconstrictors may be a feature of DEX administration, it remains unclear whether these changes are sufficient to account, if at all, for the hypertension. Despite the evidence presented above, there are reports that have not found any pressor effects of either acute or chronic DEX treatments (acute: 20 mg intravenously to human subjects (Sambhi, Weil *et al.* 1962); and chronic: 0.5 mg/day for 14 days intramuscularly to mongrel dogs (Lefer, Manwaring *et al.* 1966)) on arterial responses to noradrenaline and angiotensin II.

Other factors contributing to increased pressor responsiveness in DEX-HT include decreased synthesis of vasodilator prostanoids and increased expression of angiotensin 1A and AVP receptors, discussed in Sections 1.4.6.2, 1.4.5.1 and 1.4.5.2, respectively.

1.4.4 Increased sympathetic nervous system activity

Several studies have evaluated the effect of DEX on sympathetic nerve activity and the role of sympathetic nervous system as a mediator of DEX-HT, but with conflicting results. This is, in part, due to the methods used to measure sympathetic nerve function. There are no published reports evaluating the role of sympathetic nervous system in DEX-HT by means of ganglionic blockade. However, there are several other pieces of evidence from both direct (muscle sympathetic activity) and indirect (expression of adrenergic receptors, catecholamine synthesis, plasma catecholamine and plasma and tissue

neuropeptide Y) assessments of sympathetic nerve activity in DEX-HT which are presented below.

1.4.4.1 Changes in adrenergic receptors

DEX can alter the balance of α1-adrenergic receptor availability in vascular smooth muscles (Haigh and Jones 1990). In DDT1 MF2 hamster smooth muscle cell culture, DEX (10^{-6} M) was shown to result in 2.8 ± 0.7 (mean ± SEM) fold increase in the expression of α1B adrenergic receptor genes and 1.8 ± 0.2-fold increase in the expression of α1-β adrenergic receptors (Sakaue and Hoffman 1991). As discussed in Section 1.5.3, these alterations may contribute to the increase in vascular reactivity and pressor responsiveness seen in DEX-treated humans and experimental animals (Handa, Kondo *et al.* 1984; Russo, Fraser *et al.* 1989; Russo, Fraser *et al.* 1990; Nakamoto, Suzuki *et al.* 1991; Pirpiris, Sudhir *et al.* 1992).

1.4.4.2 Changes in catecholamine synthetic pathway

Tyrosine hydroxylase: Kumai *et al.* showed that hypertension in rats induced by subcutaneous DEX injections at 1 mg/kg/day for 2 days was associated with elevated adrenaline and noradrenaline levels in plasma and adrenal medulla; and increased expression and activity of tyrosine hydroxylase, a rate-limiting enzyme that converts L-tyrosine to dihydrophenylalanine (precursor for dopamine) (Kumai, Asoh *et al.* 2000). They have also demonstrated that inhibition of tyrosine hydroxylase with α-methyl-p-tyrosine reversed DEX-HT (Kumai, Asoh

et al. 2000). Intravenous DEX (2 mg, single dose) in normotensive human subjects resulted in elevated plasma dopamine and adrenaline levels that could be blocked by the tyrosine hydroxylase inhibitor alpha-methyl-p-tyrosine (Watanabe, Noshiro *et al.* 1995).

Phenylethanolamine N-methyltransferase: The activity of phenylethanolamine *N*-methyltransferase (PNMT), an enzyme that converts noradrenaline to adrenaline, in peripheral tissues (atria, ventricle and skeletal muscle) was significantly increased with chronic subcutaneous DEX treatment at 1 mg/kg/day for 12-14 days in both intact and adrenalectomised rats (Kennedy and Ziegler 1991; Kennedy, Elayan *et al.* 1993). The increase in activity, which was secondary to DEX-induced increase in PNMT level rather than activation of existing enzyme, was associated with restoration of adrenalectomy-induced decrease in adrenaline production in the atria (Kennedy and Ziegler 1991). In another experiment, these authors demonstrated that administration of a highly selective peripheral PNMT inhibitor in adrenalectomised DEX-induced hypertensive rats successfully normalised blood pressure (Kennedy, Elayan *et al.* 1993).

Whilst these studies suggest a role for tyrosine hydroxylase and non-adrenal PNMT in the pathogenesis of DEX-HT, it is not possible to draw any definitive conclusions about the role of increased sympathetic activity in DEX-HT as both tyrosine hydroxylase and PNMT activities are very indirect measures of sympathetic function.

1.4.4.3 Changes in neuropeptide Y

Neuropeptide Y (NPY) is a 36 amino acid peptide that is found in abundance within neurons both in the central (Adrian, Allen *et al.* 1983; Allen, Adrian *et al.* 1983) and peripheral (Gu, Polak *et al.* 1983; Lundberg, Terenius *et al.* 1983) nervous system. In the periphery, it coexists with noradrenaline in sympathetic neurons that innervate the blood pressure-controlling structures: blood vessels, heart and kidneys (Sundler, Bottcher *et al.* 1993). It is released upon sympathetic stimulation and thus, is used as an index of sympathetic activity. NPY can modulate vascular tone by inhibiting the release of noradrenaline and NPY itself at the presynaptic NPY receptors (Haass, Cheng *et al.* 1989; Pernow and Lundberg 1989). At the postsynaptic receptor, NPY causes direct vasoconstriction (especially coronary, cerebral, mesenteric and renal vascular beds) (Edvinsson, Ekblad *et al.* 1984; Echtenkamp and Dandridge 1989; Tanaka, Mori *et al.* 1997) and enhances the vasoconstricting effect of vasopressors including noradrenaline and histamine (Edvinsson, Ekblad *et al.* 1984).

A role for NPY in GC-HT was proposed following observations that DEX can influence NPY gene expression and tissue content in neuroendocrine tissue and cell lines (Corder, Pralong *et al.* 1988; Wilding, Gilbey *et al.* 1993; Myrsen, Ahren *et al.* 1996; Myrsen-Axcrona, Karlsson *et al.* 1997). DEX-induced NPY expression in islet cells (*in vivo* DEX dose 2 mg/kg/day, intraperitoneal injections, 12 days) (Myrsen, Ahren *et al.* 1996) and insulin-producing cell line RINm5F (*in vitro* DEX concentration 100 nM, 5 days) (Myrsen-Axcrona, Karlsson *et al.* 1997) has been demonstrated. Increases in rat hypothalamic NPY mRNA (Wilding,

Gilbey *et al.* 1993) and content (Corder, Pralong *et al.* 1988; Wilding, Gilbey *et al.* 1993) have also been shown following DEX treatment (0.4mg/kg/day, subcutaneously (Wilding, Gilbey *et al.* 1993) - 0.5 mg/kg/day, intraperitoneally (Corder, Pralong *et al.* 1988)). The only evaluation of plasma NPY levels in glucocorticoid hypertension was conducted by Tabarin *et al.* who found that plasma NPY was not elevated in either hypertensive (n = 15) or normotensive patients (n = 11) with Cushing's syndrome (Tabarin, Minot *et al.* 1992). There is insufficient evidence to conclude that changes in plasma or tissue NPY content play a role in DEX-HT as direct measurement of NPY tissue content and plasma level, consequent on alterations in its formation, release and clearance, in DEX-HT has not been reported.

1.4.4.4 Changes in plasma noradrenaline and adrenaline levels

DEX effects on plasma noradrenaline and adrenaline concentrations are inconsistent in the literature (Table 1.4). Acute DEX (2.5, 25 and 250 μg or approximately 0.01, 0.1 and 1 mg/kg, respectively, given subcutaneously) did not alter plasma adrenaline and noradrenaline levels in normal rats (Brown and Fisher 1986). On the other hand, rats made hypertensive with 2-day DEX injections (1 mg/kg/day, given subcutaneously) had significantly raised plasma adrenaline and noradrenaline (Kumai, Asoh *et al.* 2000). In another study in rats, 0.1 mg/kg subcutaneous DEX raised plasma adrenaline but did not alter plasma noradrenaline concentration (Silvan, Martinez-Mateos *et al.* 2007).

Similar variations in plasma adrenaline and noradrenaline concentrations were documented in normotensive human subjects following DEX treatment (Rothschild, Langlais *et al.* 1984; Watanabe, Noshiro *et al.* 1995) (Table 1.3).

Whilst plasma adrenaline and noradrenaline concentrations have been used as an index of sympathetic activity, they have limitations. Static measurements are influenced by changes in renal function and hence, plasma catecholamine clearance. Discrepancies probably also reflect differences in species studied, dose and duration of DEX treatments.

Table 1.3: Changes in plasma noradrenaline and adrenaline concentrations induced by DEX treatment in normotensive humans and rats

Species	DEX dose	Plasma NAdr	Plasma Adr	Reference
Human	2 mg, i.v. *stat.*	↑	↓	(Watanabe, Noshiro *et al.* 1995)
Human	1 mg, p.o. *stat.*	↔	↔	(Rothschild, Langlais *et al.* 1984)
Rat	0.01, 0.1, 1 mg/kg, s.c. *stat.*	↓	↓	(Brown and Fisher 1986)
Rat	1 mg/kg, s.c. 2 days	↑	↑	(Kumai, Asoh *et al.* 2000)
Rat	0.1 mg/kg, s.c. *stat.*	↔	↑	(Silvan, Martinez-Mateos *et al.* 2007)

Adr: adrenaline, NAdr: noradrenaline.

1.4.4.5 Muscle sympathetic activity

Direct assessment of sympathetic vasomotor drive to skeletal muscle has been evaluated in six healthy male subjects, treated with oral DEX (3 mg/day) for five days. DEX significantly increased systolic blood pressure from a pre-DEX pressure of 115 ± 1 to 125 ± 2 mmHg (mean ± SEM, $P < 0.01$) but completely suppressed resting spontaneous sympathetic activity in five subjects and markedly

reduced it in the other (Macefield, Williamson *et al.* 1998). Stimulated sympathetic activity induced by cold pressor stimulus, end-inspiratory and end-expiratory apnoea were also attenuated by DEX (Macefield, Williamson *et al.* 1998).

1.4.4.6 Summary

Although indirect methods have provided some useful information about the effects of DEX on sympathetic nerve activity, direct recording of sympathetic nerve traffic remains a more reliable technique (Grassi and Esler 1999). Based on the data of Macefield *et al.* using the latter technique, it is evident that DEX-HT, at least in humans, is not due to increased sympathetic drive (Macefield, Williamson *et al.* 1998).

1.4.5 Excess vasopressor hormone

1.4.5.1 Angiotensin II

DEX (4 mg/kg, intraperitoneally) given to rats 16 and 24 hours before sacrifice significantly increased plasma and liver renin substrate (angiotensinogen) without significant alteration in plasma renin activity (Eggena and Barrett 1988). In DEX-HT in rats (2.5 mg DEX/L drinking water, approximately 30-60 μg/day or 0.17-0.27 mg/kg/day), plasma renin substrate was increased (Okuno, Suzuki *et al.* 1981) but plasma renin activity was within normal range (Okuno, Suzuki *et al.* 1981; Suzuki, Handa *et al.* 1982). The absence of raised plasma renin activity in these studies suggests that glucocorticoid-induced increase in plasma renin substrate does not necessarily indicate activation of the renin-angiotensin system.

Another way of evaluating the role of angiotensin II in the development of DEX-HT is by utilising angiotensin II receptor blockers or angiotensin converting enzyme inhibitors in *in vivo* models. Suzuki *et al.* found that DEX (2.5 mg/L drinking water, approximately 30-60 μg/day or 0.17-0.27 mg/kg/day) raised blood pressure, daily urine volume, urinary sodium excretion and fluid intake without altering plasma renin activity (Suzuki, Handa *et al.* 1982). There was partial prevention of DEX-HT with the angiotensin antagonist saralasin and partial reversal with both saralasin and angiotensin converting enzyme inhibitor SQ14225 without significant differences in volume status, as indicated by body weight, daily urine volume and fluid intake, between the groups. The blood pressure lowering effects of saralasin and SQ14225 were abolished by bilateral

nephrectomy (Suzuki, Handa *et al.* 1982). These results highlight a partial contribution of vasoconstrictor angiotensin II in the development of DEX-HT but do not differentiate whether this is due to angiotensin II excess or glucocorticoid-induced increase in angiotensin II sensitivity.

Apart from its vasoconstrictive capacity, angiotensin II stimulates angiogenesis, vascular smooth muscle hypertrophy and hyperplasia, myocardial hypertrophy and vascular extracellular matrix synthesis (Ferrario and Chappell 2008). It is also a powerful stimulus of superoxide production by the mitochondria, via the activation of mitochondrial ATP-sensitive potassium channel openers, and NAD(P)H oxidase pathway (Griendling, Minieri *et al.* 1994; Kimura, Zhang *et al.* 2005) (Figure 1.2). The role of oxidative stress including NAD(P)H oxidase-mediated superoxide in DEX-HT is discussed in Section 1.5.7.

1.4.5.2 Arginine vasopressin

Administration of arginine vasopressin (AVP) to normotensive rats resulted in dose dependent increases in mean arterial pressure (Iijima and Malik 1988). This increase was accentuated by DEX administration (1.8 mg.kg/week, given as weekly subcutaneous injections for 2 weeks). Administration of $d(CH_2)_5Tyr(Me)AVP$, an AVP V_1 receptor antagonist, reduced mean arterial pressure in DEX-treated rats but not in control rats (Iijima and Malik 1988). The contribution of AVP to the pathogenesis of DEX-HT appears to be mediated by increased expression of the V_{1a} AVP receptor due to increased mRNA stability

(Murasawa, Matsubara *et al.* 1995) and not increased plasma AVP concentration (Nakamoto, Suzuki *et al.* 1991).

1.4.5.3 Endothelin

DEX has been shown to induce endothelin release from cultured human umbilical vein endothelial cells (Huang, Whitworth *et al.* 1995) and cultured rat and rabbit vascular smooth muscle cells (Kanse, Takahashi *et al.* 1991; Roubert, Viossat *et al.* 1993). Plasma endothelin level was reported to be increased in rats receiving DEX (2 mg/kg/day for 12 days) (Takahashi, Suda *et al.* 1991). A 50% increase in circulating endothelin concentration was also reported in human subjects treated with another synthetic glucocorticoid, prednisolone (50 mg on day 1, 25 mg on days 2 and 3, and 10mg on days 4 and 5) (Borcsok, Schairer *et al.* 1998). It is unclear whether this association represents the pathological process responsible for DEX-HT. Further *in vivo* studies using an endothelin antagonist in DEX-HT models is necessary to confirm this hypothesis.

1.4.5.4 Other vasoconstrictors

The influences of other vasoconstrictors such as catecholamines and NPY have been discussed in Sections 1.5.4.2 and 1.5.4.3, respectively.

1.4.6 Deficiency in vasodilator hormone

Of the naturally-occurring vasodilators, atrial natriuretic peptide, prostanoids and nitric oxide have been examined in DEX-HT models. There are no data on the role of other vasodilators (eg endothelium-derived hyperpolarizing factor) in the pathogenesis of DEX-HT.

1.4.6.1 Atrial natriuretic peptide

The role of atrial natriuretic peptide (ANP) in DEX-HT is controversial. Currently available evidence from both *in vivo* and *in vitro* studies indicates conflicting results on the effect of DEX on tissue and plasma ANP concentrations. On one hand, plasma atrial natriuretic peptide (ANP) concentrations were significantly lower in rats made hypertensive with subcutaneous DEX infusions at low dosages (1, 2, 5 and 10 μg/day) (Tonolo, Fraser *et al.* 1988). In these rats, the ANP values were negatively correlated with blood pressure (Tonolo, Fraser *et al.* 1988). On the other hand, DEX treatment (1mg/day or 4 mg/kg/day, subcutaneously for 2 days) increased expression of atrial, ventricular and pulmonary ANP gene, and plasma ANP levels in both intact and adrenalectomised rats (Gardner, Hane *et al.* 1986). The DEX-induced increases in plasma ANP and atrial ANP mRNA levels were independent of volume status as they were not suppressed by water

deprivation for 96 hours prior to sacrifice and sample collection (Gardner, Hane *et al.* 1986). Garcia *et al.* demonstrated that the synthesis and release of ANP by the atria of adrenalectomised rats are regulated by DEX (0.1 mg/kg/day via miniosmotic pump subcutaneous infusion for 5 days) and can only occur when co-administered with a mineralocorticoid which exerts a permissive effect on the regulatory role of DEX on ANP production (Garcia, Debinski *et al.* 1985). In another study, ANP levels from atrial slices and extract obtained from DEX (0.1 mg/kg/day, intraperitoneal injection, 4 days)-treated rats were significantly higher compared to control rats but were not reproducible by *in vitro* incubation of atrial slices with varying concentrations of DEX (10^{-7}- 10^{-4} M, for 1 and 4 hours) (Lachance, Garcia *et al.* 1986). The latter result was likely due to inadequate incubation time.

It is unclear whether the contrasting effects of DEX on tissue and plasma ANP concentrations are related to the dose and administration of DEX and/or variations in experimental conditions, rat strain or model. Nevertheless, the role of ANP availability and activity in DEX-HT merits further investigation.

1.4.6.2 Prostanoids

The notion that a reduction in vasodilator prostanoids plays a role in the development of DEX-HT arose from observations in *in vitro* studies that DEX can inhibit the biosynthesis of prostaglandins via the inhibition of phospholipase A_2 activity, mediated by a transferable phopholipase A_2 inhibitory protein (Flower

and Blackwell 1979; Hirata, Schiffmann *et al.* 1980; Russo-Marie and Duval 1982), and subsequent reduction in arachidonic acid.

The roles of prostaglandins and prostacyclins in the development of DEX-HT have been examined, but with conflicting results. The discrepancies may be ascribed to variability in species and experimental protocols. There have been reports indicating that hypertension in rats due to DEX (3 mg/L, drinking water, approximately 146-160 μg/day, 7 days) was associated with decreased urinary excretion of PGI-M, a marker of prostacyclin (PGI_2) biosynthesis (Falardeau and Martineau 1989). Handa *et al.* concluded that DEX-HT in the rat (DEX dose: 0.1 mg/day or 0.5 mg/kg/day, orally) was associated with sustained inhibition of prostaglandin synthesis based on their finding of reduced urinary prostaglandin E_2 (PGE_2) excretion prior to the onset of hypertension (Handa, Kondo *et al.* 1984). There are no *in vivo* studies in humans evaluating the role of prostanoids in DEX-HT but studies using cultured human umbilical vein endothelial cells showed that thrombin- and histamine-stimulated prostacyclin (PGI_2) (Lewis, Campbell *et al.* 1986; Huang, Whitworth *et al.* 1995) and histamine-stimulated PGE_2 (Lewis, Campbell *et al.* 1986) release from this human cell line were inhibited by DEX (10^{-7} M or approximately 0.04 μg/mL (Lewis, Campbell *et al.* 1986) and 1μg/mL(Huang, Whitworth *et al.* 1995)).

On the other hand, Nasjletti *et al.* demonstrated that DEX-HT in rats (DEX dose: 2.5 mg/kg/week, given subcutaneously) was associated with an increase in circulating and urinary excretion of PGE_2 in the setting of reduced renomedullary

production (Nasjletti, Erman *et al.* 1984). This was attributed to decreased degradation of this vasodilator prostaglandin in the kidney and other extrapulmonary tissues (Nasjletti, Erman *et al.* 1984). This conclusion was further supported by another study which found increased renal and urinary PGE_2 and 6-oxo-$PGF_{1\alpha}$, a stable derivative of PGI_2, in DEX-induced hypertensive rats (DEX dose: 2.5 mg/L drinking water or approximately 0.3 mg/kg/day) (Codde and Beilin 1985). Furthermore, they have shown that cod liver oil diet prevented DEX-HT despite causing a fall in vasodilator prostaglandins (Codde and Beilin 1985). In a recent study from our own laboratory, low dose DEX (1 μg/rat/day, subcutaneous injection) resulted in hypertension in rats without altering urinary PGI_2 (Zhang, Hu *et al.* 2008).

Whilst there are data in keeping with the hypothesis that DEX-HT is linked to a reduction in vasodilator prostanoids, it remains unclear if this is a significant cause of DEX-HT.

1.4.6.3 Nitric oxide

Nitric oxide (NO) deficiency due to administration of nitric oxide synthase inhibitors (Rees, Palmer *et al.* 1989; Wen, Li *et al.* 2000a) or endothelial nitric oxide synthase (eNOS) gene inactivation (Huang, Huang *et al.* 1995) is associated with hypertension. Although there are no published data on the role of NO based on acute NO synthase blockade or sequential blockade of vasoactive systems in DEX-HT, there is accumulating evidence suggesting a role for NO deficiency in

the pathogenesis of DEX-HT. Plasma nitrate/nitrite, a marker of total body NO synthesis, are reduced in rats (Mondo, Yang *et al.* 2006) and mice (Wallerath, Witte *et al.* 1999; Wallerath, Godecke *et al.* 2004) made hypertensive by DEX treatment. The reduced availability of NO might result from a range of influences on the NO biosynthetic pathways: i) alteration in the activity and expression of NOS ii) decreased availability of tetrahydrobiopterin (BH_4), a NOS cofactor, iii) decreased NO precursor L-arginine and iv) increased NO removal via its interaction with superoxide to form peroxynitrite (Figure 1.5).

Altered nitric oxide synthase expression: DEX substantially suppressed the expression of eNOS mRNA and protein in cultured human and bovine endothelial cells, as well as in aorta, kidney and liver of DEX-induced hypertensive rats (Wallerath, Witte *et al.* 1999). Furthermore, the hypertensive effect of DEX seen in wild type mice was not evident in their eNOS knockout counterparts (Wallerath, Godecke *et al.* 2004). This is compatible with the proposal that DEX-HT involves downregulation of eNOS gene expression and resultant decrease in vasodilator NO.

Decreased tetrahydrobiopterin availability: Tetrahydrobiopterin (BH_4) is an essential cofactor for all the nitric oxide synthase isoforms (Schmidt, Werner *et al.* 1992) (Figure 1.5). Simmons *et al.* demonstrated that DEX-induced decrease in intracellular BH_4 content in cultured rat cardiac microvascular endothelial cells, mediated by suppression of guanosine triphosphate (GTP) cyclohydrolase gene expression, was associated with suppressed nitrogen oxide production (Simmons,

Ungureanu-Longrois *et al.* 1996). In another study, *ex vivo* analysis of aortic segments of DEX (5 mg/kg, subcutaneous implant)-induced hypertensive rats revealed decreased GTP cyclohydrolase gene expression, dampened eNOS activity, increased vasoconstrictor response to phenylephrine and absent vascular contraction to NOS inhibitor N^{ω}-nitro-L-arginine (Johns, Dorrance *et al.* 2001). Based on these results, they proposed that BH_4 deficiency consequent on downregulation of GTP cyclohydrolase results in eNOS-dependent regulation of vascular contractility and may play a role in the development of GC-HT.

In contrast, BH_4 administration *in vivo* in DEX-hypertensive rats did not alter systolic blood pressure (Miao, Zhang *et al.* 2007).

Decreased L-arginine availability: Nitric oxide is synthesized from L-arginine via the catalytic action of NOS with co-production of L-citrulline (Figure 1.5). Induced depletion of L-arginine in rats resulted in hypertension and decreased NO synthesis, as evidenced by reduced urinary nitrate and cyclic GMP (Wakabayashi, Yamada *et al.* 1994), illustrating the importance of L-arginine in the maintenance of nitric oxide homeostasis. However, L-arginine supplementation did not prevent or reverse DEX-HT (Li, Fraser *et al.* 1997; Hu, Zhang *et al.* 2006). This could mean that either L-arginine deficiency is not a predominant feature of DEX-HT or there is a defective L-arginine delivery system that results in a state of relative intracellular L-arginine deficiency. DEX-induced abnormalities in L-arginine transport have been demonstrated in cardiac microvascular endothelial cells

(Simmons, Ungureanu-Longrois *et al.* 1996). The state of L-arginine transporter in the DEX-induced hypertensive model has not been examined.

Increased nitric oxide inactivation: NO has a very short half life. Under normal circumstances, it diffuses rapidly across cell membrane into red blood cells where it is removed by its interaction with haemoglobin (Azarov, Huang *et al.* 2005). It can also be inactivated within the vessel wall by its interaction with superoxide to form a powerful oxidant, peroxynitrite (Pacher, Beckman *et al.* 2007). This reaction occurs faster that the removal of superoxide by superoxide dismutase. In the presence of vascular oxidative stress, endothelial NO can be rapidly quenched by excess superoxide resulting in a state of NO deficit. The role of oxidative stress in DEX-HT will be reviewed in Section 1.6.

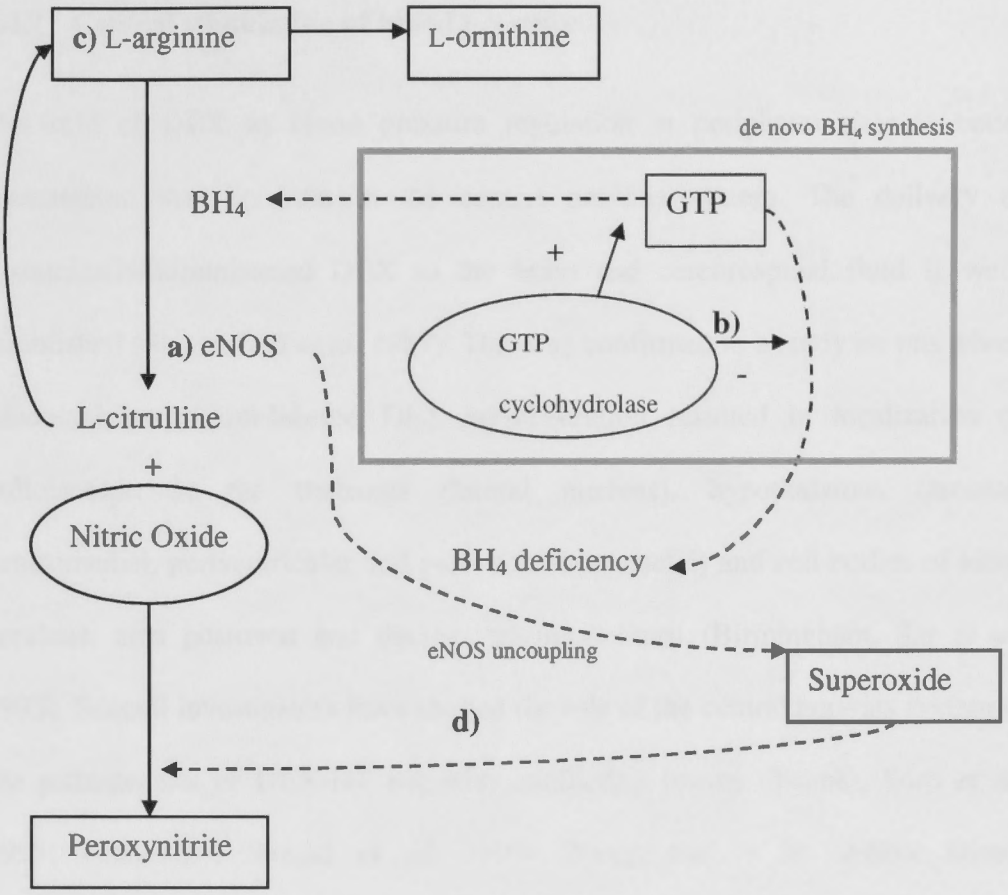

Figure 1.5: Biochemical pathways controlling NO bioavailability. DEX treatment can decrease NO by altering four main pathways marked in this diagram. **a)** Downregulation of eNOS or decrease in eNOS activity by DEX can decrease NO synthesis; **b)** Downregulation of GTP cyclohydrolase by DEX results in decreased de novo BH_4 biosynthesis and BH_4 deficiency; **c)** Decrease in L-arginine availability due to alterations to its transporter by DEX; **d)** DEX-induced oxidative stress increases NO inactivation through peroxynitration, a reaction that is significantly faster than dismutation of superoxide by superoxide dismutase. BH_4: tetrahydrobiopterin, eNOS: endothelial nitric oxide synthase, GTP: guanosine triphosphate.

1.4.7 Central stimulation of blood pressure

The role of DEX in blood pressure regulation at peripheral sites is better documented than its role in the central nervous system. The delivery of systemically-administered DEX to the brain and cerebrospinal fluid is well-established (Siegal, Soti *et al.* 1997). This was confirmed in a study on rats where subcutaneous tritium-labeled DEX administration resulted in localization of radioisotope in the thalamus (lateral nucleus), hypothalamus (arcuate, ventromedial, periventricular and paraventricular nuclei) and cell bodies of locus ceruleus, area postrema and nucleus tractus solitarii (Birmingham, Sar *et al.* 1993). Several investigators have studied the role of the central nervous system in the pathogenesis of DEX-HT but with conflicting results (Tonolo, Soro *et al.* 1993; Nakamoto, Suzuki *et al.* 1995; Wang, Ou *et al.* 2005). Direct microinjections of DEX into bilateral rat nucleus tractus solitarii resulted in a transient hypertensive response acutely at lower doses (12.5 and 25 pmol) and a longer hypertensive response at higher doses (50 and 100 pmol) (Wang, Ou *et al.* 2005). The increase in blood pressure was found to be mediated by glucocorticoid receptor-independent interaction with $GABA_A$ and $GABA_B$ receptors and glucocorticoid-receptor dependent non-transcriptional activation of phosphtidylinositol 3-kinase/protein kinase Akt pathway. However, the possibility of systemic absorption and DEX interactions at peripheral sites was not accounted for in this study. In contrast, intracerebroventricular DEX (1 and 10 μg/kg/day for 7 days in dogs (Nakamoto, Suzuki *et al.* 1995), and approximately 1 μg/kg/day for 24 days in rats (Tonolo, Soro *et al.* 1993)) lowered blood pressure. In the

former study, co-administration of intracerebroventricular glucocorticoid receptor antagonist, RU38486, abolished the antihypertensive effects (Nakamoto, Suzuki *et al.* 1995). Differences in dosages, treatment duration and central sites of DEX administration may account for these discrepancies. Nevertheless, the role of the central nervous system in the pathogenesis of DEX-HT remains unclear.

1.5 REACTIVE OXYGEN SPECIES

Reactive oxygen species (ROS) at low levels under normal physiological conditions play a pivotal role in innate immunity, cell signalling and regulation of vascular integrity. They consist of biologically active oxygen radicals (superoxide, hydroxyl, carbonate, peroxyl and alkoxyl radicals) and highly reactive non-radicals (hydrogen peroxide, hypochlorus acid, fatty acid hydroperoxides, reactive aldehydes and singlet oxygen) which are generated in a constant fashion as by-products of normal cellular metabolism (Bayir 2005) (Table 1.4). Superoxide and hydrogen peroxide are generated from one and two electron reduction of molecular oxygen respectively. These two ROS molecules serve as precursors of other ROS through a cascade of reactions catalysed by a host of antioxidant enzymes. Superoxide is unstable in aqueous environment and is rapidly dismutated by superoxide dismutase (SOD) to hydrogen peroxide. This in turn is detoxified by catalase and glutathione peroxidase into water and oxygen.

Table 1.4: Reactive oxygen species

Oxygen radicals	Highly reactive non radicals
Superoxide	Hydrogen peroxide
Hydroxyl	Hypochlorus acid
Carbonate	Fatty acid hydroperoxides
Peroxyl	Reactive aldehydes
Alkoxyl	Singlet oxygen

The antioxidant enzymes and low molecular weight antioxidant molecules such as glutathione and ascorbate are responsible for maintaining ROS at normal physiological levels (Crawford and Davies 1994). Imbalance between ROS production and antioxidant defence leads to oxidative stress. This phenomenon is linked to various pathologies including cardiovascular diseases, hypertension, neurodegenerative diseases, cancer, inflammatory conditions and diabetes mellitus (Dhalla, Temsah *et al.* 2000; Sayre, Smith *et al.* 2001; Valko, Leibfritz *et al.* 2007).

1.6 REACTIVE OXYGEN SPECIES AND HYPERTENSION

Patients with essential hypertension have higher levels of free radical production, lower NO availability, lower levels of vitamin E and SOD, and higher concentrations of lipid peroxidation product malondialdehyde than normotensive controls (Kumar and Das 1993; Armas-Padilla, Armas-Hernandez *et al.* 2007). Hypertension due to unilateral renal artery stenosis in pigs (Lerman, Nath *et al.* 2001) and chronic angiotensin II infusion (10 ng/kg/min) in rats (Reckelhoff, Zhang *et al.* 2000) and pigs (Haas, Krier *et al.* 1999) was accompanied by increased F_2-isoprostane, a product of arachidonic acid peroxidation. There was overproduction of aortic superoxide in spontaneously hypertensive rats (Wu, Millette *et al.* 2001) which could be prevented by tempol, an antioxidant, at the pre-hypertensive stage (Nabha, Garbern *et al.* 2005). Hypertensive Dahl salt-sensitive rats displayed elevated urinary excretions of F_2-isoprostane and 8 hydroxy 2′ deoxyguanosine (another biomarker of oxidative stress) (Kushiro, Fujita *et al.* 2005), raised superoxide production in the mesenteric microvasculature detected by tetranitroblue tetrazolium dye and increased plasma hydrogen peroxide levels (Swei, Lacy *et al.* 1997). Additionally, experimental induction of oxidative stress in normotensive rats, by reduction of tissue glutathione synthase content with an inhibitor buthionine sulfoximine (30 mmol/L drinking water for 2 weeks), led to hypertension (Vaziri, Wang *et al.* 2000).

ROS can result in hypertension through the loss of NO-mediated vasodilatation; sodium and water retention consequent on increased sodium reabsorption,

glomerular damage and nephron loss; central stimulation of sympathetic outflow; and impaired carotid baroreceptor responses (Harrison, Gongora *et al.* 2007).

1.7 REACTIVE OXYGEN SPECIES AND DEXAMETHASONE-INDUCED HYPERTENSION

The concept that oxidative stress is important in the pathogenesis of DEX-HT emerged from a range of experimental evidence.

1.7.1 Experimental evidence for dexamethasone-induced oxidative stress

Iuchi *et al.* demonstrated that pre-treatment of human umbilical vein endothelial cells with DEX enhanced ROS generation in a time and dose-dependent manner (Iuchi, Akaike *et al.* 2003). They have also shown that patients with glucocorticoid excess have increased immunostaining of nitrotryrosine residue, a stable biomarker of NO radical-derived oxidants, in the skeletal muscle vasculature. However, immunohistochemical staining for nitrotyrosine in adrenal, thymus, kidney and liver tissues from DEX-induced hypertensive rats did not demonstrate any changes compared to controls (Tan, Schyvens *et al.* 2005).

In another study, bilateral adrenalectomy and treatment with the glucocorticoid antagonist RU486 resulted in attenuation of elevated hydroethidine staining while DEX injection in adrenalectomised rats restored the oxidative reaction of hydroethidine (Suzuki, Swei *et al.* 1995).

Lucigenin-enhanced chemiluminescence is widely used for the study of oxidative stress in various animal models of cardiovascular diseases (Rajagopalan, Kurz *et al.* 1996; Dobrian, Schriver *et al.* 2001; Wu, Millette *et al.* 2001; Paravicini, Gulluyan *et al.* 2002). *Ex vivo* analysis of aorta from DEX-induced hypertensive rats showed increased NAD(P)H-activated lucigenin-enhanced chemiluminescence (Mondo, Yang *et al.* 2006a). These authors have also demonstrated increased plasma superoxide concentration measured using the Fenton reaction method in DEX-induced hypertensive rats (Mondo, Yang *et al.* 2006).

Because of the limitations associated with direct detection of reactive oxygen and nitrogen species in clinical settings, biomarkers of oxidative modifications, which are more stable, have been used to assess physiological and pathological redox states (Dalle-Donne, Rossi *et al.* 2006). Among the biomarkers, F_2-isoprostanes, prostaglandin $F_{2\alpha}$-like compounds, are reliable markers of oxidative stress and free radical-catalysed lipid peroxidation of esterified arachidonic acid (Dalle-Donne, Rossi *et al.* 2006). Plasma F_2-isoprostane was increased in DEX-HT in rats (Zhang, Croft *et al.* 2004; Miao, Zhang *et al.* 2007).

To date, there is no convincing evidence for increased ROS production in DEX-HT in humans. There was, however, some evidence implicating oxidative stress in endogenous GC-HT in humans. Iuchi *et. al.* demonstrated increased vascular production of peroxynitrite (through immunostaining of nitrotyrosine residues in vascular tissues) in a patient with HT associated with Cushing's syndrome (Iuchi,

Akaike *et al.* 2003), but cortisol treatment in healthy humans did not result in a significant increase in urinary F_2-isoprostane excretion. (Kelly JJ, Mangos GJ and Whitworth JA, unpublished data)

1.7.2 Effect of antioxidants on dexamethasone-induced hypertension

In rats, hypertension induced by DEX was reversed and prevented by tempol, a superoxide scavenger (Zhang, Croft *et al.* 2004). Additionally, drugs with antioxidant properties such as N-acetylcysteine (Krug, Zhang *et al.* 2008), atorvastatin (Mondo, Yang *et al.* 2006; Mondo, Yang *et al.* 2006a) and folic acid (Miao, Zhang *et al.* 2007) ameliorated DEX-HT in rats suggesting a role for oxidative stress (see below).

1.7.2.1 Tempol

Improvement in DEX-HT following tempol treatment was not accompanied by reduction in F_2-isoprostane levels (Zhang, Croft *et al.* 2004). Tempol, a membrane permeable antioxidant, may modify intracellular ROS which are not detectable by plasma F_2-isoprostane concentrations.

1.7.2.2 N-Acetylcysteine

The hypotensive effect of N-acetylcysteine may be mediated by increase in NO-mediated vasodilatation (Girouard, Chulak *et al.* 2003), antioxidant properties via replenishing intracellular cysteine required for the synthesis of tissue glutathione (Ruffmann and Wendel 1991), and down-regulation of NAD(P)H oxidase

activities and expression (Zhang, Fujii *et al.* 2004). In DEX-treated rats, N-acetylcysteine partially prevented the development but had no effect on established hypertension (Krug, Zhang *et al.* 2008).

1.7.2.3 Atorvastatin

Atorvastatin given orally at 50 mg/kg/day for 14 days prevented DEX-HT in rats (Mondo, Yang *et al.* 2006). Accompanying this blood pressure response, DEX-induced hypertensive rats on atorvastatin also showed suppressed aortic superoxide production, measured using the lucigenin-enhanced chemiluminescence assay; upregulation of eNOS mRNA and improved acetylcholine-induced vasodilatation (Mondo, Yang *et al.* 2006). This study showed that hypertension due to DEX is in part mediated by oxidative stress.

1.7.2.4 Antioxidant vitamins

Folic acid supplementation prevented and partially reversed DEX-HT in the rat (Miao, Zhang *et al.* 2007). This antihypertensive effect of folic acid was not accompanied a significant decrease in plasma homocysteine, increase in tetrahydrobiopterin (BH_4) or decreased F_2-isoprostane concentrations (Miao, Zhang *et al.* 2007). However, the possibility of a decrease in intracellular ROS by folic acid has not been excluded. There are no published data on the effects of antioxidant vitamins such as vitamins C and E in DEX-HT.

1.7.3 Altered expression and activity of antioxidant enzymes

Changes in the availability and activity of endogenous antioxidant enzymes, such as SODs, catalase, thioredoxin reductase and GSH-related enzymes, are seen in response to oxidative stress (Wassmann, Wassmann *et al.* 2004). Rajashree and Puvanakrishnan found that hypertensive DEX-treated rats had increased tissue markers of lipid peroxidation (thiobarbituric acid reactants), decreased catalase and SOD levels in the heart but not in the kidney (Rajashree and Puvanakrishnan 1999). They also demonstrated a decrease followed by a subsequent increase in glutathione S-transferase and glutathione peroxidase activity with DEX treatment (Rajashree and Puvanakrishnan 1999). Furthermore, oxidative stress induced by DEX in veal calves was associated with activation of glutathione peroxidase (Carletti, Cantiello *et al.* 2007). It is likely that there is an element of a compensatory induction, at transcriptional level, of antioxidant protein and enzymes in response to exposure to ROS (Crawford and Davies 1994).

1.7.4 Inhibition of superoxide-generating enzymes

ROS reduction by inhibition of the different superoxide synthetic pathways has provided further evidence for a role for ROS in DEX-HT in the rat. (See below.)

1.8 ROLE OF VASCULAR ROS IN GC-HT

There is increasing evidence implicating vascular ROS in the pathogenesis of hypertension (Touyz and Schiffrin 2004; Harrison, Gongora *et al.* 2007). Superoxide is produced first and through a cascade of catalytic processes, other ROS are generated. Although a variety of enzymes contribute to production of superoxide, the predominant sources in the vasculature are NAD(P)H oxidase, xanthine oxidase, uncoupled eNOS, and mitochondria (Cai and Harrison 2000). (Figure 1.6)

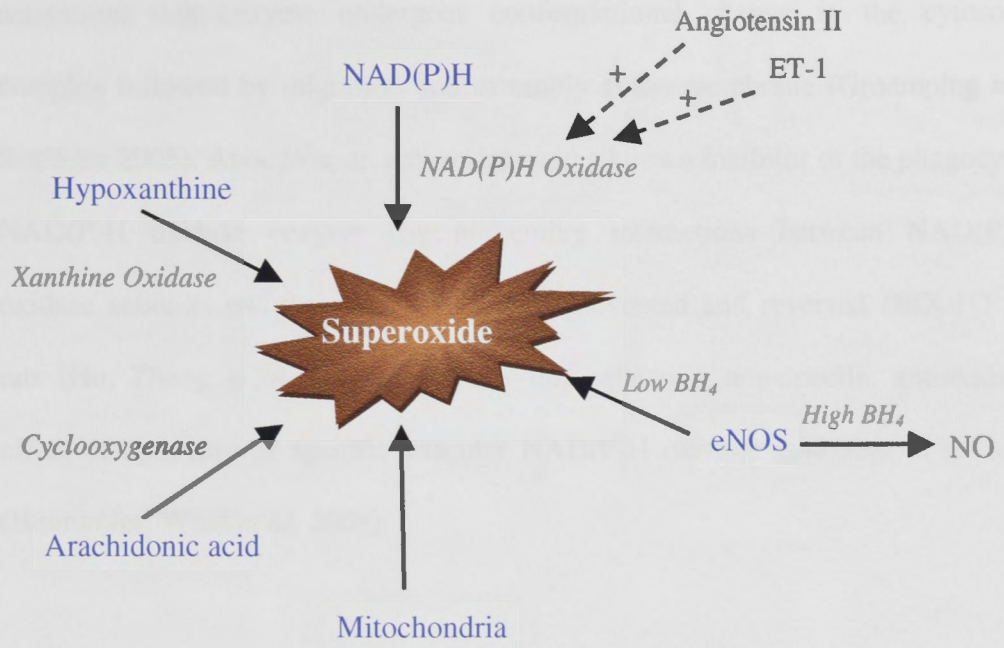

Figure 1.6: Major sources of superoxide in the vasculature. Ang II: angiotensin II, BH_4: tetrahydrobiopterin, ET-1: Endothelin-1, NAD(P)H: reduced nicotinamine adenine dinucleotide phosphate, NO: nitric oxide.

1.8.1 NAD(P)H oxidase

NAD(P)H oxidase is one of the major producers of vascular superoxide, expressed in all layers of the blood vessel wall (Pagano, Ito *et al.* 1995; Pagano, Clark *et al.* 1997; Wang, Pagano *et al.* 1998; Sorescu, Weiss *et al.* 2002). It is a multimeric enzyme composed of a membrane-bound catalytic domain (gp91phox/Nox2, Nox1 or Nox4), regulatory cytosolic subunits (p22phox, p47phox, p67phox, p40phox) and low molecular weight G-protein (Rac 1 or Rac 2) (Bengtsson, Gulluyan *et al.* 2003; Lassegue and Clempus 2003). Upon

activation, this enzyme undergoes conformational change in the cytosolic complex followed by migration and assembly at the membrane (Groemping and Rittinger 2005). Apocynin, an antioxidant and a known inhibitor of the phagocytic NAD(P)H oxidase enzyme (by preventing interactions between NAD(P)H oxidase subunits p47phox and gp91phox), prevented and reversed DEX-HT in rats (Hu, Zhang *et al.* 2006). Whether this reflects a non-specific antioxidant effect of apocynin or specific vascular NAD(P)H oxidase inhibition is unclear (Heumuller, Wind *et al.* 2008).

Superoxide production by NAD(P)H oxidase can be stimulated by angiotensin II (Figure 1.6). In an *in vitro* study, incubation of vascular smooth muscle cells with angiotensin II resulted in increased superoxide production, largely mediated by activation of both NADH and NAD(P)H oxidases (Griendling, Minieri *et al.* 1994). The angiotensin II AT1 receptor antagonist losartan (25 mg/kg/day, in drinking water for 2 days) significantly decreased vascular superoxide production, as assessed by lucigenin-enhanced chemiluminescence, in angiotensin II-induced hypertension in rats. This demonstrated a role for the angiotensin type 1 receptor in NAD(P)H oxidase stimulated superoxide production. In our laboratory, treatment with losartan at a dose known to fully prevent ACTH-HT, partially prevented and reversed DEX-HT in rats (He 2008).

Further examination of the role of NAD(P)H oxidase enzyme using other strategies such as NAD(P)H oxidase subunit knockout mice, will be necessary to confirm its role in DEX-HT.

1.8.2 Xanthine oxidase

Xanthine oxidase catalyses the oxidation of hypoxanthine and xanthine to uric acid, with superoxide formed as by-products. Whilst this superoxide-generating pathway is implicated in the development of hypertension in spontaneously hypertensive (Nakazono, Watanabe *et al.* 1991; Suzuki, DeLano *et al.* 1998) and Dahl salt-sensitive rats (Swei, Lacy *et al.* 1999), it has been shown not to be the major source of superoxide in ACTH-HT in the rat as the xanthine oxidase inhibitor allopurinol (200 mg/kg/day, given orally) failed to prevent and reverse ACTH-HT despite lowering plasma uric acid (Zhang, Chan *et al.* 2005). In contrast, allopurinol (0.4 mg/mL drinking water, approximately 45 mg/kg/day) was shown to be effective in lowering mean blood pressure in high dose DEX-induced hypertensive rats (0.5 mg/kg/day) (Wallwork, Parks *et al.* 2003). One of the limitations of this study was the use of a high dose DEX-HT model. High DEX dose is known to result in significant weight loss due to plasma volume contraction and skeletal muscle catabolism (Tonolo, Fraser *et al.* 1988); and consequently activate the renin-angiotensin-aldosterone system, increase endogenous glucocorticoid levels (Stricker, Vagnucci *et al.* 1979) and suppress ANP production (Sebaai, Lesage *et al.* 2002). Further clarification of the role of xanthine oxidase inhibition in the prevention of DEX-HT, using a much lower DEX dose so as to minimise these confounding effects is necessary.

1.8.3 Uncoupling of eNOS

Fully-reduced BH_4 serves as an important cofactor for endothelial nitric oxide synthase (eNOS) which catalyses the conversion of L-arginine to L-citrulline and NO (Figure 1.5). Decreased BH_4 availability, which promotes eNOS uncoupling, leads to the formation of superoxide instead of NO (Vasquez-Vivar, Kalyanaraman *et al.* 1998).

DEX-HT (5 mg subcutaneous DEX pellet delivering approximately 0.79 mg/kg/day) in the rat is associated with downregulation of vascular GTP cyclohydrolase I, the rate-limiting enzyme for *de novo* biosynthesis of BH_4 (Mitchell, Dorrance *et al.* 2003). Abnormal endothelium-dependent vasorelaxation in the aortic rings of the DEX-induced hypertensive rats was corrected by sepiapterin, a BH_4 donor (Mitchell, Dorrance *et al.* 2003). However, *in* vivo administration of BH_4 failed to prevent DEX-HT (10 µg/rat/day, given subcutaneously) in the rat despite appropriate increases in plasma biopterin levels (Miao, Zhang *et al.* 2007).

In a BH_4-free environment, L-arginine did not inhibit superoxide production but rather, augmented superoxide generation that could only be reversed by the addition of reduced BH_4 (Vasquez-Vivar, Martasek *et al.* 2002). L-Arginine supplementation did not prevent, reverse or exacerbate DEX-HT (10 µg/rat/day, given subcutaneously) in the rat (Li, Fraser *et al.* 1997). As eNOS is downregulated by DEX treatment (Wallerath, Witte *et al.* 1999; Schafer,

Wallerath *et al.* 2005), its involvement in superoxide production via its uncoupled state is unlikely to be significant. Results from recent studies using *in vivo* sepiapterin (which increases BH_4 production via a salvage pathway involving the conversion of sepiapterin to dihydrobiopterin and then, to BH_4) and the NOS inhibitor N-nitro-L-arginine (which minimises eNOS acitivity and thus, eNOS uncoupling) in DEX-induced hypertensive rats were consistent with this proposal (Thida, Earl *et al.* 2010). Sepiapterin did not prevent or reverse DEX-HT in rats despite significantly increased total plasma biopterin concentrations (Thida, Earl *et al.* 2010). N-Nitro-L-arginine did not relieve DEX-HT but exacerbated it (Thida, Earl *et al.* 2010).

These findings showed that oxidative stress due to eNOS uncoupling does not play a significant role in the pathogenesis of DEX-HT.

1.8.4 Mitochondria

Whilst the main function of mitochondria is to produce adenosine triphosphate via electron transfer in the electron transport chain resulting in reduction of oxygen to water, it also results in superoxide formation in the event of electron leakage within this chain. Complex I and III are the primary source of superoxide within the mitochondria. Approximately 0.2-2% of oxygen used by the mitochondria is reduced to superoxide in this electron transport chain (Madamanchi and Runge 2007). As a charged radical, superoxide produced within the mitochondria does not diffuse across the mitochondrial membrane into the cytosol readily (Han,

Antunes *et al.* 2003). It exits the organelle through voltage dependent anion channels and more commonly, as membrane-permeable hydrogen peroxide following its dismutation by intermembrane Cu, Zn-superoxide dismutase (Han, Antunes *et al.* 2003).

Apart from being an important source of superoxide, the mitochondrion is also a target of oxidative injury (Madamanchi and Runge 2007). Oxidative damage to the mitochondria is known to damage mitochondrial DNA, compromise oxidative phosphorylation potentials, decrease energy production and lead to additional production of mitochondrial reactive oxygen species (Madamanchi and Runge 2007). Mitochondrial DNA damage is increasingly recognised as an important etiological factor in cardiovascular disease including hypertension (Ramachandran, Levonen *et al.* 2002; Ballinger 2005).

Mitochondrial superoxide overproduction has also been implicated in the pathogenesis of hypertension in some models. El Midaoui *et al.* demonstrated that hypertension in rats treated chronically with glucose is associated with increased mitochondrial superoxide production (El Midaoui, Elimadi *et al.* 2003). In these rats, oral supplementation of alpha-lipoic acid (500 mg/kg rat chow) blunted the increase in cardiac mitochondrial superoxide and prevented hypertension. Despite this observation, the sequential relationship between these factors remains unclear. It was also uncertain whether the blood pressure lowering effect was due to the antioxidant properties of alpha-lipoic acid or the direct result of a lowered mitochondrial superoxide level. The role of mitochondrial-derived superoxide

and the effect of alpha-lipoic acid on DEX-HT have not been examined previously.

1.8.5 Cyclooxygenase

Endothelial cyclooxygenase is involved in regulation of vascular tone, endothelial function and pressor reactivity to agonists. Arachidonic acid metabolism by endothelial cyclooxygenase is a source of superoxide anions as demonstrated in studies on cerebral arteries in cats and dogs (Kontos, Wei *et al.* 1985; Cosentino, Sill *et al.* 1994).

The role of cyclooxygenase-related superoxide overproduction in DEX-HT has not been fully evaluated. Aspirin, a non-selective cyclooxygenase inhibitor with antioxidant properties, tended to prevent DEX-HT ($P < 0.07$) in rats but failed to reverse it (Zhang, Miao *et al.* 2007). This modest effect could be due to its non-specific antioxidant properties or aspirin-induced stimulation of NO production via eNOS acetylation (Taubert, Berkels *et al.* 2004) and increased cyclic GMP (Grosser and Schroder 2003) rather than inhibition of cyclooxygenase-related oxidative stress. Furthermore, indomethacin treatment potentiated the hypertensive effect of low dose DEX (0.1 mg/kg/day, given orally) in dogs (Nakamoto, Suzuki *et al.* 1992). However, the extent of oxidative stress was not evaluated in this study. The hypertensive response could be a consequence of relative imbalance of vasodilator and vasoconstrictor prostaglandins from the DEX and indomethacin doses used.

Whether oxidative stress due to cyclooxygenase pathway has a role in DEX-HT remains to be determined.

1.8.6 Summary

There is a body of evidence implicating oxidative stress in the pathogenesis of DEX-HT. DEX-HT is associated with raised plasma F_2-isoprostane and lucigenin-enhanced chemiluminescence. In rats, DEX-HT is prevented and reversed by antioxidants tempol, apocynin, folic acid, N-acetylcysteine and aspirin. Oxidative stress in DEX-HT has been shown to involve the NAD(P)H oxidase pathway but not uncoupled eNOS. The role of xanthine oxidase-stimulated superoxide production in DEX-HT needs further evaluation. The role superoxide produced by the mitochondria and cyclooxygenase in DEX-HT has not been evaluated.

1.9 DIFFERENCES BETWEEN NATURALLY-OCCURING AND SYNTHETIC GLUCOCORTICOID-INDUCED HYPERTENSION

DEX, the most potent synthetic glucocorticoid, is commonly used for study of the generic effects of glucocorticoid in different disease states and in various biological pathways. DEX however exhibits some features that are different from those of naturally-occurring glucocorticoids. The similarities and differences between DEX- and ACTH-HT are summarised below. ACTH-HT is explicable in terms of ACTH-stimulated cortisol (Whitworth, Saines *et al.* 1984; Connell,

Whitworth *et al.* 1987) and corticosterone (Mangos, Turner *et al.* 2000) secretions in humans and rats, respectively.

1.9.1 Similarities

1.9.1.1 Rapid onset

Development of GC-HT, due to both naturally-occurring and synthetic glucocorticoid hormones, is rapid. Hypertension due to oral cortisol at supraphysiological doses (80 and 200 mg/day) is evident within 24 hours with the peak blood pressure occurring at day 4 or 5 of treatment in humans (Connell, Whitworth *et al.* 1987; Kelly, Tam *et al.* 1998). ACTH administration produces rapid onset of hypertension in sheep (Scoggins, Allen *et al.* 1979), rats (Turner, Wen *et al.* 1998) and humans (Connell, Whitworth *et al.* 1987; Whitworth 1992). Similarly, DEX raises blood pressure in rats (10 μg/rat/day, subcutaneously) (Zhang, Croft *et al.* 2004; Hu, Zhang *et al.* 2006; Krug, Zhang *et al.* 2008), dogs (0.5 mg/kg/day, orally) (Nakamoto, Suzuki *et al.* 1991; Nakamoto, Suzuki *et al.* 1992) and humans (3 mg/day, orally) (Pirpiris, Sudhir *et al.* 1992) within 1-2 days.

1.9.1.2 No requirement for salt loading or volume expansion

In both forms of GC-HT, salt loading and volume expansion are not prerequisites for their hypertensinogenic effects. Excess sodium is not required for the development of GC-HT. DEX raises blood pressure independent of sodium and intravascular volume expansion in man (Whitworth, Gordon *et al.* 1989).

Likewise, ACTH-HT is not entirely dependent on this mechanism even though sodium excess can magnify its hypertensive response in both man and sheep (Humphrey, Fan *et al.* 1983; Whitworth, Saines *et al.* 1985). Furthermore, dietary sodium restriction (15 mmol/day) did not prevent ACTH-HT (1 mg/day, given intramuscularly) in man despite limiting the mineralocorticoid effects (Connell, Whitworth *et al.* 1988). Cortisol-induced hypertension developed in sheep following sodium depletion (urinary sodium loss of 603 ± 49 mmol) although the extent of the increase was less than that in control sheep (Mills, Coghlan *et al.* 1986).

Cortisol, at maximal physiological doses, exhibits mineralocorticoid activity. However, spironolactone blocked the mineralocorticoid effects of cortisol without preventing the blood pressure rise (Williamson, Kelly *et al.* 1996). In addition, the administration of intravenous deoxycorticosterone (1 mg/day or 40 μg/hour) in man for 5 days reproduced the antinatriuretic properties of cortisol without the hypertensive effects (Whitworth, Saines *et al.* 1984).

1.9.1.3 Nitric oxide-redox imbalance

As discussed in the earlier sections, both DEX- and ACTH-HT are associated with increased superoxide production and decreased NO bioavailability.

Plasma biomarkers of oxidative stress and NO availability: Plasma F_2-isoprostanes, reliable markers of lipid peroxidation and systemic oxidative stress,

were elevated in both ACTH- (Zhang, Jang *et al.* 2003; Zhang, Chan *et al.* 2005; Miao, Zhang *et al.* 2007) and DEX-HT in rats (Zhang, Croft *et al.* 2004; Miao, Zhang *et al.* 2007). Similarly, plasma reactive nitrogen intermediates (nitrate/nitrite), a marker of NO availability, are reduced in cortisol- (Kelly, Tam *et al.* 1998), corticosterone-(Mangos, Turner *et al.* 2000), ACTH- (Wen, Li *et al.* 2000; Turner, Mangos *et al.* 2001) and DEX-HT (Wallerath, Godecke *et al.* 2004; Mondo, Yang *et al.* 2006; Mondo, Yang *et al.* 2006a; Miao, Zhang *et al.* 2007).

Responses to antioxidants and BH_4 supplementation: Both ACTH- and DEX-HT were prevented and reversed by antioxidants: folic acid (Miao, Zhang *et al.* 2007), N-acetylcysteine (Mondo, Zhang *et al.* 2006; Krug, Zhang *et al.* 2008) and superoxide scavenger tempol (Zhang, Jang *et al.* 2003; Zhang, Croft *et al.* 2004). Hypertension due to both ACTH and DEX was prevented and reversed by apocynin (Zhang, Chan *et al.* 2005; Hu, Zhang *et al.* 2006) implicating a role for superoxide-generating NAD(P)H oxidase in this condition. Oxidative stress in these models of hypertension was not due to uncoupling of eNOS as hypertension was not prevented by administration of BH_4 (Zhang, Pang *et al.* 2004; Miao, Zhang *et al.* 2007).

1.9.2 Differences

Despite the evidence implicating oxidative stress and NO-superoxide imbalance, blood pressure responses to treatments known to modify the synthesis of NO and superoxide were variable.

1.9.2.1 Response to L-arginine

As discussed earlier, L-arginine deficiency is not a characteristic of DEX-HT. L-Arginine treatment (500 mg/kg/day) increased plasma nitrate/nitrite (NOx) concentrations but failed to prevent hypertension in DEX-treated rats (Li, Fraser *et al.* 1997; Hu, Zhang *et al.* 2006). In contrast, ACTH-HT is associated with decreased plasma L-arginine, L-citrulline and NOx concentrations (Wen, Li *et al.* 2000). Established ACTH-HT was prevented and partially reversed by L-arginine, but not D-arginine supplementation (Turner, Wen *et al.* 1996; Wen, Li *et al.* 2000).

The blood pressure lowering effect of L-arginine in corticosterone- and ACTH-HT is largely due to restoration of NO by increased availability of NOS substrate as increases in blood pressure with both corticosterone- and ACTH treatments were prevented by L-arginine but not D-arginine (Turner, Wen *et al.* 1996; Mangos, Turner *et al.* 2000); and co-administration of L-arginine and the competitive NOS inhibitor, N-nitro L-arginine negated the blood pressure lowering effect of L-arginine in ACTH-HT (Wen, Li *et al.* 2000a).

1.9.2.2 Urinary 20-hydroxyeicosatetraenoic acid

ACTH-HT, but not DEX-HT, is associated with increased urinary 20-hydroxyeicosatetraenoic acid excretion (Zhang, Hu *et al.* 2008).

20-Hydroxyeicosatetraenoic acid (20-HETE) is a cytochrome P450-derived arachidonic acid metabolite that has potent vasoconstrictive properties. Synthesis of 20-HETE can be inhibited by NO (Roman 2002). Overproduction of 20-HETE in ACTH-HT might be due to NO deficiency although this does not explain the findings in DEX-HT.

1.9.2.3 Response to glucocorticoid receptor antagonism

Dihydroepiandrosterone, an endogenous steroid with anti-glucocorticoid activity, prevented DEX-HT (Shafagoj, Opoku *et al.* 1992) but not ACTH-HT (Li, Wen *et al.* 1996).

DEX-HT was prevented by the glucocorticoid antagonist RU486 at a dose (50 mg subcutaneous pellet) that did not reverse weight loss (Kalimi 1989). With ACTH-HT, a dose of RU486 (70 mg/kg every third day) that reversed weight loss did not modify blood pressure (Li, Wen *et al.* 1999). Partial prevention of the blood pressure rise was seen with high dose RU486 (70 mg/kg/day) (Li, Wen *et al.* 1999).

These differences suggest glucocorticoid receptor activation is more predominant in DEX-HT.

1.9.2.4 Response to vasopressin antagonism

Vasopressin antagonism with the AVP V_1 receptor antagonist [l-(β-mercapto-β, β-cyclopentamethylene propionic acid) 2-(O-methyl)-Tyrosine]-AVP significantly decreased mean arterial pressure in DEX-induced hypertensive rats but not in saline-treated control rats (Iijima and Malik 1988). Conversely, ACTH-HT was not modified by either acute or chronic inhibition of the AVP V_{1a} receptor using OPC 21268 (Fraser, Turner *et al.* 2000) at a dose proven to be effective in blocking V_1 receptors (Burrell, Phillips *et al.* 1994).

1.9.2.5 Response to aspirin

Aspirin, a non-selective cyclooxygenase inhibitor and an antioxidant, prevented and partially reversed ACTH-HT but not DEX-HT in rats (Zhang, Miao *et al.* 2007). The postulated antihypertensive mechanisms of aspirin in the ACTH-HT model include inhibition of cyclooxygensase- and NAD(P)H oxidase-mediated superoxide production, decrease in superoxide-mediated NO inactivation, increase in NO production and increase in cyclic GMP availability. The reason for the differences between DEX- and ACTH-HT is unclear.

1.9.2.6 Response to neomycin

Neomycin attenuates the blood pressure rise in rats following ACTH, corticosterone or prednisolone but not DEX (Fraillon, Wynne *et al.* 1984). It remains unclear whether the blood pressure changes were due to altered patterns of enterohepatic handling and metabolism or the intrinsic properties of neomycin.

1.9.3 Summary

The observed differences between naturally-occuring GC-HT and DEX-HT suggest that hypertension due to these glucocorticoids involves different pathophysiological perturbations of NO-redox imbalance.

1.10 SUMMARY- MECHANISMS OF DEXAMETHASONE-INDUCED HYPERTENSION

There is convincing evidence indicating that sodium retention with a resultant volume expansion is not a mechanism of DEX-HT. Whilst the major cause for DEX-HT remains unclear, there is a body of evidence implicating nitric oxide-redox imbalance, in part, due to increased vascular superoxide production. The likely source of superoxide is the NAD(P)H oxidase pathway. DEX-HT is also associated with increased total peripheral resistance and heightened pressor response to vasocontrictors but not raised sympathetic activity. The roles of endogenous vasoconstrictors and vasodilators in the pathogenesis of DEX-HT are variable, with possible links to NO, prostanoids, angiotensin II, arginine vasopressin, endothelins, catecholamines, neuropeptide Y and atrial natriuretic peptide.

1.11 PROJECT HYPOTHESES

The hypotheses of this project were that:

1. increase in TPR will be essential to raise blood pressure with DEX.

2. there is ROS overproduction from mitochondria in GC-HT and hypertension can be prevented and reversed by inhibiting mitochondrial superoxide production using alpha-lipoic acid.

3. allopurinol, a xanthine oxidase inhibitor, can prevent and reverse DEX-HT by means of ROS reduction.

4. propranolol, a β-adrenergic receptor blocker and lipid peroxidase inhibitor, can prevent GC-HT.

5. DEX-HT is associated with increased production of 20-HETE and specific inhibition of 20-HETE production will reverse DEX-HT.

1.12 GENERAL AIMS OF THIS PROJECT

The main aim of this project was to evaluate the mechanisms of DEX-HT, namely the haemodynamic mechanisms, the role of oxidative stress and NO deficiency.

The role of β-adrenergic receptor blockade in DEX-HT and metabolic effects of DEX in rats were also evaluated. In some experiments, evaluations of both DEX- and ACTH-HT were conducted for comparison purposes.

1.13 SPECIFIC AIMS OF THIS PROJECT

This project comprised 7 studies (Table 1.5).

Two studies examined the haemodynamic mechanisms of DEX-HT. The first evaluated the haemodynamic characteristics of DEX-HT in the rat (Chapter 3). This was followed by evaluation of the role of TPR and conductance in DEX-HT (Chapter 4). The roles of mitochondrial superoxide (Chapters 5 and 6) and lipid peroxidation (Chapter 8) were evaluated in both DEX- and ACTH-HT. In Chapter 7, the role of xanthine oxidase, another source of reactive oxygen species, was examined in DEX-HT. The role of β-adrenergic activity (Chapter 8) and 20-HETE (Chapter 9) in the pathogenesis of DEX-HT were also evaluated. Metabolic profiles of DEX-induced hypertensive rats were documented in Chapter 10.

Table 1.5: Studies in this project

HAEMODYNAMICS

Chapter 3: Haemodynamic profile of DEX-HT in the rat

Chapter 4: The role of total peripheral resistance and conductance in DEX-HT in the rat

OXIDATIVE STRESS

Chapters 5 & 6: Role of mitochondrial superoxide in GC-HT in the rat

Chapter 7: Role of xanthine oxidase in DEX-HT in the rat

Chapter 8: The effects of adrenergic receptor antagonism and lipid peroxidation inhibition using propranolol in GC-HT in the rat

NITRIC OXIDE DEFICIENCY

Chapter 9: Role of 20-hydroxyeicosatetraenoic acid in DEX-HT in the rat

OTHER MECHANISMS/ OBSERVATIONS

The role of adrenergic receptors- as in **Chapter 8** above

Chapter 10: Metabolic profiles of DEX-HT in rats

CHAPTER 2

Materials and Methods

2.1 ETHICS

This project was approved by the Animal Experimentation Ethics Committee (Approval numbers: J.HB.17.03, J.HB.20.05, J.HB.22.06 and J.HB.24.06).

2.2 EXPERIMENTAL ANIMALS

Rats are used in the study of GC-HT because of the relevance of this model to human GC-HT (Whitworth, Schyvens *et al.* 2001; Whitworth, Zhang *et al.* 2006).

Male Sprague-Dawley rats with an initial body weight of 180-280 g were used in this project (Figure 2.1). This outbred stain is one of the most widely used animals in experimental hypertension. Only male rats are used to minimise gender-related variability to the results. These rats were purchased from Animal Resource Centre, Perth. This certified facility produces and sells laboratory animals that are free from pathogens. (http://www.arc.wa.gov.au/overview.php)

Figure 2.1: Male Sprague-Dawley albino rat

The rats were housed in a purpose-built laboratory in John Curtin School of Medical Research, Australian National University. The laboratory has ducted air conditioning (21 ± 1 °C) and operates 12-hour light/dark cycles. The rats were housed communally in groups of 2-3 per cage. An individually-ventilated caging system was used (Techniplast, Buguggiate, Italy) (Figure 2.2). These cages were made of transparent plastic and thus, allowed interaction and socialisation. The cages were lined with aspen wood chip bedding (Tapvei, Finland). The animals had free access to standard rat chow (Gordon's Specialty Stockfeeds Pty. Ltd., Yanderra, Australia) and tap water.

Figure 2.2: Individually-ventilated caging system

2.3 STUDY DESIGN

This project consisted of 7 studies which followed a general experimental protocol for animal handling, treatment and tail cuff blood pressure measurement. There was inter-study variability with regard to the treatments, surgical procedures and assays.

The main experimental protocol consisted of 3 main phases- acclimatisation, control and treatment periods (Figure 2.3).

2.3.1 Acclimatisation period

The rats were allowed to familiarise with the environment, handling and blood pressure measuring equipment prior to any experimental procedure for 1-2 weeks after their arrival.

2.3.2 Control period

Two baseline tail cuff blood pressure and body weight measurements were obtained prior to drug administration on day C4 (4 days prior to treatment) and C2 (2 days prior to treatment). The prefix "C" represents control days.

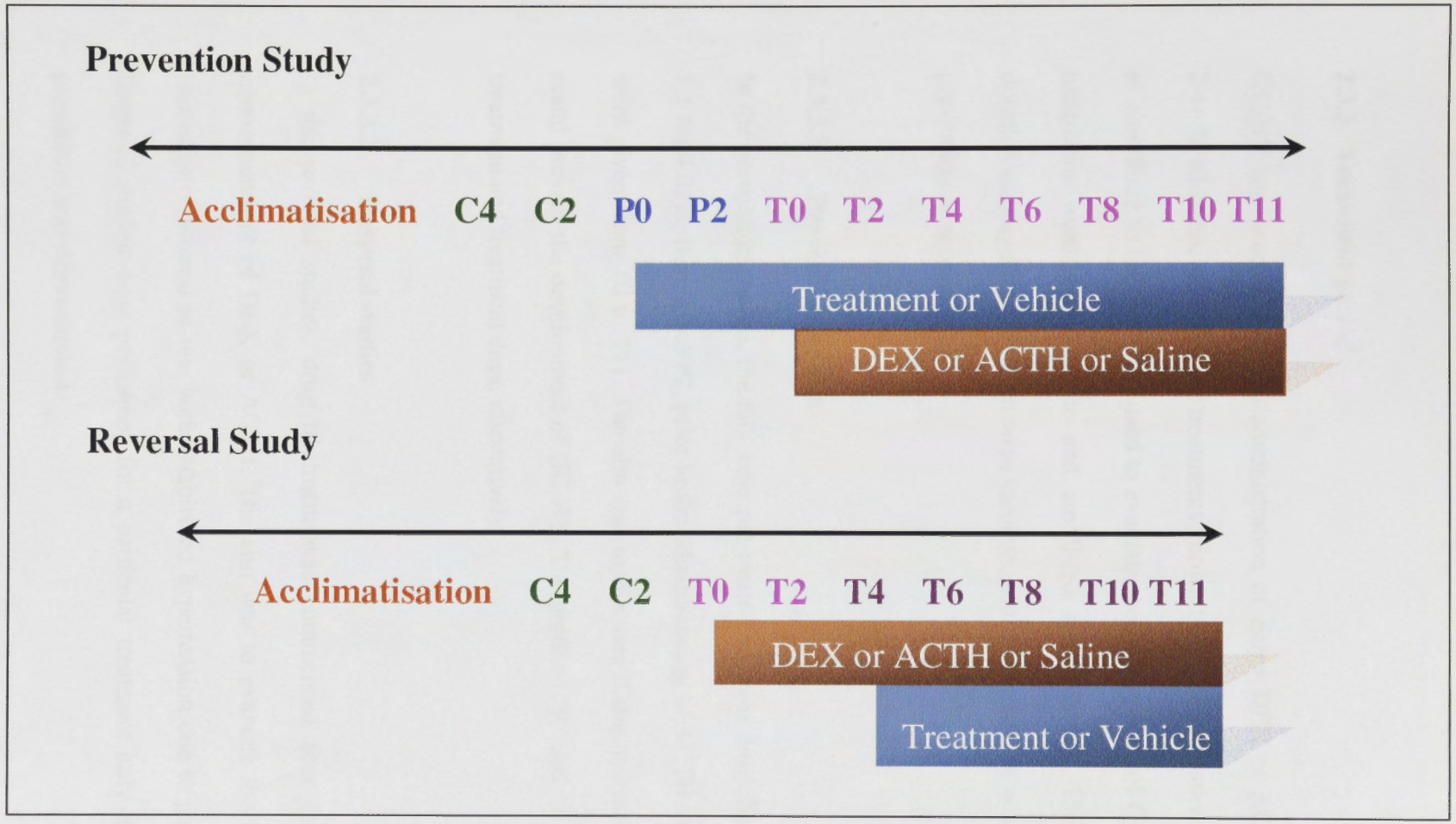

Figure 2.3: Timeline of experimental protocol

2.3.3 Treatment period

GC-HT was produced by the administration of either DEX or ACTH (Section 2.4). In addition, several other treatments known to inhibit the pathways proposed to contribute to GC-HT were used to evaluate the mechanisms of GC-HT. These treatments were study-specific and are listed in Table 2.1. The timing and duration of drug administration were variable, and determined by whether it was a prevention or reversal study.

2.3.3.1 Prevention studies

In the prevention studies, the rats were pre-treated with the drugs listed on Table 2.1 for 4 days, from P0 to P2, prior to the administration of ACTH or DEX which were given from T0 to T11. The aim was to evaluate if the treatment of interest could prevent the development of GC-HT. The prefixes "P" and "T" denote pre-treatment and treatment days, respectively.

2.3.3.2 Reversal studies

In the reversal studies, drug treatment was commenced four days after the commencement of DEX or ACTH. The aim was to evaluate the effect of the treatment of interest in rats with established hypertension due to glucocorticoid. Reversal studies were performed for a particular treatment only if a complete prevention was demonstrated.

Table 2.1: Summary of studies and drug treatments

Chapter	Study Title	Saline/DEX/ ACTH (s.c)	Other treatments
3	Haemodynamic profile of DEX-HT in the rat	DEX/Saline	Vehicle (Saline), gavage
4	Role of total peripheral resistance and conductance in DEX-HT in the rat	DEX/Saline	Minoxidil or Vehicle (Saline), gavage
5	Effects of GC on rat kidney mitochondrial superoxide	DEX/ACTH/ Saline	Nil
6	Role of mitochondrial superoxide in GC-HT in the rat	DEX/ACTH/ Saline	Alpha lipoic acid or Vehicle (Ground food), p.o.
7	Role of xanthine oxidase in DEX-HT in the rat	DEX/Saline	Allopurinol or Vehicle (Ground food), p.o.
8	Effects of adrenergic receptor antagonism and lipid peroxidation inhibition using propranolol in GC-HT in the rat	DEX/ACTH/ Saline	Propranolol or Vehicle (Ground food), p.o.
9	Role of 20-hydroxyeicosatetraenoic acid in DEX-HT in the rat	DEX/Saline	HET0016 or Vehicle (Lecithin), i.p.
10	Metabolic profiles of DEX-HT in rats	DEX/Saline	Vehicle (Saline), gavage

During the control and treatment phases, indirect SBP readings were measured on alternate days using tail-cuff plethysmography (See Section 2.5.1).

2.4 DRUG ADMINISTRATION PROTOCOL

The preparation and administration of DEX and ACTH are discussed here but that of other drugs in the relevant chapters.

2.4.1 Dexamethasone preparation and administration

DEX is a synthetic glucocorticoid which has very active glucocorticoid activity and minimal mineralocorticoid activity (Rang, Dale *et al.* 2007).

DEX solution was prepared by diluting 1mL of 4 mg/mL stock solution (DBL dexamethasone sodium phosphate, David Bull Laboratories, Mulgrave, Australia) in 29 mL sterile saline (0.9 % NaCl). The final concentration of the DEX solution was 131.57 μg/mL DEX sodium phosphate which contains 100 μg/mL DEX.

DEX was injected subcutaneously once daily at a dose of 20 μg/rat (0.2 mL/rat, approximately 0.06 mg/kg body weight) in the haemodynamic and metabolic studies (Chapter 3, 4 and 10) and at a dose of 10 μg/rat (0.1 mL/rat, approximately 0.03 mg/kg body weight) for the other studies. Equivalent volumes of normal saline were used in control rats for these studies. The timing and duration of DEX or vehicle treatments is discussed separately in each study.

The solution was drawn into a 1 mL syringe and injected subcutaneously using a 25 gauge needle (Terumo Medical Corporation, Elkton, USA). The rat was restrained gently but firmly under a towel to prevent movements during the subcutaneous DEX injection after the tail-cuff SBP and body weight measurements.

2.4.2 ACTH preparation

The ACTH preparation used (tetracosactrin 1 mg/mL, Synacthen Depot, Novartis Pharmaceuticals, Sydney, Australia) is a synthetic polypeptide that consists of the first 24 of 39 amino acids found in the endogenous ACTH molecule. ACTH suspension was prepared by diluting 1mL of 1 mg/mL stock suspension in 4 mL sterile saline (0.9 % NaCl). The final concentration of the preparation was 0.2 mg/mL. The dose administered was 0.2 mg/kg/day (0.1 mL/100g/day, subcutaneous injections). Equivalent volume of normal saline was used in control rats.

As with DEX treatment, ACTH was administered subcutaneously using the technique described in Section 2.4.1.

2.5 BLOOD PRESSURE MEASUREMENT

2.5.1 Indirect blood pressure measurement

2.5.1.1 Equipment and procedures

Blood pressure was measured in conscious rats using the indirect tail-cuff sphygmomanometer (Figure 2.4). Experiments were performed in the morning on alternate days, in a separate quiet room within the laboratory. The rats were placed in plastic restrainers on a heating plate (39-40°C, SDR Clinical Technology, Sydney, Australia) for approximately 12 minutes before recording the SBP readings. This caused tail artery vasodilation which was necessary for the detection of the oscillatory pulse wave by the pneumatic sensor bulbs and pulse transducers (Narco Biosystems, Houston, USA). The bulbs, which were securely taped to the tail using adhesive tapes (Leukofix, Smith & Nephew Pty Ltd., Mount Waverley, Australia) were connected to the pneumatic transducers. Analogue signals were amplified by an amplifier (PA100, SDR Clinical Technology, Sydney, Australia) and converted to digital signals by a Biopac MP100 processor (Biopac Systems Inc., Goleta, USA). The blood pressure data were then acquired using the HyperRat software (SDR Clinical Technology, Sydney, Australia) on a Macintosh computer.

Systolic blood pressure readings were acquired by inflating a pneumatic cuff that was applied to the base of the rat tail (proximal to the pneumatic bulb sensor). The cuff, which was powered by an electrosphygmomanometer (Narco Biosystems,

Houston, USA) was inflated to 225 mmHg to occlude the tail artery and then deflated. The return of the pulse signal during deflation marked the SBP. The SBP readings were recorded on the computer.

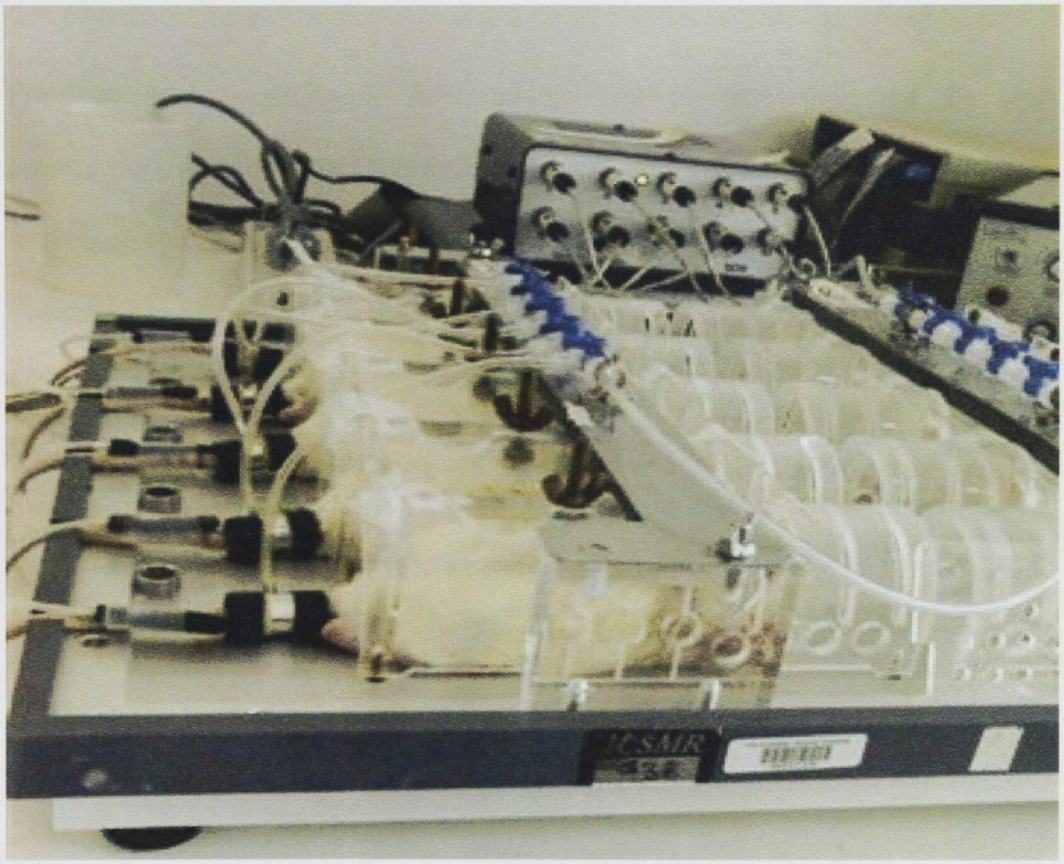

Figure 2.4: Tail-cuff sphygmomanometer

Up to 30 readings were recorded from each rat and the mean of the four median recordings, among which the difference was less than 10 mmHg, were accepted as the SBP.

2.5.1.2 Validation and maintenance

This method has been previously compared with the 'gold standard' of a direct blood pressure measurement technique using a biotelemetry system with both giving similar blood pressure results (Fraser, Turner *et al.* 2001).

Prior to each experiment, the maximal air pressure delivered by the electrosphygmomanometer for cuff inflation was checked using a mercury sphygmomanometer. The tubing and occlusion cuffs were also checked for air leaks prior to any actual blood pressure recordings.

2.5.2 Direct blood pressure measurement

Direct blood pressure measurements were carried out only in the haemodynamic experiments (Chapters 3 and 4).

2.5.2.1 Equipment and surgical procedures

Following the induction of general anaesthesia using pentobarbitone (see Section 2.8.2 below), the rats were placed on a heating pad (surface temperature 38-40°C, D.L.C Australia Pty. Ltd., Hoppers Crossing, Australia) in a dorsally recumbent position. The ventral aspect of the neck was shaved using an electric clipper (Thrive, Daito Electric Machine Ind Co, Ltd, Osaka, Japan). A midline ventral skin incision was made to expose the strap muscles of the neck. Subsequent surgical procedures were performed using a stereomicroscope (Leica MZ7$_5$, Leica Microscopy Systems Ltd, Heerbrugg, Switzerland). Haemostasis was achieved

using a battery operated cautery. Blunt dissection along the direction of the muscle fibres exposed the trachea and thyroid gland. Further blunt dissection laterally towards the left of the animal exposed the left jugular vein and left common carotid artery. Approximately 2 cm of the left common carotid artery was gently isolated from the adherent connective tissues, vagus and cervical sympathetic nerves. Once the artery was isolated, three 5/0 silk sutures (B.Braun Surgical, Melsungen, Germany) were passed around the artery and placed approximately 1 cm apart- one at the cranial end, the other one at the caudal end and the third in the middle between the cranial and caudal sutures. The cranial suture was tied to occlude the carotid artery. The middle and caudal sutures were tied loosely around the artery. A micro vascular clamp (HD-S, S&T, Neuhausen, Switzerland) was placed over the caudal suture to prevent bleeding during the insertion of the catheter tip transducer (Mikro-Tip SPR-320; Millar Instruments Inc., Houston, USA). To insert the Millar catheter, an incision was made to the artery between the cranial and middle sutures using a 25 gauge needle with its sharp tip bent at 90°. Using the same needle, the Millar catheter was introduced into the artery in the direction of the heart. The middle suture was tightened to prevent bleeding when the artery clip was removed. The Millar catheter was advanced to the level of the aortic arch. Both the middle and caudal sutures were tightened to secure the catheter to the carotid artery. The Millar catheter was then connected to a bridge amplifier and the PowerLab® data acquisition system (AD Instruments, Sydney, Australia). The latter was connected to a computer running the Chart™5 for Windows software (AD Instruments, Sydney, Australia). The

mean arterial pressure, systolic and diastolic blood pressures were recorded on the computer.

2.5.2.2 Calibration and maintenance

The Millar catheter was calibrated with a pressure gauge calibration kit consisting of an aneroid sphygmomanometer prior to each use.

The catheter was soaked in enzyme cleaner (Tergazyme, Alconox Inc., White Plains, USA) after each use to remove any blood clot or protein build-up that might affect the accuracy of the pressure transducer.

2.6 HEART RATE MEASUREMENT

Heart rate was measured using the tail-cuff sphygmomanometry, non-invasively and Millar catheter, invasively.

2.6.1 Via tail-cuff sphygmomanometry

Heart rate measurements were obtained via this technique as reported in Chapter 10. During the acquisition of SBP readings, heart rate data were also acquired and recorded. The arterial pulsations were detected via the pneumatic pressure transducers and amplified. The signals were digitalised and recorded. Each sine wave was counted as a beat.

Up to 30 readings were recorded. Readings that were < 200 and > 500 beats/min were excluded as these were not within the physiological ranges for rats and were likely to be artefactual. All the other heart rate readings were averaged and accepted as the heart rate.

2.6.2 Via Millar carotid artery transducer

Heart rate measurements were also measured invasively using the Millar catheter in the haemodynamic studies (Chapters 3 and 4). The arterial pulsations were detected by the transducer, acquired by the PowerLab®, amplified by the bridge amp and recorded by the computer running the Chart™5 for Windows software. The number of sine waves per minute was used as heart rate.

2.7 METABOLIC MEASUREMENTS

Metabolic assessments were performed using stainless steel metabolic cages (Mascot Wire Works Pty Ltd., Sydney, Australia) where the rats were housed singly for 24 hours on alternate days through 12-hour light/dark cycles (Figure 2.5). The construct of this caging system enables measurements of 24-hour food and water intakes and urine volume. Under each cage is a removable stainless steel funnel that collects urine and faeces. The lower part of the funnel is a specially-designed pipe that can separate urine and faeces. A graduated plastic container is attached to the end of the funnel for urine collection. Attached to the cages are food canisters that also support water bottles.

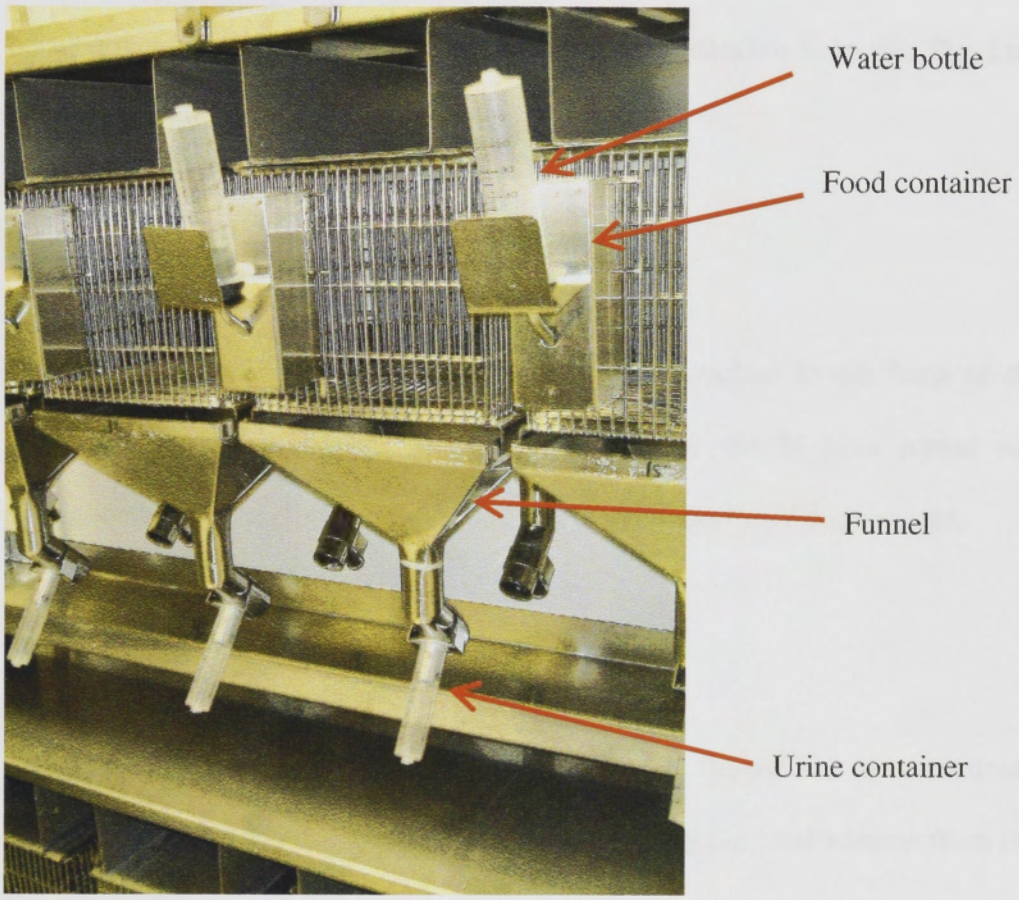

Figure 2.5: Metabolic cages

2.7.1 Body weight

Body weight was measured after tail cuff experiments using a multi-function balance that allows weighing of moving animals. (Australian Scientific Pty. Ltd., Kotara, Australia).

2.7.2 Food intake

Pellet rat food was placed in the food container attached to the front of the metabolic cage. The amount of food ingested over the 24 hour period was determined by subtracting the final food weight from the initial food weight.

2.7.3 Water intake

The graduated water bottle was filled with tap water. The amount of water drunk over the 24 hour period was calculated by subtracting the final volume from the initial volume.

2.7.4 Urine volume

Urine was collected into the graduated container at the bottom of the funnel (Figure 2.5). Urine volume was measured and documented. Two milliliters of urine was collected into Eppendorf tubes and stored in a -70°C freezer. Urinary sodium, potassium and creatinine were analysed at the ACT Pathology, The Canberra Hospital.

2.8 ANAESTHETIC AND SURGICAL PROCEDURES

2.8.1 Presurgical treatment

The animals were given the final doses of all treatments prior to surgery.

2.8.2 Anaesthesia

All surgical procedures were carried out under general anaesthesia, achieved by either using intraperitoneal pentobarbitone sodium (Nembutal 60mg/mL, Merial Australia Pty. Ltd., Sydney, Australia) or isoflurane (Laser Animal Health, Pharmachem, Eagle Farm, Australia) inhalational anaesthesia.

Pentobarbitone was used to anaesthetise animals in the haemodynamic (Chapters 3 and 4), metabolic (Chapter 10) and the 20-HETE studies (Chapter 9). Pentobarbitone (60 mg/kg or 0.1 mL/100g body weight) was drawn into a 1 mL syringe with a 25 gauge needle. The rat was restrained gently but firmly under a towel to prevent movements during the intraperitoneal injection. The right hind leg was abducted at the hip joint and at the same time, the hindquarter was lifted up. This allowed the abdominal viscera to fall anteriorly with gravity and minimise inadvertent puncture of the abdominal viscera. The injection was made at a site between the liver and the bladder, approximately 1 cm to the right of the midline. Before the injection, the syringe was withdrawn to ensure that the needle was not in the bladder or a blood vessel. Following the injection, the rat was returned to the cage until anaesthesia was achieved. During longer surgical

procedures, such as in the haemodynamic studies (Chapters 3 and 4), additional bolus doses of pentobarbitone were required (6 mg/hour or 0.1 mL/ hour) to maintain satisfactory anaesthesia.

Isoflurane inhalational anaesthesia was used in the remainder of the studies (Chapters 5, 6, 7 and 8). It was administered with oxygen (2 L/min) via a vaporiser (Tec 5 Vaporizer, Datex-Ohmeda, Helsingborg, Sweden). Induction of anaesthesia was attained in an anaesthetic chamber using 4 % isoflurane concentration. Isoflurane administration via a nose cone was continued at 2 % to maintain anaesthesia throughout the entire surgical procedure.

The level of anaesthesia was checked by stretching the hind foot outward and pinching the paw pad firmly. If the rat did not retract the foot or move from this manoeuvre, satisfactory anaesthesia had been achieved.

2.8.3 Haemodynamic experiments

2.8.3.1 Principles of haemodynamics

Haemodynamics is the study of physics that governs the blood flow within the cardiovascular system. The fundamental principle of haemodynamics in the cardiovascular system is based on the Poiseuille's Law which states that the flow of fluid through a series of tubes is proportional to the pressure difference between the 2 ends of a tube and conductance, but inversely proportional to resistance (Figure 2.6).

$$Q = \frac{\Delta P r^4 \pi}{\eta L 8}$$

$$= \Delta P \left(\frac{r^4}{\eta L} \right) \left(\frac{\pi}{8} \right)$$

$$= \Delta P \left(\frac{1}{R} \right) \left(\frac{\pi}{8} \right)$$

Figure 2.6: Poiseuille's Law. Q=flow rate, ΔP= difference in pressure between the ends of a tube, r = radius of the tube, η = viscocity, L = length of the tube, $\pi/8$ = proportionality constant and $r^4/\eta L$ = conductance.

When applied to the cardiovascular system, this equation gives the formula:

Mean Arterial Pressure = Cardiac Output x Total Peripheral Resistance

Cardiac output (CO) and total peripheral resistance (TPR) are the fundamental parameters that determine arterial pressure. The blood pressure and CO are measured, whilst TPR is calculated by dividing mean arterial pressure by CO. CO,

which is the minute output of blood from the heart, is dependent on the heart rate and stroke volume. TPR is the sum of the resistance of all peripheral vasculature in the systemic circulation. Total peripheral conductance (TPC), which is reciprocal of TPR, is the blood flow normalised to MAP in all peripheral vasculature. Determination of CO and TPR in a hypertensive model allows characterisation of the haemodynamic profile of the increase in blood pressure and thus, contributes to better understanding of the pathogenesis of hypertension in that model.

In Chapters 3 and 4, rats underwent surgical procedures that enabled measurements of haemodynamic parameters. In the central haemodynamic experiments, the mean arterial pressure (described in Section 2.5.2), heart rate (described in Section 2.6.2) and cardiac output were measured. In the regional haemodynamic experiments, the mean arterial pressure, and blood flow measurement of the left renal, left common iliac and anterior mesenteric arteries were measured.

2.8.3.2 Principles of ultrasonic transit-time flowmetry

Haemodynamic parameters were measured using an electronic flow detection unit or flowmeter (Transonic T106 Small Animal Blood Flowmeter, Transonic System Inc., Ithaca, USA) with enhanced frequency resolution and volume flow-sensing probes (Transonic 3SS and 1RB perivascular probes, Transonic System Inc., Ithaca, USA). This system uses an ultrasonic transit-time principle to sense blood

flow in vessels positioned within the flow probe acoustic-sensing window, independent of flow velocity profile, turbulence and haematocrit.

The flow probe consists of 2 ultrasonic transducers, which act as both transmitters and receivers for the ultrasonic beam, within the flow-sensor body and a fixed acoustic reflector (Figure 2.7). An ultrasonic wave transmitted from transducer 1 intersects the vessel, is reflected off the acoustic probe reflector, again intersects the vessel in the reverse direction and is received by transducer 2 (Figure 2.7). The flowmeter accurately measures the transit time which is the time taken for the ultrasonic signals to travel from one transducer to the other.

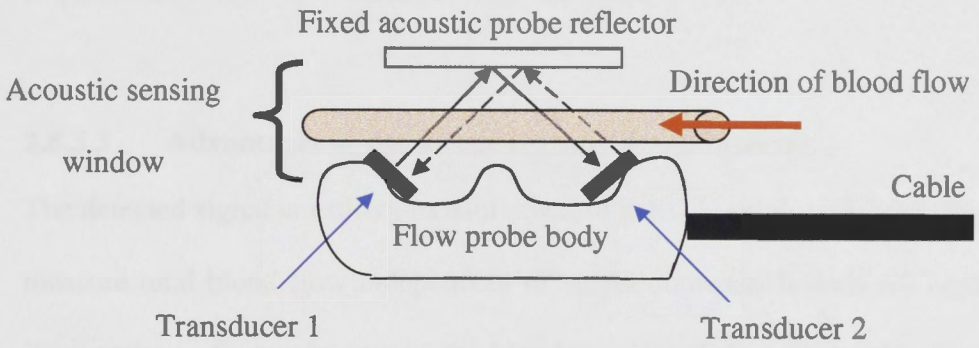

Figure 2.7: Basic structural components of aTransonic perivascular ultrasonic volume flow-sensing probe. ——► upstream transit-time cycle, - - -► downstream transit-time cycle.

Ultrasonic signals travelling back and forth alternately traverse the flowing blood in the upstream and downstream directions. During the upstream transit-time

measurement cycle, the ultrasonic signal travels against blood flow. This results in an increase in transit time by a factor dependent on blood flow. The downstream transit-time measurement cycle, where the ultrasonic signal travels with blood flow, is associated with a reduction in transit time by the same magnitude as during the upstream cycle. The difference in integrated transit times between the upstream and downstream cycles is a measure of volume flow rather than velocity (Drost 1978).

The flowmeter automatically detects the scaling and individual calibration factors of flow probe attached to it. It is also attached to an external data acquisition device (PowerLab® data acquisition system). Prior to each recording, the data acquisition device was calibrated to the flowmeter.

2.8.3.3 Advantages of ultrasonic transit-time flowmetry

The detected signal is a direct measurement of net volume flow. Ultrasonic probes measure total blood flow independent of vessel diameter. It does not require the flow probe to fit snugly around the blood vessel and thus, is suitable for vessels smaller than the acoustic window. This is because ultrasonic beams that do not intersect the vessels do not contribute to the volume flow integral. This technique does not require zero calibration and it is, therefore, not subjected to offset and zero adjustment inaccuracies. It is also not affected by vessel-probe alignment, haematocrit and flow turbulence.

2.8.3.4 Disadvantages of ultrasonic transit-time flowmetry

Acoustic couplant or gel is required to fill the area within the acoustic window completely in acute study. Presence of gas bubbles within this space will affect the transmitted signals. Another disadvantage is the need to perform surgical implantation of flow-sensing probe.

2.8.3.5 Initial preparation

Once anaesthesia had been achieved, the rat was placed on a heating pad (surface temperature 38-40 °C) in a dorsally recumbent position. The rat was given maintenance intravenous fluid replacement (0.9 % NaCl) via a tail vein intravenous cannula (24 G Optiva IV catheter, Medex Medical Ltd, Haslingden, Great Britain) using a micro-processor controlled syringe pump (Model 22; Harvard Apparatus Ltd., South Natick, USA) at a rate of 1 mL/hour. All surgical procedures were performed using a stereomicroscope (Leica MZ7$_5$, Leica Microscopy Systems Ltd, Heerbrugg, Switzerland).

The ventral aspect of the neck was shaved with an electric clipper. The left common carotid artery was cannulated for direct blood pressure and heart rate measurements, as described in Sections 2.5.2 and 2.6.2, respectively.

2.8.3.6 Cardiac output measurement

Cardiac output (CO) was measured using the Transonic 3SS perivascular probe. This probe was connected to the flowmeter that had been connected to the PowerLab® data acquisition system. Cardiac measurements were recorded by the computer using the Chart™ 5 software.

Mechanical ventilation: With measurement of cardiac haemodynamics, the rat was mechanically-ventilated using a small animal ventilator (Harvard Apparatus Ltd., South Natick, USA) via a tracheal cannula. The trachea was visible through the ventral midline neck incision made for left common carotid cannulation procedure. The adherent connective tissue was dissected away using a blunt curved forceps. The ventral aspect of the 3rd intercartilage space was incised. Haemostasis was achieved using a cautery. A tracheal cannula with Luer adapter (Harvard Apparatus, Holliston, USA) was inserted into the trachea, secured and connected to the ventilator. The respiratory rate was set to 80 breaths per minute. Supplemental oxygen (2 mL/min) was administered to the rat via the ventilator.

Cardiac output measurement: Bilateral thoracotomy was performed to expose the heart and aorta. The pericardium was opened and ascending aorta was isolated by blunt dissection. The 3SS perivascular probe was positioned around the ascending aorta. Acoustic gel (SurgiLube; W. Fougera & Co, Melville, USA) was deposited into the acoustic window of the probe adjacent to the artery to replace the air space.

After at least 20 minutes stabilisation, cardiac output measurements were recorded at 1 min intervals for 10 min. These values were then averaged.

2.8.3.7 Regional blood flow measurements

Regional blood flow was measured using the Transonic 1RB perivascular probe (Transonic System Inc., Ithaca, USA) connected to the same blood flow meter. Data acquisition was as described in cardiac output measurement.

Midline laparotomy was performed in anaethesised rats. The intestines were gently deflected to expose the left kidney. The left renal artery, found posterior to the larger renal vein, was carefully located and dissected. The 1RB perivascular probe was then placed around the artery. The left common iliac artery blood flow was used as a marker of hindquarter blood flow. The iliac artery, immediately below the bifurcation of the terminal abdominal aorta, was located and gently dissected before placing the 1RB perivascular probe around it. For mesenteric blood flow measurement, the anterior mesenteric artery was gently dissected to allow the placement of the 1RB perivascular probe. Acoustic gel was deposited into the acoustic window of the probe next to the artery, replacing the air space. All the blood flow measurements were recorded after at least 20 minutes stabilisation.

2.8.4 Sacrifice and blood collection procedures

In the haemodynamic studies (Chapters 3 and 4), rats were sacrificed after the haemodynamic experiments. In the other studies, (Chapters 5-9), the rats were sacrificed once general anaesthesia had been attained. Bilateral thoracotomy was performed (if not already done for other experiments e.g. cardiac output

measurements) to expose the heart. The pericardial sac was dissected away. All the rats were sacrificed via exsanguination. This was performed by right ventricular puncture using an 18 gauge needle and a 10 mL syringe. Blood was aspirated slowly to prevent haemolysis. Approximately 6-8 mL of blood could be collected from each rat.

Blood was collected into different tubes, depending on the assays required for the different studies. This is discussed in Section 2.9.

2.8.5 Organ weight determination

2.8.5.1 Thymus gland

The thymus gland was gently dissected away from the adjacent structures using blunt forceps. It was placed on an absorbent paper to move excess blood and moisture before being weighed using an electronic balance (Sartorius Analytical, Goettingen, Germany). The weight was expressed as mg/100 g body weight.

2.8.5.2 Adrenal glands

The adrenal glands were located and removed via a median laparotomy incision. Using a pair of blunt curved forceps, the adherent connective tissue was dissected away. Blood and excess moisture were removed using an absorbent paper. The weights of these glands, obtained using an electronic balance, were averaged and expressed as mg/100 g body weight.

2.9 HAEMATOCRIT ESTIMATION

Blood was collected into heparinised capillary tubes and centrifuged. Haematocrit was measured using a micro-haematocrit reader (Hawksley and Sons Ltd., Sussex, England). Data were expressed as percentage of red blood cells per total volume of blood.

2.10 BIOCHEMICAL ASSAYS

2.10.1 Plasma nitrite and nitrate assay

2.10.1.1 Principles

Determination of NO is difficult due to its short half life and its highly reactive nature (Knowles and Moncada 1994). Therefore, measurement of nitrite and nitrate (NOx), which are stable end products of NO, in plasma is often used as an indicator of total body NO production. Quantitating nitrite alone is inadequate as nitrite in whole blood is rapidly oxidised to nitrate by haemoglobin prior to plasma preparation. Hence, both nitrite and nitrate have to be measured.

Nitrate is measured as nitrite after enzymatic reduction by nitrate reductase. Nitrite is measured by the Griess colorimetric reaction. The optical density is measured using a microplate reader at a wavelength of 540 nm.

2.10.1.2 Materials

This assay was performed using reagents provided in a commercially available kit (Endogen, Pierce, Rockford, IL, USA). The kit consisted of the following reagents:

10x Reagent diluent. This is a Hepes based buffer containing detergent and preservatives. One in 10 dilution was performed using deionised water to give 1x reagent diluent.

Nitrate reductase diluent. This is a phosphate based buffer containing preservatives.

Nitrate reductase. This lyophilised enzyme was reconstituted by adding 1 mL nitrate reductase diluent into the given vial. One in 2.5 dilution was performed on the reconstituted nitrate reductase concentrate. The diluted enzyme was used directly in the assay.

Reduced β-nicotinamide adenine dinucleotide (NADH). This lyophilised reagent was reconstituted by adding 1 mL deionised water into the given vial. Prior to use, 1 in 2 dilution was performed using deionised water.

Nitrite standard. This is a solution of sodium nitrite at 2000 μM in water with preservatives.

Nitrate standard. This is a solution of sodium nitrate at 1000 μM in water with preservatives.

Griess reagent I. This is a solution of sulphanilamide in 2 M hydrochloric acid.

Griess reagent II. This is a solution of N-(1-Naphthyl) ethylenediamine in 2 M hydrochloric acid.

2.10.1.3 Sample preparation

Briefly, blood was collected into tubes (BD Vacutainer, Franklin Lakes, USA) containing 3.2 % buffered sodium citrate (0.109 M). Plasma was prepared by centrifuging the blood tubes at 3500 rpm (relative centrifugal force 2465 G) for 15 min at 4 °C. Plasma was stored at -70°C until assayed.

Plasma samples were thawed immediately prior to use. These were spun for 5 minutes at 13000 rpm at 4 °C. Approximately 300 μL of the sample's plasma was aliquoted into ultrafiltration tubes (Ultraforce-MC 30 000 NMWL filter unit, Millipore Corp., Bedford, USA) and spun for 25 minutes at 13 000 rpm at 4 °C. The filtrate was used directly in the assay.

2.10.1.4 Procedures

Standard curves for both nitrite and nitrate were constructed. Nitrite standards were prepared by sequential dilutions of 2000 μM stock nitrite solution with a

Hepes-based buffer containing detergent and preservatives (1x reagent diluent) to give the following concentrations: 200, 100, 50, 25, 12.5, 6.25 and 3.125 μM. Nitrate standards were prepared by sequential dilutions of 1000 μM stock nitrate with 1x reagent diluent to give the following concentrtions: 100, 50, 25, 12.5, 6.25 and 3.125 μM. Plain 1x reagent diluent was used as a zero standard. 200 μL of 1x reagent diluent was pipetted into duplicate blank wells.

Nitrate Assay Procedures: The nitrate standards (50 μL), controls *ie.* unspiked and spiked (20μM nitrate) pooled plasma (25 μL each) and ultrafiltered plasma samples (25 μL) were pipetted into the wells of a 96-well plate (NUNC Brand Products, Roskilde, Denmark). The controls and plasma samples were further diluted with 25 μL 1x reagent diluent.

Diluted NADH (25 μL) was added to the standard and sample wells. Following this, 25 μL of diluted nitrate reductase was added to the standard and sample wells (except the blank wells).

The plate was then incubated at 37 °C for 30 minutes before Griess Reagents I and II (50 μL each) were added to the standard and sample wells (except the blank wells).

Nitrite Assay Procedure: Similarly, the nitrite standards (50 μL), controls *ie.* unspiked and spiked (20μM nitrate) pooled plasma (25 μL each) and ultrafiltered

plasma samples (25 µL) were pipetted into the wells of a 96-well plate. The controls and plasma samples were further diluted with 25 µL 1x reagent diluent.

Instead of NADH and nitrate reductase enzyme, 50 µL 1x reagent diluent was added to the standard and sample wells (except the blank wells).

The plate was also incubated at 37 °C for 30 minutes before Griess Reagents I and II (50 µL each) were added to the standard and sample wells (except the blank wells).

Both nitrate and nitrite assay plates were incubated for another 10 minutes at room temperature (22- 25 °C) to allow the colour to develop. Absorbances for each well were read at 540 ± 20 nm after blanking against the blank wells using a microplate reader (THERMOmax Microplate Reader, Molecular Devices, California, USA).

2.10.1.5 Performance

Linearity: The standard curves for nitrate and nitrite constructed as per the method described in Section 2.9.1.4 had a correlation coefficient of 1.00 each.

Precision: Spiked (with 20 µM nitrate) and unspiked pooled rat plasma samples were run multiple times in the same assay to determine the intra-assay precision. The mean, standard deviation (SD) and the precision numbers which represent the

percent coefficient of variance (% CV) for the concentrations of nitrate determined in the assay are summarised in Table 2.2 below.

Table 2.2: Assay precision

Quality Controls	Mean	SD	% CV
Unspiked plasma	16.9	0.09	5.2
Plasma + 20 μM nitrate	38.03	1.74	4.6

CV: coefficient of variance; SD: Standard deviation.

2.10.1.6 Analysis

The net optical density for the standards and samples were calculated by subtracting the average zero standard optical density from the optical density for each standard and sample. The average optical densities for each standard versus nitrate and nitrite concentrations were plotted. The optical densities for each sample were then plotted on the standard curves. Total nitrate and nitrite concentrations can be extrapolated from these graphs.

2.10.2 Serum uric acid assay

2.10.2.1 Principle

The uric acid assay was based on the method described by Trivedi (Trivedi, Rebar *et al.* 1978). Oxidation of uric acid to allantoin by uricase leads to the production of hydrogen peroxide. In the presence of peroxidase, the reaction of hydrogen

peroxide with 4-aminoantipyrine and 2, 4, 6-tribromo-3-hydroxybenzoic acid forms a quinoneimine dye. The change in absorbance at 548 nm is proportional to the uric acid concentration in the sample.

2.10.2.2 Materials and procedures

The serum uric acid assay was performed by ACT Pathology at The Canberra Hospital. This laboratory is accredited by NATA.

This assay was performed on the ARCHITECT® c8000 (Abbot Laboratories, Abbott Park, USA) automated assay system using reagents provided in a commercially available kit (Abbott Clinical Chemistry, Abbott Park, USA) consisting of a single reagent solution. The active ingredients of the solution are 4-aminoantipyrine (0.5 mmol/L), 2, 4, 6-tribromo-3-hydroxybenzoic acid (1.75 mmol/L), uricase (> 120 U/L), peroxidase (> 500 U/L) and TRIS buffer 50 mmol/L.

2.10.2.3 Sample preparation

Blood was collected into serum tubes (BD Vacutainer, Franklin Lakes, USA). Blood was allowed to clot for at least 1 hour and serum was prepared by centrifuging the blood tubes at 3500 rpm (relative centrifugal force 2465 G) for 15 min at 4 °C. Serum was stored at -70 °C until assayed.

2.10.3 Urinary sodium and potassium

2.10.3.1 Principle

Ion-selective electrodes for sodium and potassium use membranes selective to each of these ions. Voltage or electrical potential that is generated across the membranes between the reference and measuring electrodes (in accordance with the Nernst equation) is compared to previously determined voltages and thus, converted into ion concentration.

2.10.3.2 Materials and procedures

The urinary sodium and potassium assays were performed by ACT Pathology at The Canberra Hospital using the ICT Na^+, K^+, Cl^- reagent kit on the ARCHITECT® c8000 (Abbot Laboratories, Abbott Park, USA) automated assay system.

2.10.3.3 Sample preparation

Urine was collected using the metabolic cages as described in Section 2.7.4 and kept at -70 °C until assayed.

2.10.4 Urinary creatinine assay

2.10.4.1 Principle

Creatinine in the urine reacts with picrate to form a creatinine-picrate complex at an alkaline pH. The rate of increase in absorbance at 500 nm due to the formation

of creatinine-picrate complex is directly proportional to the concentration of creatinine in the urine sample.

2.10.4.2 Materials and procedures

This assay was performed by ACT Pathology at The Canberra Hospital using a two-reagent kit consisting of sodium hydroxide (0.25 mol/L) and picric acid (20.5 mmol/L) on an automated assay system (ARCHITECT® c8000, Abbot Laboratories, Abbott Park, USA).

2.10.4.3 Sample preparation

Urine was collected using the metabolic cages as described in Section 2.7.4 and kept at -70 °C until assayed.

2.11 DETECTION OF REACTIVE OXYGEN SPECIES

2.11.1 Lucigenin-enhanced chemiluminescence assay

2.11.1.1 Principle

Lucigenin-enhanced chemiluminescence was used to determine superoxide production in rat aortic segments resected following sacrifice. The reaction of lucigenin (bis-*N*-methylacridinium nitrate) with superoxide in its cationic state through a series of reactions resulted in the formation of an unstable dioxetane compound that emits a photon as it decomposes. This can be detected in the scintillation/luminescence counter.

2.11.1.2 Materials

All solutions were prepared fresh prior to each assay. All chemicals were purchased from Sigma-Aldrich (St Louis, MO, USA).

Hepes-buffered Krebs solution. This solution consists of 100 mM NaCl, 5 mM KCl, 1 mM $MgSO_4$, 2 mM K_2HPO_4, 25 mM $NaHCO_3$, 11 mM glucose, 20 mM Na-Hepes and 2 mM $CaCl_2$, pH 7.4.

NAD(P)H solution. This is a solution of NAD(P)H at 1 mM in Hepes-buffered Krebs solution. It is stored away from light at 4 °C.

Sodium diethyldithiocarbamate (DETC). This is a solution of DETC at 1 M in warm (37 °C) Hepes-buffered Krebs solution.

Lucigenin solution. This is a solution of lucigenin at 500 μM in warm (37 °C) Hepes-buffered Krebs solution. It is kept away from light.

Incubation solution. This is a solution of DETC at 13.5 mM and NAD(P)H at 0.1 mM in Hepes-buffered Krebs solution.

Assay solution. This is a solution of NAD(P)H at 0.1 mM in Hepes-buffered Krebs solution.

2.11.1.3 Sample preparation

After sacrificing the rat, a 1-2 cm segment of the thoracic aorta was resected. The aortic segment was washed in saline solution and the adherent connective tissue was carefully dissected. It was bisected and kept on ice in Hepes-buffered Krebs solution until it was ready to be incubated.

2.11.1.4 Procedures

All the aortic segments were incubated for 30 minutes at 37 °C in incubation solution. NAD(P)H was added to activate NAD(P)H oxidase, the main source of superoxide In the vasculature. The superoxide dismutase inhibitor diethylthiocarbamate (DETC) was used to prevent dismutation of existing superoxide. After incubation, the aortic segments were placed in individual wells of a black 96-well plate containing the assay solution. Lucigenin was added to the wells prior to analysis to give a final concentration of 5 μM.

The plates were read in a scintillation detector (TopCount NXT Microplate Scintillation & Luminescence Counter, PerkinElmer, Woodbridge, Canada). Twelve successive readings were recorded.

The aortic segments were dried at 60 °C for 1-2 days and the dry weight of each segment was recorded.

2.11.1.5Analysis

The first 2 and the last 2 readings from the blank and sample wells were excluded and the mean luminescence, expressed as counts per second (counts/s), was calculated. The mean values from the blank wells were subtracted from the sample wells. The net results were then adjusted to aortic weight by dividing the net luminescence by dry weight of the corresponding aortic tissue and expressed as counts per second per mg of dry wt (counts/s/mg).

2.11.2 Kidney mitochondrial superoxide analysis

The method for this assay is described in Chapter 5.

2.11.3 F_2-isoprostane concentration

2.11.3.1 Principle

The F_2-isoprostane family is a group of chemically stable prostaglandin F_2-like compounds generated during peroxidation of unsaturated fatty acids in membrane phospholipids, namely arachidonic acid. They have been shown to be reliable markers of lipid peroxidation and oxidative stress *in vivo*. (Morrow, Hill *et al.* 1990; Morrow and Roberts 1996; Patrono and FitzGerald 1997)

2.11.3.2 Sample preparation

Blood was collected into blood tubes (BD Vacutainer, Franklin Lakes, USA) containing 5.4 mg K_2EDTA and 2 mg glutathione. Plasma was prepared by centrifuging the blood tubes at 3500 rpm (relative centrifugal force 2465 G) for 15

min at 4 °C. Butylated hydroxyltoluene was added to plasma samples (final concentration 0.2 mg/mL) before being stored at -70 °C until assayed.

2.11.3.3 Procedures

Plasma F_2-isprostane was assayed by Associate Professor Kevin Croft, University of Western Australia using stable isotope dilution capillary gas/ electron capture negative ionization mass spectrometry (Mori, Croft *et al.* 1999).

2.12 STATISTICAL ANALYSIS AND DATA PRESENTATION

Results were expressed as mean ± SEM. SBP, body weight, heart rate (Chapter 8), urine volume (Chapter 10) and food and water consumption (Chapter 10) measurements between and within groups were analysed by repeated-measure analysis of variance, with Greenhouse-Geisser adjustment for multisample asphericity. Comparisons between groups for thymus weight and adrenal weight, haemodynamic parameters, biochemical assay results (plasma NOx, serum urate, plasma F_2-isoprostane), blood glucose level, haematocrit, aortic lucigenin-enhanced chemiluminescence, flow cytometric results and food and water consumption were carried out using unpaired t-tests. To minimise the family-wise type 1 error, the Ryan-Holm stepdown Bonferroni procedure was applied to the raw P values to give P'.

CHAPTER 3

Haemodynamic Profile of Dexamethasone-Induced Hypertension in the Rat

3.1 INTRODUCTION

The haemodynamics of DEX-HT have been evaluated in both humans (Pirpiris, Sudhir *et al.* 1992) and dogs (Nakamoto, Suzuki *et al.* 1991). DEX-HT in humans (3 mg/day) was associated with increased TPR without any change in CO (Pirpiris, Sudhir *et al.* 1992). Whilst these are useful data depicting the haemodynamic patterns of DEX-HT, little is known about the regional flow patterns contributing to the raised TPR. In dogs, DEX-HT (0.5 mg/kg/day) was found to be associated with increased TPR and decreased CO (Nakamoto, Suzuki *et al.* 1991). Whether these changes represent features necessary for the development of DEX-HT has not been previously evaluated. In that study, only CO, TPR and renal blood flow were evaluated leaving other haemodynamic parameters unexamined. Furthermore, the relevance of the dog model of DEX-HT to that in humans remains unclear. For the purpose of examining the mechanisms of GC-HT, the rat is generally more applicable to the human situation (Whitworth, Schyvens *et al.* 2001; Whitworth, Zhang *et al.* 2006).

Haemodynamic profiles of cortisol- and ACTH-HT have been evaluated. Cortisol-induced hypertension (50 mg orally, every 6 hours for 5 days) in man was associated with a rise in CO and renal vascular resistance but no change in calculated TPR (Connell, Whitworth *et al.* 1987). The beta-adrenergic receptor blocker atenolol prevented the increase in CO but not the blood pressure increase in cortisol-hypertensive human subjects (Pirpiris, Yeung *et al.* 1993). ACTH-HT in rats has been shown to be associated with increased CO and renal vascular

resistance (Wen, Fraser *et al.* 1998) In another series of experiments, Wen *et al.* demonstrated that ramipril successfully prevented both ACTH-HT and rise in renal vascular resistance, whereas neither preventing rise in CO nor decreasing TPR altered ACTH-HT in the rat (Wen, Fraser *et al.* 1999). These studies showed that increase in renal vascular resistance is necessary for the development of ACTH-HT. In sheep, ACTH-HT was also associated with increased CO but prevention of CO increase by β-adrenoreceptor blockade did not modify the rise in blood pressure (Graham, Allen *et al.* 1980). Because of the differences between ACTH-HT and DEX-HT described in Chapter 1, inferences cannot be drawn about DEX-HT based on these results in ACTH-HT.

In this study, we evaluated the central and regional haemodynamic profiles of DEX-HT using ultrasonic transit-time flowmetry. This method has been validated for measurement of cardiac output and regional blood flow in rats (Wen, Li *et al.* 1996).

3.2 METHODS

3.2.1 Experimental animals

This study was approved by the Animal Experimentation Ethics Committee of the Australian National University (Protocol No. J.HB.22.06). Forty one male Sprague-Dawley rats (initial body weight of 200-250 g) were housed and acclimatised as described in Sections 2.2 and 2.3 of Chapter 2. Nineteen rats

(sham treatment, n = 9 and DEX, n = 10) were used in the central haemodynamic study and 22 rats (sham treatment, n = 11 and DEX, n = 11) in the regional haemodynamic study. These rats received saline by gavage (0.1 mL/100 g body weight/day, from day P0) and subcutaneous saline (0.2 mL/rat/day) or DEX injections (20 μg/rat/day, s.c.) from day T0-T11.

3.2.2 Blood pressure and body weight measurements

Non-invasive systolic blood pressure (SBP) was measured in conscious rats between 9-11 am on alternate days using the tail-cuff method described in Section 2.5.1. Body weights were measured on alternate days after the tail-cuff SBP measurements.

Direct blood pressure measurements were recorded under pentobarbitone anaesthesia (60 mg/kg, i.p.) on the last day of experiment (T11) where the mean arterial pressure (MAP), systolic and diastolic blood pressures (DBP) and heart rate (HR) were measured using a catheter tip pressure transducer (Mikro-Tip SPR-320; Millar Instruments Inc., Houston, USA) that was inserted into the left carotid artery and advanced to the level of the aortic arch. Surgical approaches for cardiac output and regional flow measurements are described in Section 2.8.3.

3.2.3 Calculation of other haemodynamic parameters

The following formulae were used to calculate the other haemodynamic parameters.

- Cardiac Index (CI) = CO/ 100 g body weight
- Stroke Volume (SV) = CO/HR
- Stroke Index (SI) = CI/HR
- Total peripheral resistance (TPR) = MAP/CO
- Total peripheral conductance (TPC) = 1/TPR
- Regional vascular resistance = MAP/Regional blood flow
- Regional vascular conductance = 1/ Regional vascular resistance

3.2.4 Haematocrit estimation

After the haemodynamic experiments, the animals were sacrificed via exsanguination. Blood was collected for haematocrit estimation as described in Section 2.9 of Chapter 2.

3.2.5 Thymus and adrenal weights

Thymus wet weight, expressed relative to body weight (grams thymus weight per 100 g body weight), was used as a marker of glucocorticoid activity. The surgical technique is described in Section 2.8.5.1 of Chapter 2.

Adrenal wet weight, expressed relative to body weight (grams adrenal weight per 100 g body weight), was used to assess the efficacy of DEX administration. The surgical technique is described in Section 2.8.5.2 of Chapter 2.

3.2.6 Statistical analysis

Results were expressed as mean ± SEM. Statistical analysis were as described in Section 2.12 of Chapter 2.

3.3 RESULTS

3.3.1 Tail-cuff systolic blood pressure

Sham injections with sterile saline did not alter SBP (T0: 126 ± 3, T10: 124 ± 2 mmHg, n = 21). DEX significantly increased SBP from 123 ± 2 on day T0 to 142 ± 2 mmHg on day T10 (n = 20, $P < 0.0005$). In comparison with saline-treated rats (n = 20), SBP in the DEX-treated group (n = 21) was significantly higher ($P < 0.0005$) (Figure 3.1).

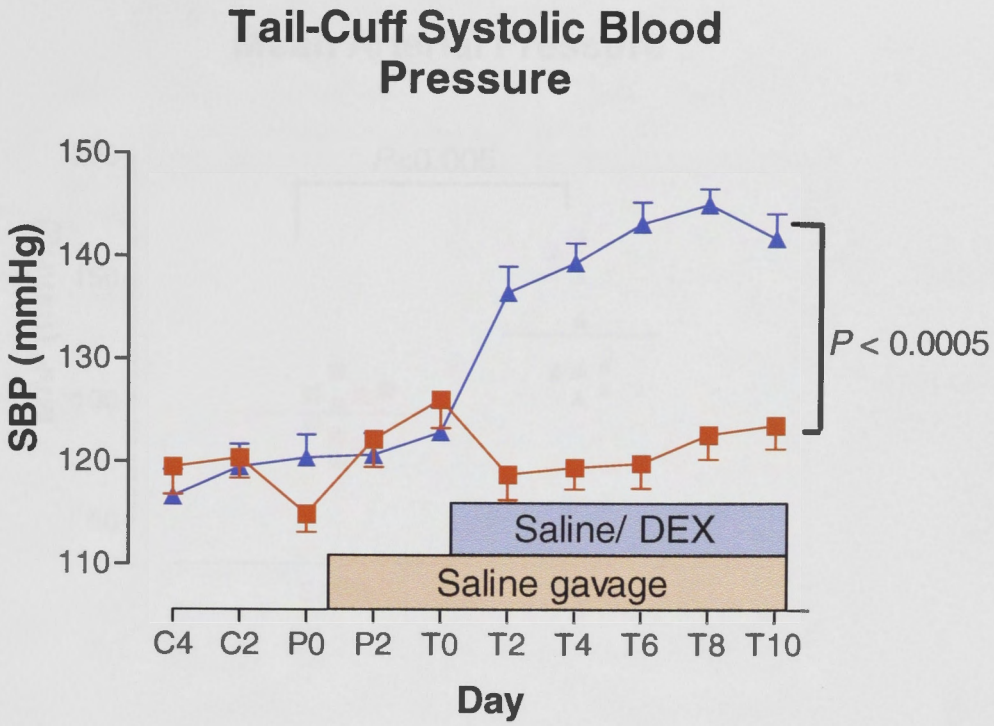

Figure 3.1: Tail-cuff systolic blood pressure. ■ Saline, n = 20; ▲ DEX, n = 21.

3.3.2 Central haemodynamics

DEX-treated rats (n = 10) had significantly higher MAP ($P < 0.005$), systolic and diastolic blood pressure ($P < 0.005$) (Figure 3.2), TPR ($P < 0.05$) and lower TPC ($P < 0.005$) (Figure 3.3) in comparison to the sham treatment group (n = 9). There was no significant difference in HR, CO, CI, SV and SI between DEX (n = 9) and sham (n = 10) treatment groups (Figures 3.4-3.6, Table 3.1).

Mean Arterial Pressure

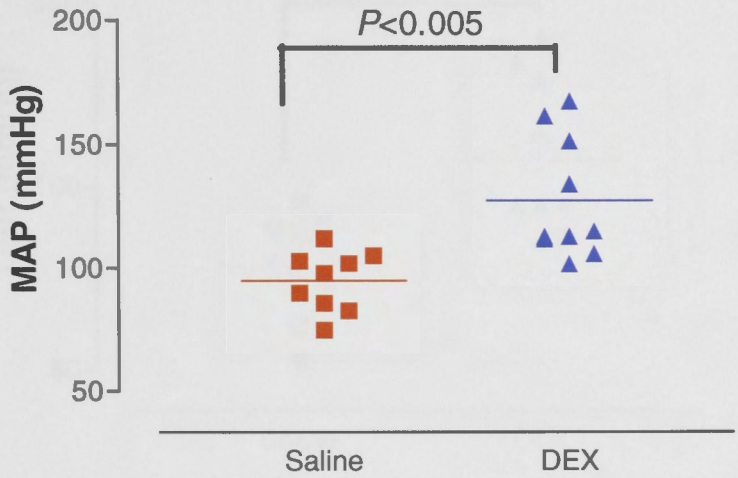

Direct Systolic Blood Pressure

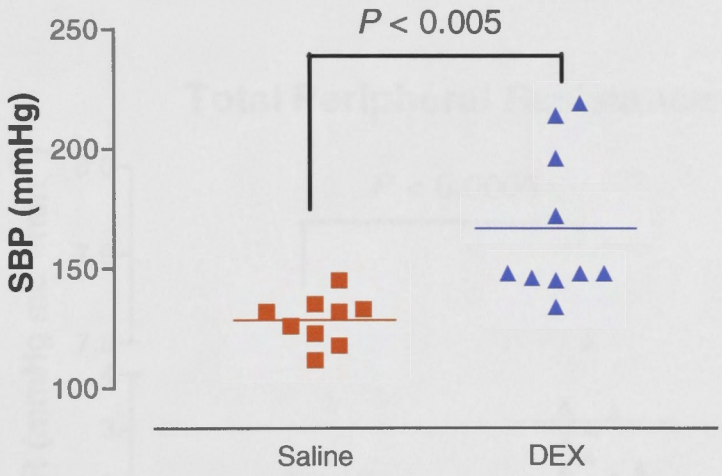

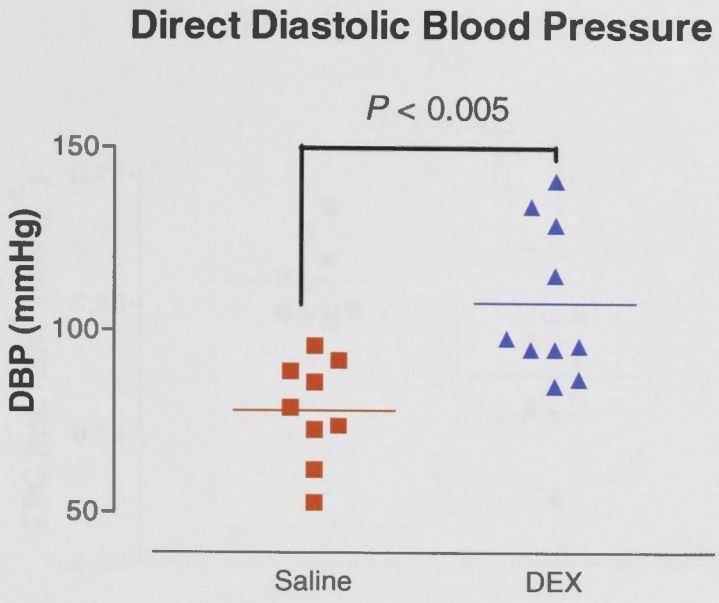

Figure 3.2: Comparisons of blood pressure readings between sham and DEX treatments. ■ Saline, n = 9; ▲ DEX, n = 10.

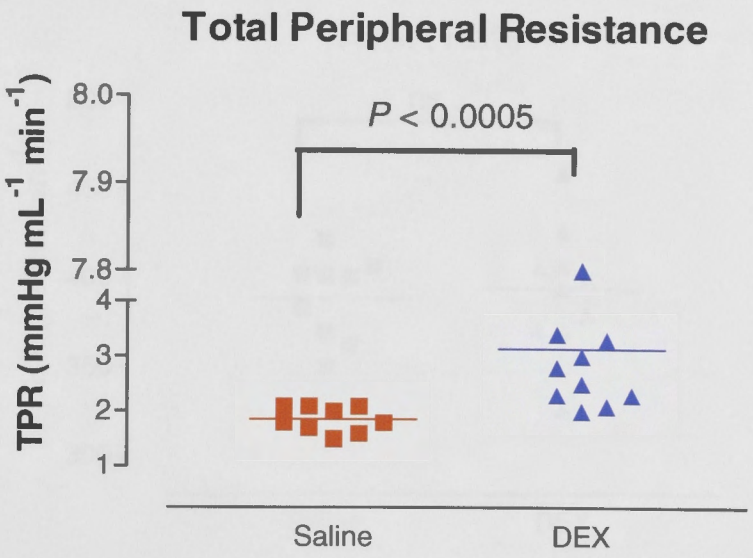

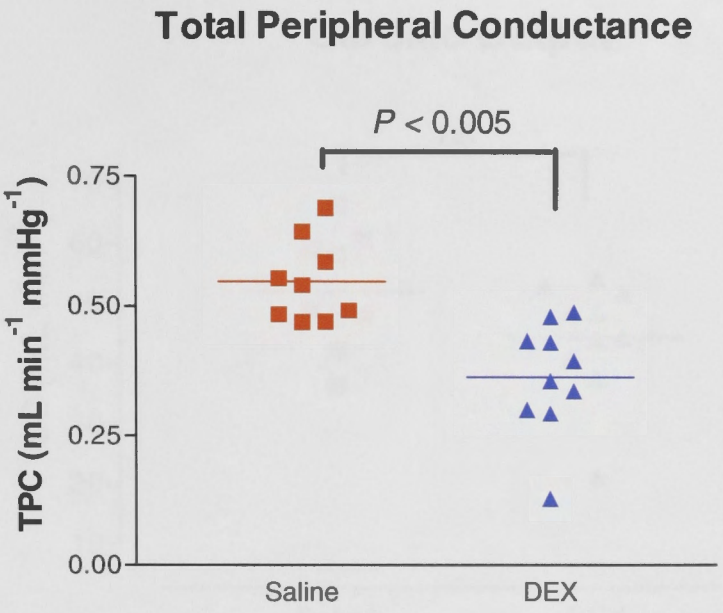

Figure 3.3: Comparisons of total peripheral resistance and total peripheral conductance between sham and DEX treatments. ■ Saline, n = 9; ▲ DEX, n = 10.

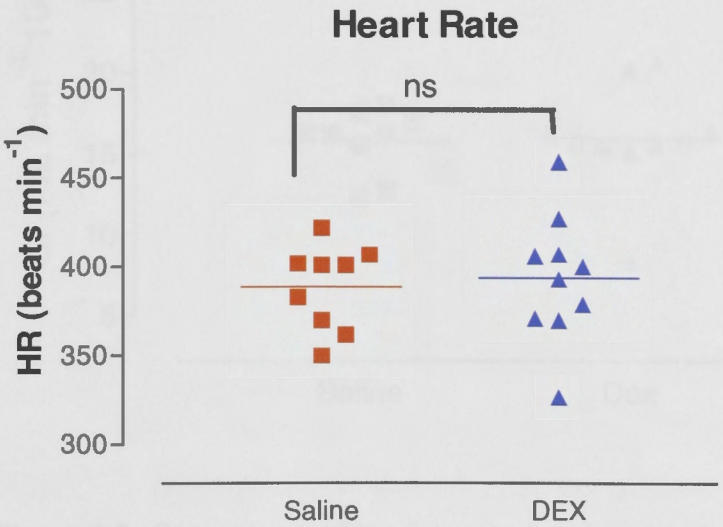

Figure 3.4: Comparisons of heart rate between sham and DEX treatments. ■ Saline, n = 9; ▲ DEX, n = 10.

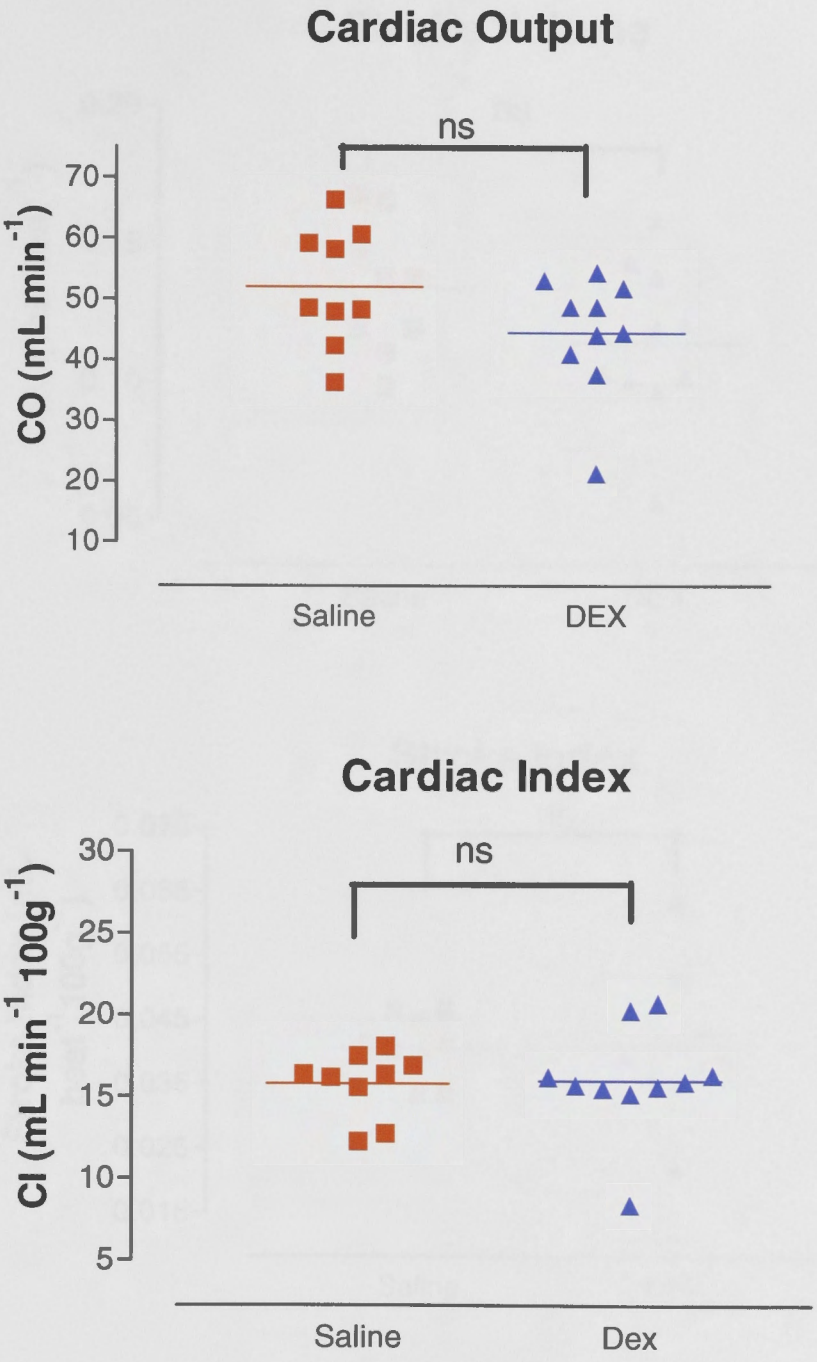

Figure 3.5: Comparisons of cardiac output and cardiac index between sham and DEX treatments. ■ Saline, n = 9; ▲ DEX, n = 10.

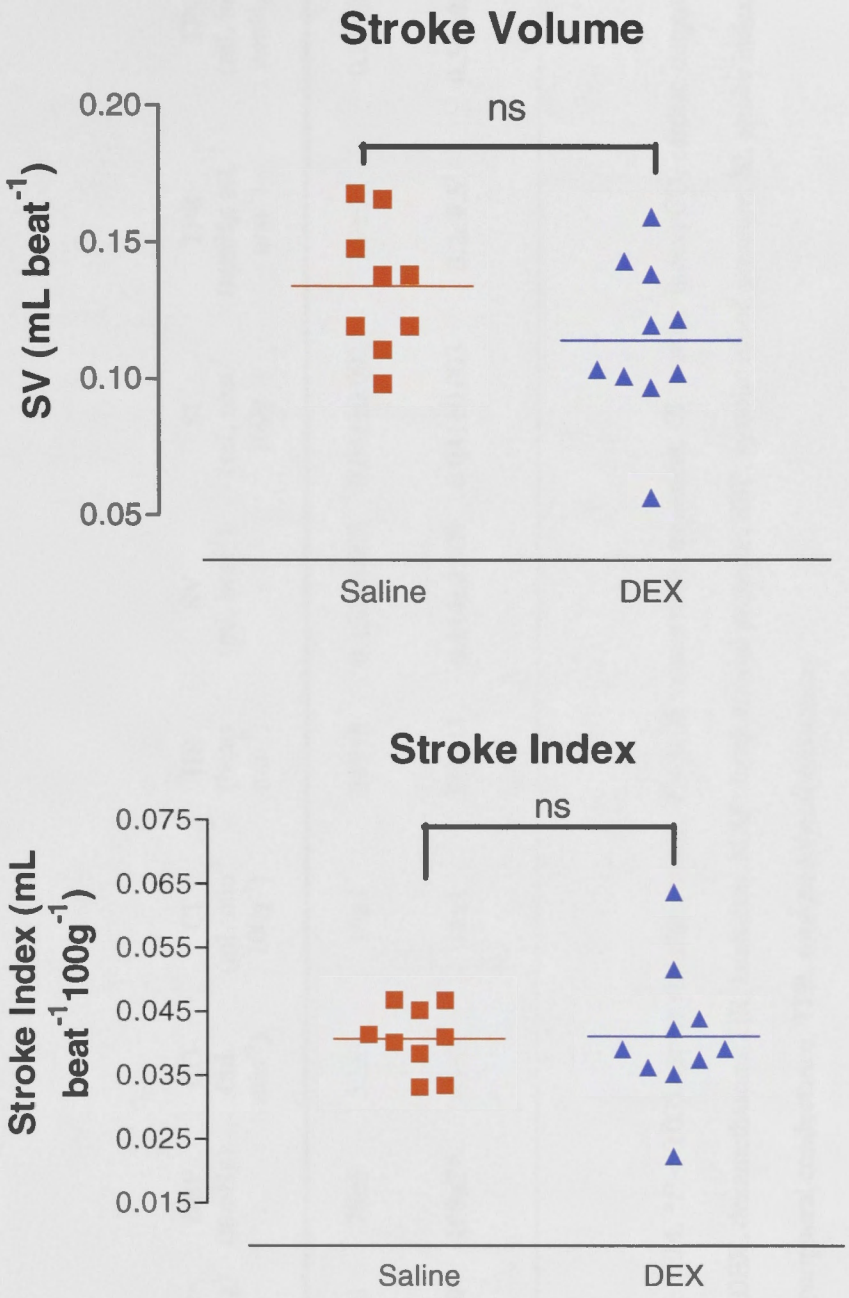

Figure 3.6: Comparisons of stroke volume and stroke index between sham and DEX treatments. ■ Saline, n = 9; ▲ DEX, n = 10.

Table 3.1: Central haemodynamic effects of sham and DEX treatments

Treatment Groups	MAP (mmHg)	SBP (mmHg)	DBP (mmHg)	CO (mL min^{-1})	CI (mL min^{-1} $100g^{-1}$)	HR (beats min^{-1})	SV (mL $beat^{-1}$)	SI (mL $beat^{-1}$ $100g^{-1}$)	TPR (mmHg mL^{-1} min^{-1})	TPC (mL min^{-1} $mmHg^{-1}$)
Sham n = 9	95±4	128±3	78±5	52±3	16±1	389±8	0.134±0.008	0.041±0.002	1.9±0.1	0.55±0.03
DEX n = 10	**127±8***	**167±10***	**108±7***	45±3	16±1	394±11	0.114±0.009	0.041±0.003	**3.2±0.5†**	**0.36±0.03***

Data were expressed as mean ± SEM. *$P < 0.005$ versus sham treatment, †$P < 0.05$ versus sham treatment. CI, cardiac index; CO, cardiac output; DBP, diastolic blood pressure; DEX, dexamethasone; HR, heart rate; MAP, mean arterial pressure; SBP, systolic blood pressure; SI, stroke index; SV, stroke volume; TPC, total peripheral conductance; TPR, total peripheral resistance.

3.3.3 Regional haemodynamics

In comparison with sham treatment (n = 11), DEX treatment (n = 11) increased MAP ($P < 0.05$), SBP ($P < 0.005$) and DBP ($P < 0.05$) (Figure 3.7) but did not significantly change renal, mesenteric or common iliac blood flow, vascular resistance or vascular conductance measurements (Figures 3.8-3.10, Table 3.2).

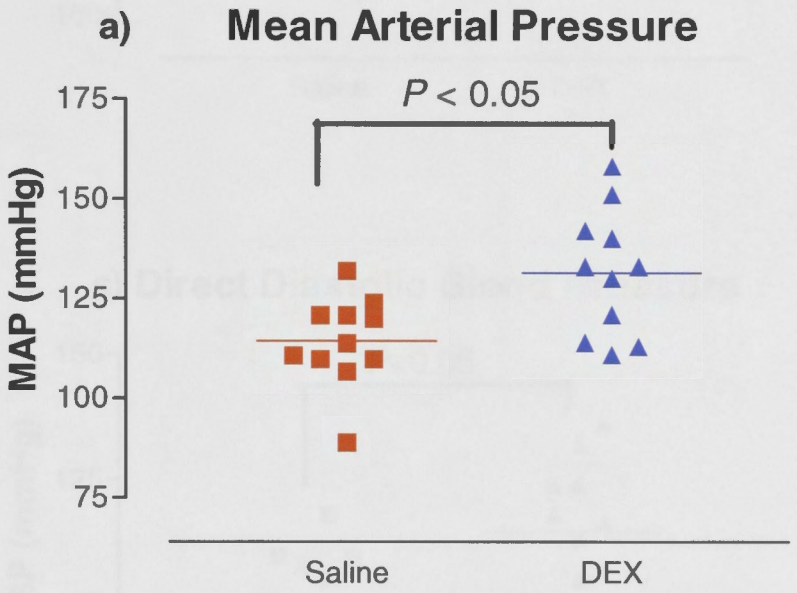

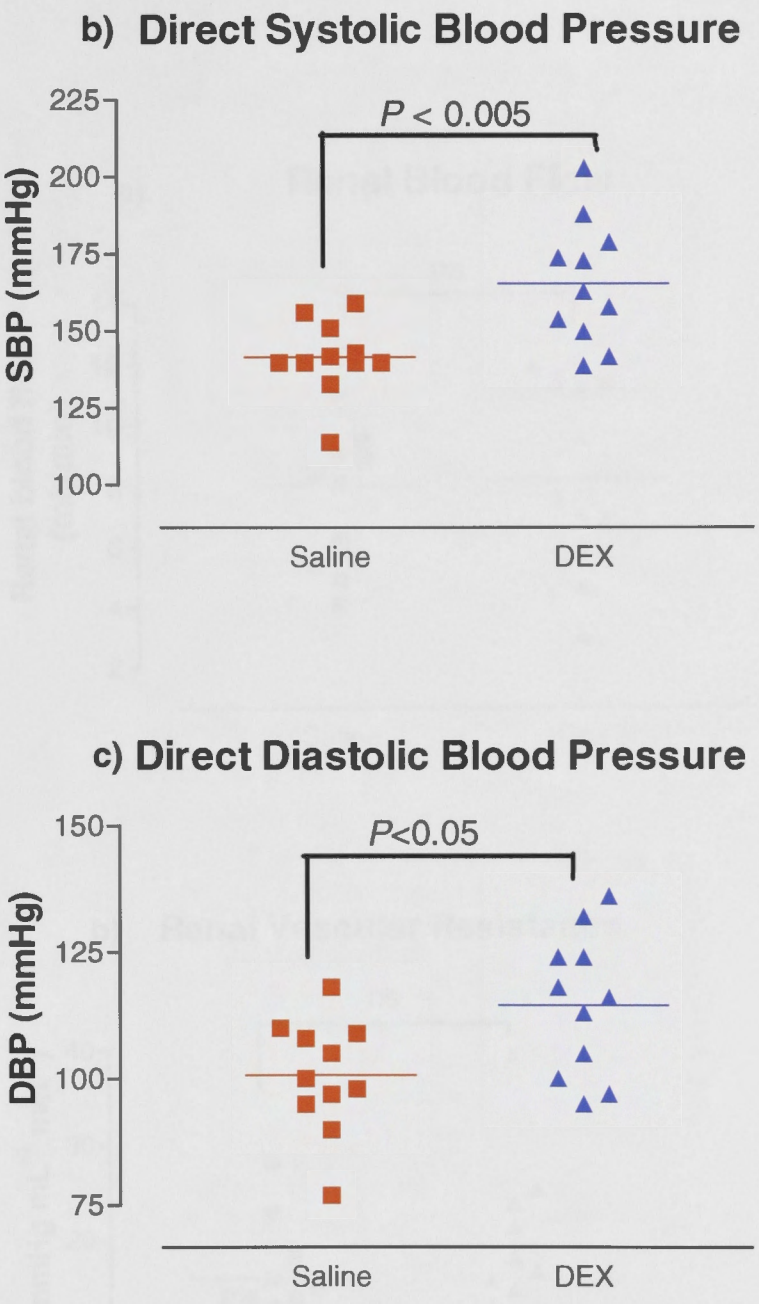

Figure 3.7: Comparisons of blood pressure readings between sham and DEX treatments. ■ Saline, n = 11; ▲ DEX, n = 11.

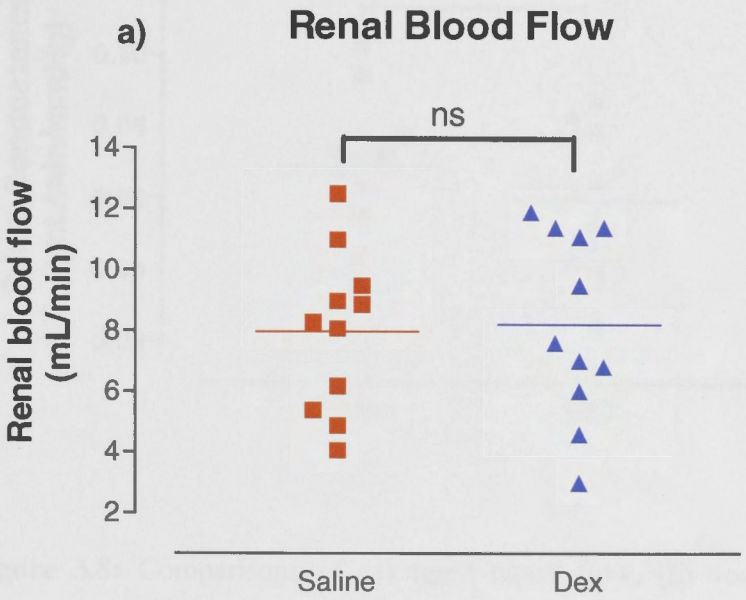
a)
Renal Blood Flow
ns
Renal blood flow (mL/min)
14
12
10
8
6
4
2
Saline
Dex

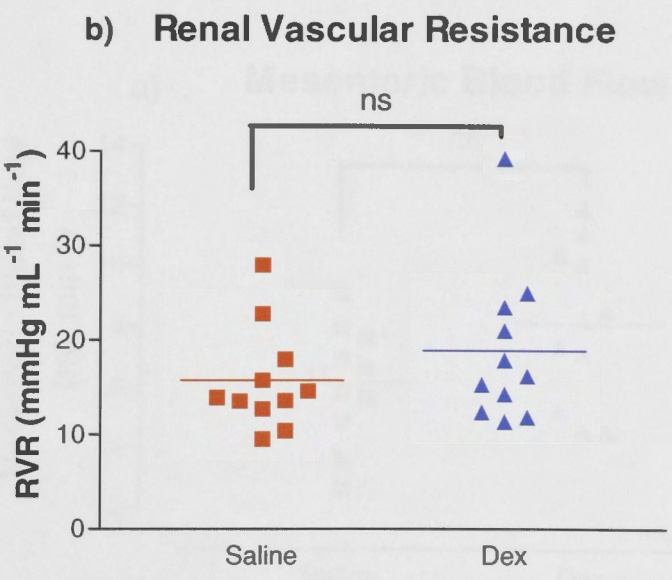
b)
Renal Vascular Resistance
ns
RVR (mmHg mL-1 min-1)
40
30
20
10
0
Saline
Dex

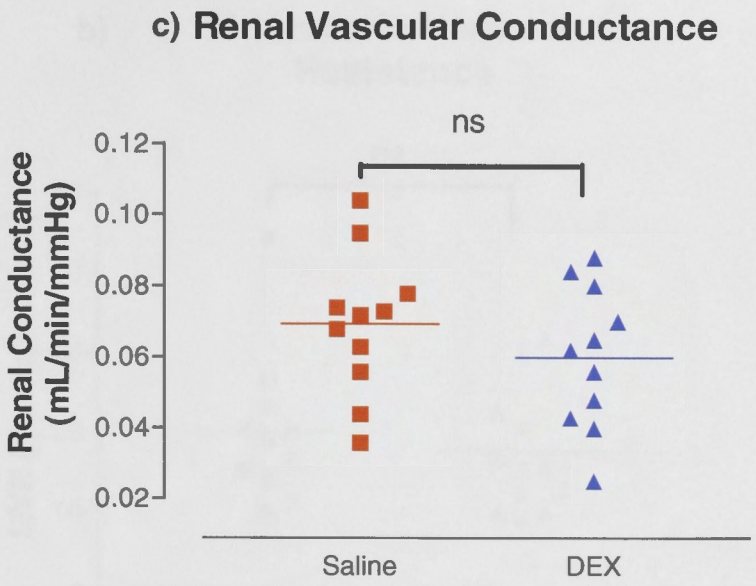

Figure 3.8: Comparisons of **(a)** renal blood flow, **(b)** vascular resistance and **(c)** vascular conductance in saline and DEX treatments. ■ Saline, n = 11; ▲ DEX, n = 11.

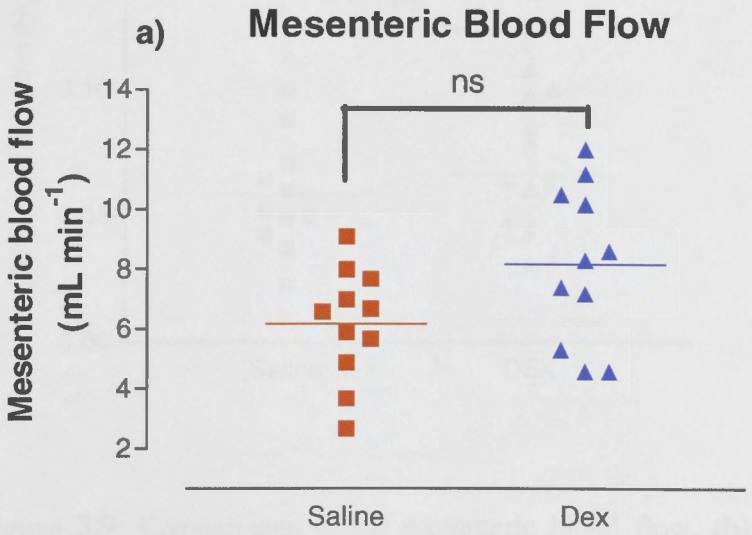

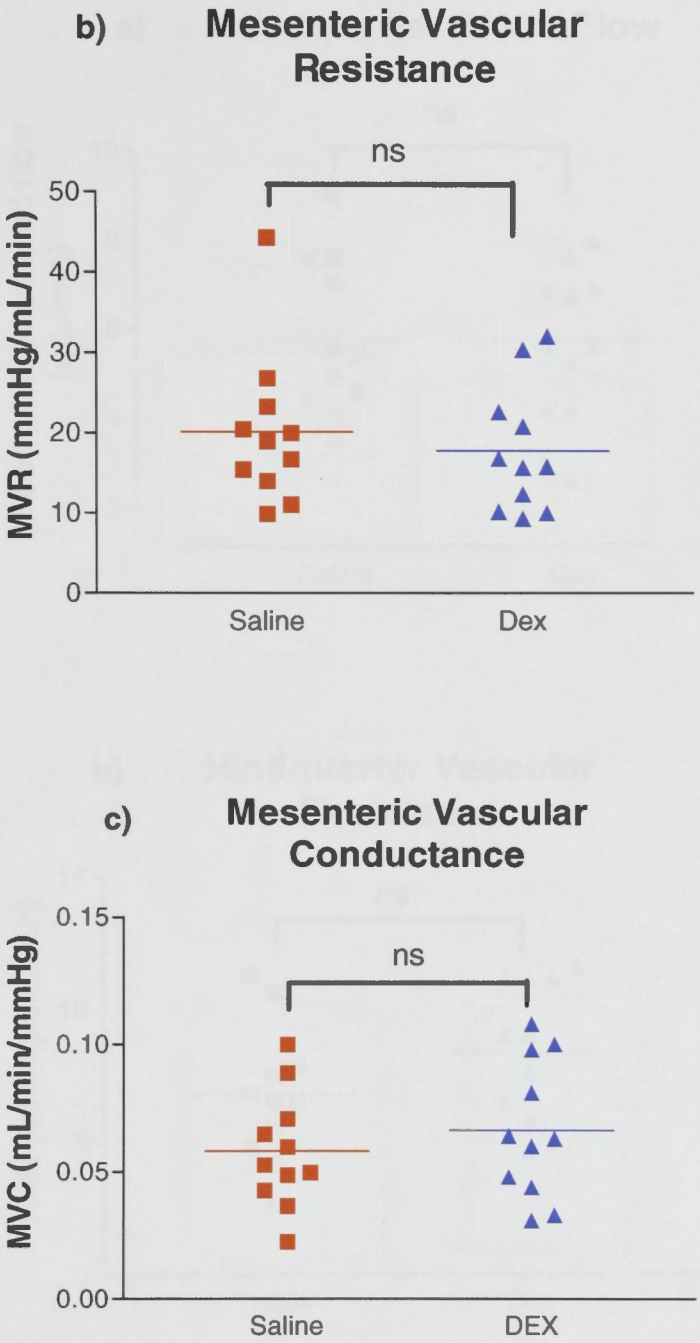

Figure 3.9: Comparisons of **(a)** mesenteric blood flow, **(b)** vascular resistance and **(c)** vascular conductance in saline and DEX treatments. ■ Saline, n = 11; ▲ DEX, n = 11.

a) Hindquarter Blood Flow

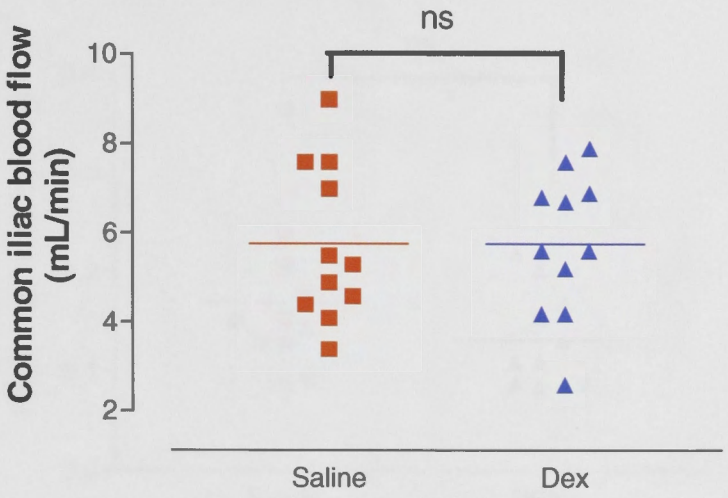

b) Hindquarter Vascular Resistance

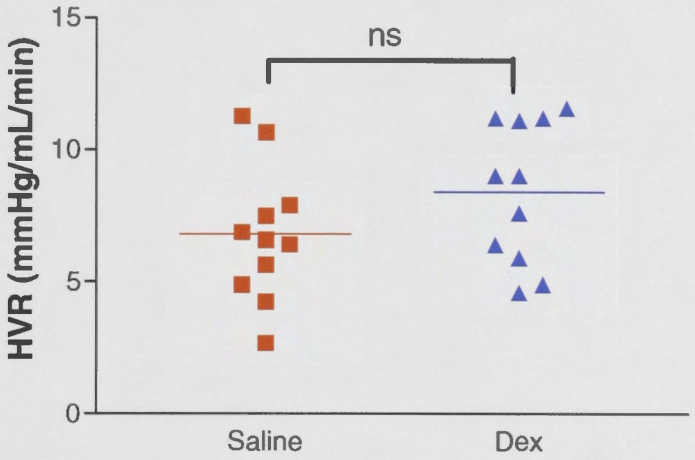

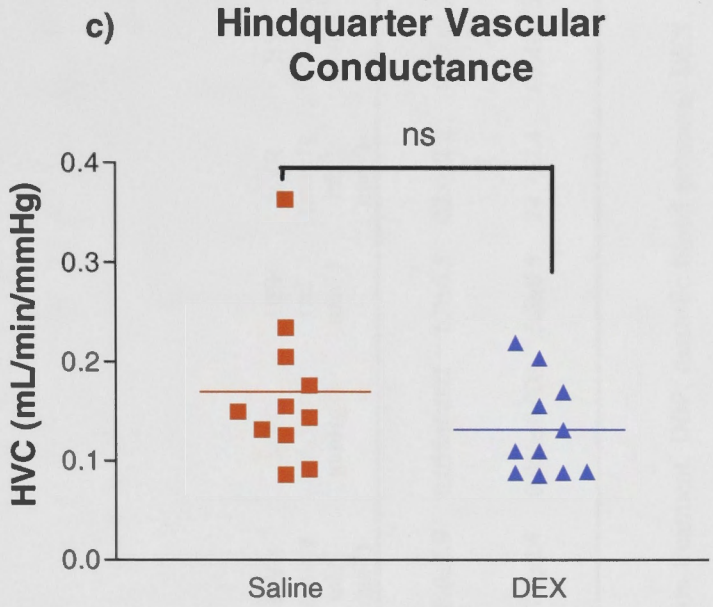

Figure 3.10: Comparisons of hindquarter blood flow, vascular resistance and vascular conductance in saline and DEX treatments. ■ Saline, n = 11; ▲ DEX, n = 11.

Table 3.2: Regional haemodynamic effects of sham and DEX treatments

Treatment Groups	MAP (mmHg)	SBP (mmHg)	DBP (mmHg)	RBF (mL min^{-1})	RVR (mmHg mL^{-1} min^{-1})	RVC (mL min^{-1} $mmHg^{-1}$)	MBF (mL min^{-1})	MVR (mmHg mL^{-1} min^{-1})	MVC (mL min^{-1} $mmHg^{-1}$)	HBF (mL min^{-1})	HVR (mmHg mL^{-1} min^{-1})	HVC (mL min^{-1} $mmHg^{-1}$)
Sham n=11	114±3	142±4	101±4	8.0±0.8	16.0±1.6	0.069±0.006	6.0±0.6	20.0±2.9	0.058±0.007	6.0±0.5	22.0±2.2	0.05±0.01
DEX n=11	**132±5**†	**166±6***	**115±4**†	8.2±0.9	18.9±2.5	0.060±0.006	8.2±0.8	17.8±2.4	0.066±0.008	5.8±0.5	24.7±2.4	0.04±0.04

Data were expressed as mean ± SEM. *$P < 0.005$ versus sham treatment, $^{\dagger}P < 0.05$ versus sham treatment. DBP, diastolic blood pressure; DEX, dexamethasone; HBF, hindquarter blood flow; HVC, hindquarter vascular conductance; HVR, hindquarter vascular resistance; MAP, mean arterial pressure; MBF, mesenteric blood flow; MVC, mesenteric vascular conductance; MVR, mesenteric vascular resistance; RBF, renal blood flow; RVC, renal vascular conductance; RVR, renal vascular resistance; SBP, systolic blood pressure.

3.3.4 Body weight

There was an initial decrease in body weight from 285 ± 4 g on day T0, following the initiation of DEX treatment, to 277 ± 4 g on day T2 ($P < 0.0005$) (Figure 3.11). Subsequently, body weight remained stable at that level throughout the entire treatment period (n = 21). On the other hand, rats on sham treatment gained weight progressively over the entire experimental period from 280 ± 7 g on day T0 to 328 ± 7 g on day T11 (n = 20, $P < 0.0005$).

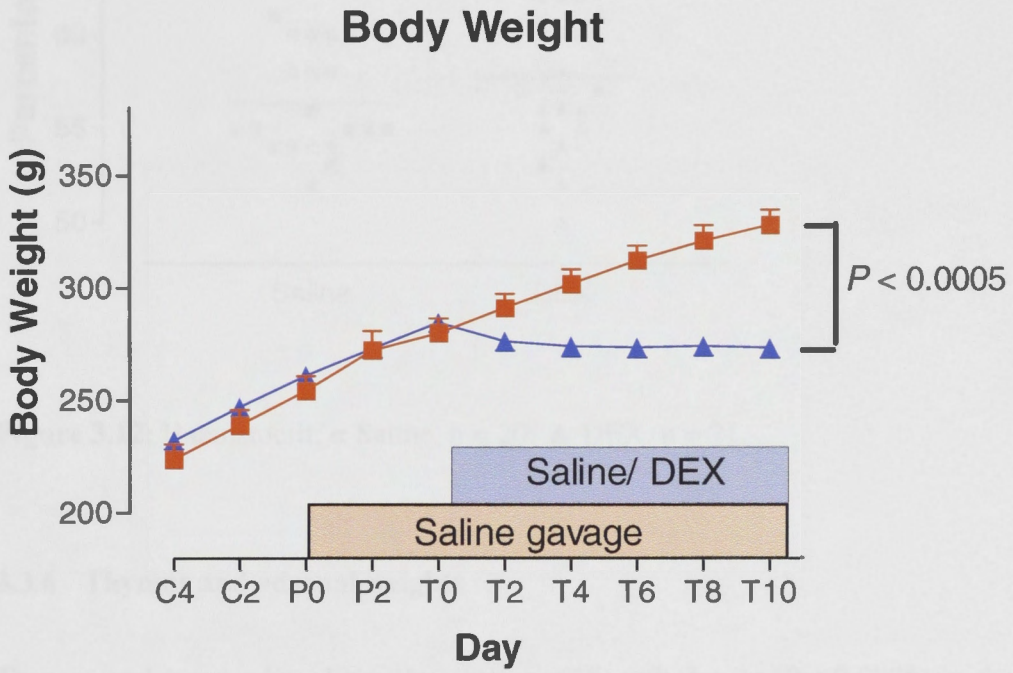

Figure 3.11: Body weight. ■ Saline, n = 20; ▲ DEX, n = 21.

3.3.5 Haematocrit

There was no significant difference in haematocrit between saline (56 ± 1%, n = 20) and DEX-treated rats (58 ± 1%, n = 21) (Figure 3.12).

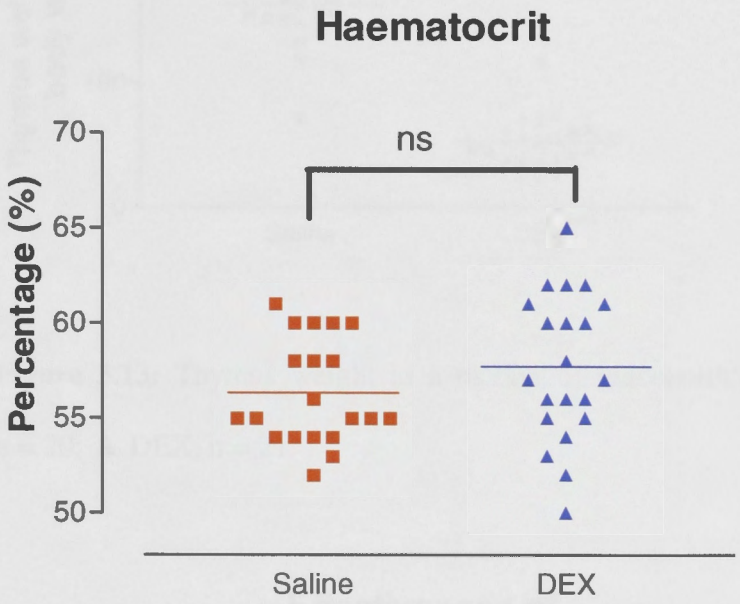

Figure 3.12: Haematocrit. ■ Saline, n = 20; ▲ DEX, n = 21.

3.3.6 Thymus and adrenal weights

Thymus and mean adrenal weights were significantly lower ($P < 0.0005$) in the DEX-treated group (thymus: 53 ± 5; adrenal: 3.9 ± 0.2 mg/100 g body weight, n = 21) compared with sham treatment group (thymus: 163 ± 9; adrenal: 6 ± 0.2 mg/100 g body weight, n = 20) (Figures 3.13 and 3.14).

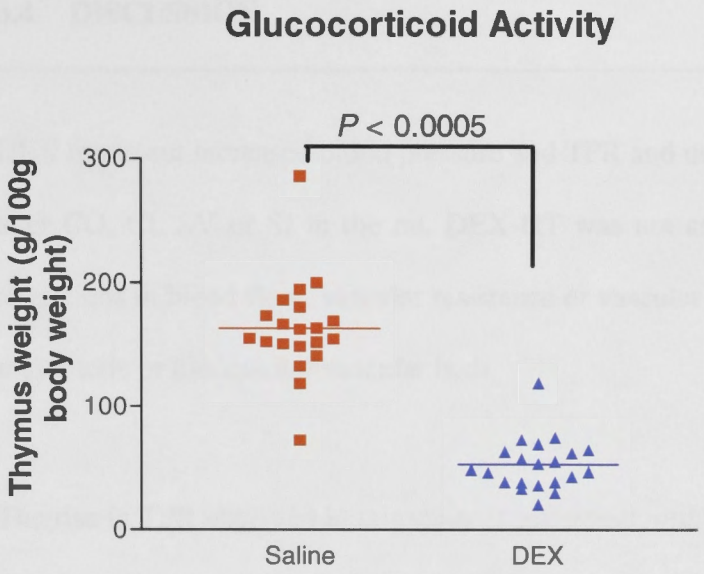

Figure 3.13: Thymus weight as a marker of glucocorticoid activity. ■ Saline, n = 20; ▲ DEX, n = 21.

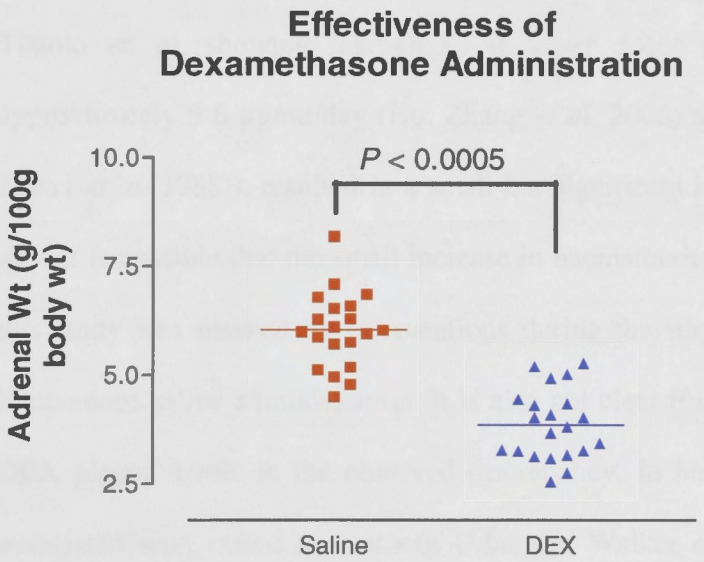

Figure 3.14: Adrenal weight as a marker of effective DEX administration. ■ Saline, n = 20; ▲ DEX, n = 21.

3.4 DISCUSSION

DEX treatment increased blood pressure and TPR and decreased TPC; but did not alter CO, CI, SV or SI in the rat. DEX-HT was not associated with significant alterations in blood flow, vascular resistance or vascular conductance in the renal, mesenteric or hindquarter vascular beds.

The rise in TPR observed in this study is consistent with the results obtained from DEX-hypertensive humans (Pirpiris, Sudhir *et al.* 1992) and dogs (Nakamoto, Suzuki *et al.* 1995). It is unlikely that alterations in blood viscosity, which could in turn alter vascular resistance and conductance, contribute to the increase in TPR in DEX-HT. In this study, DEX-HT was not associated with any change in haematocrit. This finding was different from those reported by Hu *et. al.* and Tonolo *et. al.* showing that DEX, at lower doses (20 μg/kg/day which is approximately 5-6 μg/rat/day (Hu, Zhang *et al.* 2006) and 2 μg/rat/day (Tonolo, Fraser *et al.* 1988)), resulted in a small but significant increase in haematocrit in rats. It is possible that the small increase in haematocrit due to DEX treatment in this study was masked by interventions during the surgical procedures such as intravenous saline administration. It is also not clear if differences in the dose of DEX played a role in the observed discrepancy. In humans, DEX-HT was not associated with raised haematocrit (Mangos, Walker *et al.* 2006). DEX-HT in dogs was not accompanied by a significant alteration in plasma osmolality (Nakamoto, Suzuki *et al.* 1991).

Another explanation for the increase in TPR is DEX-induced changes to vascular tone. There is increasing evidence linking deficiency in the vasorelaxant nitric oxide to the pathogenesis of DEX-HT. Plasma NOx, a marker of NO synthesis, was significantly reduced in DEX-hypertensive humans (Mangos, Walker *et al.* 2006) and rodents (Wallerath, Witte *et al.* 1999; Wallerath, Godecke *et al.* 2004). There are also reports implicating DEX in potentiating vascular pressor responsiveness to noradrenaline and/or angiotensin II in humans (Pirpiris, Sudhir *et al.* 1992), rats (Handa, Kondo *et al.* 1984) and dogs (Nakamoto, Suzuki *et al.* 1991).

The observed increase in TPR and decrease in TPC may reflect cumulative changes from a number of peripheral vascular beds including those evaluated in this study. In addition, these changes could also be a consequence of alterations in a site or sites other than the renal, mesenteric or hindquarter vascular system.

This study did not show any significant differences in the blood flow, resistance or conductance in the renal, mesenteric or hindquarter vascular beds. However, acute DEX administration at a significantly higher dose (3 mg/kg or approximately 900 μg/rat/day, continuous infusion over 24 hours) in conscious rats resulted in increased MAP, and decreased renal and mesenteric blood flows and vascular conductance (Gardiner, Kemp *et al.* 1996). These differences could be due to a variety of factors such as DEX dose differences, duration of DEX treatment and the use of anaesthesia. Data obtained from studies using high DEX dose need to be interpreted with caution as volume depletion through diuresis

(Chabria and Gaitonde 1966) due to high dose DEX may confound haemodynamic assessments of DEX-HT.

In this study, haemodynamic parameters were measured under pentobarbitone general anaesthesia (60 mg/kg, intraperitoneal injection). There are reports documenting the impact of anaesthetic agents on cardiovascular measurements (Koeppen, Katz *et al.* 1979; Janssen, De Celle *et al.* 2004; Saha, Saha *et al.* 2007). Pentobarbitone (50 mg/kg, i.p.) has been shown to decrease CI and HR in mice (Janssen, De Celle *et al.* 2004). Koeppen *et al.* have also demonstrated that pentobarbitone significantly reduced renal blood flow. Mechanical ventilation can also affect haemodynamic parameters. Selldén *et al.* have shown that changing ventilatory pattern in rats under choralose general anaesthesia from spontaneous breathing to artificial ventilation resulted in a significant decrease in CO and SV; and a significant increase in MAP, HR and TPR (Sellden, Sjovall *et al.* 1986). In view of these limitations, appropriately-matched controls that also underwent similar experimental and surgical conditions were used to minimise the confounding effects associated with acute haemodynamic experiments.

Thymus and adrenal weights were used as surrogate markers of the effectiveness of DEX administration as effective DEX delivery will decrease thymus and adrenal weights. DEX induces apoptosis in thymocytes and thus, results in thymic atrophy (Sun, Dinsdale *et al.* 1992; Zavitsanou, Nguyen *et al.* 2007). Adrenal atrophy was due to suppression of endogenous glucorticoid production by exogenous DEX administration.

3.5 CONCLUSION

DEX-HT is associated with a decrease in TPC and increase in TPR. These changes cannot be ascribed simply to individual alterations in conductance or resistance in the renal, mesenteric or hindquarter circulations.

The haemodynamics of DEX-HT in rats are different from those in ACTH-HT in rats. ACTH-HT is associated with raised CO and renal vascular resistance, and DEX-HT with increase in TPR and decrease in TPC. These findings support the notion that the mechanisms of DEX-HT (synthetic glucocorticoid) are different from those of ACTH-HT (ACTH-stimulated endogenous glucocorticoid).

CHAPTER 4

Role of Total Peripheral Resistance and Conductance in Dexamethasone-Induced Hypertension in the Rat

4.1 INTRODUCTION

As shown in Chapter 3, DEX-HT in rats is associated with an increase in TPR and decrease in TPC. In this study, using ultrasonic transit-time flowmetry as described in Chapter 2, we further evaluated the role of TPR and TPC in DEX-HT in rats by the administration of the vasodilator minoxidil at a dose known to reduce TPR in rats (Wen, Fraser *et al.* 1999).

4.2 METHODS

4.2.1 Experimental animals

This study was approved by the Animal Experimentation Ethics Committee of the Australian National University (Protocol No. J.HB.22.06). The general methodology for this study was as described in Chapters 2 and 3 (Section 3.2).

Twenty rats weighing 200-250 g were randomly divided into 2 groups, with 10 rats in each group.

1. Minoxidil (15mg/kg/day, gavage) + saline (0.2 mL/rat/day, sc)

2. Minoxidil (15mg/kg/day, gavage) + DEX (20 μL/rat/day, sc)

Minoxidil suspension (15 mg/mL) was prepared daily by mixing minoxidil powder (Sigma-Aldrich, St. Louis, USA) in 0.9% NaCl solution. All rats received minoxidil suspension (15 mg/kg/day or 0.1 mL/100 g body weight) by gavage daily between 3-4 pm for 16 days from P0 to T11. From day T0-T11, one group was co-administered DEX (n = 10), and the other group, saline (n = 10) via subcutaneous injections daily between 3-4 pm.

4.2.2 Blood pressure and body weight measurement

Tail-cuff SBP measurement was performed on alternate days at 9-11 am using the method as described in Sections 2.5.1 (Chapter 2) and 3.2.2 (Chapter 3). Body weights were measured on alternate days after the tail-cuff SBP measurements.

Direct blood pressure and heart rate (HR) measurements were recorded as per the method described in Sections 2.5.2 and 2.6.2 of Chapter 2; and Section 3.2.2 of Chapter 3. In this study, only central haemodynamic profiles were evaluated. Surgical approaches for CO measurements are described in Section 2.8.3.

4.2.3 Calculation of other haemodynamic parameters

The following haemodynamic parameters were calculated.

- Cardiac Index (CI) = CO/ 100 g body weight
- Stroke Volume (SV) = CO/HR

- Stroke Index (SI) = CI/HR
- TPR = MAP/CO
- TPC = 1/TPR

4.2.4 Haematocrit estimation

Haematocrit estimation was performed as described in Sections 2.9 and 3.2.4.

4.2.5 Thymus and adrenal weights

Thymus wet weight, expressed relative to body weight (grams thymus weight per 100 g body weight), was used as a marker of glucocorticoid activity. Adrenal wet weight, expressed relative to body weight (grams adrenal weight per 100 g body weight), was used to assess DEX treatment efficacy. The surgical methods were as described in Section 2.8.5.1 of Chapter 2.

4.2.6 Statistical analysis

Data from this study was compared with central haemodynamic data from rats described in Chapter 3, which were used as controls.

Controls:

1. Vehicle (saline, 0.1 mL/100 g, gavage) + Saline (0.2 mL/rat, s.c.), n = 9

2. Vehicle (saline, 0.1 mL/100 g, gavage) + DEX (20 μL/rat, s.c.), n = 10

Results were expressed as mean ± SEM. Statistical analysis were as described in Section 2.12 of Chapter 2.

4.3 RESULTS

4.3.1 Tail-cuff systolic blood pressure

DEX treatment increased tail-cuff SBP from 125 ± 4 to 140 ± 3 mmHg (T0-T10, $P < 0.005$, n = 9) whilst sham injections with saline did not alter SBP (T0: 128 ± 4 to T10: 120 ± 4 mmHg, n = 10). Tail-cuff SBP in the DEX-treated group (n = 10) was significantly higher than in the sham treatment group ($P < 0.005$, n = 9). Tail-cuff SBP in the minoxidil + DEX group tended to rise from day T0 to day T10 but was not statistically significant ($P = 0.086$, n = 10). Minoxidil treatment did not alter SBP in saline-treated rats (Figure 4.1).

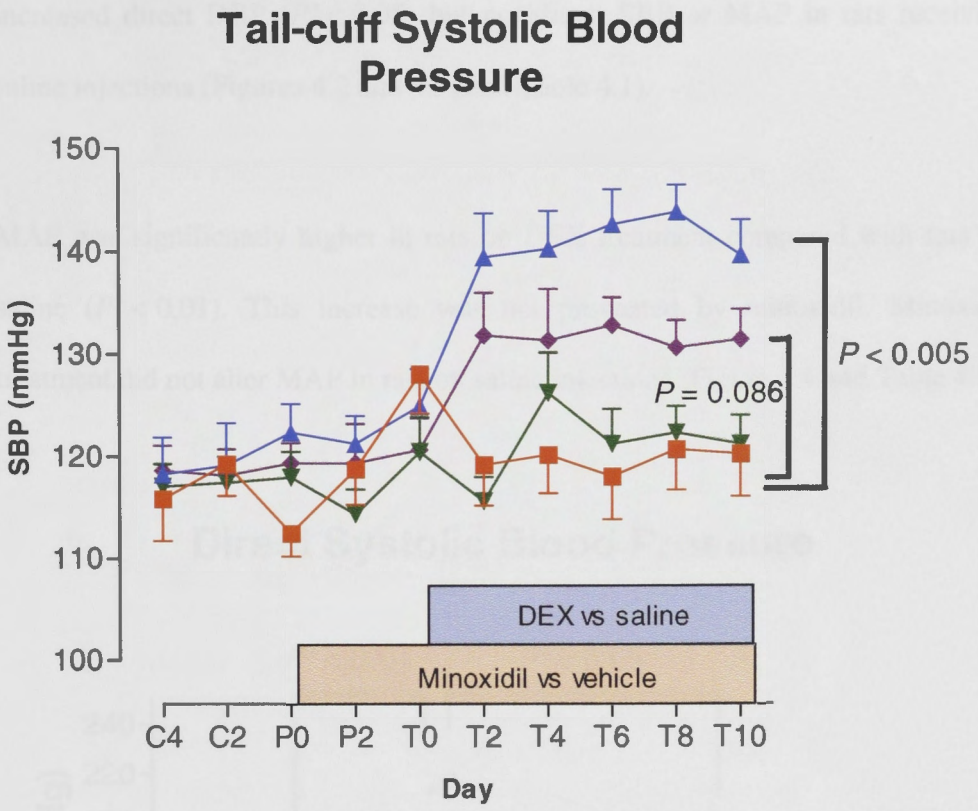

Figure 4.1: Tail-cuff SBP. ■ Vehicle + Saline, n = 9; ▲ Vehicle + DEX, n = 10; ▼ Minoxidil + Saline, n = 10; ♦ Minoxidil + DEX, n = 10.

4.3.2 Direct blood pressure measurements

Both direct systolic and diastolic blood pressure (DBP) measurements obtained on the last day of experiment (T11) were significantly higher in the DEX-treated rats compared with saline-treated control rats. Rats on minoxidil + DEX treatments had significantly lower SBP than those on DEX treatment alone ($P' < 0.05$). However, there was no significant difference in direct DBP between DEX- and minoxidil + DEX-treated rats. Interestingly, minoxidil treatment significantly

increased direct DBP ($P' < 0.05$) but not direct SBP or MAP in rats receiving saline injections (Figures 4.2 and 4.3; and Table 4.1).

MAP was significantly higher in rats on DEX treatment compared with rats on saline ($P' < 0.01$). This increase was not prevented by minoxidil. Minoxidil treatment did not alter MAP in rats on saline injections (Figure 4.4 and Table 4.1).

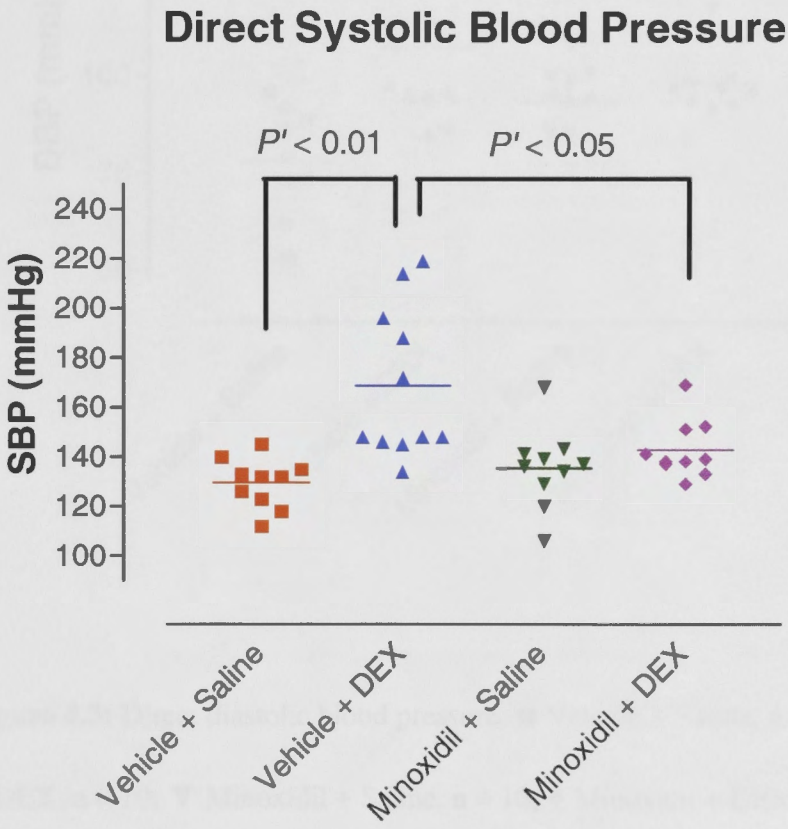

Figure 4.2: Direct systolic blood pressure. ■ Vehicle + Saline, n = 9; ▲ Vehicle + DEX, n = 10; ▼ Minoxidil + Saline, n = 10; ♦ Minoxidil + DEX, n = 10.

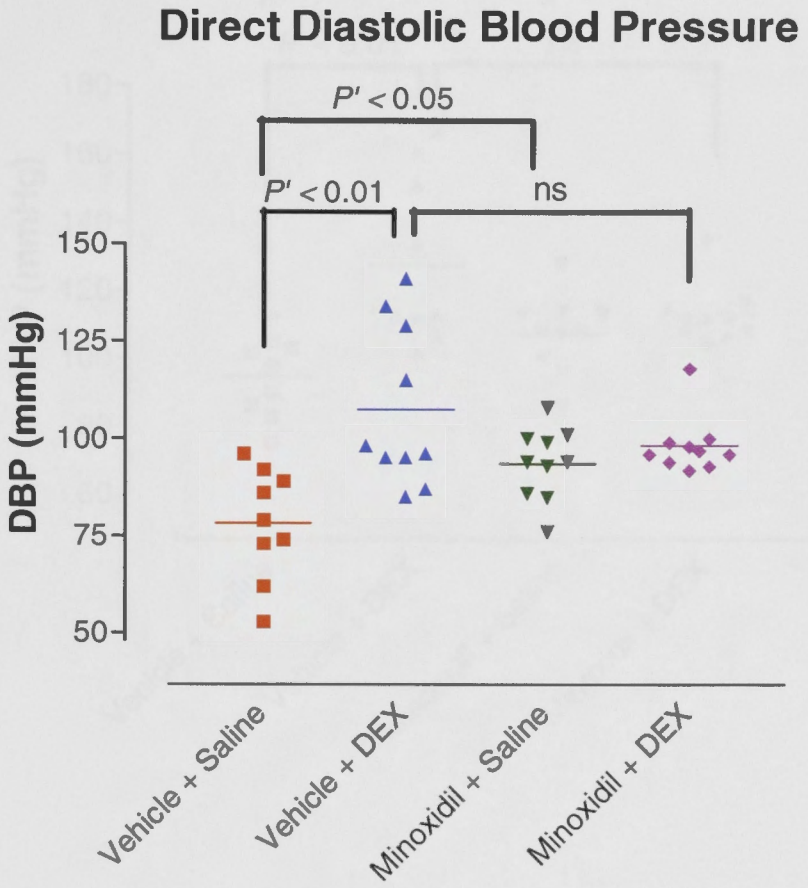

Figure 4.3: Direct diastolic blood pressure. ■ Vehicle + Saline, n = 9; ▲ Vehicle + DEX, n = 10; ▼ Minoxidil + Saline, n = 10; ♦ Minoxidil + DEX, n = 10.

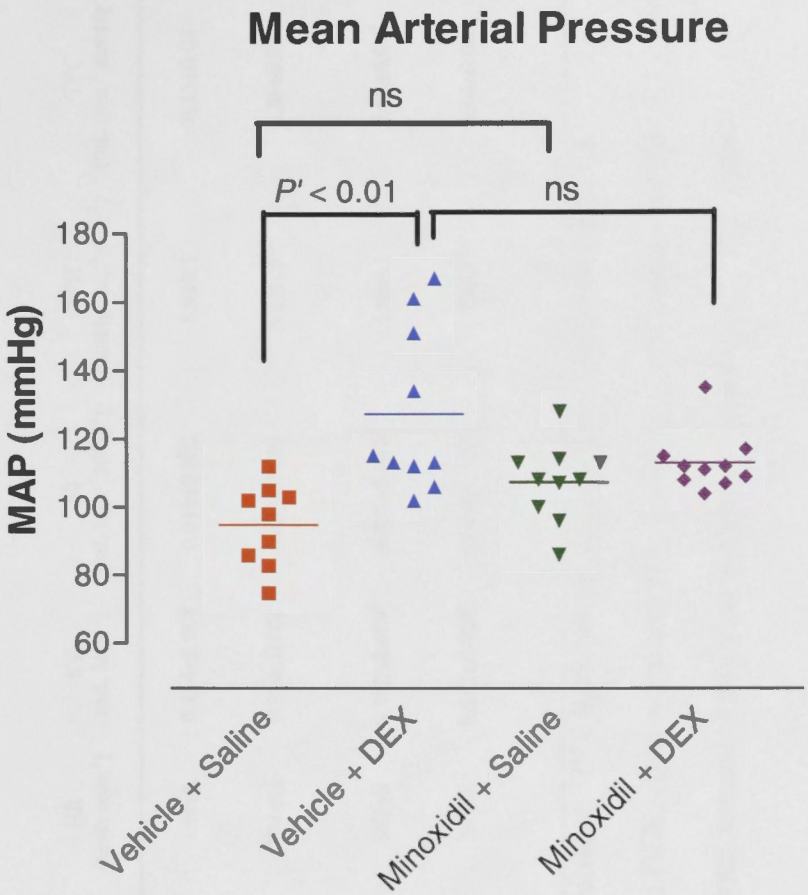

Figure 4.4: Mean arterial pressure. ■ Vehicle + Saline, n = 9; ▲ Vehicle + DEX, n = 10; ▼ Minoxidil + Saline, n = 10; ♦ Minoxidil + DEX, n = 10.

Table 4.1: Central haemodynamic effects of sham and dexamethasone treatments with and without minoxidil

Treatment group	MAP (mmHg)	SBP (mmHg)	DBP (mmHg)	CO (mL min^{-1})	CI (mL min^{-1} $100g^{-1}$)	HR (beats min^{-1})	SV (mL $beat^{-1}$)	SI (mL $beat^{-1}100g^{-1}$)	TPR (mmHg mL^{-1} min^{-1})	TPC (mL min^{-1} $mmHg^{-1}$)
Sham n = 9	95±4	128±3	78±5	52±3	16±1	389±8	0.134±0.008	0.041±0.002	1.9±0.1	0.55±0.03
DEX n = 10	**127±8***	**167±10***	**108±7***	45±3	16±1	394±11	0.114±0.009	0.041±0.003	**3.2±0.5***	**0.36±0.03***
Minoxidil + sham n = 10	107±4	135±5	**94±3†**	**70±4†**	**22±2†**	383±9	**0.182±0.009†**	**0.057±0.005†**	1.6±0.1	**0.65±0.04†**
Minoxidil + DEX n = 10	**113±3***	**143±4‡**	98±2	**72±4‡**	**25±1‡**	395±8	**0.182±0.010‡**	**0.064±0.003‡**	**1.6±0.1‡**	**0.64±0.04‡**

Data were expressed as mean ± SEM. $*P' < 0.01$ versus sham treatment; $^{\dagger}P' < 0.05$ versus sham; $^{\ddagger}P' < 0.05$ versus DEX. CI, cardiac index; CO, cardiac output; DBP, diastolic blood pressure; DEX, dexamethasone; HR, heart rate; MAP, mean arterial pressure; SBP, systolic blood pressure; SI, stroke index; SV, stroke volume; TPC, total peripheral conductance; TPR, total peripheral resistance.

4.3.3 Haemodynamic effects

4.3.3.1 Heart rate

Heart rate was not significantly altered by DEX or minoxidil treatments (Figure 4.5 and Table 4.1).

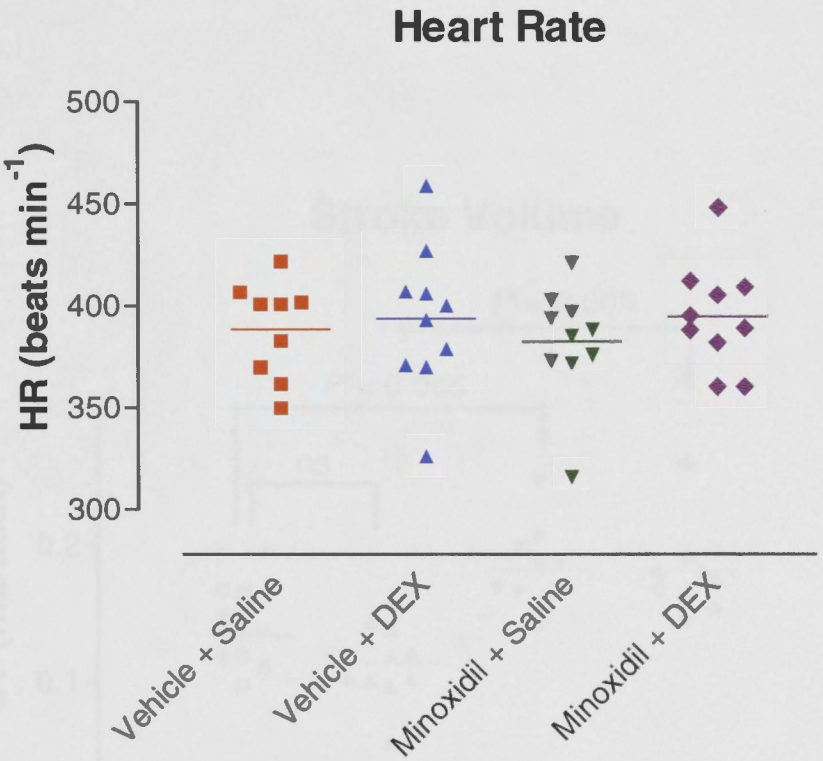

Figure 4.5: Heart rate. ■ Vehicle + Saline, n = 9; ▲ Vehicle + DEX, n = 10; ▼ Minoxidil + Saline, n = 10; ♦ Minoxidil + DEX, n = 10.

4.3.3.2 Stroke volume and stroke index

There was no significant difference in SV and SI between the DEX-treated and sham groups. In comparison with the sham group, rats on minoxidil + sham treatments had significantly higher SV ($P' < 0.005$) and SI ($P' < 0.05$). Similarly, minoxidil + DEX treatments resulted in significantly higher SV ($P' < 0.005$) and SI ($P' < 0.005$) compared with DEX treatment alone (Figures 4.6 and 4.7; and Table 4.1).

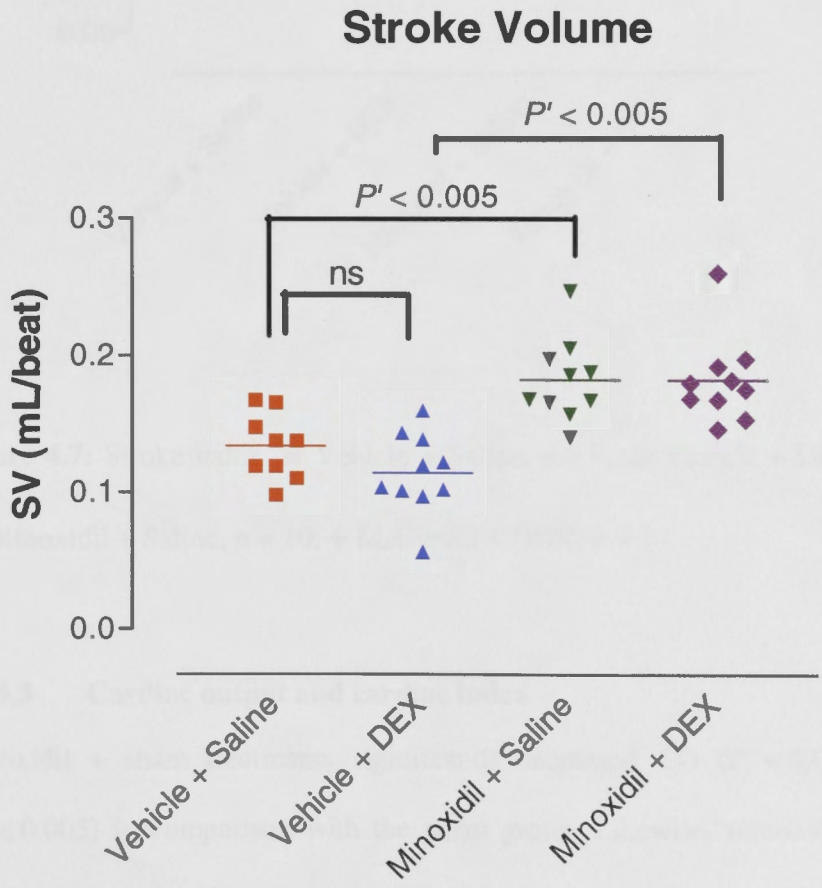

Figure 4.6: Stroke volume. ■ Vehicle + Saline, n = 9; ▲ Vehicle + DEX, n = 10; ▼ Minoxidil + Saline, n = 10; ♦ Minoxidil + DEX, n = 10.

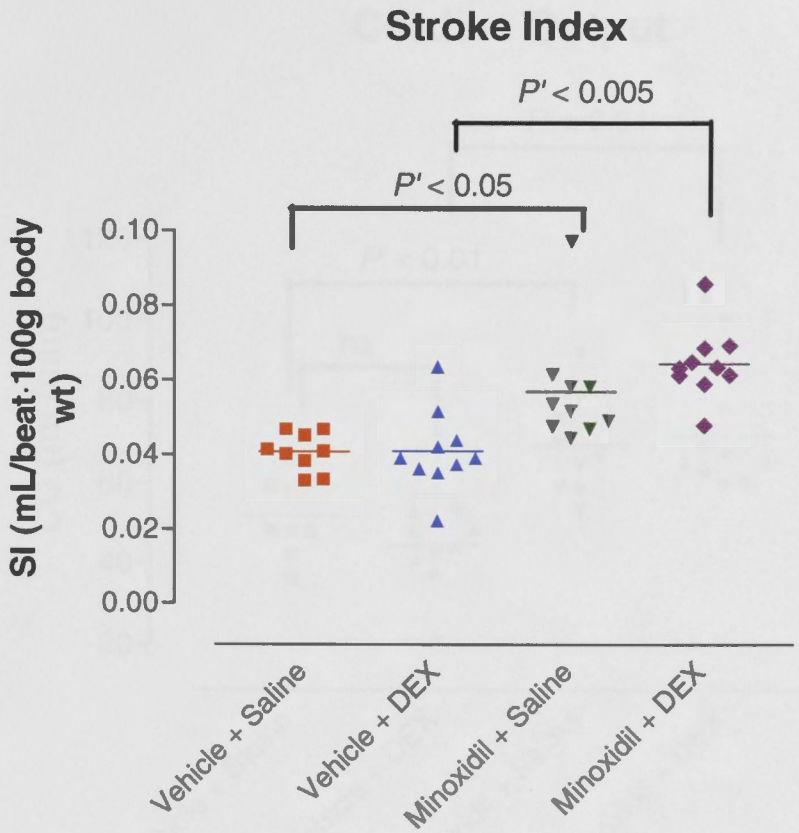

Figure 4.7: Stroke index. ■ Vehicle + Saline, n = 9; ▲ Vehicle + DEX, n = 10; ▼ Minoxidil + Saline, n = 10; ♦ Minoxidil + DEX, n = 10.

4.3.3.3 Cardiac output and cardiac index

Minoxidil + sham treatments significantly increased CO ($P' < 0.01$) and CI ($P' < 0.005$) in comparison with the sham group. Likewise, minoxidil + DEX-treated rats had significantly higher CO ($P' < 0.01$) and CI ($P' < 0.005$) compared with DEX-treated rats (Figures 4.8 and 4.9; and Table 4.1).

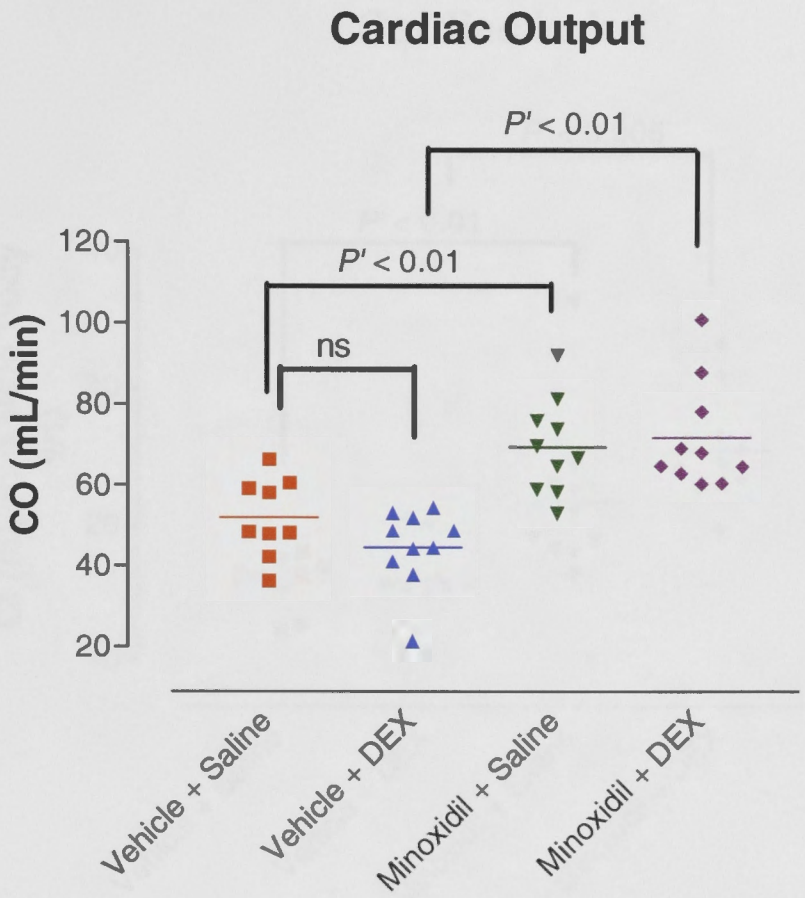

Figure 4.8: Cardiac output. ■ Vehicle + Saline, n = 9; ▲ Vehicle + DEX, n = 10; ▼ Minoxidil + Saline, n = 10; ♦ Minoxidil + DEX, n = 10.

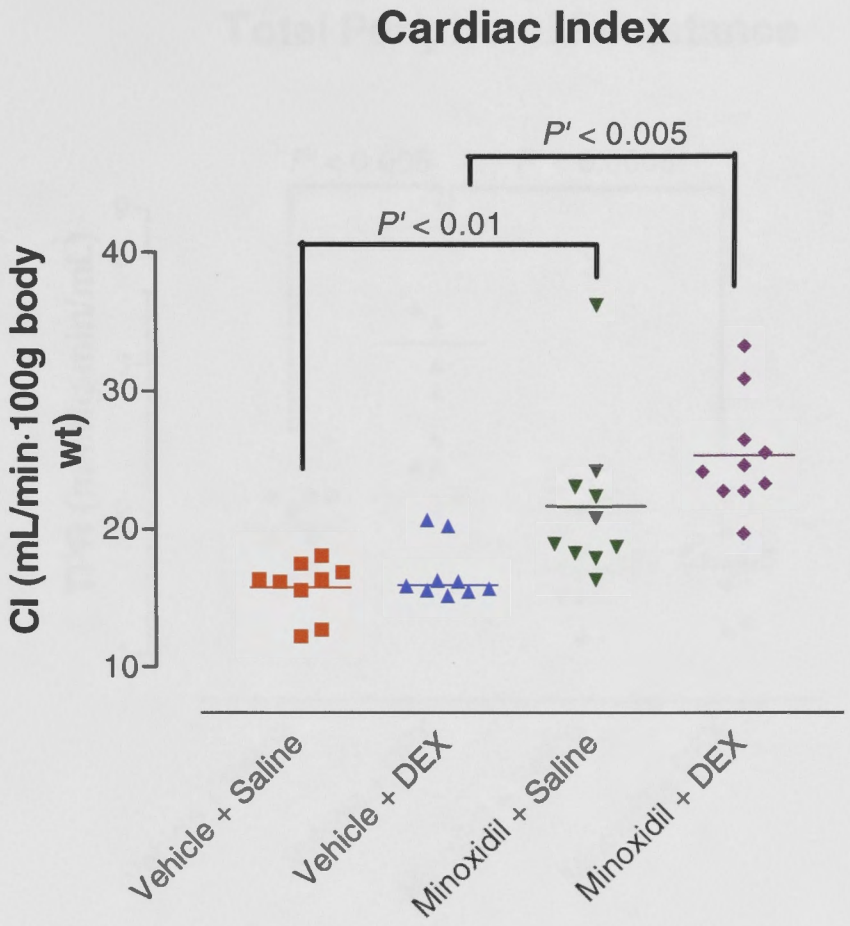

Figure 4.9: Cardiac index. ■ Vehicle + Saline, n = 9; ▲ Vehicle + DEX, n = 10; ▼ Minoxidil + Saline, n = 10; ♦ Minoxidil + DEX, n = 10.

4.3.3.4 Total peripheral resistance

TPR was significantly increased in the DEX-treated group compared with the sham treatment group ($P' < 0.05$) and was significantly lower in the minoxidil + DEX-treated group in comparison to DEX-treated group ($P' < 0.05$) (Figure 4.10 and Table 4.1).

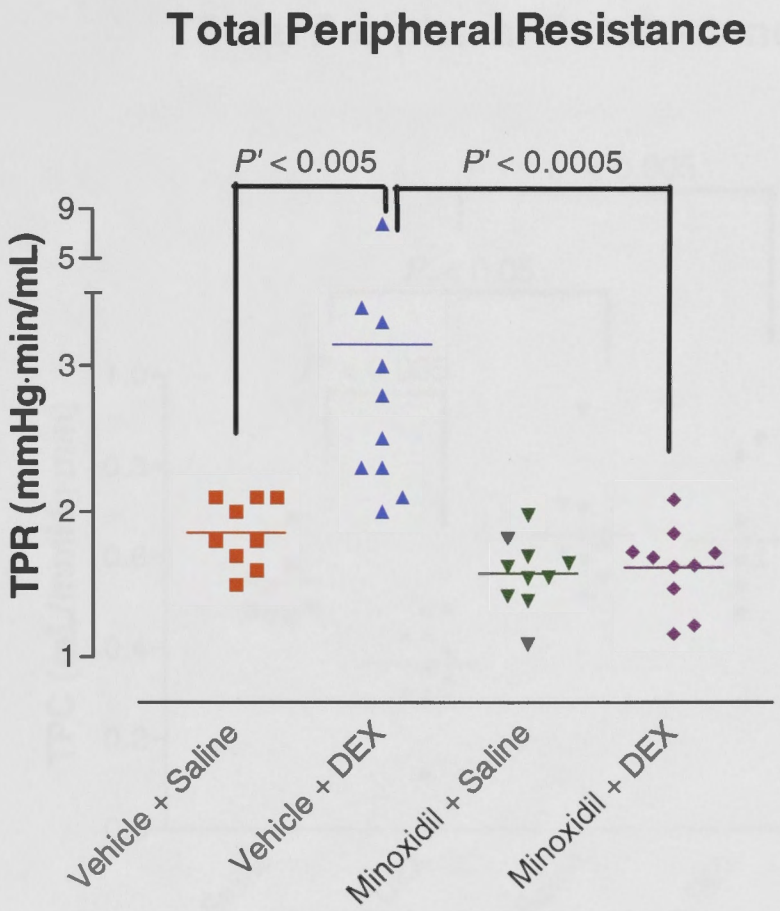

Figure 4.10: Total peripheral resistance. ■ Vehicle + Saline, n = 9; ▲ Vehicle + DEX, n = 10; ▼ Minoxidil + Saline, n = 10; ♦ Minoxidil + DEX, n = 10.

4.3.3.5 Total peripheral conductance

TPC in the DEX-treated group was significantly lower than in the sham treatment group ($P' < 0.005$). Rats on minoxidil + DEX had significantly higher TPC than those on DEX without minoxidil ($P' < 0.005$). Minoxidil + sham treatments significantly increased TPC in comparison to sham treatment ($P' < 0.05$) (Figures 4.11 and Table 4.1).

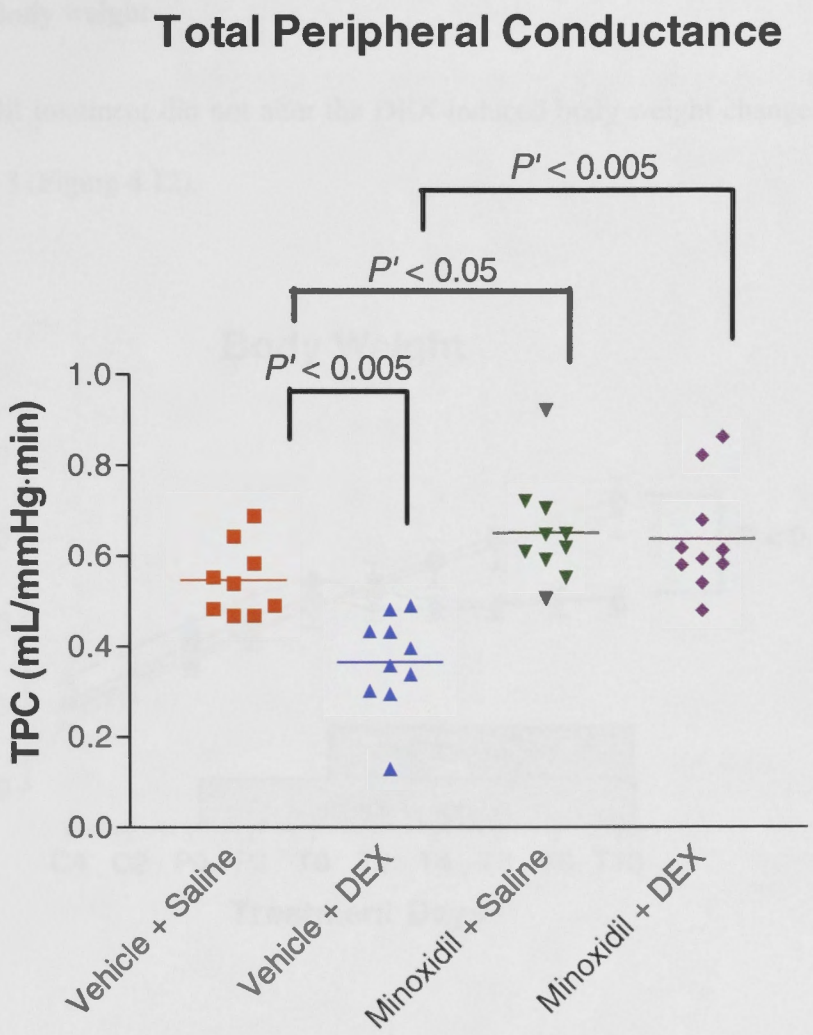

Figure 4.11: Total peripheral conductance. ■ Vehicle + Saline, n = 9; ▲ Vehicle + DEX, n = 10; ▼ Minoxidil + Saline, n = 10; ♦ Minoxidil + DEX, n = 10.

4.3.4 Body weight

Minoxidil treatment did not alter the DEX-induced body weight changes seen in Chapter 3 (Figure 4.12).

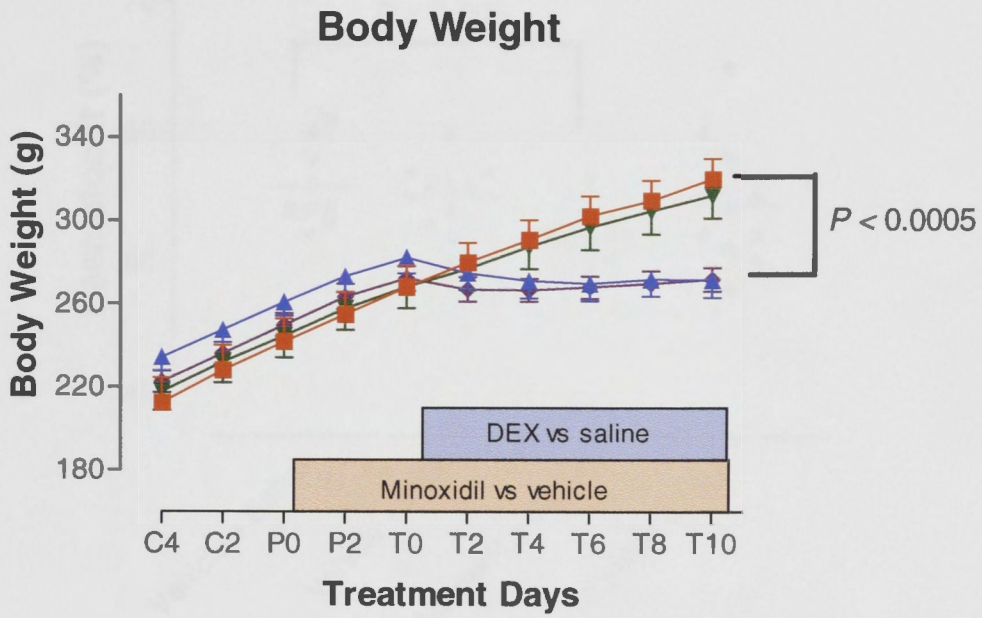

Figure 4.12: Body weight. ■ Vehicle + Saline, n = 9; ▲ Vehicle + DEX, n = 10; ▼ Minoxidil + Saline, n = 10; ♦ Minoxidil + DEX, n = 10.

4.3.5 Haematocrit

There was no significant difference in haematocrit between DEX-treated and sham rats (sham: 56 ± 1.1, n=9; DEX: 55 ± 0.9 %, n = 10). Minoxidil + sham treatments produced a significant decrease in haematocrit compared with sham treatment alone (sham: 56 ± 1.1, n = 9; minoxidil + sham: 52 ± 0.6 %, n = 10,

$P < 0.005$). This decrease was not seen in minoxidil + DEX-treated rats (DEX: 55 ± 0.9; minoxidil + DEX: 55 ± 1.6 %, n = 10 each) (Figure 4.13).

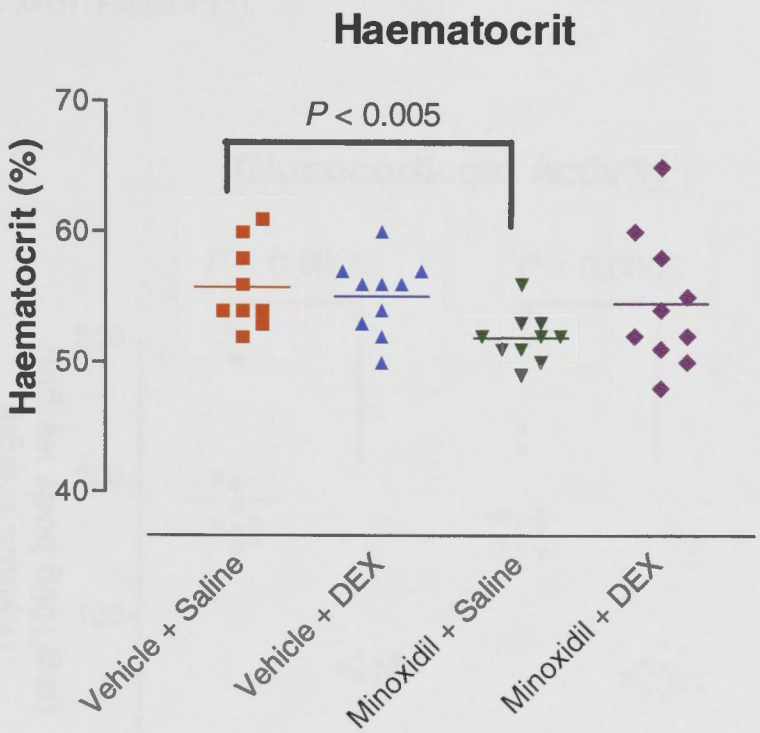

Figure 4.13: Haematocrit. ■ Vehicle + Saline, n = 9; ▲ Vehicle + DEX, n = 10; ▼ Minoxidil + Saline, n = 10; ♦ Minoxidil + DEX, n = 10.

4.3.6 Thymus and adrenal weights

DEX treatment, regardless of the presence of minoxidil treatment, resulted in significant decreases in thymus (saline: 185 ± 14, n = 9 versus DEX: 60 ± 3, n = 10 and minoxidil + saline: 172 ± 10, n=10 versus minoxidil + DEX: 60 ± 4

mg/100g, n = 10; both $P < 0.0005$) (Figure 4.14) and mean adrenal weights (saline: 5.7 ± 0.2, n=9 versus DEX: 3.7 ± 0.3, n = 10 and minoxidil + saline: 5.6 ± 0.4, n = 10 versus minoxidil + DEX: 3.6 ± 0.1 mg/100g, n = 10; both $P < 0.0005$) (Figure 4.15).

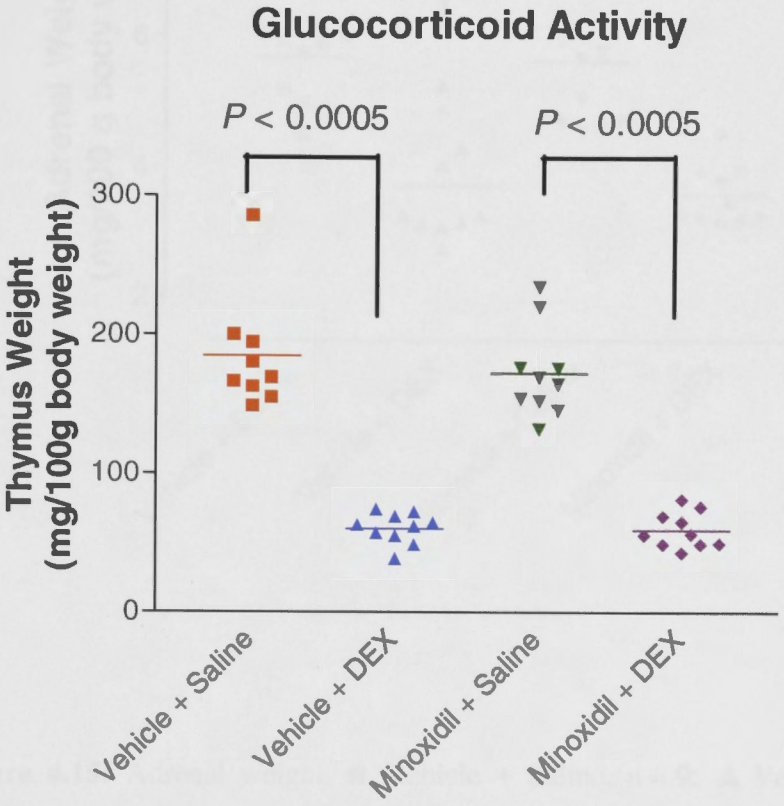

Figure 4.14: Thymus weight. ■ Vehicle + Saline, n = 9; ▲ Vehicle + DEX, n = 10; ▼ Minoxidil + Saline, n = 10; ♦ Minoxidil + DEX, n = 10.

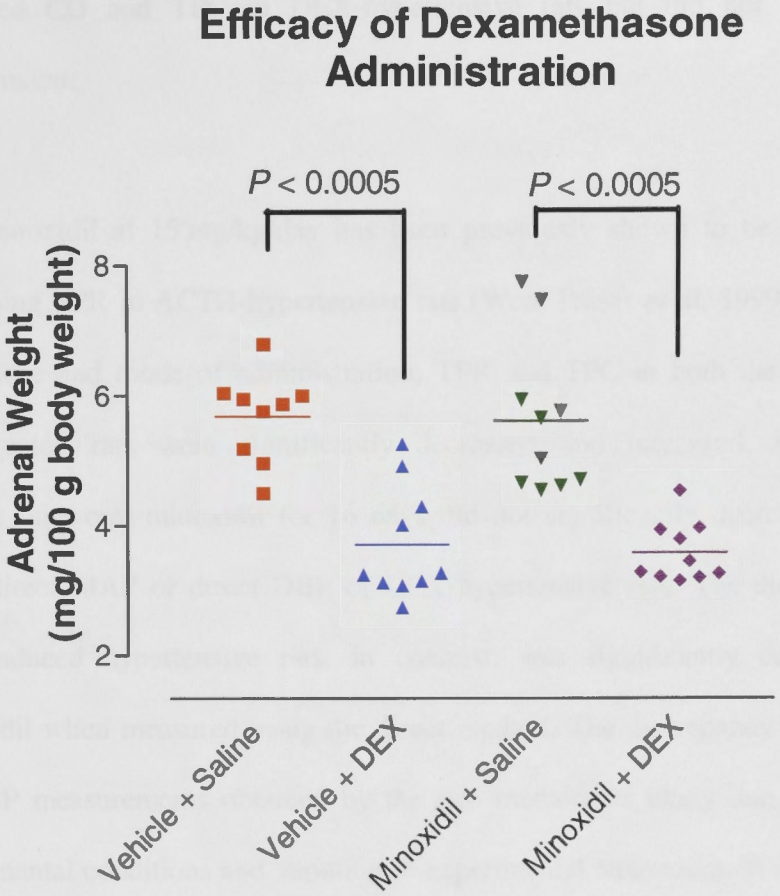

Figure 4.15: Adrenal weight. ■ Vehicle + Saline, n = 9; ▲ Vehicle + DEX, n = 10; ▼ Minoxidil + Saline, n = 10; ♦ Minoxidil + DEX, n = 10.

4.4 DISCUSSION

As shown in Chapter 3, DEX-HT in the rat is associated with raised TPR and reduced TPC. Minoxidil treatment for 16 days significantly decreased TPR and

increased CO and TPC in DEX-hypertensive rats but did not prevent the hypertension.

Oral minoxidil at 15 mg/kg/day has been previously shown to be effective in decreasing TPR in ACTH-hypertensive rats (Wen, Fraser *et al.* 1999). Using the same dose and mode of administration, TPR and TPC in both the saline- and DEX-treated rats were significantly decreased and increased, respectively. Despite this, oral minoxidil for 16 days did not significantly decrease tail-cuff SBP, direct MAP or direct DBP of DEX-hypertensive rats. The direct SBP of DEX-induced hypertensive rats, in contrast, was significantly decreased by minoxidil when measured using the direct method. The discrepancy observed in the SBP measurements obtained by the two methods is likely due to different experimental conditions and variation in experimental techniques. With the direct method, the rats were anaesthetised and mechanically-ventilated. Limitations associated with these manoeuvres have been discussed in Chapter 3. Tail-cuff SBP, on the other hand, was obtained in restrained conscious animals without the undesirable side effects of general anaesthesia and mechanical ventilation. The tail-cuff system is a reliable method for assessing SBP in rats. It was previously shown, in our hands, to produce results that are comparable to telemetry (Fraser, Turner *et al.* 2001).

Although direct SBP of DEX-hypertensive rats was significantly reduced by minoxidil, increases in direct MAP and DBP due to DEX were not significantly lowered. Furthermore, DBP in the minoxidil + saline group was significantly

increased compared with the saline-only group. There are 2 possible explanations for this absence of blood pressure lowering effect of minoxidil. Firstly, changes in TPR and TPC are not critical to the development of DEX-HT, though they might contribute to the maintenance of the hypertensive state. Secondly, the blood pressure lowering effect of minoxidil may have been offset by volume factors. CO and CI, in both the minoxidil + saline- and minoxidil + DEX-treated rats were increased. As there was no change in HR between the treatment groups, minoxidil-induced elevations in CO and CI were also associated with increases in SV and SI in the saline and DEX-treated rats. It is likely that these increases counteracted all the vasodilator effect of minoxidil. The mechanism responsible for the increases in CO and CI and the loss of blood pressure lowering effect of minoxidil, is mainly related to plasma volume expansion. In this study, we observed a decrease in haematocrit due to minoxidil in the saline-treated group. Several studies have also suggested that minoxidil treatment resulted in plasma and blood volume expansion in rats (Leenen and Prowse 1987; Sanz, Lopez Novoa *et al.* 1990; Tsoporis, Fields *et al.* 1991). In the present study, minoxidil did not alter haematocrit in the DEX-HT rats despite increasing CO and CI. It remains unclear if DEX can inhibit the fall in haematocrit due to minoxidil.

The reduction of both thymus and adrenal weights were signs of effective DEX delivery to these animals.

4.5 CONCLUSION

Concomitant treatment with the vasodilator minoxidil prevented the rise in TPR and decrease in TPC but did not completely prevent the rise in blood pressure due to DEX, which in this case was associated with increase in CO and CI. Thus, raised TPR and decrease in TPC are features of DEX-HT that may not be critical for production of DEX-HT and may be overcome by increase in CO.

CHAPTER 5

Effects of Glucocorticoid on Rat Kidney Mitochondrial Superoxide

5.1 INTRODUCTION

The mitochondrion is an important source of ROS, primarily the superoxide radical and consequently its dismutation product, hydrogen peroxide, which can form highly reactive hydroxyl radicals. It consumes approximately 90% of the cell's oxygen and 1-4% of oxygen reacting with the mitochondrial respiratory chain is incompletely reduced to ROS (Richter 1988; Lenaz 1998). The electron transport chain is generally accepted as the main source of ROS in the mitochondria. Based on studies in isolated mitochondria utilising different substrates or inhibitors to support or inhibit cell respirations, it is concluded that the main sites of superoxide generation within the electron transport chain are complex I (NADH dehydrogenase) and III (cytochrome bc_1 complex) with the release of superoxide towards the mitochondrial matrix (Muller, Liu *et al.* 2004). The electron transport chain is, however, not the only major supply of ROS within the mitochondria. Recent studies on neural tissues have revealed that alpha-ketoglutarate dehydrogenase, an important Kreb cycle enzyme, also contributes to ROS generation in the mitochondria (Starkov, Fiskum *et al.* 2004; Adam-Vizi 2005; Tretter and Adam-Vizi 2005).

Besides being the producer of ROS, the mitochondrion is also susceptible to oxidative injury. Overproduction and the resultant accumulation of mitochondrial-derived ROS can damage mitochondrial components such as mitochondrial DNA and membrane, leading to mitochondrial dysfunction which can further exacerbate mitochondrial ROS production.

As there are a number of different pathways contributing to the production of superoxide in cells apart from the mitochondria such as the NAD(P)H oxidase, xanthine oxidase and eNOS in its uncoupled form (Chapter 1), proper assessment of mitochondrial superoxide production requires analysis at this subcellular level. Furthermore, superoxide generated by the mitochondria does not permeate the inner mitochondrial membrane and is compartmentalised within this organelle away from the cytosol (Han, Antunes *et al.* 2003).

The aim of this study was to establish and validate a simple quantitative assay to detect superoxide within the mitochondria and to determine the effect of glucocorticoids in kidney mitochondrial superoxide levels.

5.2 METHODS

This study was approved by the Animal Experimentation Ethics Committee of the Australian National University (Protocol No. J. HB. 20.05).

5.2.1 Mitochondrial superoxide detection

One of the methods includes analysing superoxide oxidation products in isolated mitochondrial particles. First, mitochondria from rat kidney were isolated using differential ultra-centrifugation of cell suspension prepared from homogenised kidney. This process was based on a method described previously (Pallotti and Lenaz 2001). The mitochondrial content was standardised by quantitation of the

protein content using the Bradford method (Bradford 1976) (BioRad, Gladesville, Australia) using bovine serum albumin as standard. After staining the isolated mitochondria with a number of fluorogenic probes- nonylacridine orange to identify mitochondrial particles, 1,1',3,3,3',3'-hexamethylindodicarbocyanine iodide ($DiIC_1(5)$) to assess mitochondrial membrane potential and dihydroethidine to assess superoxide generation (all fluorogenic probes were purchased from Molecular Probes, Invitrogen, USA), the stained isolated mitochondria were assessed via flow cytometry (Mattiasson 2004; Mattiasson 2004a). This technique was abandoned as this multi-step process involved in this method was time-consuming and not suitable for analysis of a large number of fresh specimens on the days the animals were sacrificed. Instead, I utilised another fluorescent method which involved analysing mitochondrial superoxide in intact live cells. Analysis of mitochondria in live cells bypasses this tedious process of mitochondrial isolation. It also allows for separation of artefacts of isolated mitochondrial preparations from actual signals generated by mitochondrial superoxide.

In this latter technique, a novel fluorogenic probe, triphenylphosphonium-hydroethidine (Mito-HE) (MitoSOX™ Red, Molecular Probes, Invitrogen, USA), which is a derivative of hydroethidine (HE) was used. HE is widely used to detect intracellular superoxide anion. It reacts with superoxide to form ethidium (Etd^+) and its hydroxylated product (HO- Etd^+) both of which become highly fluorescent when intercalated with cellular nucleic acids (Robinson, Janes *et al.* 2006). Mito-HE is derived by linking a triphenylphosphonium cation to the HE

moiety. The positive charge in the phosphonium group allows Mito-HE to selectively accumulate in the mitochondria of live cells with 100-1000 fold affinity, as described in other compounds with the phosphonium side-chain (Ross, Kelso *et al.* 2005). Mito-HE is oxidised in the similar manner to HE to result in the formation of Mito- Etd^+ which fluoresces following excitation.

As Mito-HE accumulates in mitochondria as a function of mitochondrial membrane potential, cells were also stained with $DiIC_1(5)$, a mitochondrial potentiometric probe to ensure that cell treatment with Mito-HE did not depolarise mitochondrial membrane. This phenomenon can lead to extra-mitochondrial oxidation of Mito-HE causing false positive results. $DiIC_1(5)$ is a cationic cyanine dye which penetrates the cytosol of eukaryotic cells and accumulates in cells in response to membrane potential (Shapiro, Natale *et al.* 1979; Shapiro 2000). It however, accumulates mainly in the mitochondria with active membrane potentials at concentrations below 100 nM.

5.2.2 Principles of flow cytometry

Flow cytometry is a powerful tool that allows multi-parametric analysis of cells within a heterogenous cell population. It uses the principles of light excitation and scattering to generate specific data of cells such as size, granularity or complexity, phenotype and health.

The cells, as they pass through the laser beam, scatter the light in different angles. Forward scatter (FSC) is the amount of light that scatters in the forward direction. Its magnitude is proportional to cell size. Side scatter (SSC), on the other hand, is a measure of granularity or complexity within the cell. It is a large angle scatter caused by structures within the cell. The intensity of the light scatter captured by the detectors is converted to voltage pulse which is then presented graphically.

Fluorescent molecules are commonly used in flow cytometry to study cell characteristics. When cells treated with fluorochromes are excited by light with a correct wavelength, they emit fluorescent signals which follow the same paths as the FSC and SSC signals. These fluorescent signals travel through a series of filters and mirrors to reach the detector for that particular wavelength. Fluorescence data are collected via the same method as FSC and SSC data. The intensity of the fluorescence is converted into voltage signals proportional to the emissions emitted. All of the voltage pulses are collected and presented graphically as in Figure 5.2.

5.2.3 Single cell suspension

Rats were sacrificed under anaesthesia using the method described in Section 2.8 of Chapter 2. The left kidney was located and removed via a median laparotomy incision. The left rat kidney was harvested and immediately placed in chilled phosphate buffered saline (PBS). Perinephric fat and serosal membrane were trimmed, before cutting the kidney into smaller pieces. The kidney was then

homogenised manually using a cell sieve and a 5 mL syringe plunger in a petri dish containing 10 mL of chilled PBS. The cells were then filtered using a 2000 μm cell filter.

5.2.4 Standardisation of cell number

Trypan blue (Fluka, Seelze, Germany) was used to stain dead cells. The cells were counted using a Neubauer haemocytometer (Brightline®, American Optical Corporation, Buffalo, USA) counting chamber and a microscope at 100x magnification. In a viable cell preparation, the proportion of dead cells should be less than 20%. A total cell count of $2.0x10^6$ per sample was required for flow cytometry analysis.

5.2.5 Mitochondrial staining

The cells were incubated with Mito-HE and $DiIC_1(5)$. The approximate excitation and emission (Ex/Em) spectral peaks for Mito-HE are 510/580 and for $DiIC_1(5)$ are 638/658 nm. These two dyes are compatible as the fluorescent products for Mito-HE and $DiIC_1(5)$ are efficiently excited by the 488 and 633 nm lasers, respectively without overlap in their emission peaks.

Mito-HE and $DiIC_1(5)$ were reconstituted with dimethylsulfoxide (DMSO) to 5 mM and 3 mM respectively. These stock solutions were further diluted using PBS to the required concentrations. The DMSO and PBS solutions used on Mito-HE were percolated with nitrogen. Mito-HE (final concentration 2 μM, see

validation study below) and $DiIC_1(5)$ (final concentration 10 nM) solutions were added to the cells and incubated for 10 minutes at 37 °C. All samples were prepared in duplicate.

5.2.6 Flow cytometric analysis

The cells were analysed immediately after incubation with Mito-HE and $DiIC_1(5)$. The cells were protected from light at all times to prevent quenching of fluorescence signals.

Flow cytometric analysis was performed using a FACSort BD (Becton Dickinson, San Jose, USA) flow cytometer equipped with 488 nm Argon and 633 nm diode lasers. Excitation of the Mito-HE oxidation products was performed using the 488 nm laser. The emissions generated by Mito-HE oxidation products were detected by the FL2 channel. This channel can detect emissions in the wavelength range of 585 ± 30 nm. $DiIC_1(5)$ was excited by the 633 nm laser and the emissions were detected by the FL4 channel. This channel can detect emissions in the wavelength range of 660 ± 20 nm.

Data acquisition and analysis were performed using the CellQuest software (Becton Dickinson Immunocytometry Systems, San Jose, USA).

Based on light scattering properties in the FSC and the SSC modes, the cells were gated to exclude cell debris (Figure 5.1). Dead cells are recognised flow

cytometrically by very low fluorescence and relatively low FSC and SSC. This gate was drawn to cover a large SSC area to ensure all cell lines from the kidneys were covered, whilst excluding cell debris.

Using the "medium" sampling rate, 15000 gated events per sample were analysed.

The geometric mean fluorescence intensity (MFI) was used. The geometric MFI values of the samples were obtained by subtracting fluorescence of the stained specimen, obtained in the region marked M2 in Figure 5.2b, with autofluorescence of unstained specimen obtained in the region marked M1 in Figure 5.2a.

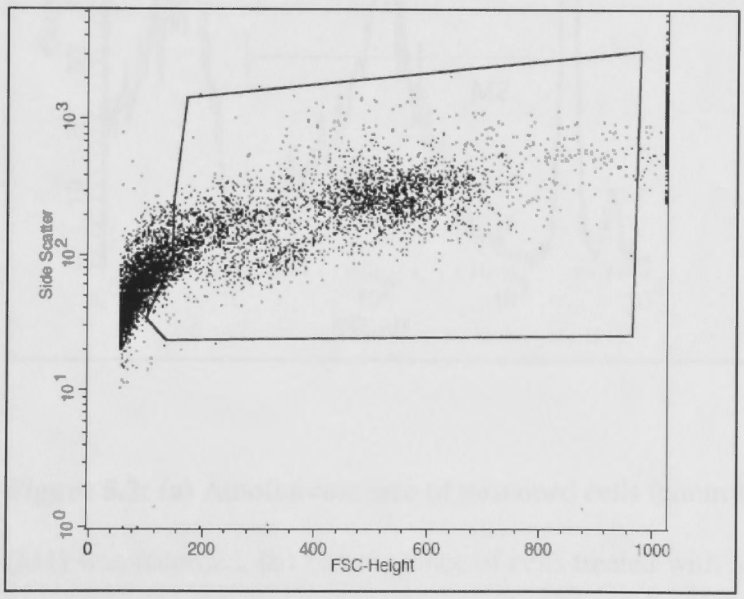

Figure 5.1: Cells were gated to exclude debris. FSC = forward scatter.

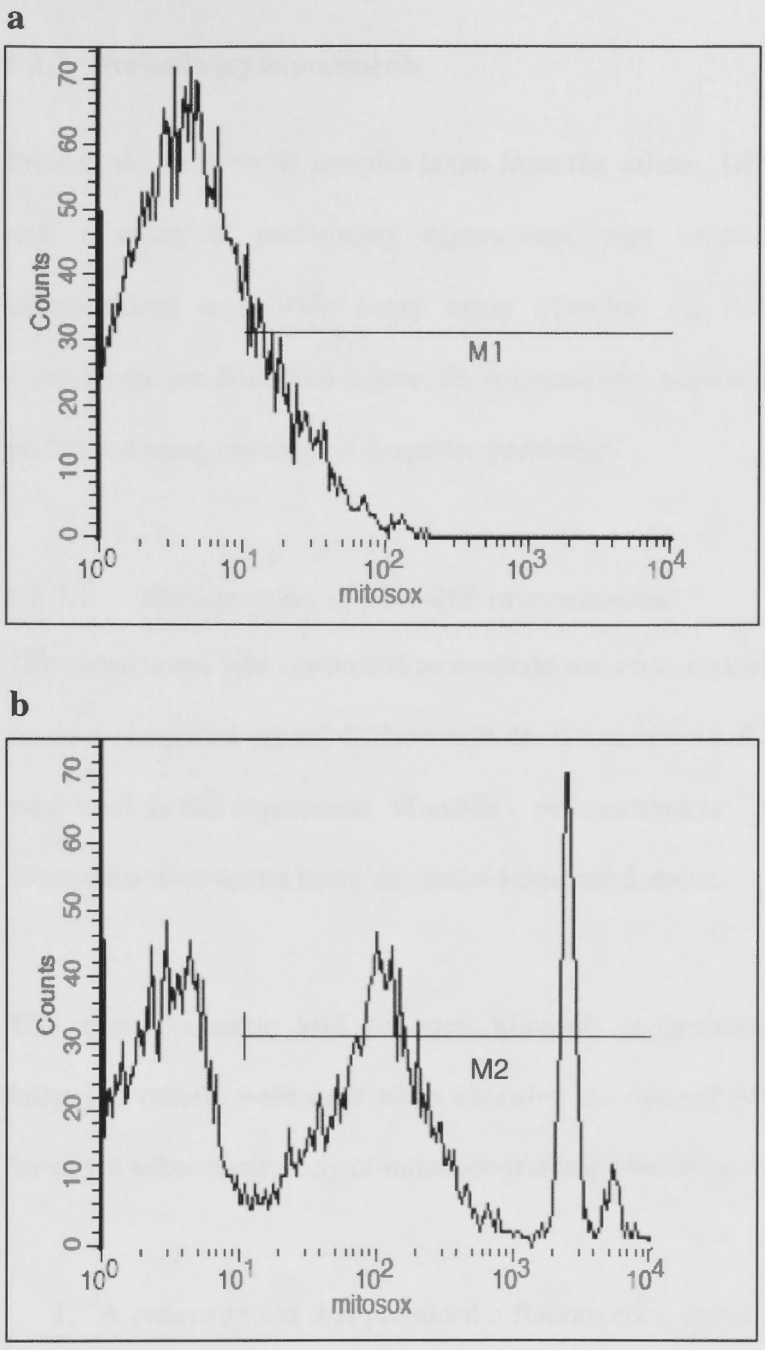

Figure 5.2: (a) Autofluorescence of unstained cells (control) in the marked region (M1) was recorded. **(b)** Fluorescence of cells treated with Mito-HE in the marked region (M2) was recorded. Net geometric MFI was calculated by subtracting the geometric MFI obtained in M2 region from M1 region.

5.2.7 Preliminary experiments

Prior to the analysis of samples taken from the saline-, DEX and ACTH-treated rats, a series of preliminary experiments were conducted to validate the mitochondrial superoxide assay using Mito-HE via flow cytometry. These experiments are described below. Flow cytometric acquisition and analysis were performed using the method described previously.

5.2.7.1 Optimisation of Mito-HE concentration

This experiment was conducted to evaluate the concentration of Mito-HE which resulted in optimal signal. Kidney cells from four untreated Sprague-Dawley rats were used in this experiment. Mito-HE concentrations of 1 to 10 μM with 1 μM increments were tested using the method described above.

The mean geometric MFI for each Mito-HE concentration was plotted. The following criteria were used when choosing the optimal Mito-HE concentration for use in subsequent study of mitochondrial superoxide generation:

1. A concentration that produced a fluorescence signal that was not affected by background autofluorescence.

2. A concentration that was not cytotoxic. Changes in cell morphology due to cell damage can alter the scatter properties of the cells.

3. A concentration that produced maximal separation of negative and positive population at the above flow cytometric settings.

5.2.7.2 Positive control

Antimycin A (Sigma-Aldrich, St Louis, USA) is a mixture product originating from *Streptomycin kitazawensis* which consists of Antimycin A1 and A3a (Nakayama, Okamoto *et al.* 1956). It blocks the mitochondrial electron transport chain at the Complex III and results in the breakdown of the proton gradient across the inner mitochondrial membrane and thus, the mitochondrial membrane potential (Campo, Kinnally *et al.* 1992; Pham, Robinson *et al.* 2000). Antimycin A, at concentrations ranging from 2 to 20 μM, can also increase mitochondrial superoxide production in both isolated mitochondrial preparations and live cells (Du, Daniels *et al.* 2006; Meany, Poe *et al.* 2006; Robinson, Janes *et al.* 2006; Mukhopadhyay, Rajesh *et al.* 2007). I used 5 μM Antimycin A to establish a positive control to validate mitochondrial superoxide generation with Mito-HE. To ensure that this concentration did not collapse the mitochondrial membrane potential, a phenomenon that could lead to a false positive Mito-HE signal, cells were counterstained with $DiIC_1(5)$.

Antimycin A (MW 548.7) was reconstituted in 95% ethanol to give a 400 μM solution. It was further dissolved in PBS before being used to incubate the cells at a final concentration of 5 μM. Cells were incubated with Antimycin A for 15 minutes prior to staining with Mito-HE and $DiIC_1(5)$. The geometric MFI for both dyes were evaluated using the flow cytometric analysis method described above.

5.2.7.3 Negative control

Tiron or sodium dihydroxybenzene disulfonate (Fluka, Steinheim, Germany), a membrane permeable superoxide mimetic agent, was used to lower superoxide in the mitochondria. It has been widely used in concentrations of 10-30 mM to evaluate the biological responses of superoxide *in vitro* (Hein and Kuo 1998; MacKenzie and Martin 1998; Arimura, Egashira *et al.* 2001). (Kondo-Nakamura, Shintani-Ishida *et al.*). Tiron (5 mM) has also been successfully used to inhibit carbon monoxide-induced superoxide production in cardioblastic H9c2 cells *in vitro*. It was reported that brief exposure (approximately 15 min) of cells to concentrations of 50 and 100 mM resulted in no cytotoxicity (Krishna, Liebmann *et al.* 1992). In the present study, I used 5 mM Tiron to establish a negative control to validate mitochondrial superoxide generation with Mito-HE.

Tiron (MW 314.20), which was prepared in PBS, was added to the cells to give a final concentration of 50 mM before the addition of Mito-HE and $DiIC_1(5)$ dyes.

5.2.8 Assessment of kidney mitochondrial superoxide in GC-HT

In this part of the study, mitochondrial superoxide in kidney cells of rats treated with saline, DEX or ACTH were evaluated.

5.2.8.1 Experimental animals

Male Sprague-Dawley rats (initial body weight of 250-270 g) were housed and acclimatised as described in Sections 2.2 and 2.3 of Chapter 2.

The rats were treated with ACTH (0.2 mg/kg/day), DEX (0.03 mg/kg/day) or sterile saline (vehicle for ACTH and DEX, 0.9% NaCl, 0.1 mL/rat/day) for 12 days (T0-T11) after 4 control days (C4-C1).

Group 1. Sterile saline (n = 16, of which 10 rats were pooled from the studies in Chapter 6)

Group 2. ACTH (n = 15, of which 10 rats were pooled from the studies in Chapter 6)

Group 3. DEX (n = 15, of which 10 rats were pooled from the studies in Chapter 6)

5.2.8.2 Systolic blood pressure and body weight measurements

The animals underwent second-daily tail cuff experiments from day T0 until day T10 at 9-11 am using the method as described in Section 2.5.1 of Chapter 2. Body weight measurements were recorded on alternate days after the tail-cuff SBP measurements.

5.2.8.3 Thymus weight

At the end of the experiment, these rats were sacrificed under anaesthesia. Thymus resection and blood sampling procedures were as described in Sections 2.8.5.1 and 2.8.4 of Chapter 2, respectively.

Thymus wet weight, expressed relative to body weight (grams thymus weight per 100 g body weight), was used as a marker of glucocorticoid activity.

5.2.8.4 Kidney mitochondrial Mito-HE fluorescence analysis

Mito-HE fluorescence intensity was used as a marker of mitochondrial superoxide availability. The kidneys were harvested, prepared for Mito-HE staining and analysed using flow cytometry as described in Sections 5.2.3 to 5.2.6 (above).

5.2.8.5 Kidney mitochondrial $DiIC_1(5)$ fluorescence analysis

$DiIC_1(5)$ fluorescence intensity was used to determine the mitochondrial membrane potential. The method for this analysis was described in Sections 5.2.5 and 5.2.6 (above).

5.2.9 Statistical analysis

Results were expressed as mean ± SEM. Statistical analysis were as described in Section 2.12 of Chapter 2.

5.3 RESULTS

5.3.1 Preliminary experiments

5.3.1.1 Optimisation of Mito-HE concentration

Concentrations up to 3 μM resulted in a steady increase in Mito-HE geometric MFI. This signal plateaued at concentrations between 3-6 μM and declined at

concentrations > 6 μM (Figure 5.3 and Table 5.1). To minimise risk of cytotoxicity initiated by Mito-HE, which might in turn result in cell and mitochondrial damage, a concentration 1 μM below the concentration that produced the maximal geometric MFI (ie 2 μM) was chosen.

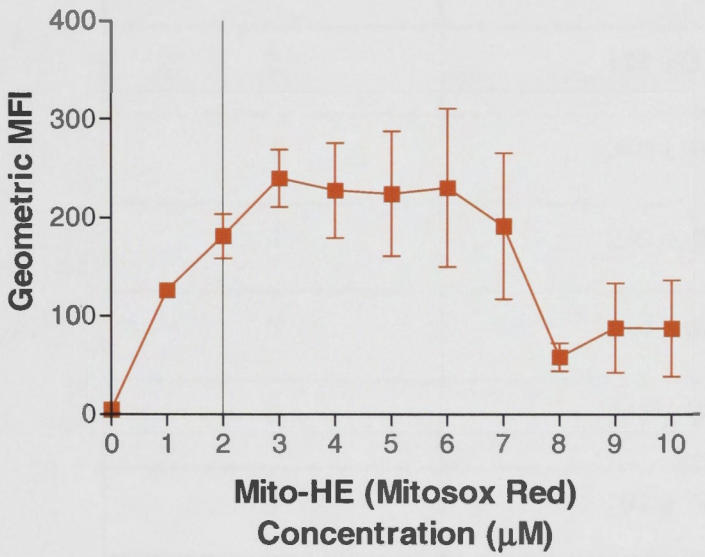

Figure 5.3: Mito-HE titration curve, n = 4.

Table 5.1: Mito-HE geometric mean fluorescence intensity generated by the different Mito-HE concentrations

Mito-HE concentration	Geometric MFI (mean ± SEM)
0	5 ± 1
1	126 ± 7
2	181 ± 23
3	240 ± 29
4	228 ± 48
5	224 ± 63
6	230 ± 80
7	191 ± 74
8	59 ± 14
9	88 ± 45
10	88 ± 49

5.3.1.2 Positive control

Cells pre-treated with 5 μM Antimycin A had significantly higher Mito-HE fluorescence (694 ± 105, n = 6) compared with untreated cells (control, 213 ± 27, n = 6, $P < 0.005$) (Figure 5.4). Antimycin A at 5 μM did not significantly reduce

mitochondrial membrane potential as indicated by $DiIC_1(5)$ geometric MFI (control: 136 ± 49 and Antimycin A: 72 ± 12, n = 6 each, *ns*) (Figure 5.5).

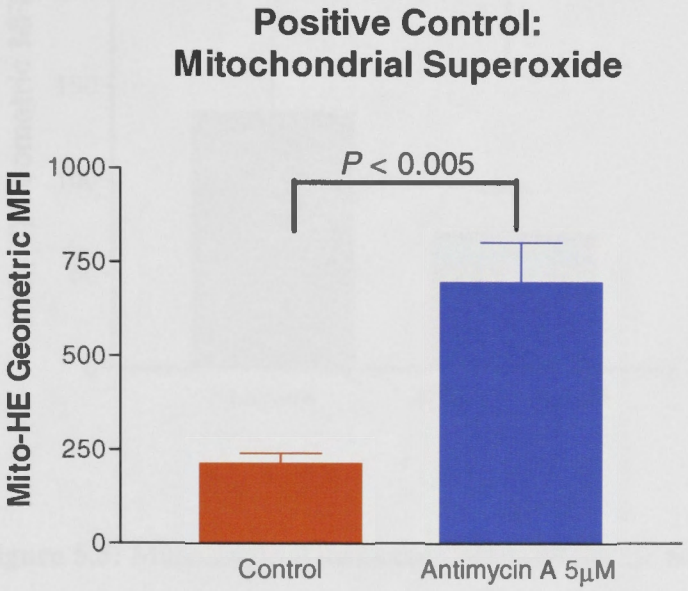

Figure 5.4: Mitochondrial superoxide availability for the positive control established using Antimycin A. Control, n = 6, Antimycin A, n = 6.

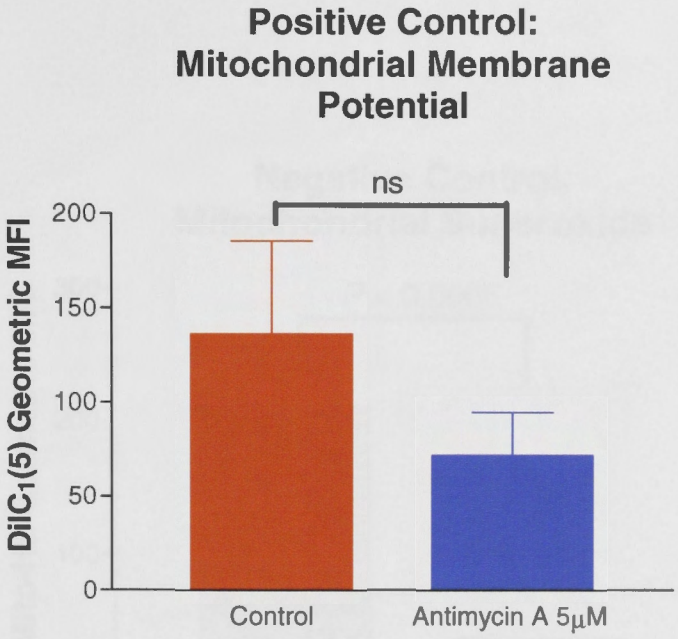

Figure 5.5: Mitochondrial membrane potential for the positive control established using Antimycin A. Control, n = 6, Antimycin A, n = 6, ns = not significant.

5.3.1.3 Negative control

Tiron at 50 mM resulted in significant reduction in Mito-HE geometric MFI (37 ± 6, n = 6) compared to controls (213 ± 27, n = 6, $P < 0.0005$) (Figure 5.6). At this concentration, Tiron did not significantly alter mitochondrial membrane potential as represented by $DiIC_1(5)$ geometric MFI (control: 136 ± 49 and Tiron: 115 ± 34, n = 6 each, *ns*) (Figure 5.7).

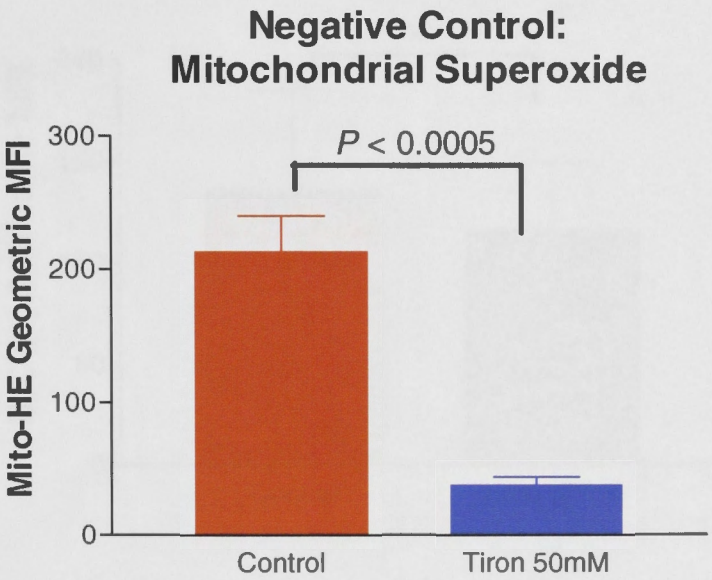

Figure 5.6: Mitochondrial superoxide availability for the negative control established using Antimycin A. Control, n = 6, Tiron, n = 6.

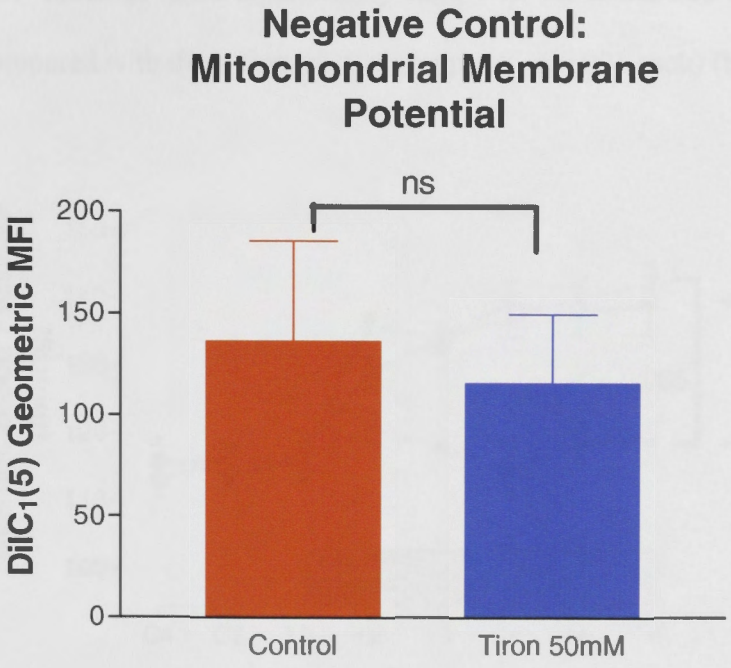

Figure 5.7: Mitochondrial membrane potential for the negative control established using Tiron. Control, n = 6, Tiron, n = 6, ns = not significant.

5.3.2 Assessment of kidney mitochondrial superoxide in GC-HT

5.3.2.1 Systolic blood pressure

SBP was significantly elevated in DEX-treated rats from 116 ± 2 mmHg on day T0 to 142 ± 3 mmHg on day T10 (n = 15, $P < 0.0005$). Similarly, SBP in ACTH-treated rats was significantly raised from 116 ± 3 mmHg on day T0 to 139 ± 5 mmHg on day T10 (n =15, $P < 0.0005$). Saline did not alter SBP (T0: 116 ± 2 mmHg, and T10: 119 ± 3 mmHg, n = 16, *ns*) (Figure 5.8).

SBP readings were significantly higher in the DEX and ACTH-treated groups compared with the saline-treated groups ($P' < 0.001$ each) (Figure 5.8).

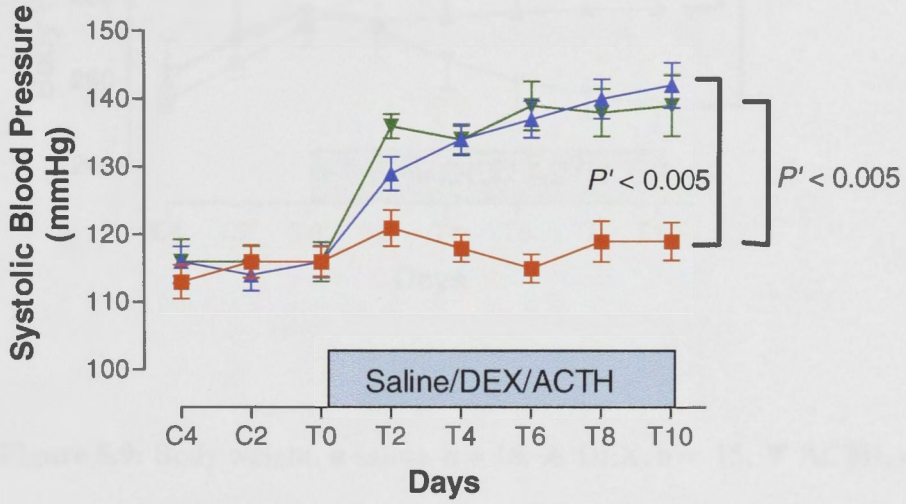

Figure 5.8: Systolic blood pressure. ■ saline, n = 16, ▲ DEX, n = 15, ▼ ACTH, n = 15.

5.3.2.2 Body weight

There was a significant weight increase in rats treated with saline from day T0 (273 ± 5 g) to day T10 (310 ± 5 g, n = 15, $P < 0.0005$). DEX-treated rats had no significant body weight change between day T0 (277 ± 9 g) to day T10 (277 ± 8 g, n = 15, *ns*). Rats on ACTH treatment had progressive weight loss from 276 ± 8 g on day T0 to 254 ± 6 g (n = 16, $P < 0.0005$) (Figure 5.9).

Overall, rats treated with DEX and ACTH had significantly lower body weight than those on saline treatment ($P' < 0.001$ each) (Figure 5.9).

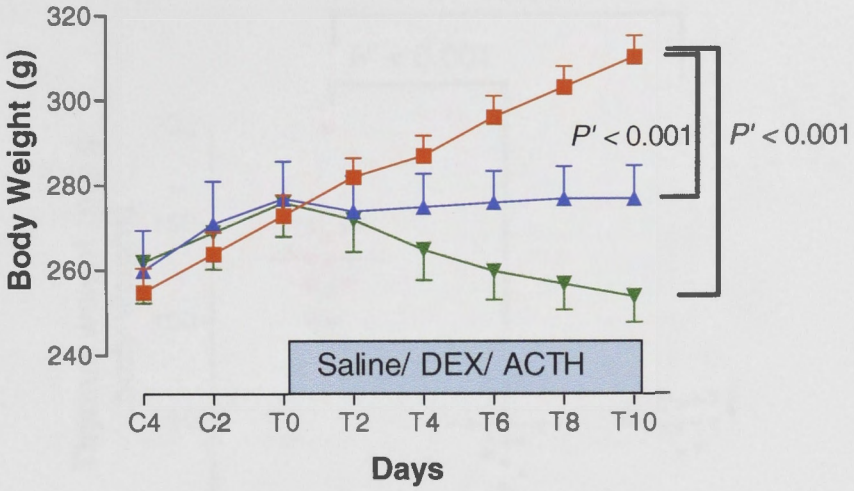

Figure 5.9: Body weight. ■ saline, n = 16, ▲ DEX, n = 15, ▼ ACTH, n = 15.

5.3.2.3 Thymus weight

Thymus weight in DEX- (47 ± 5 mg/g body weight, n = 15) and ACTH-treated rats (59 ± 10 mg/g body weight, n = 15) was significantly lower compared to saline-treated rats (132 ± 7 mg/g body weight, n = 16, $P' < 0.001$ each) (Figure 5.10).

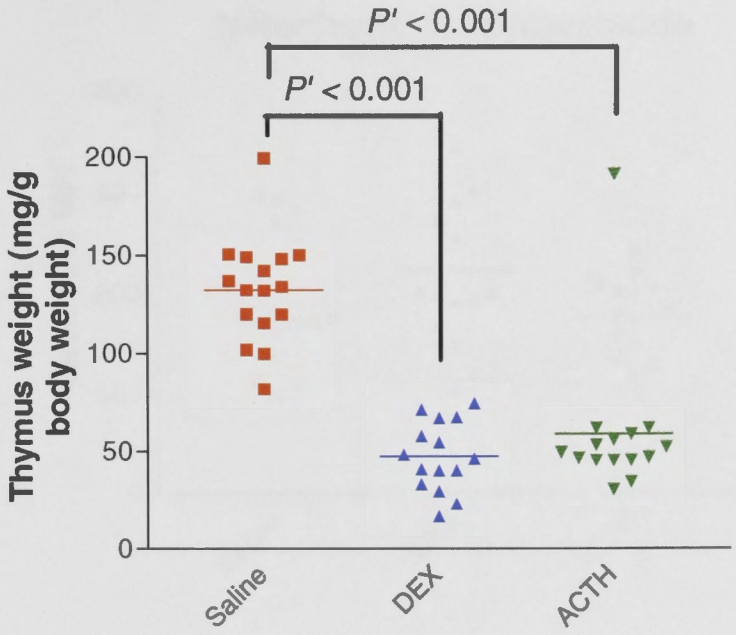

Figure 5.10: Thymus weight. ■ saline, n = 16, ▲ DEX, n = 15, ▼ ACTH, n = 15.

5.3.2.4 Kidney mitochondrial Mito-HE fluorescence analysis

There was no difference in kidney mitochondrial Mito-HE fluorescence intensity between the (DEX- 223 ± 20, n = 15) and ACTH-treated groups (176 ± 9, n = 15) compared with saline-treated group (188 ± 16, n = 16, *ns*) (Figure 5.11).

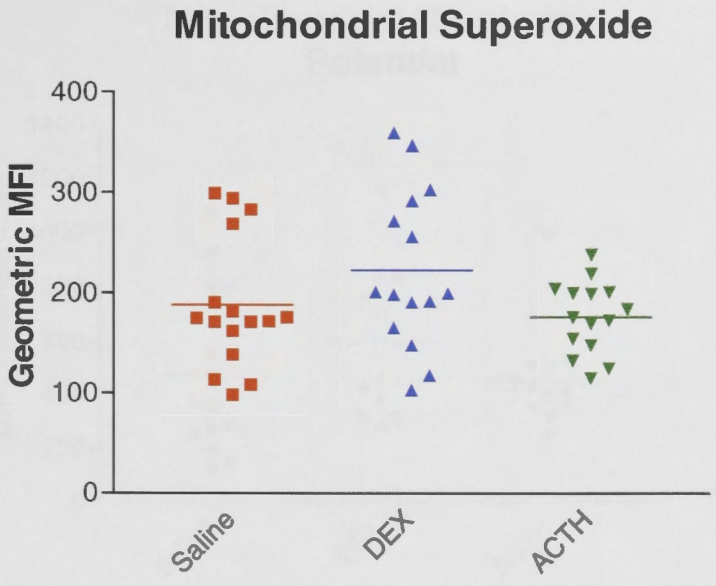

Figure 5.11: Kidney mitochondrial Mito-HE geometric mean fluorescence intensity as marker of mitochondrial superoxide availability. ■ saline, n = 16, ▲ DEX, n = 15, ▼ ACTH, n = 15.

5.3.2.5 Kidney mitochondrial $DiIC_1(5)$ fluorescence intensity

There was no difference in kidney mitochondrial $DiIC_1(5)$ fluorescence intensity between DEX- (599 ± 75, n = 13) and ACTH- (451 ± 49, n = 13) treated groups compared with saline-treated group (476 ± 82, n = 14, *ns*).

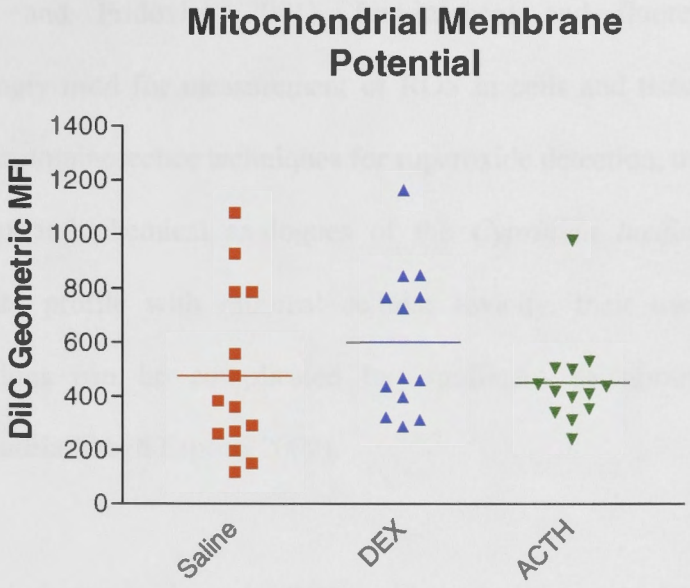

Figure 5.12: Kidney mitochondrial $DiIC_1(5)$ mean fluorescence intensity as marker of mitochondrial membrane potential. ■ saline, n = 14, ▲ DEX, n = 13, ▼ ACTH, n = 13.

5.4 DISCUSSION

Laboratory assessment of reactive oxygen species remains very challenging. Superoxide, the first ROS to be generated, has a very short half life. Its rapid dismutation by MnSOD and interaction with other compounds make its detection rather difficult and arduous. Earlier techniques which employed spectrophotometry such as cytochrome c reduction, adenochrome formation and nitroblue tetrazolium are associated with limited specificity and sensitivity

(Tarpey and Fridovich 2001). Luminescent and fluorescent probes are increasingly used for measurement of ROS in cells and tissues. Despite claims that chemiluminescence techniques for superoxide detection, using probes such as lucigenin and chemical analogues of the *Cyprinida luciferin*, offer a better sensitivity profile with minimal cellular toxicity, their use in mitochondrial preparations can be complicated by significant background reactions with mitochondria (Degli Esposti 2002).

Information on mitochondrial ROS has been based largely on studies performed on mechanically-isolated mitochondrial preparations or submitochondrial particles. Mechanical isolation of mitochondria from their natural cellular environment through differential centrifugation can affect the bioenergetics of the electron transport chain. Nohl *et al.* argued that previous claims that mitochondrial ROS production are byproducts of cellular respirations may simply reflect bioenergetic artefacts consequent on mechanical mitochondrial isolation (Nohl, Gille *et al.* 2005). Some workers examined mitochondrial ROS in intact live cells to avoid this artefact though this remains challenging experimentally (Dawson, Gores *et al.* 1993; Vanden Hoek, Shao *et al.* 1997; Duranteau, Chandel *et al.* 1998). Whilst this is possible for detection of hydrogen peroxide which is membrane permeable and stable, the detection of mitochondrial superoxide in live cells becomes more problematic as it is heavily affected by mitochondrial superoxide dismutase, a tightly regulated superoxide scavenger within the mitochondria. Furthermore, their activity varies with the different cell lines. One

of the techniques that is increasingly used is *in situ* evaluation of mitochondrial superoxide using a novel fluorescence dye, Mito-HE.

In this experiment, Mito-HE probe was used in flow cytometry to detect mitochondrial superoxide in live cells. The use of flow cytometry allows a large number of cells to be analysed rapidly. Simultaneous quantitative measurements of a number of parameters such as mitochondrial superoxide and membrane potential, or other markers are also possible with this technique. In addition, cell debris can also be excluded from analysis. With this method, which only detects fluorescence associated with particles, lower Mito-HE concentrations can be used. Whilst 5 μM is recommended for other fluorometric techniques, lower Mito-HE concentrations can be used in flow cytometry. In this study, we have shown that Mito-HE concentration of more than 5 μM can result in reductions in mitochondrial membrane potentials and decrease uptake and fluorescence of Mito-HE in this cell preparation. It is also important to do parallel assessment of mitochondrial membrane potential to ensure that cell treatments, including Mito-HE dye loading itself, do not depolarise the mitochondria in the cells as Mito-HE requires a membrane potential across the inner mitochondrial membrane to accumulate there. Otherwise, Mito-HE can be oxidised elsewhere in the cell and result in falsely positive signals for mitochondrial superoxide.

There are also a number of limitations associated with the use of the HE-based assay. Superoxide reacts with Mito-HE to form two highly fluorescent compounds, HO-Mito-Etd^+ and Mito-Etd^+ that can be detected optimally by

excitation wavelengths of 396 and 510 nm respectively. HO-Mito-Etd$^+$ is more specific for superoxide whilst Mito-Etd$^+$ can be generated by other non-specific oxidation products (Robinson, Janes *et al.* 2006). Standard lasers available on flow cytometers can excite fluorophores at 488 and 405 nm. Whilst excitation wavelength at 488 nm fluoresces Mito-HE oxidation product very well, its specificity can be enhanced by using lower excitation wavelengths (eg 405 nm when used for flow cytometry) (Robinson, Janes *et al.* 2006). However, at this near ultraviolet wavelength, the autofluorescence can be intense and may be difficult to exclude fully from flow data analysis. In this study, a flow cytometer with an excitation wavelength of 488 nm was used as the issue associated with decreased specificity was accounted for by having a saline-treated control group in the study. Any increase in fluorescent signal generated by the glucocorticoid-induced hypertensive group in comparison with the control group could therefore be presumed to correlate with mitochondrial superoxide. Another limitation with the use of a fluorescent dye is that Mito-HE is prone to photo-oxidation and its oxidation product susceptible to photo-bleaching. Thus light exposure needs to be kept to a minimum during the experiment as was done in this study.

Antimycin A and Tiron were used as positive and negative controls respectively to validate mitochondrial superoxide generation with Mito-HE. The validation studies described in Sections 5.2.6 and 5.2.7 showed that Mito-HE can detect an increase in kidney mitochondrial superoxide induced biochemically using Antimycin A and a decrease due to the scavenging effect of Tiron. Although Antimycin A can result in loss of mitochondrial membrane potential, a

phenomenon known to result in the uptake of Mito-HE in sites other than the mitochondria, the concentration used in this study (5 μM) did not affect the membrane potential. Tiron at 50mM also did not significantly reduce mitochondrial membrane potential, and thus is unlikely to affect the specificity of the results. The main limitation of these controls was that the stimulation and inhibition of mitochondrial superoxide were done in *in vitro* rather than in *in vivo* models. However, the latter was not feasible given the toxicity of these agents.

In this study, cells from the kidney were used for several reasons. Firstly, the kidney is a highly-vascularised organ, rich in resistance blood vessels. Secondly, the kidney is relevant to GC-HT. We have previously shown that ACTH-HT, a model mainly mediated by cortisol, is associated with increased renal vascular resistance (Wen, Fraser *et al.* 1998; Wen, Fraser *et al.* 1999). Furthermore, the rise in BP due to ACTH in rats was accompanied by reductions in iNOS and eNOS gene expression in the kidney (Lou, Wen *et al.* 2001).

Although the Mito-HE probe has mainly been used in high performance liquid chromatography and fluorescent microscopy, I have independently developed a method for its use in flow cytometry for our laboratory with technical assistance from Dr Harpreet Vohra (Flow Cytometry Resource Facility, John Curtin School of Medical Research). Since the development of this technique for use in the studies of the role of mitochondrial superoxide in GC-HT (current chapter and Chapter 6), there have been a number of other researchers who have published work using Mito-HE in flow cytometry. Table 5.1 summarises the studies to date

using Mito-HE in flow cytometry. Whilst there were similarities with the flow technique used in these studies, such as the use of 488 nm excitation wavelength, there were also several important differences that need to be highlighted.

Most of these authors used 5 μM Mito-HE, as per the manufacturer's protocol (Product information via http://probes.invitrogen.com/media/pis/mp36008.pdf) which was developed using live bovine pulmonary epithelial cells, MRC5 human lung fibroblasts and mouse 3T3 fibroblasts for used in fluorescence microscopy. Thus, the concentration for optimal fluorescence without causing cytotoxicity for other cell lines cannot be assumed. The optimal Mito-HE concentration needs to be individually optimised and assessed based on the different cell lines and experimental conditions.

Another fundamental difference between the present study and some of those listed on Table 5.1 was the concurrent determination of the mitochondrial membrane potential. This is a crucial step as uptake of Mito-HE into mitochondria is a function of mitochondrial membrane potential (Robinson, Janes *et al.* 2008). False positive results can be a consequence of collapsed mitochondrial membrane potential rather than excess mitochondrial superoxide production. Only a few studies performed this crucial analysis (Zhang, Soboloff *et al.* 2006; Dvorak, Payne *et al.* 2007; Payne, Weber *et al.* 2007; Cordero, De Miguel *et al.* 2010). These investigators assessed the mitochondrial membrane potential to assess mitochondrial integrity but failed to recognise the confounding effect of collapsed mitochondrial membrane potential on fluorescence analysis using Mito-HE.

Furthermore, validations with positive and negative controls were not performed in some of the studies listed (Table 5.2).

Some of these authors have validated the flow cytometric technique with confocal microscopy and confirmed that the fluorescence signal due to the oxidation products of Mito-HE was indeed a consequence of mitochondrial superoxide production. Using confocal microscopy, Mukhopadhyay *et al* also showed that Mito-HE staining is enhanced in dead cells (Mukhopadhyay, Rajesh *et al.* 2007). Nevertheless, dead and damaged cells have already being excluded from the present study and further analysis using confocal microscopy is unlikely to provide any extra information.

Table 5.2: Use of Mito-HE in flow cytometry

Cell Type	Method	Mito-HE concentration (μM)	Positive Control	Negative Control	Membrane Potential Assessment	References
Human promyelocytic (HL-60) cells	Flow cytometry	5	Atractyloside	-	JC-1	(Zhang, Soboloff *et al.* 2006)
Oesophageal adenocarcinoma (Seg 1) cells	Flow cytometry	5	-	-	Mitotracker Red	(Dvorak, Payne *et al.* 2007)
Colon carcinoma (HCT 116) cells	Flow cytometry	5	Deoxycholate	-	Mitotracker Red	(Payne, Weber *et al.* 2007)
Human diffuse large cell lymphoma (OCI-Ly 19), Human Burkitts Lymphoma (Ramos), normal human B cells	Flow cytometry	5	-	-	-	(Brookes, Morse *et al.* 2007)
Human hepatoma (HepG2, H9C2) cells	Flow cytometry	5	-	-	-	(Lund, Peterson *et al.* 2007)
HCAEC	Flow cytometry	5	-	-	-	(Rajesh, Mukhopadhyay *et al.* 2007)

Cell Type	Method	Mito-HE concentration (μM)	Positive Control	Negative Control	Membrane Potential Assessment	References
Rat embryonic ventricular myocardial (H9c2) cells and HCAEC	Flow cytometry, confocal microscopy	5	Antimycin A, Paraquat	Cell-permeable SOD	-	(Mukhopadhyay, Rajesh *et al.* 2007a)
HCAEC, PMVEC	Flow cytometry	5	Antimycin A, doxorubicin	Cell-permeable SOD	-	(Mukhopadhyay, Rajesh *et al.* 2007)
Human spermatozoa	Flow cytometry, confocal microscopy	2	Rotenone	-	-	(Koppers, De Iuliis *et al.* 2008)
Blood mononuclear cells	Flow cytometry	1	-	-	Mitotracker Red	(Cordero, De Miguel *et al.* 2010)

HCAEC = human coronary artery endothelial cells , HPMVEC = Human pulmonary micorvascular endothelial cells, SOD = superoxide dismutase.

The *in vivo* physiological studies verified previous findings that both ACTH and DEX increased SBP in rats (Zhang, Jang *et al.* 2003; Hu, Zhang *et al.* 2006). This increase in blood pressure was accompanied by a decrease in thymus weight implicating increased glucocorticoid activity induced by ACTH and DEX injections; and oxidative stress as indicated by an increase in plasma F_2-isoprostane concentration (Ong, Zhang *et al.* 2008) (Sections 6.3.7, 8.3.7, 11.2). In this study, however, ACTH and DEX did not result in a significant increase in Mito-HE geometric MFI despite producing blood pressure elevation. Possibly the increase in mitochondrial superoxide generation in GC-hypertensive rats was not large enough for a change to be detected. Another possible explanation is that Mito-HE oxidation by superoxide (rate constant of ~10^6 M^{-1} s^{-1}) produced in the impermeable compartment could not surpass the efficacy of endogenous mitochondrial superoxide dismutase (rate constant > 10^9 M^{-1} s^{-1}). Nevertheless, this study did not find any evidence that mitochondrial superoxide plays a major role in the pathogenesis of GC-HT.

5.5 CONCLUSION

In this study, kidney mitochondrial superoxide was not increased in glucocorticoid-induced hypertensive rats, suggesting that mitochondrial superoxide does not play a significant role in the pathogenesis of glucocorticoid hypertension.

The role of mitochondrial superoxide in GC-HT is further evaluated and discussed in Chapter 6.

CHAPTER 6

Role of Mitochondrial Superoxide in Glucocorticoid-Induced Hypertension in the Rat

6.1 INTRODUCTION

Mitochondrial ROS have been implicated in the pathogenesis of hypertension. Treatment with alpha-lipoic acid, an antioxidant that can improve mitochondrial function (Hagen, Ingersoll *et al.* 1999), prevented both hypertension and mitochondrial ROS overproduction due to hyperglycemia in rats (El Midaoui, Elimadi *et al.* 2003) and thus suggested a role for mitochondrial ROS in this form of experimental hypertension. Mitochondrial superoxide dismutase deficiency has been shown to be linked with susceptibility to hypertension with aging and high salt intake in mouse (Rodriguez-Iturbe, Sepassi *et al.* 2007). The role of mitochondrial ROS overproduction in the development of glucocorticoid-induced hypertension is unclear.

Alpha-lipoic acid is a naturally-occuring short chain fatty acid that serves as an important cofactor for many enzyme complexes including mitochondrial respiratory enzymes. Exogenously-administered alpha-lipoic acid has been shown to be an effective antioxidant. Urinary F_2-isprostane concentration, a biomarker of lipid peroxidation, was significantly reduced after treatment with 600 mg/day alpha-lipoic acid orally for 2 months in humans (Marangon, Devaraj *et al.* 1999). Apart from this, alpha-lipoic acid has also been shown to improve mitochondrial function. A single dose of alpha-lipoic acid (100 mg/kg i.p.) resulted in improvement in mitochondrial function, determined by mitochondrial oxygen consumption and complex I, II and IV activities, in endotoxemic rats (Vanasco, Cimolai *et al.* 2008). Furthermore, alpha-lipoic acid supplementation (0.5% w/w)

improved the average mitochondrial membrane potential in old rats hepatocytes to that of young rats (Hagen, Ingersoll *et al.* 1999). Mitochondrial membrane potential is another indicator of mitochondrial health as it reflects the metabolic activity and integrity of mitochondrial membrane (Distelmaier, Koopman *et al.* 2008).

6.2 METHODS

This study was approved by the Animal Experimentation Ethics Committee of the Australian National University (Protocol No. J. HB. 20.05). Male Sprague-Dawley rats were housed and acclimatised as described in Sections 2.2 and 2.3 of Chapter 2. The general methodology for this study was as described in Chapter 2.

Alpha-lipoic acid powder (Sigma, St. Louis, USA) was administered by mixing in ground food and given to rats overnight (16-18 hours). Normal saline (0.9% NaCl, 0.1 mL/rat/day), DEX (10 μg/rat/day) and ACTH (0.2 mg/kg/day) were administered from day T0 to T11 using the technique described in Section 2.3 of Chapter 2.

The rats were randomly divided into 9 treatment groups. The alpha-lipoic acid prevention study was performed in both DEX- and ACTH-HT. The reversal study was only performed in DEX-HT as alpha-lipoic acid completely prevented DEX-HT.

Control groups

Control rats were allocated 30 g of plain ground food per rat per night (16-18 hours) from P0. Pelleted food was given during the control days and daytime (from approximately 0900 to 1700 hours) from P0.

Group 1: Saline (n = 10)

Group 2: DEX (n = 10)

Group 3: ACTH (n = 10)

Alpha lipoic acid prevention studies

In the prevention studies, rats were pre-treated with either alpha-lipoic acid (500 mg/kg in food) (El Midaoui, Elimadi *et al.* 2003) in ground food overnight (16-18 hours) from P0, 4 days before commencement of saline, DEX or ACTH injections. In another group of 4 rats, high dose alpha-lipoic acid (5 g/kg of ground food, starting at P0) was given prior to the commencement of ACTH injections from T0-T11.

Group 4. Alpha-lipoic acid + saline (n = 10)

Group 5. Alpha-lipoic acid + DEX (n = 10)

Group 6. Alpha-lipoic acid + ACTH (n = 10)

Group 7. Alpha-lipoic acid (high dose) + ACTH (n = 4)

Alpha lipoic acid reversal study

In the reversal studies, oral alpha-lipoic acid-laced food was given 4 days after the subcutaneous injections (T4-T11).

Group 8. Saline + alpha-lipoic acid (n=10)

Group 9. DEX + alpha-lipoic acid (n=10)

6.2.1 Tail-cuff blood pressure and body weight measurements

The animals underwent second-daily tail cuff experiments from day C4 until day T10 at 9-11 am using the method described in Section 2.5.1 of Chapter 2. Body weight measurements were recorded on alternate days after the tail-cuff SBP measurements.

6.2.2 Thymus weight

On day T11, rats were sacrificed under isoflurane anaesthesia. Thymus resection were as described in Section 2.8.5.1 of Chapter 2.

Thymus wet weight, expressed relative to body weight (grams thymus wet weight per 100 g body weight), was used as a marker of glucocorticoid activity.

6.2.3 Kidney Mito-HE and $DiIC_1(5)$ fluorescence

The kidneys were resected and prepared for mitochondrial superoxide determination using Mito-HE fluorescence analysis via flow cytometry technique as described in Section 5.2.3 of Chapter 5. This was used as marker of mitochondrial superoxide availability. Double staining with $DiIC_1(5)$ was performed using the technique described in Section 5.2.5 of Chapter 5 to assess mitochondrial membrane potential.

6.2.4 Blood glucose concentration

Blood was drawn via cardiac puncture as described in Section 2.8.4 of Chapter 2. A drop of blood was placed on the glucometer strip (Precision Plus Blood Glucose Electrodes, Abbott Laboratories, MA, USA) and the blood glucose concentration was read on a glucometer (MediSense 2, Abbott Laboratories, Bedford, MA, USA).

6.2.5 Plasma nitrate and nitrite assay

Plasma nitrate and nitrite (NOx) concentrations, measured using the Griess colorimetric reaction described in Section 2.10.1 of Chapter 2, were used as a marker of endogenous NO availability.

6.2.6 Plasma F_2-isoprostane assay

Plasma F_2-isoprostane concentration was used as a marker of systemic lipid peroxidation. The assay technique was described in Section 2.11.3 of Chapter 2.

6.2.7 Statistical analysis

Results were expressed as mean ± SEM. Statistical analysis were as described in Section 2.12 of Chapter 2.

6.3 RESULTS

6.3.1 Systolic blood pressure

DEX increased SBP from 115 ± 3 to 139 ± 4 mmHg (T0-T10, $P < 0.005$) and ACTH from 110 ± 3 to 133 ± 4 mmHg (T0-T10, $P < 0.0005$). Sham injection with sterile saline did not modify SBP (T0: 113 ± 2, T10: 119 ± 3 mmHg). Between group comparisons showed that SBP in the groups receiving DEX and ACTH were significantly higher than in the saline-treated group (n = 10 each, $P' < 0.001$).

6.3.1.1 Prevention studies

There was no significant change in SBP in the alpha-lipoic acid + saline group (T0: 111 ± 2, T10: 118 ± 3 mmHg, *ns*). With alpha-lipoic acid pre-treatment, DEX did not significantly increase SBP (T0: 117 ± 4, T10: 126 ± 5 mmHg, *ns*). However, there was a significant increase in SBP in ACTH-treated rats receiving

alpha-lipoic acid pretreatment (T0: 115 ± 2 to T10: 129 ± 5 mmHg, $P < 0.05$). Despite this, there was a significant decrease in SBP in the alpha-lipoic acid + ACTH group ($P' < 0.001$) when compared with the ACTH-only group, indicating partial prevention by alpha-lipoic acid. A tenfold increase in alpha-lipoic acid dose (100 mg/rat/day) did not decrease the SBP further. There was no difference in SBP between the alpha lipoic acid + saline-treated group and the saline-only group. SBP of the alpha-lipoic acid + DEX-treated group was significantly lower than that of the DEX-only group ($P' < 0.001$) (Figures 6.1a and b).

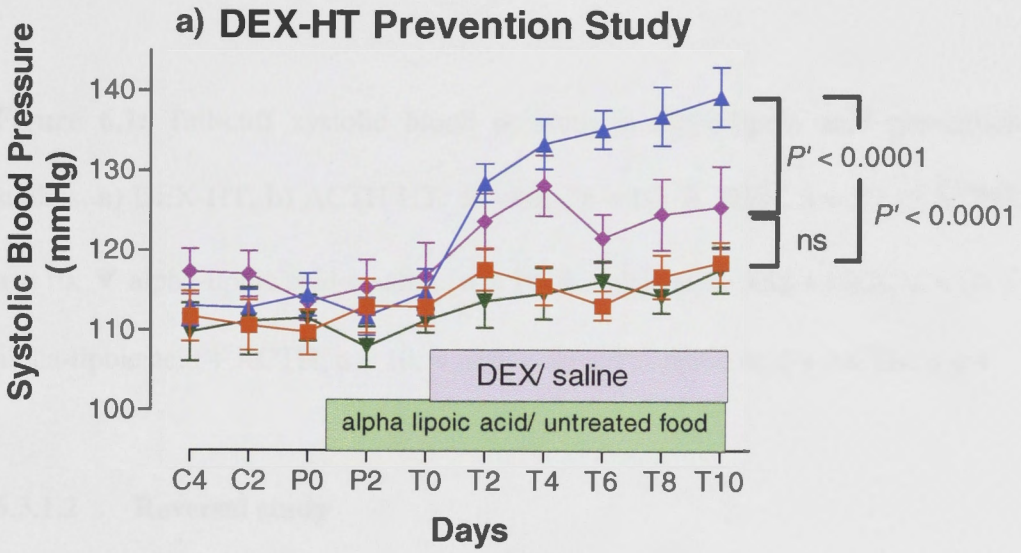

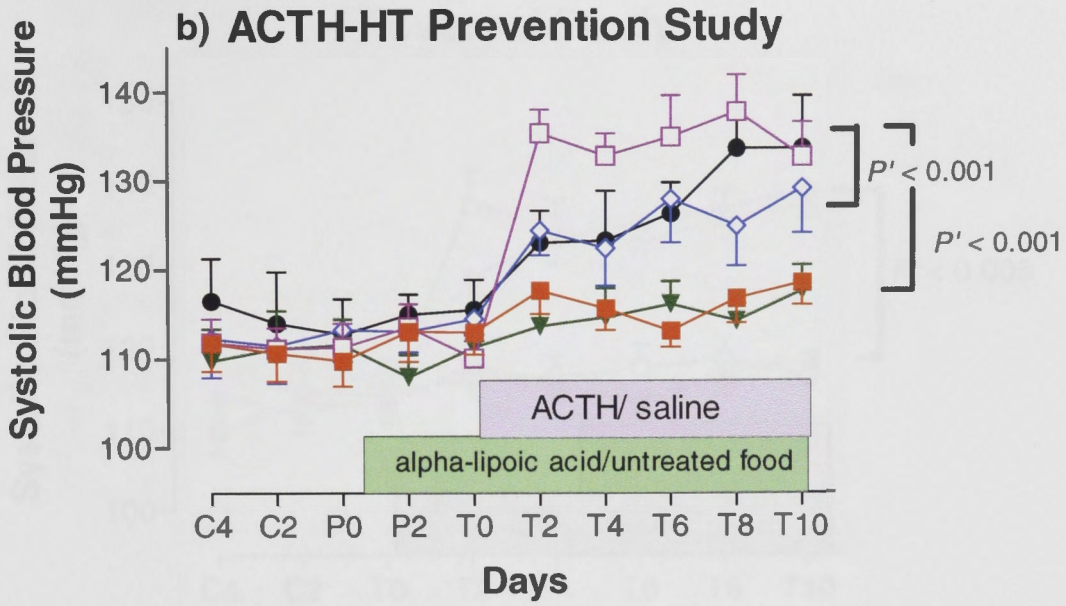

Figure 6.1: Tail-cuff systolic blood pressure in alpha-lipoic acid prevention studies. **a)** DEX-HT, **b)** ACTH-HT. ■ saline, n = 10; ▲ DEX, n = 10; □ ACTH, n = 10; ▼ alpha-lipoic acid + saline, n = 10; ♦ alpha-lipoic acid + DEX, n = 10, ◊ alpha-lipoic acid + ACTH, n = 10, ● high dose alpha-lipoic acid + ACTH, n = 4.

6.3.1.2 Reversal study

The increase in SBP due to DEX was not reversed by alpha-lipoic acid (10 mg/rat/day) treatment. Systolic BP on day T4, day 1 of alpha-lipoic acid treatment, was 134 ± 4 mmHg and on T10 was 137 ± 2 mmHg (n = 10, *ns*). As in the prevention study, alpha-lipoic acid did not alter SBP in the saline treated group (T4: 133 ± 3 mmHg; T10: 139 ± 4 mmHg, n = 10, *ns*) (Figure 6.2).

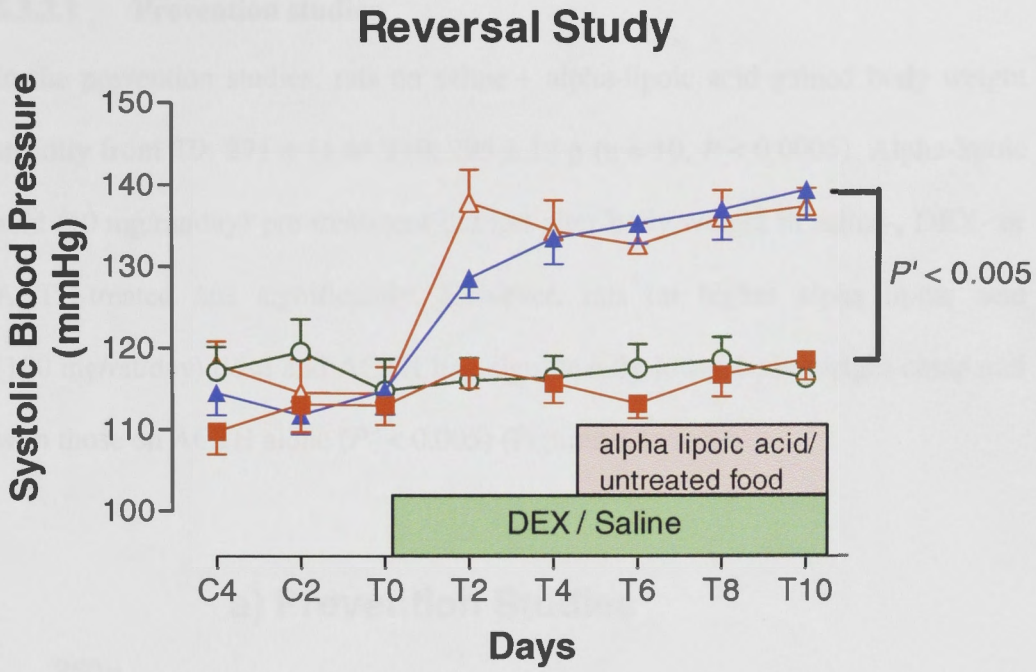

Figure 6.2: Tail-cuff systolic blood pressure in alpha-lipoic acid/ DEX-HT reversal study. ■ saline, n = 10; ▲ DEX, n = 10; ○ saline + alpha-lipoic acid, n = 10; Δ DEX + alpha-lipoic acid, n = 10.

6.3.2 Body weight

Body weight of saline-treated rats increased steadily from 270 ± 6 to 306 ± 7 g (T0-T10, $P < 0.0005$). DEX-treated rats did not gain significant body weight (T0: 272 ± 9, T10: 277 ± 7 g, T0-T10, *ns*) whilst ACTH treatment resulted in significant weight loss (from T0: 283 ± 11 to T10: 258 ± 8g, $P < 0.001$, $P < 0.0005$). In these studies, the DEX- and ACTH-treated groups showed significantly lower body weights than the saline-treated group ($P' < 0.005$).

6.3.2.1 Prevention studies

In the prevention studies, rats on saline + alpha-lipoic acid gained body weight steadily from T0: 271 ± 11 to T10: 295 ± 12 g (n = 10, $P < 0.0005$). Alpha-lipoic acid (10 mg/rat/day) pre-treatment did not alter body weight in saline-, DEX- or ACTH-treated rats significantly. However, rats on higher alpha lipoic acid (100 mg/rat/day) dose and ACTH had significantly lower body weight compared with those on ACTH alone ($P' < 0.005$) (Figures 6.3a and b).

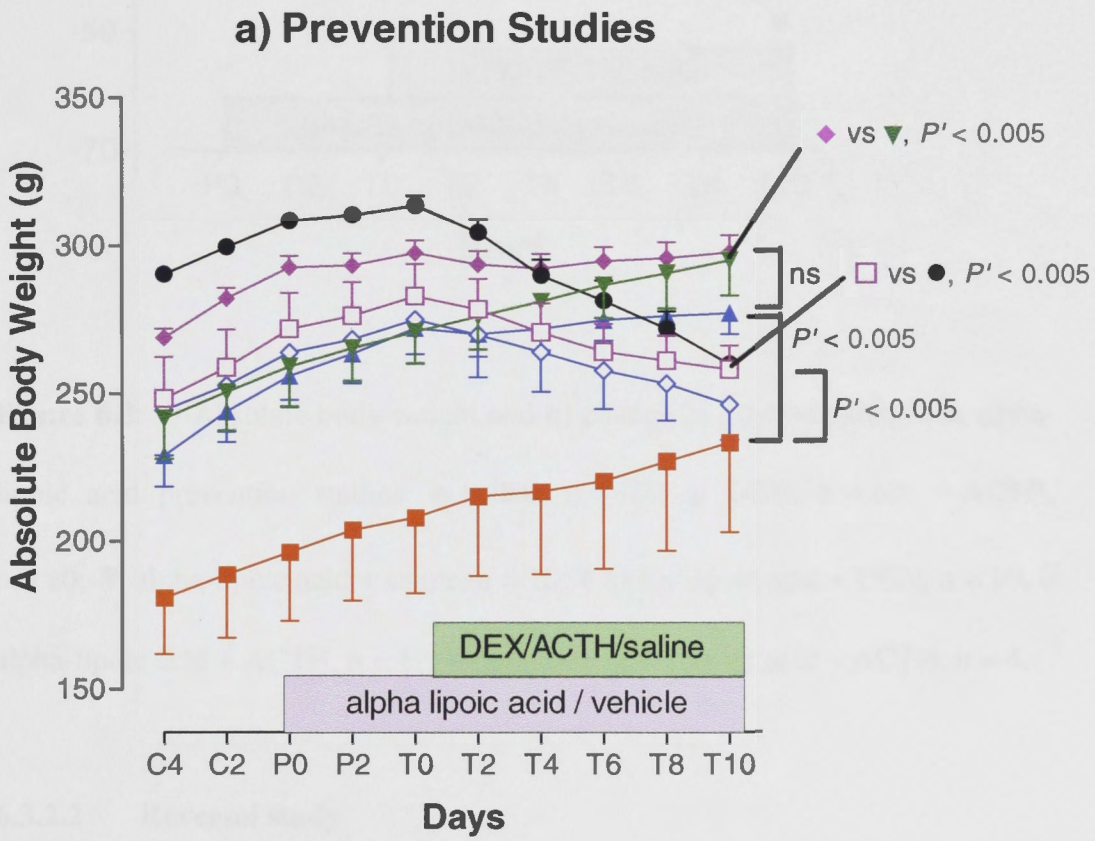

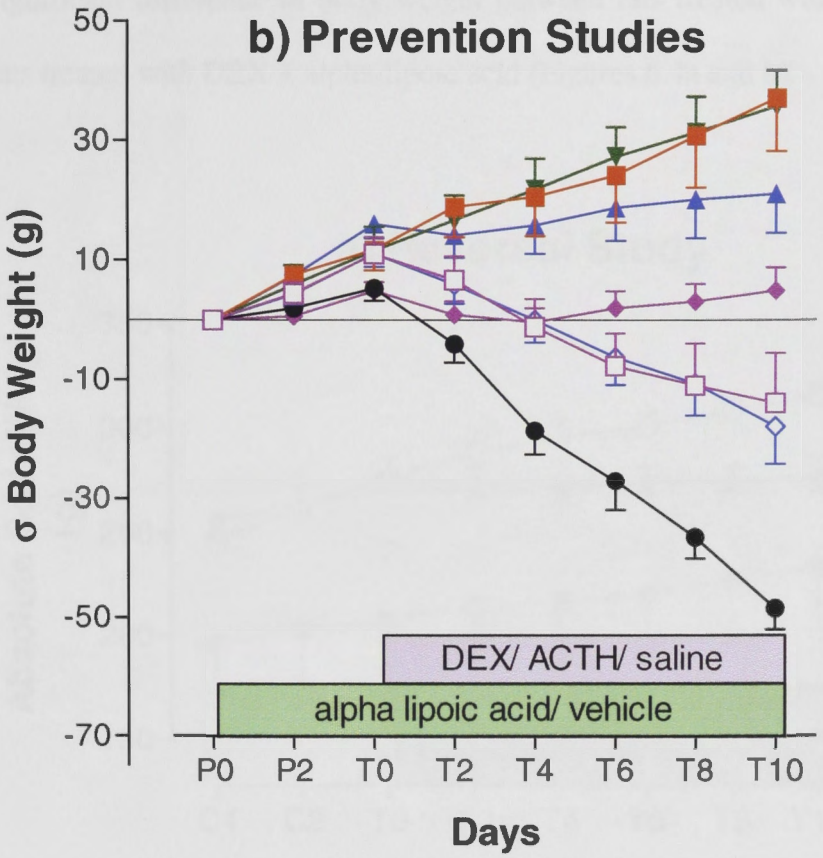

Figure 6.3: a) Absolute body weight and **b)** change (Δ) in body weight in alpha-lipoic acid prevention studies. ■ saline, n = 10; ▲ DEX, n = 10; □ ACTH, n = 10; ▼ alpha-lipoic acid + saline, n = 10; ♦ alpha-lipoic acid + DEX, n = 10, ◊ alpha-lipoic acid + ACTH, n = 10, ● high dose alpha lipoic acid + ACTH, n = 4.

6.3.2.2 Reversal study

In the reversal study, rats on DEX + alpha-lipoic acid failed to gain weight during the course of the study (from T4: 277 ± 10 to T10: 278 ± 8 g, n = 10, *ns*) whilst those on saline + alpha-lipoic acid gained weight progressively from day 276 ± 10 g on day T4 to 296 ± 10 g on day T10 (n = 10, $P' < 0.0005$). There was no

significant difference in body weight between rats treated with DEX alone and rats treated with DEX + alpha-lipoic acid (Figures 6.4a and b).

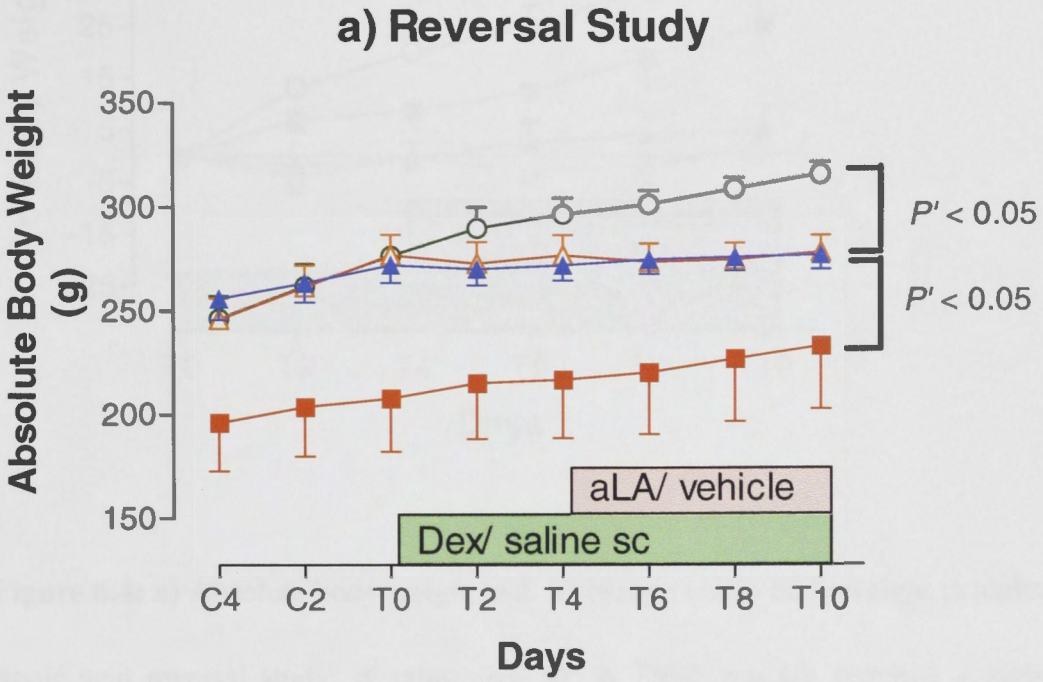

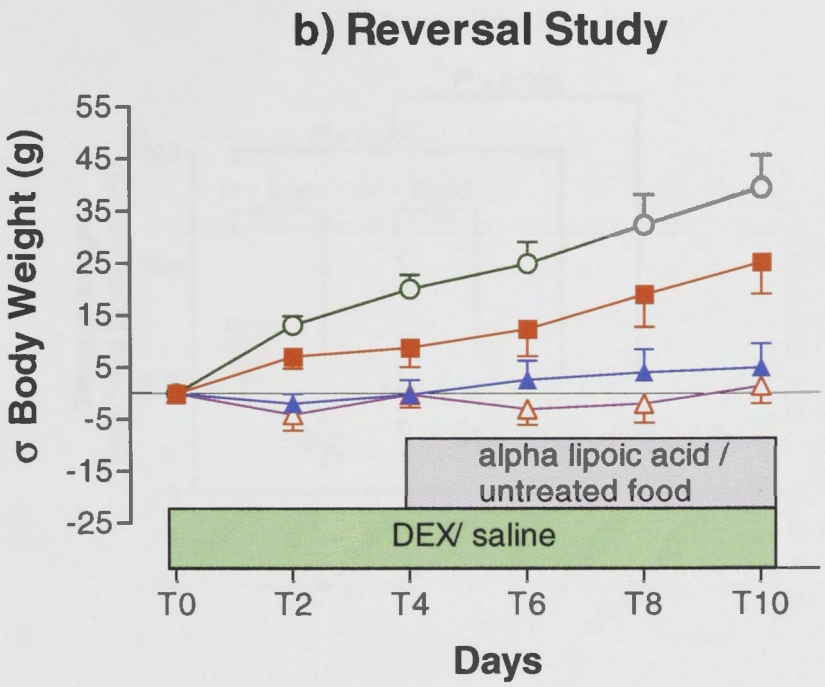

Figure 6.4: a) Absolute body weight and, **b)** change (Δ) in body weight in alpha-lipoic acid reversal study. ■ saline, n = 10; ▲ DEX, n = 10; ○ saline + alpha lipoic acid, n = 10; △ DEX + alpha lipoic acid, n = 10.

6.3.3 Thymus weight

Thymus wet weight was significantly lower with DEX and ACTH treatments compared with saline ($P'<0.005$) regardless of the presence of alpha-lipoic acid treatment ($P'<0.005$) (Figure 6.5 and Table 6.1).

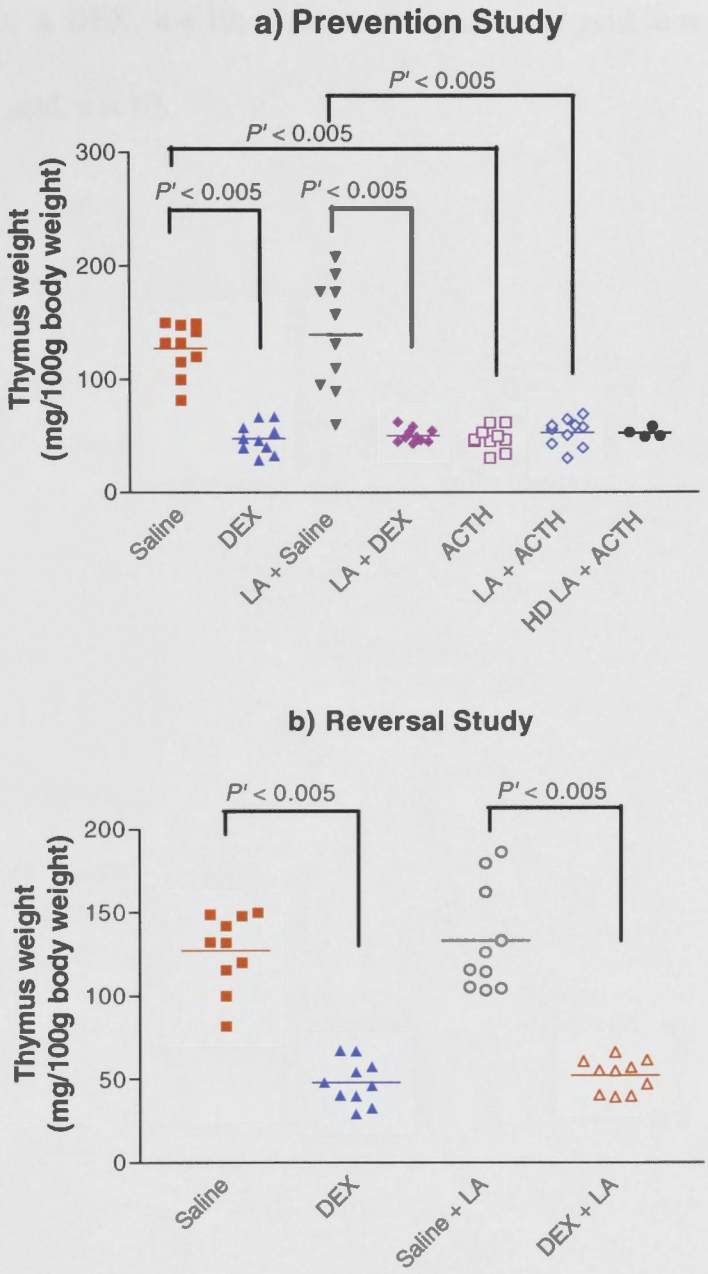

Figure 6.5: a) Thymus weight in the prevention study: ■ saline, n = 10; ▲ DEX, n = 10; □ ACTH, n = 10; ▼ alpha-lipoic acid (LA) + saline, n = 10; ♦ alpha-lipoic acid + DEX, n = 10, ◊ alpha-lipoic acid + ACTH, n = 10, ● high dose alpha-lipoic acid (HD LA) + ACTH, n = 4, **b)** Thymus weight in the reversal study: ■ saline,

n = 10; ▲ DEX, n = 10; ○ saline + alpha-lipoic acid, n = 10; △ DEX + alpha-lipoic acid, n = 10.

Table 6.1: Biological measurements for alpha lipoic acid studies.

Groups	Thymus (mg/100g body weight)	Adrenal (mg/100g body weight)	Blood Glucose (mmol/L)	Plasma NOx (μM)	Plasma F_2-Isoprostane (nmol/L)	Mito-HE (geometric MFI)	$DiIC_1(5)$ (geometric MFI)
Saline	127 ± 7.2	8 ± 0.5	11 ± 0.3	9.3 ± 1.2	4.7 ± 0.3	198 ± 15	73 ± 8
DEX	48 ± 4.1*	5 ± 0.2*	9 ± 0.4*	12.3 ± 0.9	7.1 ± 0.6*	223 ± 21	107 ± 18
ACTH	48 ± 3.2*	41 ± 4.4*	11 ± 0.6	8.2 ± 0.8	5.4 ± 0.4	196 ± 7	110 ± 13
LA + saline p	140 ± 15.8	8 ± 0.2	11 ± 0.6	13.0 ± 1.5	4.9 ± 0.3	201 ± 11	184 ± 12*
LA + DEX p	50 ± 2.0§	6 ± 0.2§†	10 ± 0.3	11.2 ± 1.0	5.7 ± 0.2†	220 ± 18	131 ± 8
LA + ACTH p	53 ± 3.7§	43 ± 3.5§	10 ± 0.5	13.1 ± 3.4	5.4 ± 0.3	217 ± 13	152 ± 20
HD LA + ACTH p	53 ± 2.1	47 ± 2.1	13 ± 1.1	8.1 ± 1.0	4.6 ± 0.6	273 ± 10$^{\text{¤}}$	125 ± 6
Saline + LA r	133 ± 10.0	7 ± 0.5	12 ± 0.5*	12.7 ± 2.3	5.4 ± 0.2	166 ± 18	161 ± 10*
DEX + LA r	52 ± 3.1$^{\#}$	5 ± 0.4$^{\#}$	12 ± 0.8†	10.9 ± 1.5	5.6 ± 0.5	178 ± 20	134 ± 12

LA: alpha-lipoic acid, HD LA: high dose alpha-lipoic acid, p: prevention, r: reversal. * $P' < 0.05$ vs saline, § $P' < 0.005$ vs LA + saline prevention, $^{\#}P' < 0.01$ vs saline + LA reversal, $^{\dagger}P' < 0.05$ vs DEX, $^{\text{¤}}P' < 0.0005$ vs ACTH.

6.3.4 Adrenal weight

The adrenal weight for rats on DEX treatment was significantly lower than in those on saline injections ($P' < 0.0005$) (Figure 6.6a and Table 6.1). ACTH treated rats had significantly higher adrenal weight than saline treated rats (Figure 6.6b and Table 6.1). Alpha-lipoic acid partially prevented the fall in adrenal weight due to DEX in the prevention study ($P' < 0.01$) (Figure 6.6a). This effect was not observed in the DEX-HT reversal or ACTH-HT prevention studies (Figures 6.6 a and b).

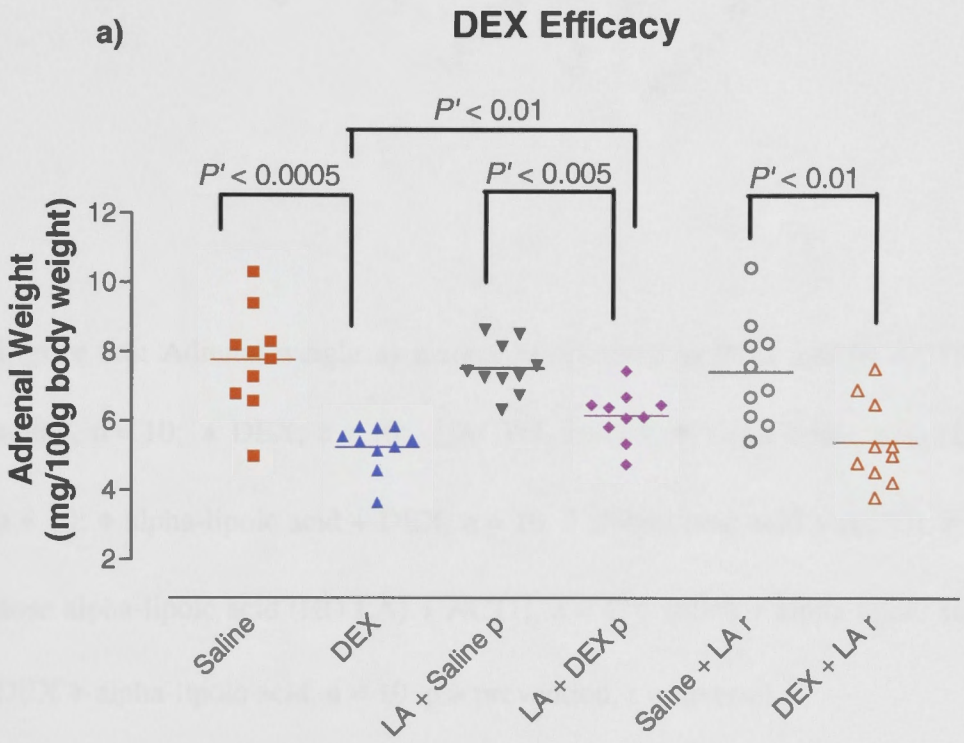

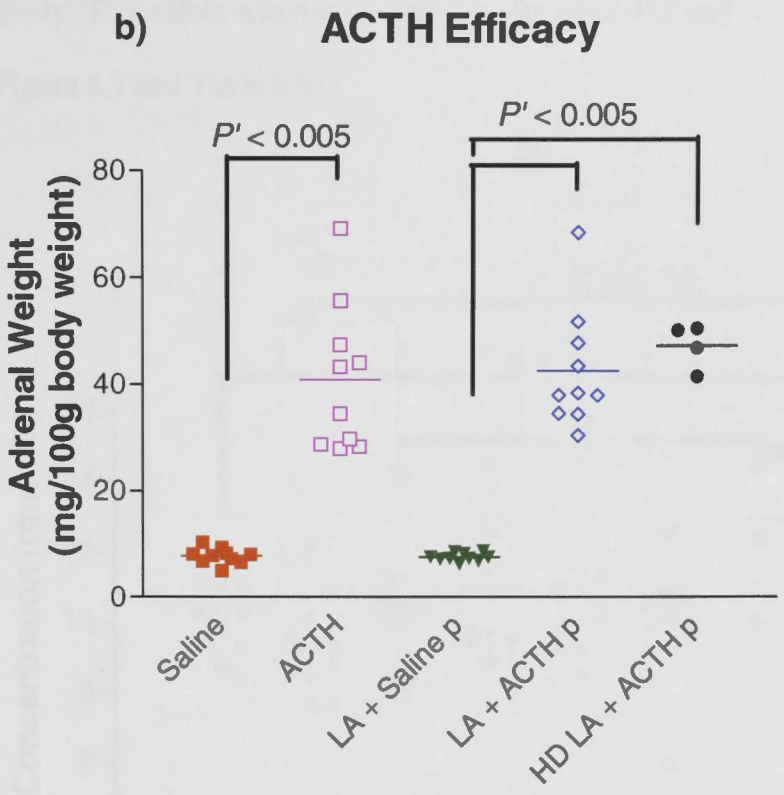

Figure 6.6: Adrenal weight as marker of effective **a)** DEX and **b)** ACTH delivery. ■ saline, n = 10; ▲ DEX, n = 10; □ ACTH, n = 10; ▼ alpha-lipoic acid (LA) + saline, n = 10; ♦ alpha-lipoic acid + DEX, n = 10, ◊ alpha-lipoic acid + ACTH, n = 10, ● high dose alpha-lipoic acid (HD LA) + ACTH, n = 4, ○ saline + alpha-lipoic acid, n = 10; Δ DEX + alpha-lipoic acid, n = 10. p = prevention, r = reversal.

6.3.5 Blood glucose concentration

Neither DEX nor ACTH altered the blood glucose concentrations in rats. Alpha lipoic acid increased blood glucose concentration in saline and DEX-treated rats in the

reversal study. This effect was not observed in the DEX-HT and ACTH-HT prevention studies (Figure 6.7 and Table 6.1).

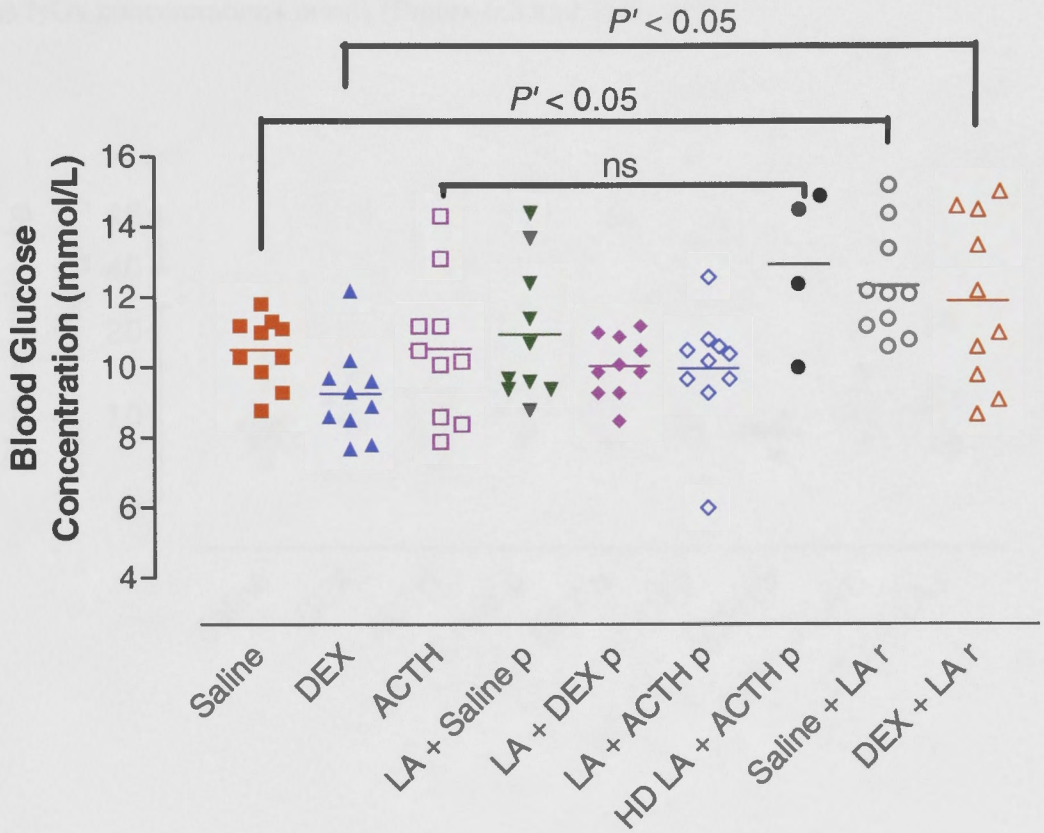

Figure 6.7: Blood glucose concentration. ■ saline, n = 10; ▲ DEX, n = 10; □ ACTH, n = 10; ▼ alpha-lipoic acid (LA) + saline, n = 10; ♦ alpha-lipoic acid + DEX, n = 10, ◊ alpha-lipoic acid + ACTH, n = 10, ● high dose alpha lipoic acid (HD LA) + ACTH, n = 4, ○ saline + alpha-lipoic acid, n = 10; Δ DEX + alpha-lipoic acid, n = 10. p = prevention, r = reversal.

6.3.6 Plasma nitrate and nitrite concentration

There was no significant difference in plasma NOx concentration in DEX- and ACTH-treated rats compared with saline-treated rats. Alpha-lipoic acid also did not alter the plasma NOx concentrations in rats (Figure 6.8 and Table 6.1).

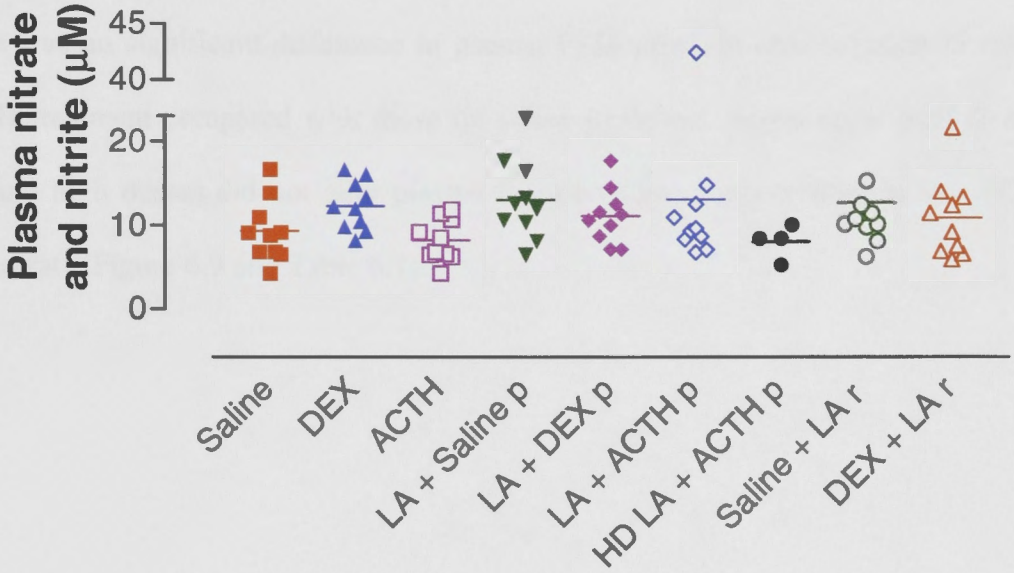

Figure 6.8: Plasma nitrate and nitrite concentration. ■ saline, n = 10; ▲ DEX, n = 10; □ ACTH, n = 10; ▼ alpha-lipoic acid (LA) + saline, n = 10; ♦ alpha lipoic acid + DEX, n = 10, ◊ alpha-lipoic acid + ACTH, n = 10, ● high dose alpha-lipoic acid (HD LA) + ACTH, n = 4, ○ saline + alpha-lipoic acid, n = 10; Δ DEX + alpha-lipoic acid, n = 10. p = prevention, r = reversal.

6.3.7 Plasma F_2-isoprostane concentration

The DEX-treated group had significantly higher plasma F_2-isoprostane concentration compared with the saline-treated group ($P' < 0.01$). Rats pre-treated with alpha-lipoic acid before DEX treatment had significantly lower plasma F_2-isoprostane concentration than those on DEX alone ($P' < 0.05$). However, no significant difference was observed in the DEX-HT reversal study between the DEX and DEX + alpha-lipoic acid groups. There was no significant difference in plasma F_2-isoprostane concentration in rats on ACTH treatment compared with those on saline treatment. Alpha-lipoic acid (both at low and high doses) did not alter plasma F_2-isoprostane concentration in the ACTH-treated rats (Figure 6.9 and Table 6.1).

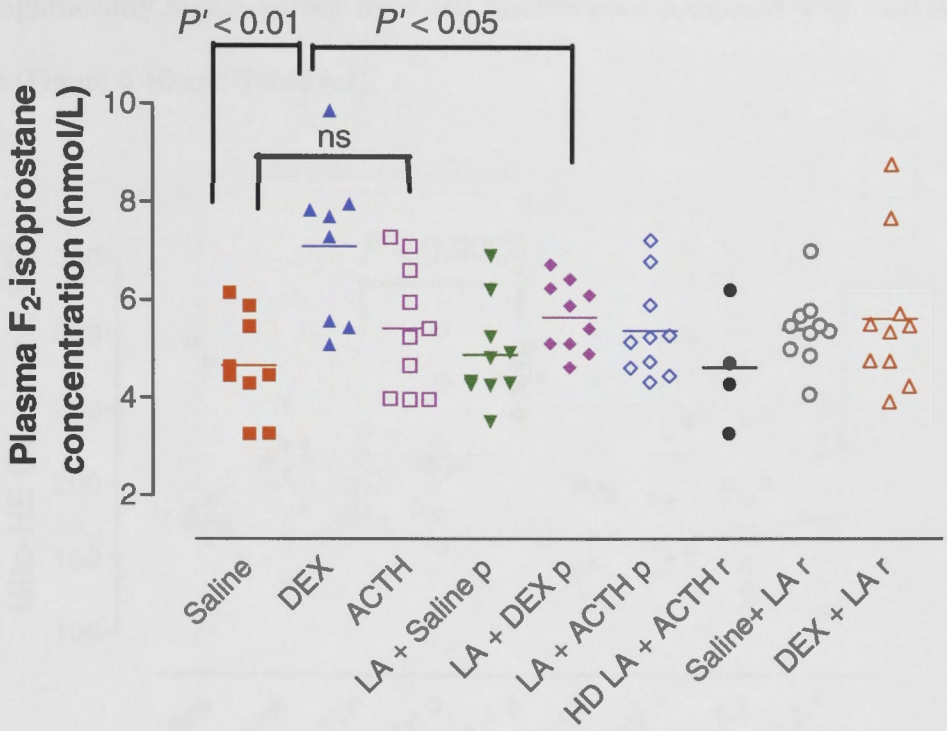

Figure 6.9: Plasma F_2-isoprostane concentration. ■ saline, n = 9; ▲ DEX, n = 8; □ ACTH, n = 10; ▼ alpha-lipoic acid (LA) + saline, n = 10; ♦ alpha-lipoic acid + DEX, n = 10, ◊ alpha-lipoic acid + ACTH, n = 10, ● high dose alpha-lipoic acid (HD LA) + ACTH, n = 4, ○ saline + alpha-lipoic acid, n = 10; Δ DEX + alpha-lipoic acid, n = 10. p = prevention, r = reversal.

6.3.8 Kidney Mito-HE fluorescence

There was no significant difference in kidney Mito-HE fluorescence between DEX- or ACTH- and saline-treated rats. Rats treated with high dose alpha-lipoic acid and ACTH

had significantly higher kidney Mito-HE fluorescence compared with ACTH treatment alone (Figure 6.10 and Table 6.1).

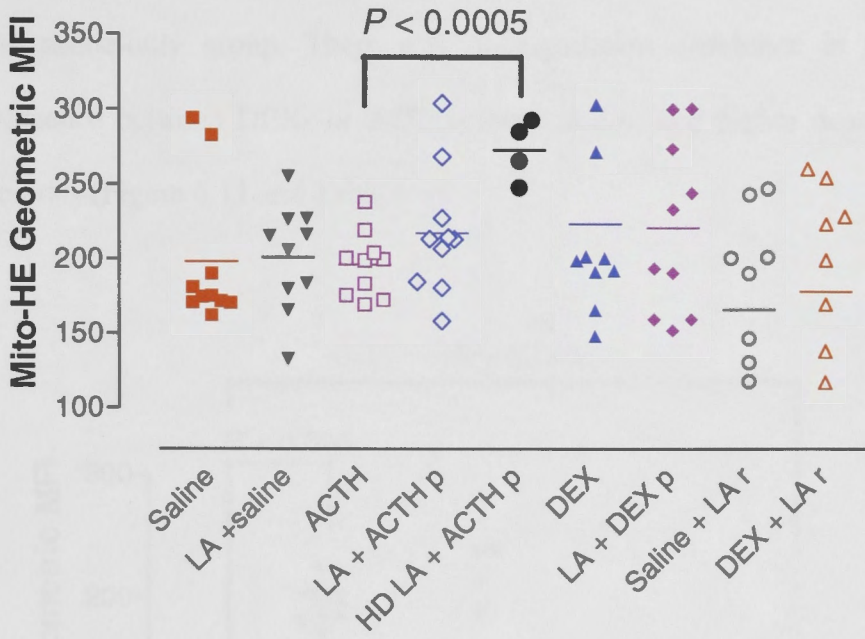

Figure 6.10: Mito-HE geometric MFI. ■ saline, n = 10; ▲ DEX, n = 10; □ ACTH, n = 10; ▼ alpha-lipoic acid (LA) + saline, n = 10; ♦ alpha-lipoic acid + DEX, n = 10, ◊ alpha-lipoic acid + ACTH, n = 10, ● high dose alpha-lipoic acid (HD LA) + ACTH, n = 4, ○ saline + alpha-lipoic acid, n = 10; Δ DEX + alpha-lipoic acid, n = 10. p = prevention, r = reversal.

6.3.9 Kidney $DiIC_1(5)$ fluorescence

$DiIC_1(5)$ mean geometric fluorescence was significantly higher in the groups which received alpha-lipoic acid (in the prevention and reversal studies) and saline compared to the saline-only group. There was no significant difference in kidney $DiIC_1(5)$ fluorescence between DEX- or ACTH- (both at low and higher dosages) and saline-treated rats (Figure 6.11 and Table 6.1).

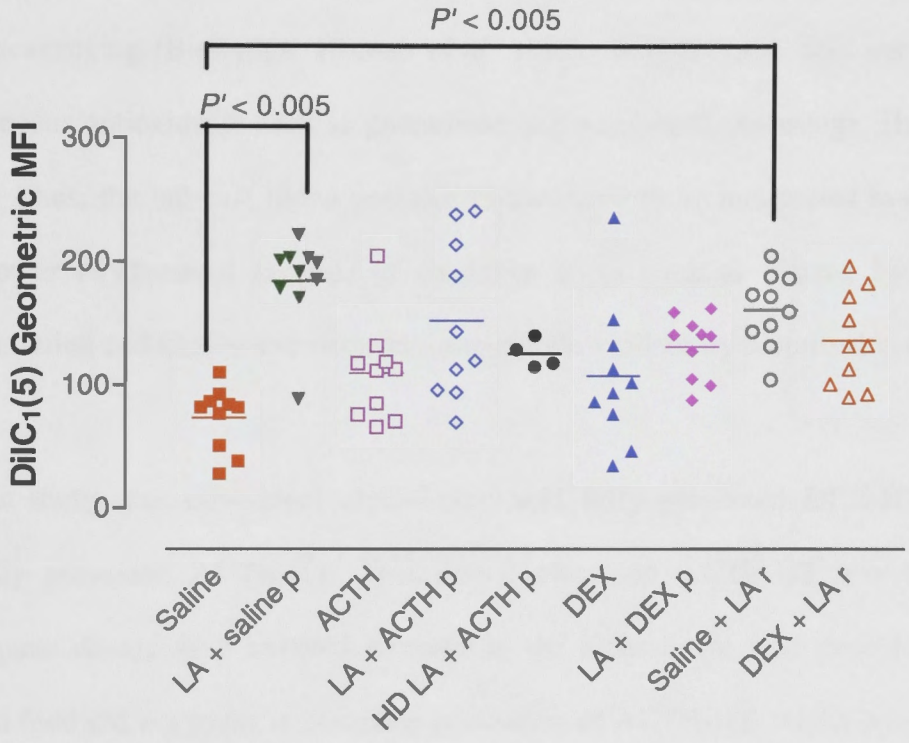

Figure 6.11: $DiIC_1(5)$ geometric MFI. ■ saline, n = 10; ▲ DEX, n = 10; □ ACTH, n = 10; ▼ alpha-lipoic acid (LA) + saline, n = 10; ♦ alpha-lipoic acid + DEX, n = 10, ◊ alpha-lipoic acid + ACTH, n = 10, ● high dose alpha-lipoic acid (HD LA) + ACTH, n = 4, ○ saline + alpha-lipoic acid, n = 10; Δ DEX + alpha-lipoic acid, n = 10. p = prevention, r = reversal.

6.4 DISCUSSION

Even though alpha-lipoic acid has been shown to be effective in improving mitochondrial function and decreasing mitochondrial superoxide in rats (Hagen, Ingersoll *et al.* 1999; El Midaoui, Elimadi *et al.* 2003), its effect is not entirely specific to mitochondria. The antioxidant effect of alpha-lipoic acid which is mediated by both the original alpha-lipoic acid compound and its metabolite dihydrolipoic acid, a more potent antioxidant, acts via a number of mechanisms such as metal chelation and direct ROS scavenging (Biewenga, Haenen *et al.* 1997). Dihydrolipoic acid can regenerate endogenous antioxidants such as glutathione and vitamin C (Biewenga, Haenen *et al.* 1997). Thus, the tail-cuff blood pressure results need to be interpreted in conjunction with other biochemical analysis of oxidative stress such as plasma F_2-isoprostane concentration and kidney mitochondrial superoxide availability described in Chapter 6.

In this study, the antioxidant alpha-lipoic acid fully prevented DEX-HT but only partially prevented ACTH-HT. This partial effect on ACTH-HT was not due to inadequate dosing as a ten-fold increase in the alpha-lipoic acid dose to 5 g/kg of ground food did not result in complete prevention of ACTH-HT. Alpha-lipoic acid was less effective in reversing established DEX-HT. Using the same dosage used in the prevention study, alpha-lipoic acid only partially reversed DEX-HT. The blood pressure lower effects of alpha-lipoic acid did not correlate directly with mitochondrial superoxide availability as demonstrated by the kidney Mito-HE assay.

The Mito-HE mean fluorescence intensity on kidney cells was not altered by DEX, ACTH or alpha-lipoic acid (500 mg/kg of ground food). However, alpha lipoic acid at 5 g/kg of ground food resulted in significantly higher Mito-HE mean fluorescence intensity. This was not associated with a decrease in mitochondrial membrane potential, a phenomenon known to result in a false increase in Mito-HE signals. It is possible that alpha-lipoic acid at a higher dose results in oxidative stress, most likely due to increased mitochondrial superoxide generation. The role of alpha-lipoic acid and its active metabolite, dihydrolipoic acid, as pro-oxidants has been reported in the literature (Biewenga, Haenen *et al.* 1997; Moini, Packer *et al.* 2002; Çakatay 2006). In this study, the increase in mitochondrial superoxide production is unlikely to translate to systemic oxidative stress given the lack of change in the plasma F_2-isoprostane concentration observed in this group, although the sample size for this group is very small and there may not have been significant power to detect a change. Another postulation is that superoxide generated within the mitochondria is not readily available to extra-mitochondrial structures. Superoxide, being a charged radical, does not permeate the mitochondrial membrane into the cytoplasm easily (Han, Antunes *et al.* 2003). It leaves the mitochondria via voltage-dependent anion channels and more commonly, as membrane-permeable hydrogen peroxide following its dismutation by intermembrane Cu, Zn-superoxide dismutase (Han, Antunes *et al.* 2003).

Plasma F_2-isoprostane concentration was significantly increased in DEX-but not ACTH-hypertensive rats. The latter finding was in contrast to previous findings that ACTH-HT was associated with raised plasma F_2-isoprostane concentration, suggesting insufficient power to detect a difference (Zhang, Wu *et al.* 2009). Pooled F_2-isoprostane

concentration data from our laboratory showed that ACTH-hypertensive rats (n = 46) had a significant higher plasma F_2-isoprostane concentration than the normotensive saline-treated rats (n = 48) (Ong, Zhang *et al.* 2008). The presence of a raised F_2-isoprostane concentration in DEX-treated rats again confirmed the role of oxidative stress in its pathogenesis. Pre-treatment with alpha-lipoic acid successfully prevented the increase of plasma F_2-isoprostane concentration due to DEX. However, alpha lipoic acid had no effect on the plasma F_2-isoprostane in established DEX-HT.

The lower blood pressure readings observed in the alpha-lipoic acid + DEX and alpha-lipoic acid + ACTH groups in the prevention studies; and DEX + alpha-lipoic acid in the reversal study were not due to inadequate dosing of DEX and ACTH. Similarly, the lower plasma F_2-isoprostane in the alpha-lipoic acid + DEX-treated group compared to DEX-only group was not a reflection of insufficient DEX administration. The effectiveness of DEX and ACTH delivery was confirmed by significant lowering of thymus weight in all groups receiving DEX or ACTH. As described in Chapter 3, excess gluococorticoid hormones results in thymocyte apoptosis and thymic involution (Sun, Dinsdale *et al.* 1992; Zavitsanou, Nguyen *et al.* 2007). Alpha lipoic acid has no effect on the GC-induced thymic involution.

Adrenal weight was also used as a surrogate marker of effective DEX and ACTH administration. DEX administration showed a reduction in adrenal weight consistent with adrenal suppression associated with exogenous glucocorticoid administration, whilst ACTH stimulation of the adrenal glands resulted in a significant increase in adrenal weight. In this study, alpha-lipoic acid did not alter the adrenal weight in either

saline- and ACTH-treated rats. It, however, partially inhibited DEX-induced reduction in adrenal weight. The reason for this remains unclear. Whether this has any correlation with DEX activity or the blood pressure reducing effect of alpha-lipoic acid effect remains to be determined. Cremer *et al.* demonstrated that oral alpha-lipoic acid at 20, 60 and 180 mg/kg body weight/day did not alter adrenal weight relative to body weight or the histology of the adrenal glands of Sprague-Dawley rats (Cremer, Rabeler *et al.* 2006). These authors, however, showed a dose-dependent decrease in body weight in rats treated with alpha-lipoic acid. Without adjusting to body weight changes, these authors found reduction in left adrenal weight only in male rats treated with 60 mg/kg body weight alpha-lipoic acid and no significant change in right adrenal weight in male rats and both adrenals in female rats. As there were no associated histopathological correlations, they concluded that this change was due to the reduction in body weight gain (Cremer, Rabeler *et al.* 2006).

In this study, treatment of alpha-lipoic acid (500 mg/kg ground food/day) did not change the body weight profile observed with saline, DEX and ACTH treatments. However, with a higher alpha-lipoic acid dose (5 g/kg ground food/day) body weight of the ACTH-treated rats fell precipitously. The rate of fall was greater in the group receiving the higher alpha-lipoic acid dose compared with the ACTH-only and alpha-lipoic acid (500 mg/kg ground food/day) + ACTH groups. A similar result was observed by Cremer *et al.* Alpha-lipoic acid has been shown to exhibit a dose dependent anti-obesity effect in Sprague-Dawley rats, independent of systemic toxicity, taste aversion or associated illness (Kim, Park *et al.* 2004). Rather, it works via the

suppression of hypothalamic AMP activated protein kinase, a fuel sensor in cells, which is activated during cellular energy depletion (Kim, Park *et al.* 2004).

In this study, blood glucose concentration was evaluated because hyperglycaemia has been shown to result in mitochondrial dysfunction (Munusamy and MacMillan-Crow 2009) and is a common feature in humans exposed to excess glucocorticoid hormones. Fasting blood glucose was significantly higher in patients with active Cushing's syndrome than those in remission (Terzolo, Allasino *et al.* 2004); and age- and sex-matched controls (Faggiano, Pivonello *et al.* 2003). In this study, however, ACTH and DEX did not alter blood glucose concentration in rats, consistent with previous findings in rats (Zhang, Pang *et al.* 2004). Interestingly, alpha-lipoic acid significantly increased glucose concentration in the reversal study involving DEX-HT and its saline control. The fact that alpha-lipoic acid increased blood glucose concentration in DEX- and saline-treated rats in the reversal study but not in the prevention study suggests that duration of alpha-lipoic acid treatment is likely to play a role. However, there is no evidence in the literature implicating alpha-lipoic acid as a cause of hyperglycemia. Rather, alpha-lipoic acid at a same dose prevented hyperglycemia in glucose-fed rats (El Midaoui, Wu *et al.* 2002).

In other studies (Chapters 7, 9), plasma NOx was decreased in DEX-HT. This decrease was not observed in the present studies on DEX- and ACTH-HT, with and without alpha-lipoic acid treatment. This may be influenced by decreased sensitivity of this assay in detecting very low plasma NOx levels seen in all group including the control and DEX-treated groups. In this study, alpha-lipoic acid did not alter the plasma NOx

concentrations in rats treated with saline, DEX or ACTH. The effect of alpha-lipoic acid on the saline-treated rats was consistent with the results seen in other studies where alpha-lipoic acid given to rats orally (20 mg/kg body weight (Amudha, Josephine *et al.* 2007) and 1 g/L drinking water (Marley, Holt *et al.* 1999) did not alter plasma NOx in normal controls. In these studies, alpha-lipoic acid prevented the rise in plasma NOx induced by cyclosporine treatment (Amudha, Josephine *et al.* 2007) and biliary cirrhosis (Marley, Holt *et al.* 1999) in rats by the inhibition of renal iNOS and total hepatic NOS respectively . In the present study, however, alpha lipoic acid did not alter plasma NOx in DEX or ACTH-treated rats. This is probably because, unlike those studies, DEX and ACTH suppresses eNOS and iNOS in rats (Wallerath, Witte *et al.* 1999; Lou, Wen *et al.* 2001).

In summary, alpha-lipoic acid fully prevented DEX-HT, partially prevented ACTH-HT and partially reversed DEX-HT without altering the kidney mitochondrial superoxide availability. This suggests that GC-HT is prevented (and DEX-HT, partially reversed) by alpha-lipoic acid through a mechanism other than mitochondrial superoxide reduction.

The differences observed between DEX- and ACTH-HT, once again, depict the different pathophysiological mechanisms contributing to the two hypertensive models.

6.5 CONCLUSION

This study suggested that mitochondrial superoxide does not play a major role in the pathogenesis of GC-HT in the rat.

CHAPTER 7

Role of Xanthine Oxidase in Dexamethasone-Induced Hypertension in the Rat

7.1 INTRODUCTION

Xanthine oxidase, best known for its role in purine degradation, has broad biological roles (Berry and Hare 2004), and is one of several sources of reactive oxygen species (ROS). In the process of converting hypoxanthine to xanthine and xanthine to uric acid, oxygen is reduced to form superoxide anions. The role of xanthine oxidase has been studied in various forms of hypertension. Inhibition of xanthine oxidase using oxpurinol lowered blood pressure in spontaneously hypertensive rats (Nakazono, Watanabe *et al.* 1991). Tungsten supplementation aimed at inhibiting xanthine oxidase also resulted in decrease in oxygen radicals and blood pressure in spontaneously hypertensive rats (Suzuki, DeLano *et al.* 1998).

The effect of xanthine oxidase inhibition on GC-HT has been examined previously. Wallwork and co-workers observed a decrease in mean blood pressure with allopurinol treatment in hypertension produced by high dose DEX (0.5 mg/kg/day). However, in our hands, allopurinol failed to prevent and reverse ACTH-HT (Zhang, Chan *et al.* 2005). This study aimed to clarify the role of xanthine oxidase inhibition in the prevention of GC-HT, using a much lower dose of DEX to minimise potential confounding effects of massive dosage.

7.2 METHODS

7.2.1 Experimental animals

This study was approved by the Animal Experimentation Ethics Committee of the Australian National University (J.HB.17.03). General methods used in this study have been described in Chapter 2. In this experiment, the rats were given either normal food or allopurinol-laced food for 18 days (from day P0 to T12) and either saline or DEX injection for 14 days (from day T0 to T13).

Thirty male Sprague-Dawley rats weighing 240-260 g were randomly divided into 4 treatment groups.

Group 1 Vehicle and saline (n=8)

Group 2 Allopurinol and saline (n= 7)

Group 3 Vehicle and DEX (n=8)

Group 4 Allopurinol and DEX (n=7)

DEX (10 µg/rat/day, s.c) and saline (0.9% NaCl, 0.1 mL/rat/day) were administered via subcutaneous injection at 1200 hours daily, as described in Section 2.4.1. Allopurinol (200 mg/kg/day, Sigma-Aldrich, St Louis, USA) was

given orally as allopurinol-laced ground food. The total allopurinol dose per cage was adjusted daily based on the weight of the animals. To ensure complete allopurinol intake, the designated rats were given drug-laced food (20 g per rat), which accounted for 90 % of their food intake, at night over 15 hours. Each morning, the remaining ground food was collected and weighed. All animals had access to the normal pellet food during the day time.

7.2.2 Systolic blood pressure and body weight measurements

SBP measurements were recorded on alternate days between 10 am to 12 noon, using the tail-cuff method described in Section 2.5.1 of Chapter 2. Body weights were recorded daily after blood pressure measurements.

7.2.3 Thymus weight measurement

The rats were sacrificed via exsanguination under isoflurane surgical anaesthesia (Section 2.8.2 of Chapter 2) and thymus wet weight, expressed relative to body weight (grams thymus weight per 100 g body weight) was used as a marker of glucocorticoid activity as described in Section 2.8.5.1.

7.2.4 Serum urate measurement

The efficacy of allopurinol treatment was evaluated by reduction in serum urate concentration, measured using the method described in Section 2.10.2 by ACT Pathology, The Canberra Hospital, Australia.

7.2.5 Plasma nitrate and nitrite assay

Plasma NOx, measured using the Griess colorimetric reaction described in Section 2.10.1, were used as a marker of endogenous NO availability.

7.2.6 Aortic lucigenin-enhanced chemiluminescence assay

This assay, which was described in Section 2.11.1, was performed as a marker of vascular superoxide production.

7.2.7 Data and statistical analysis

Results were expressed as mean $\pm$ SEM. Statistical analysis were as described in Section 2.12 (Chapter 2).

7.3 RESULTS

7.3.1 Food and allopurinol intake

After accounting for the inevitable nightly wastage of ground food, the mean food intake for allopurinol-treated rats was 20 ± 1 g/rat/15-hour night (around 98% completion) and the mean allopurinol dose consumed was 196 ± 0.5 mg/kg/day which was around 98% of the given dose.

7.3.2 Systolic blood pressure

SBP was raised by DEX but not altered by allopurinol treatment (Figure 7.1). In the DEX-treated group, SBP increased from 110 ± 2 to 126 ± 3 mmHg ($P < 0.001$). SBP was increased in the DEX compared with the saline group ($P' < 0.01$). Allopurinol did not prevent HT in DEX-treated rats and did not alter SBP in saline or DEX-treated rats.

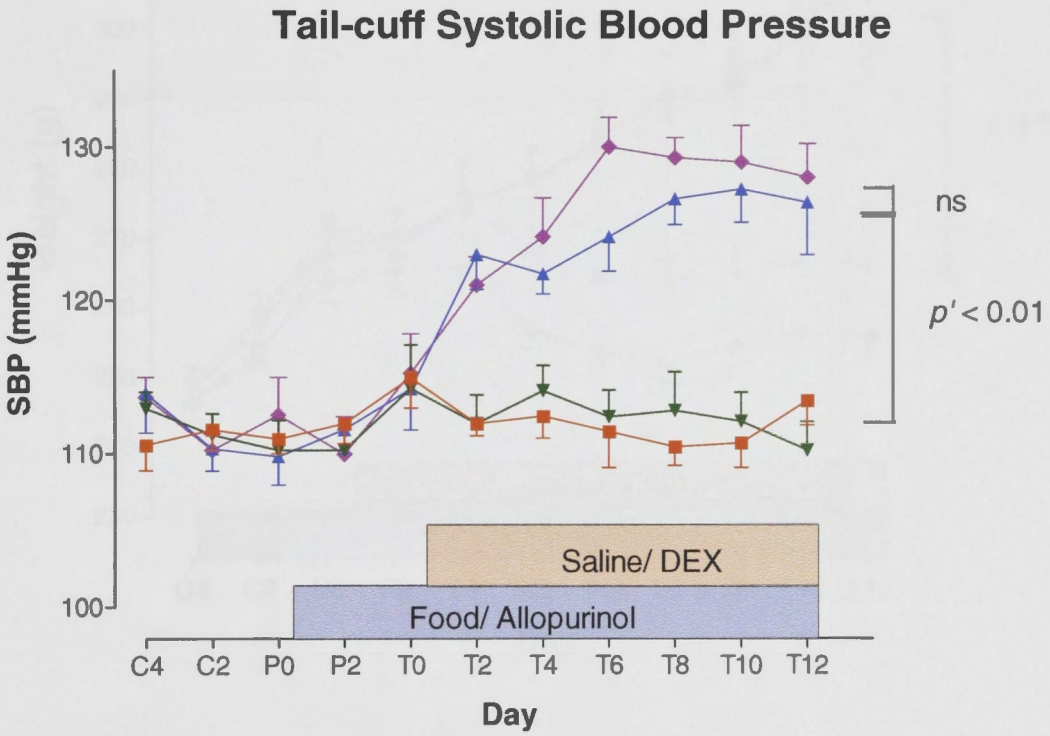

Figure 7.1: Tail-cuff SBP readings from day C4 to day T12. ■ saline only, n = 8; ▲ DEX only, n = 8; ▼ allopurinol + saline, n = 7; ♦ allopurinol + DEX, n = 7. C: control days, P: pre-treatment days, T: treatment days.

7.3.3 Body weight

Body weight fell initially in DEX-treated rats, then stabilised. These changes were not modified by allopurinol. When compared with saline, DEX-treated rats had lower mean body weight (saline: 301 ± 14 g; DEX: 267 ± 8 g, $P' < 0.01$) (Figure 7.2).

Figure 7.2: Body weight. ■ saline only, n = 8; ▲ DEX only, n = 8; ▼ allopurinol + saline, n = 7; ♦ allopurinol + DEX, n = 7. C: control days, P: pre-treatment days, T: treatment days.

7.3.4 Thymus weight

DEX significantly decreased thymus weight (saline: 134 ± 9; DEX: 53 ± 4 mg/100g body weight, $P < 0.001$) and this significant decrease due to DEX was not altered by allopurinol (allopurinol + saline: 130 ± 3; allopurinol + DEX: 53 ± 3 mg/100g body weight, n = 7 each) (Figure 7.3).

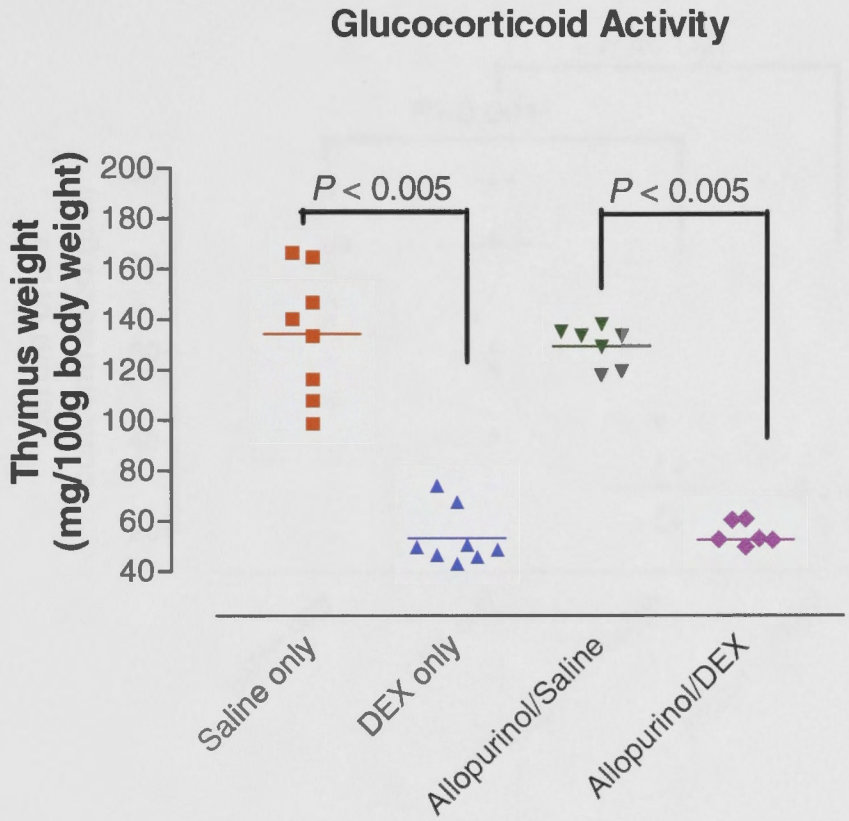

Figure 7.3: Thymus weight reduction as marker of glucocorticoid acitivity. ■ saline only, n = 8; ▲ DEX only, n = 8; ▼ allopurinol + saline, n = 7; ♦ allopurinol + DEX, n = 7.

7.3.5 Serum urate concentration

Serum urate concentrations were 76 ± 5 μmol/L in the saline- and 84 ± 13 μmol/L in the DEX-treated rats, and lower following allopurinol treatment, 30 ± 3 μmol/L saline and 28 ± 2 μmol/L DEX ($P < 0.001$) (Figure 7.4).

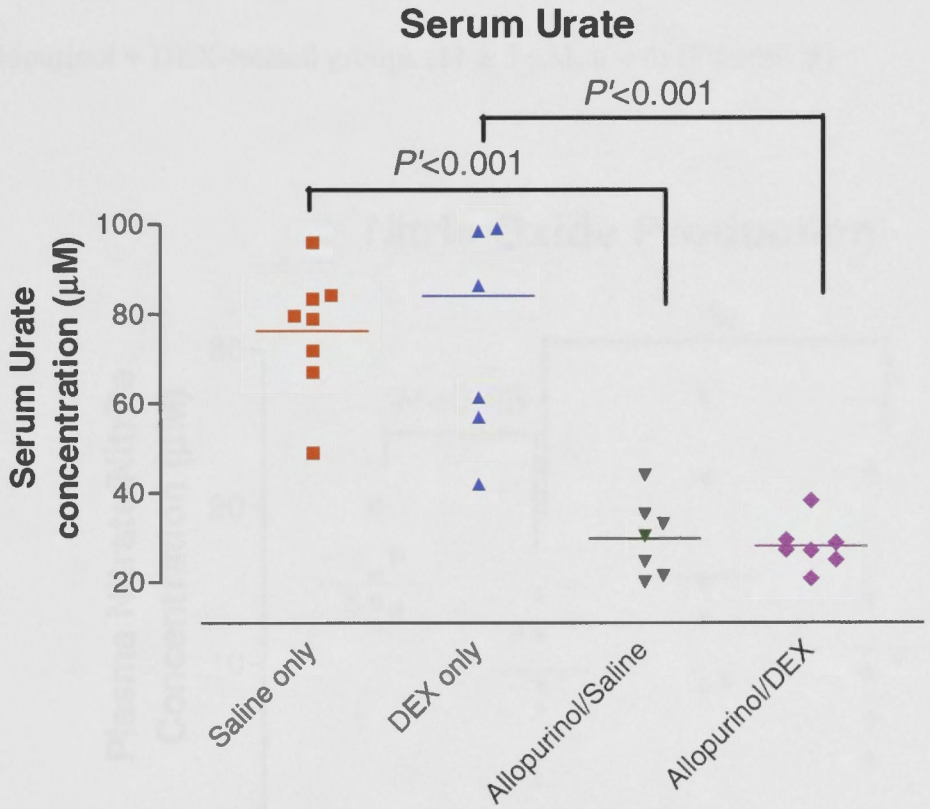

Figure 7.4: Serum urate reduction as a marker of effective allopurinol absorption. ■ saline only, n = 8; ▲ DEX only, n = 8; ▼allopurinol + saline, n = 7; ♦ allopurinol + DEX, n = 7.

7.3.6 Plasma nitrate and nitrite concentration

There was a significant decrease in plasma NOx concentrations in DEX-treated rats in comparison with saline-treated rats (saline: 15 ± 1 μM, n = 8; DEX 10 ± 2 μM, n = 6, $P' < 0.05$), but this was not prevented by allopurinol (allopurinol + DEX: 11 ± 3 μM, n = 6). There was no significant difference in plasma NOx concentrations between the allopurinol + saline- (16 ± 3 μM, n = 6) and allopurinol + DEX-treated groups (11 ± 3 μM, n = 6) (Figure 7.5).

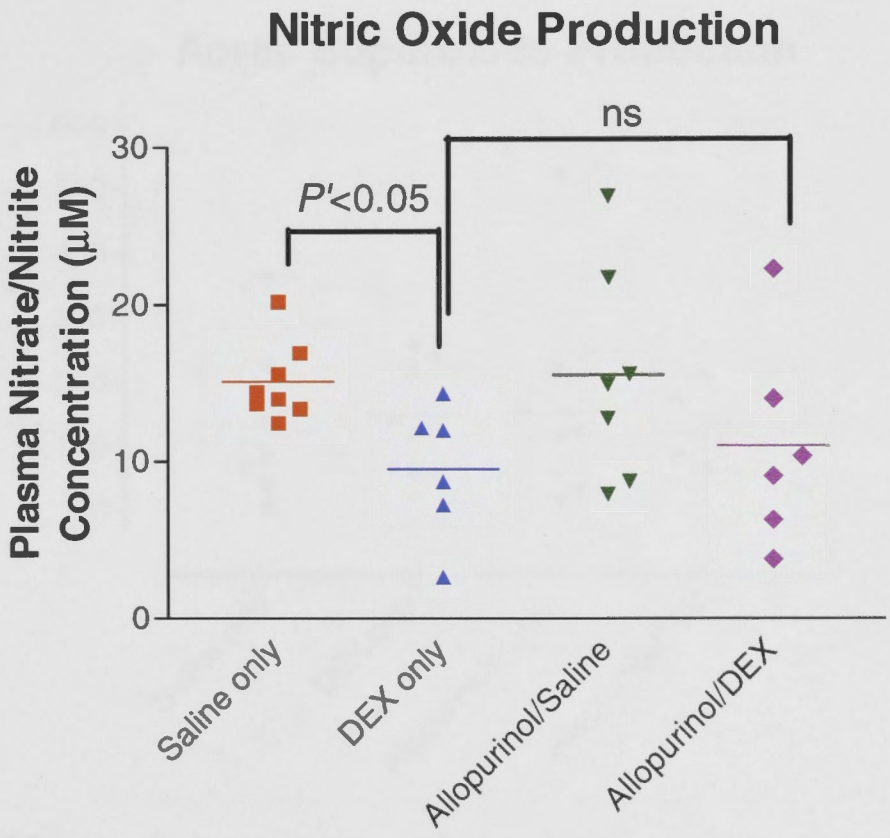

Figure 7.5: Plasma nitrate/nitrite as a marker of total body nitric oxide production. ■ saline, n = 8; ▲ DEX, n = 6; ▼ allopurinol + saline, n = 7; ♦ allopurinol + DEX, n = 6.

7.3.7 Aortic lucigenin-enhanced chemiluminescence

There was no significant difference in aortic lucigenin-enhanced chemiluminescence in saline- (182 ± 47 count/s/mg, n = 7) and DEX-treated rats (200 ± 29 count/s/mg, n = 8). Allopurinol treatment did not significantly alter the aortic lucigenin-enchanced chemiluminescence of the saline and DEX-treated groups (allopurinol + saline: 203 ± 67 count/s/mg, n = 7; allopurinol + DEX: 169 ± 22 count/s/mg, n = 7) (Figure 7.6).

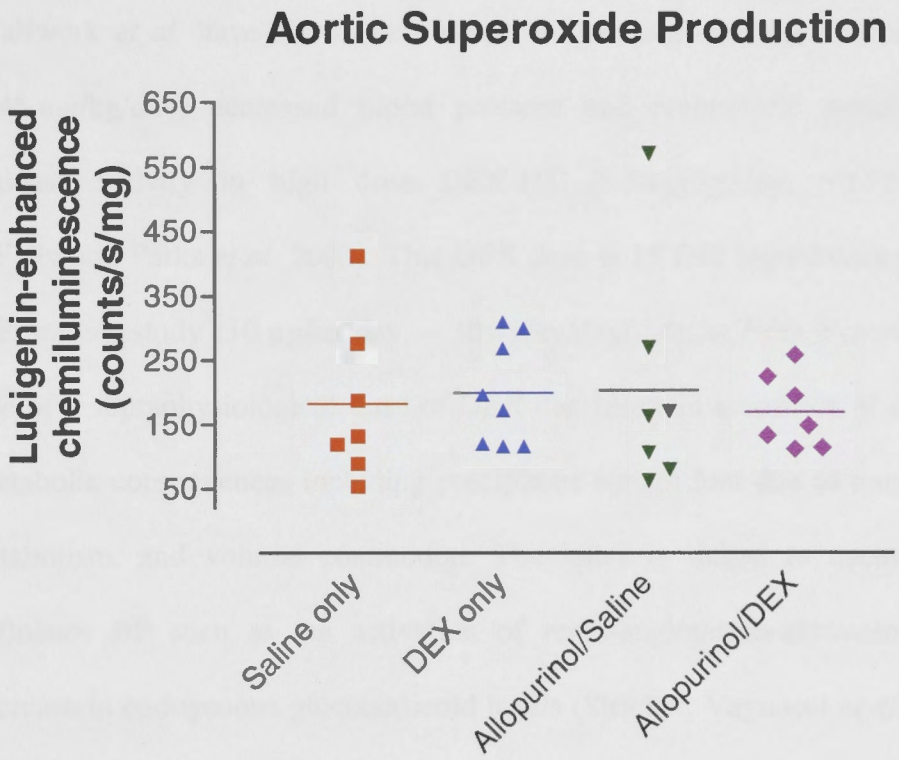

Figure 7.6: Aortic lucigenin-enhanced chemiluminescence as a marker of vascular superoxide production. ■ saline only, n = 7; ▲ DEX only, n = 8; ▼ allopurinol + saline, n = 7; ♦ allopurinol + DEX, n = 7.

7.4 DISCUSSION

As discussed in Chapter 1, ROS are generated mainly generated by the NAD(P)H oxidase and the xanthine oxidase pathways, eNOS in its uncoupled form and mitochondria. The NAD(P)H oxidase pathway (Hu, Zhang *et al.* 2006) but not uncoupling of eNOS (Li, Fraser *et al.* 1997; Hu, Zhang *et al.* 2006; Thida, Earl *et al.* 2010) plays a role in the pathogenesis of DEX-HT. The present study suggests that xanthine oxidase does not have a major role in DEX-HT.

Wallwork *et al.* have shown that allopurinol treatment (0.4 g/L drinking water, ~ 45 mg/kg/day) decreased blood pressure and cremasteric muscle xanthine oxidase activity in high dose DEX-HT (0.5 mg/kg/day, ~ 150 μg/rat/day) (Wallwork, Parks *et al.* 2003). This DEX dose is 15 fold higher than that used in the present study (10 μg/rat/day, ~ 30 μg/kg/day). Apart from hypertension, the use of a supraphysiological dose of DEX can result in a number of dose-related metabolic consequences including precipitous weight loss due to muscle and fat catabolism, and volume contraction. The latter is linked to events likely to influence BP such as the activation of renin-angiotensin-aldosterone system, increase in endogenous glucocorticoid levels (Stricker, Vagnucci *et al.* 1979) and suppression of atrial natriuretic peptide (Sebaai, Lesage *et al.* 2002). These confounding factors due to excessive DEX dose make such a model unsuitable for examining mechanisms of GC-HT. Consequently, a dose that was sufficient to induce hypertension without significant weight loss was employed in this study

(Tonolo, Fraser *et al.* 1988; Li, Fraser *et al.* 1997; Zhang, Croft *et al.* 2004; Hu, Zhang *et al.* 2006; Miao, Zhang *et al.* 2007).

Wallwork and colleagues did not report serum urate concentration. This allopurinol dose, however, did not result in any significant change in serum urate levels or SBP compared to controls (Zhang Y, unpublished data). As in a previous study (Zhang, Chan *et al.* 2005), the dose used in this study (196 ± 0.5 mg/kg/day after correcting for nightly allopurinol-laced food wastage) effectively lowered serum urate levels indicating inhibition of the xanthine oxidase pathway.

Plasma NOx concentrations were significantly decreased by DEX treatment, consistent with other published findings in rats (Mondo, Yang *et al.* 2006) and mice (Wallerath, Witte *et al.* 1999; Wallerath, Godecke *et al.* 2004). This decrease was not prevented by pretreatment with allopurinol, suggesting that DEX-induced NO deficiency was not inhibited by xanthine oxidase blockade.

Aortic lucigenin-enhanced chemiluminescence, a marker of vascular oxidative stress, was not altered by DEX and/or allopurinol. A possible explanation for this negative result is that nitric oxide-redox imbalance in the DEX-HT model is likely to be more marked in resistance vessels compared to larger vessel like the aorta. As shown in Chapter 3, DEX-HT is associated with increased in TPR, a phenomenon contributed mostly by arterioles (resistance vessels). Some may also argue that the lack of a significant difference might be a due to small sample size as similar observations were made in the ACTH-HT model (Zhang, Chan *et al.*

2005; Zhang, Miao *et al.* 2007). Using pooled data from our laboratory, ACTH-HT was associated with increased aortic lucigenin-enhanced chemiluminescence (Zhang, Chan *et al.* 2005). However, pooled data from our laboratory did not shown any significant change in luminescence in DEX-hypertensive rats compared with control rats (Figure 7.7).

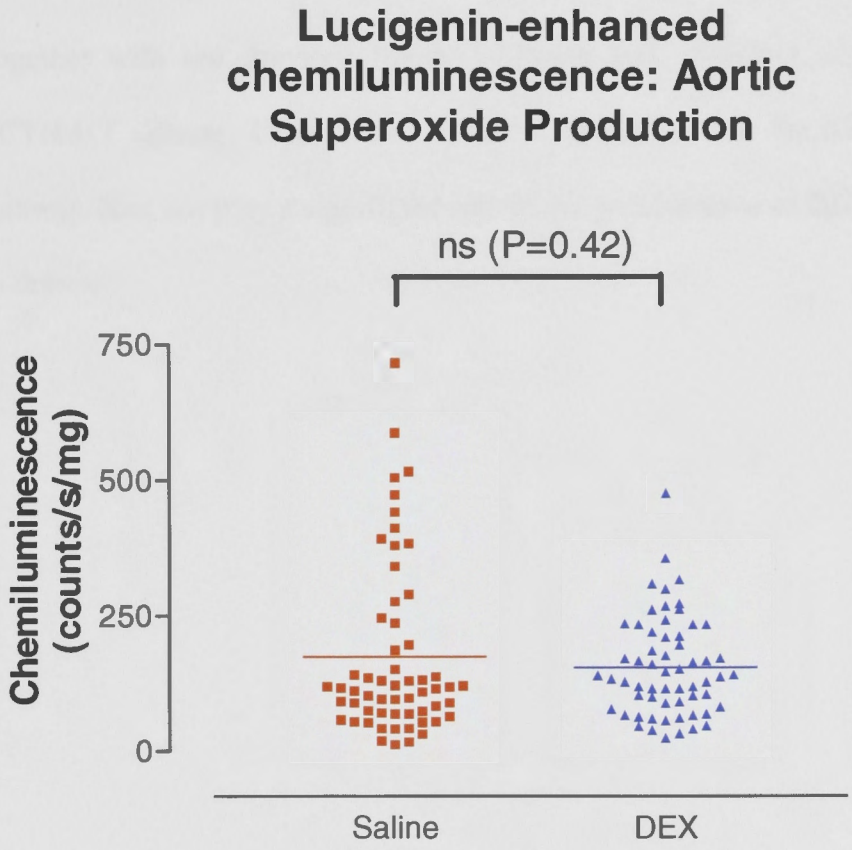

Figure 7.7: Pooled aortic lucigenin-enhanced chemiluminescence data from the High Blood Pressure Research Unit (2006-2008). ■ Saline, n = 59; ▲ DEX, n = 60.

7.5 CONCLUSION

This study shows that allopurinol is ineffective in preventing DEX-HT in the rats despite adequate inhibition of the xanthine oxidase enzyme. Thus, the xanthine oxidase pathway does not play a significant role in the pathogenesis of DEX-HT in the rat.

Together with our previous finding showing lack of effect of allopurinol on ACTH-HT (Zhang, Chan *et al.* 2005), a conclusion that the xanthine oxidase pathway does not play a significant role in the pathogenesis of GC-HT in rats can be drawn.

CHAPTER 8

Effects of Adrenergic Receptor Antagonism and Lipid Peroxidation Inhibition Using Propranolol in Glucocorticoid-Induced Hypertension in the Rat

8.1 INTRODUCTION

Stimulation of the sympathetic nerves in the adrenal medulla results in the release of catecholamines, adrenaline and noradrenaline, into the systemic circulation (Guyton and Hall 2000). Activation of adrenergic receptors by these catecholamines results in slightly prolonged but similar effects to direct sympathetic nerve stimulation. The production of noradrenaline from adrenaline in the adrenal medulla is catalysed by phenylethanolamine *N*-methyltransferase (PNMT), an enzyme regulated by adrenal glucocorticoid at transcriptional, translational and proteolytic levels (Wong, Siddall *et al.* 1995). Regulations by glucocorticoid hormones at these different levels occur independently and are different depending on the chronicity of glucocorticoid treatment (Wong, Siddall *et al.* 1995). Acute glucocorticoid replacement was shown to be associated with increased PNMT mRNA expression without a concomitant increase in PNMT enzyme activity. Chronic replacement on the other hand restored PNMT enzyme activity but decreased mRNA expression (Wong, Siddall *et al.* 1995).

Increased pressor responsiveness to noradrenaline has been observed in GC-HT in humans (Kurland and Freedberg 1951; Mendlowitz, Naftchi *et al.* 1961; Pirpiris, Sudhir *et al.* 1992), rats (Russo, Fraser *et al.* 1989; Russo, Fraser *et al.* 1990) and dogs (Nakamoto, Suzuki *et al.* 1991). In some studies, glucocorticoid treatment was associated with increases in plasma adrenaline (Kumai, Asoh *et al.* 2000; Silvan, Martinez-Mateos *et al.* 2007) and noradrenaline concentrations (Watanabe, Noshiro *et al.* 1995; Kumai, Asoh *et al.* 2000), but this is not a

universal finding (Rothschild, Langlais *et al.* 1984; Brown and Fisher 1986). Rothschild et al showed that DEX administration in human subjects resulted in raised levels of dopamine but not other catecholamines (Rothschild, Langlais *et al.* 1984). Brown and Fisher, on the other hand, were able to suppress ether-induced increases in plasma adrenaline and noradrenaline (Brown and Fisher 1986).

Whilst it has been shown previously that atenolol, a selective β1-adrenoreceptor blocker, did not prevent ACTH-HT (Wen, Fraser *et al.* 1999) in the rat, it remains unclear if complete blockade of both β1- and β2-receptors (and therefore, inhibition of myocardial and smooth muscle contractility, respectively) would be able to produce an effect.

Activation of both β1- and β2-adrenoreceptors may play a role in the pathogenesis of ACTH and DEX-HT in the rat. In this study, the role of the beta adrenergic receptors was tested using a non-selective β-adrenoreceptor blocker propranolol *in vivo*, a commonly used antihypertensive drug. Beta-adrenergic receptor blockers are useful drugs commonly used in the treatment of hypertension, cardiac failure and ischaemic heart disease. This study will also help identify the utility of β-adrenoreceptor blockers in GC-HT.

Apart from β-adrenergic antagonism, the beneficial cardiovascular effects demonstrated by β-propranolol have been related to its antioxidant effect. Propranolol has been to shown to have hydroxyl radical, hypochlorous acid,

peroxyl radical, nitric oxide radical and peroxynitrite but not superoxide scavenging activity (Gomes, Costa *et al.* 2006). This antioxidant property was associated with its intrinsic chemical properties rather than membrane stablising effect which requires a concentration significantly higher than reported serum clinical levels (Mak and Weglicki 1988). These authors subsequently found evidence that a metabolic product of propranolol ring oxidation, 4-hydroxyl propranolol, is a potent antioxidant which can provide anti-LDL oxidation and endothelial cell protection in *in vitro* experiments (Mak and Weglicki 2004). There have also been studies showing propranolol is a potent inhibitor of lipid peroxidation. These *in vitro* studies demonstrated effective inhibition of lipid peroxidation in canine sarcolemnal membranes (Mak and Weglicki 1988) and rat liver microsomes (Aruoma, Smith *et al.* 1991). Since oxidative stress, as discussed in Chapter 1, plays a significant role in glucocorticoid hypertension, the role of propranolol as a lipid peroxidation inhibitor was also examined in both ACTH and DEX-HT.

8.2 METHODS

This study was approved by the Animal Experimentation Ethics Committee of the Australian National University (Protocol No. J.HB.20.05). The general methodology for this study was as described in Chapter 2.

There were 2 sets of experiments in this study. The first evaluated the effects of propranolol on ACTH-HT and the second, on DEX-HT. Data from each of these

studies were compared with the control groups (groups 1 and 2). Seventy male Sprague-Dawley rats were randomly divided into 6 treatment groups.

8.2.1 Control groups

Group 1: Untreated ground food + saline (0.9% NaCl, 0.1mL/100g/day, sc), n = 14

Group 2: Propranolol (100 mg/kg/day)-laced ground food + saline (1 mL/kg/day, sc), n = 10.

8.2.2 ACTH-induced hypertension

Group 3: Untreated ground food + ACTH (0.2 mg/kg/day, sc), n = 13

Group 4: Propranolol-laced ground food + ACTH, n = 10

8.2.3 Dexamethasone-induced hypertension

Group 5: Untreated ground food + DEX (10 μg/rat/day), n = 13.

Group 6: Propranolol-laced food + DEX, n = 10

Propranolol (Inderal, AztraZeneca, North Ryde, Australia) was used in this study. The propranolol tablets were ground and mixed in ground rat food. Propranolol-

laced food was freshly prepared daily. The total propranolol dose per cage was adjusted daily based on weight of the animals. To ensure complete propranolol ingestion, the animals were given 20 g of ground food per rat per night over 15 hours. This was approximately 90% of their food intake at night. Each morning the remaining ground food was collected and weighed. The amount given on subsequent nights was adjusted according to the amount left over on the previous night. During the day, all animals had unlimited access to pellet food.

8.2.4 Blood pressure, heart rate and body weight measurements

Tail-cuff SBP and HR measurements were performed on alternate days at 9-11 am using the method as described in Sections 2.5.1 and 2.6.1, respectively (Chapter 2). Body weights were measured on alternate days after the tail-cuff SBP and HR measurements.

8.2.5 Thymus and adrenal weights

Thymus wet weight, expressed relative to body weight (grams thymus weight per 100 g body weight), was used as a marker of glucocorticoid activity. Adrenal wet weight, expressed relative to body weight (grams adrenal weight per 100 g body weight), was used to assess ACHT and DEX treatment efficacy. The surgical techniques were as described in Section 2.8.5.1 of Chapter 2.

8.2.6 Plasma F_2-isoprostane assay

Plasma F_2-isoprostane was used as a marker of systemic lipid peroxidation. The assay technique was described in Section 2.11.3 of Chapter 2.

8.2.7 Statistical analysis

Results were expressed as mean ± SEM. Statistical analysis were as described in Section 2.12 of Chapter 2.

8.3 RESULTS

8.3.1 Systolic blood pressure

SBP was raised by ACTH (from 110 ± 2 on day T0 to 134 ± 3 on day T12, $P <$ 0.0005) and DEX (from 114 ± 2 on day T0 to 139 ± 3 mmHg on day T12, $P <$ 0.0005) but not changed by propranolol treatment (from 111 ± 2 on day T0 to 112 ± 2 on day T12, *ns*). Propranolol treatment did not prevent ACTH- and DEX-induced hypertension in the rat. Systolic blood pressures in the propranolol + ACTH- and propranolol + DEX-treated groups were significantly higher than in the propranolol-only group ($P' < 0.001$ and $P' < 0.005$, respectively) (Figures 8.1 and 8.2).

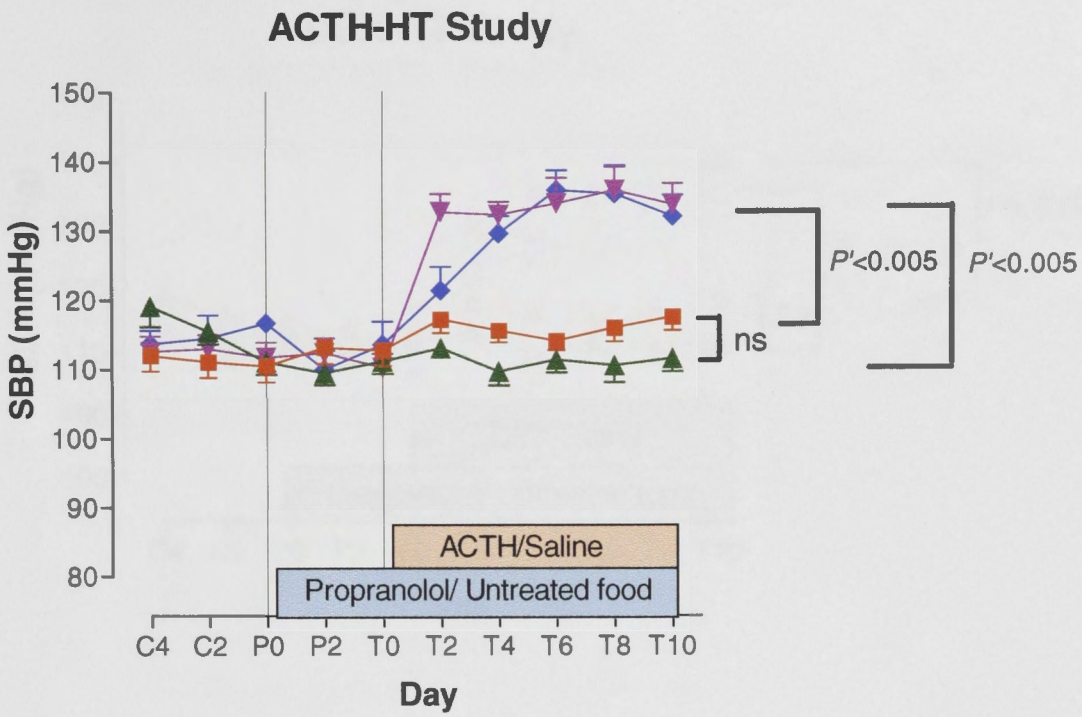

Figure 8.1: Tail-cuff SBP readings from day C4 to day T10 in the ACTH-HT prevention study. ■ Untreated food + saline, n = 14; ▲ Propranolol + saline, n = 10; ▼ untreated food + ACTH, n = 13; ♦ Propranolol + ACTH, n = 10.

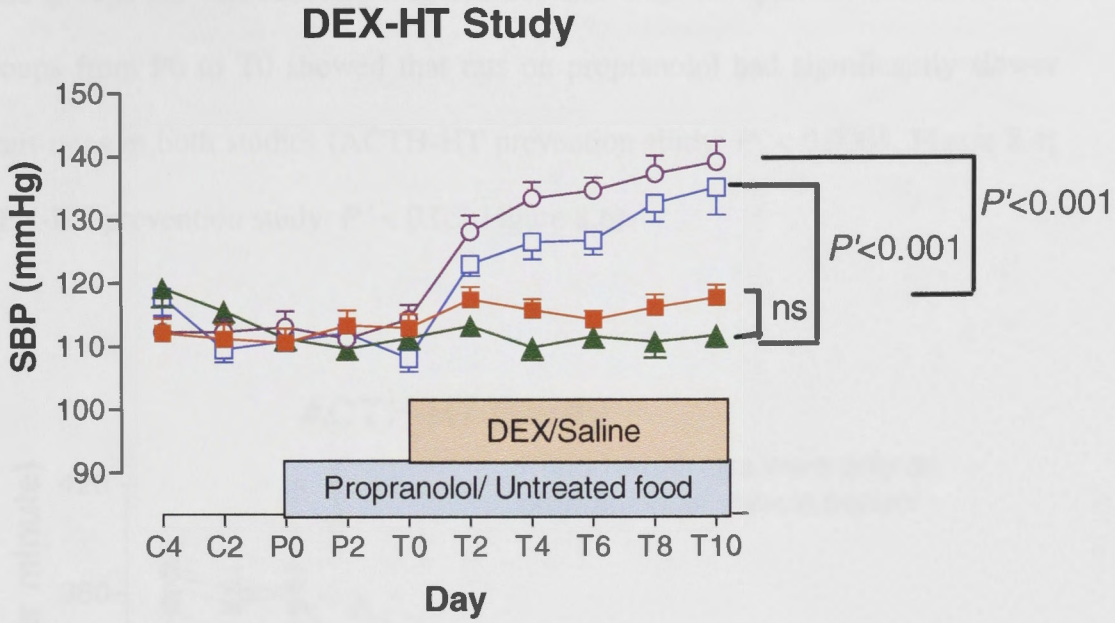

Figure 8.2: Tail-cuff SBP readings from day C4 to day T10 in the DEX-HT prevention study. ■ Untreated food + saline, n = 14; ▲ Propranolol + saline, n = 10; ○ Untreated food + DEX, n = 13; □ Propranolol + DEX, n = 10.

8.3.2 Heart rate

There was a progressive fall in the HR throughout the entire duration of the experiment in all groups (Figures 8.3 and 8.5). Therefore, in order to evaluate the effectiveness of β-adrenergic receptor blockade by propranolol, we looked at the HR profile during the initial period of propranolol treatment from day P0 to T0 (Figures 8.3 and 8.5). As the animals were only on either untreated food or propranolol between day P0 to day T0 (HR measurements were obtained prior to treatment on day T0), they were re-grouped to either propranolol or untreated

food groups for this analysis (Figures 8.4 and 8.6). Comparison between these groups from P0 to T0 showed that rats on propranolol had significantly slower heart rates in both studies (ACTH-HT prevention study: $P' < 0.0005$, Figure 8.4; DEX-HT prevention study: $P' < 0.05$, Figure 8.6).

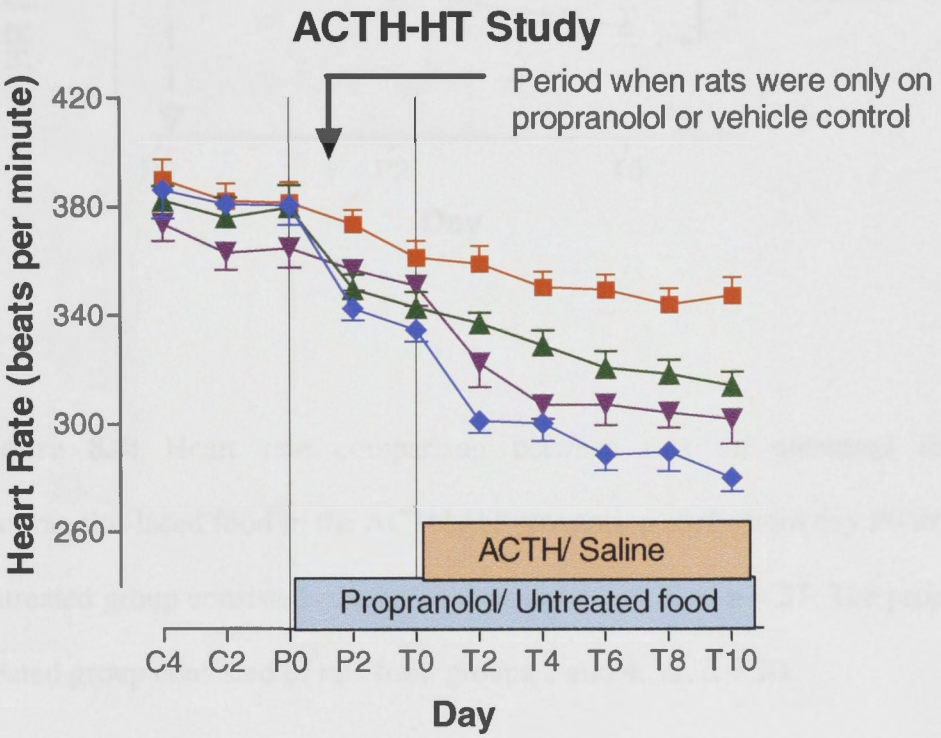

Figure 8.3: Heart rate measurements from day C4 to T10. ■ Untreated food + saline, n = 14; ▲ Propranolol + saline, n = 10; ▼ Untreated food + ACTH, n = 13; ♦ Propranolol + ACTH, n = 10.

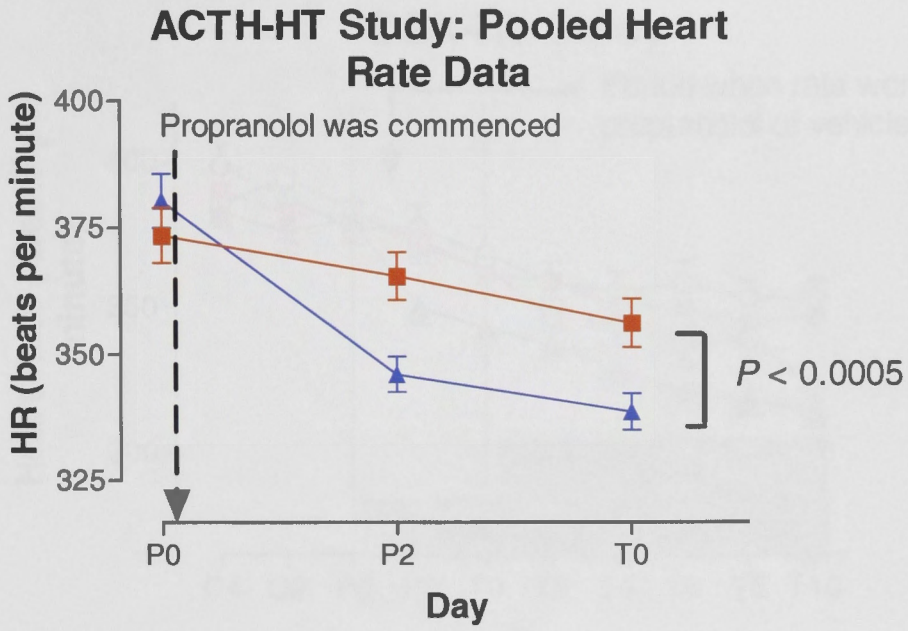

Figure 8.4: Heart rate comparison between rats on untreated food and propranolol-laced food in the ACTH-HT prevention study from day P0 to T0. The untreated group consisted of rats from groups 1 and 3, ■, n = 27. The propranolol-treated group consisted of rats from groups 2 and 4, ▲, n = 20.

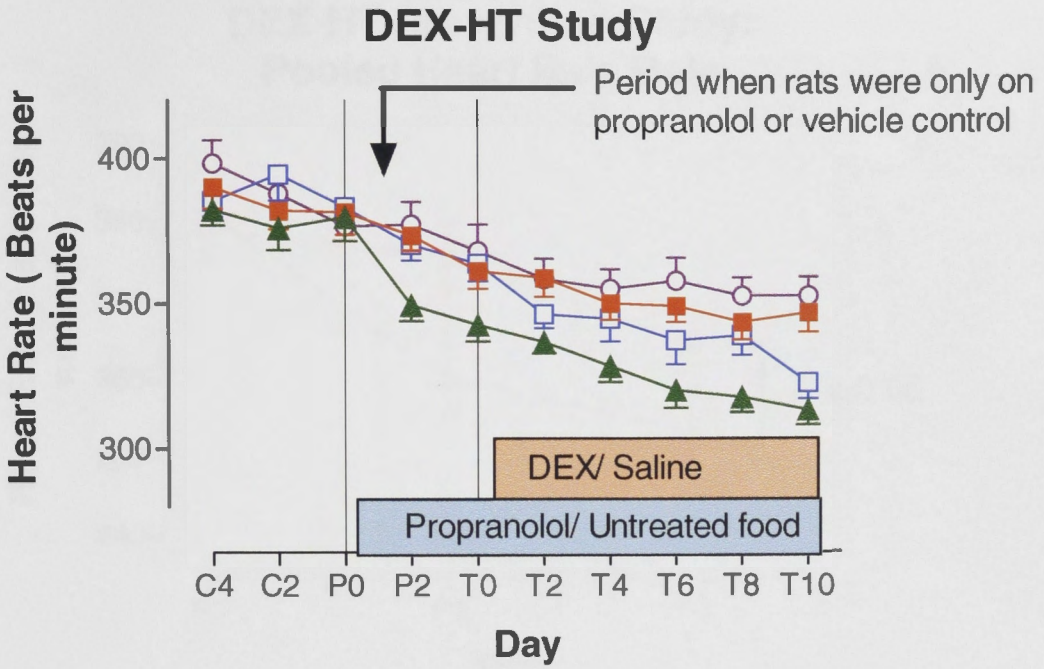

Figure 8.5: Heart rate measurements from day C4 to T0. ■ Untreated food + saline, n = 14; ▲ Propranolol + saline, n = 10; ○ Untreated food + DEX, n = 13; □ Propranolol + DEX, n = 10.

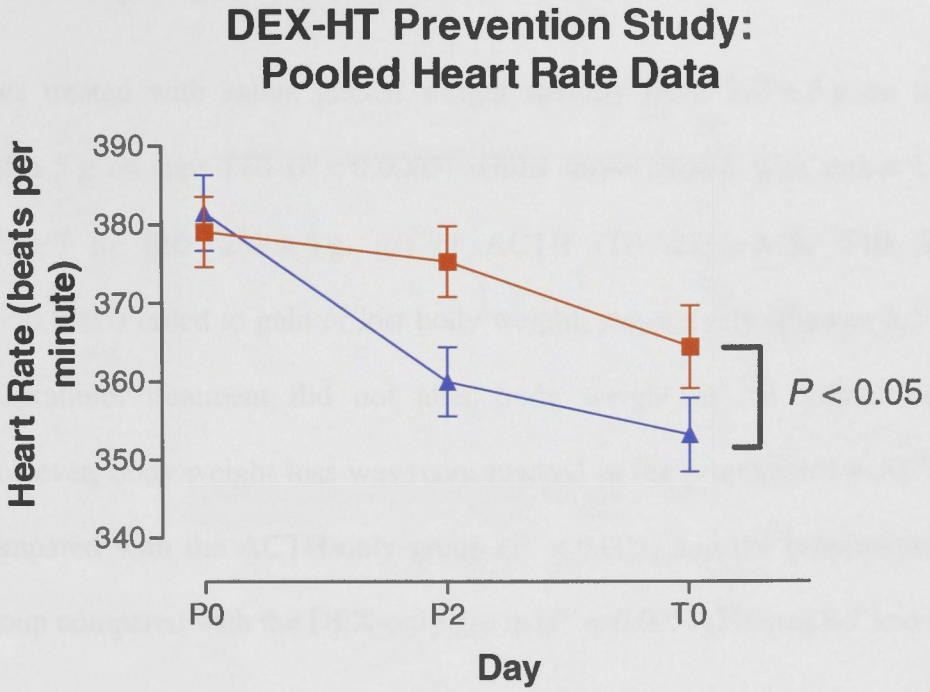

Figure 8.6: Comparison between the rats on untreated food and propranolol-laced food in the DEX-HT prevention study from day P0 to T0. The untreated group consisted of rats from groups 1 and 5, ■, n = 27. The propranolol-treated group consisted of rats from groups 2 and 6, ▲, n = 20.

8.3.3 Body weight

Rats treated with saline gained weight steadily from 273 ± 5 g on day T0 to 305 ± 5 g on day T10 ($P < 0.0005$) whilst those treated with either DEX (T0: 275 ± 7 to T10: 281 ± 6 g, *ns*) or ACTH (T0: 285 ± 8 to T10: 259 ± 6 g, $P < 0.0005$) failed to gain or lost body weight, respectively (Figures 8.7 and 8.8). Propranolol treatment did not alter body weight in the saline-treated rats. However, body weight loss was more marked in the propranolol + ACTH group compared with the ACTH-only group ($P' < 0.005$) and the propranolol + DEX group compared with the DEX-only group ($P' < 0.005$) (Figures 8.7 and 8.8).

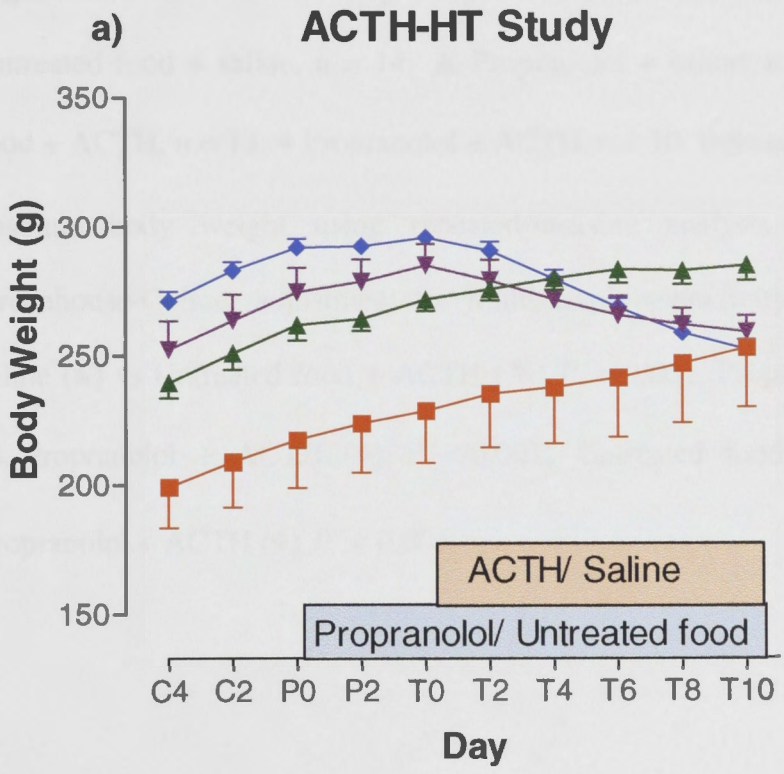

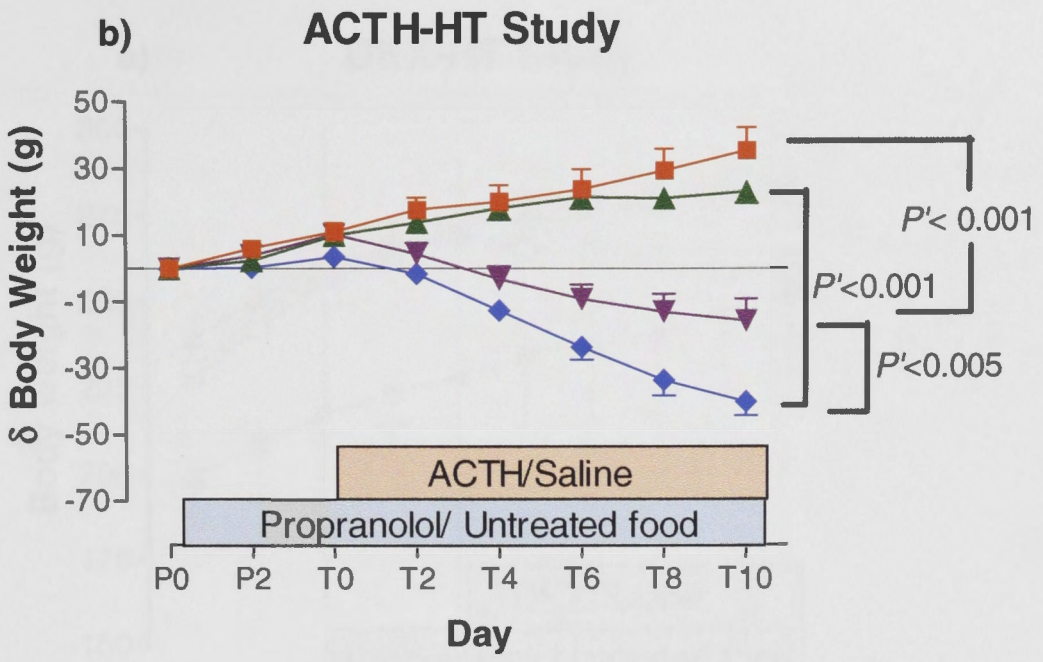

Figure 8.7: a) Absolute body weight and **b)** change (δ) in body weight. ■ Untreated food + saline, n = 14; ▲ Propranolol + saline, n = 10; ▼ Untreated food + ACTH, n = 13; ♦ Propranolol + ACTH, n = 10. Between group analysis on absolute body weight using repeated-measure analysis of variance, with Greenhouse-Geisser adjustment for multisample asphericity: Untreated food + saline (■) vs Untreated food + ACTH (▼) $P' < 0.001$; Propranolol + saline (▲) vs Propranolol + ACTH (♦) $P' < 0.001$; Untreated food + ACTH (▼) vs Propranolol + ACTH (♦) $P' < 0.005$.

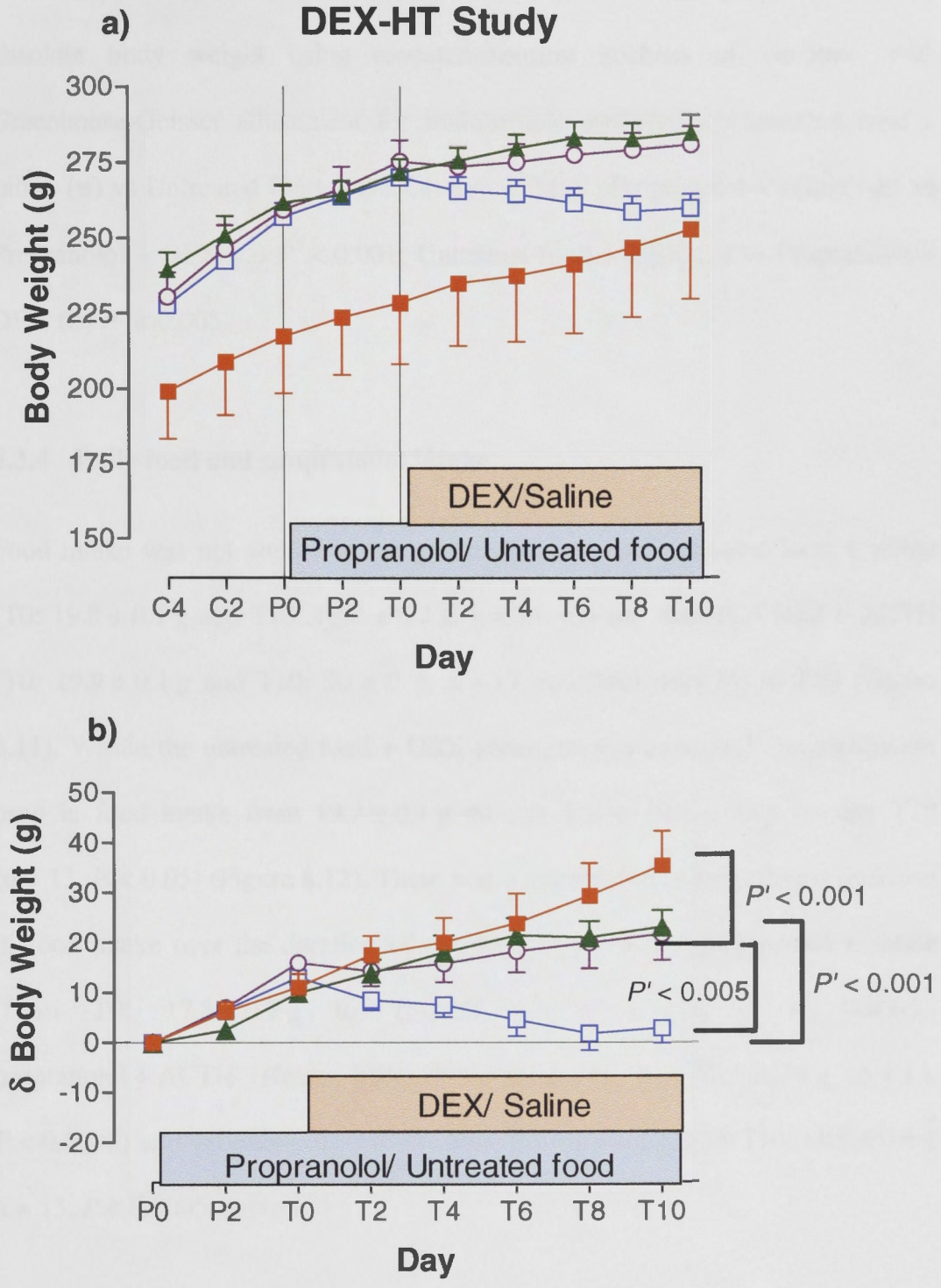

Figure 8.8: a) Absolute body weight and **b)** change (δ) in body weight. ■ Untreated food + saline, n = 14; ▲ Propranolol + saline, n = 10; ○ Untreated food

+ DEX, n = 13; □ Propranolol + DEX, n = 10. Between group analysis on absolute body weight using repeated-measure analysis of variance, with Greenhouse-Geisser adjustment for multisample asphericity: Untreated food + saline (■) vs Untreated food + DEX (○) $P' < 0.001$; Propranolol + saline (▲) vs Propranolol + DEX (□) $P' < 0.001$; Untreated food + DEX (○) vs Propranolol + DEX (□) $P' < 0.005$.

8.3.4 Daily food and propranolol intake

Food intake was not altered in the groups that received untreated food + saline (T0: 19.8 ± 0.1 g and T10: 19.8 ± 0.2 g, n = 14, *ns*) and untreated food + ACTH (T0: 19.9 ± 0.1 g and T10: 20 ± 0 g, n = 13, *ns*) from days P0 to T10 (Figure 8.11). Within the untreated food + DEX group, there was a small but significant drop in food intake from 19.7 ± 0.1 g on day T0 to 19.1 ± 0.3 g on day T10 (n = 13, $P < 0.05$) (Figure 8.12). There was a progressive and significant decrease in food intake over the duration of this experiment in the propranolol + saline (from T0: 17.5 ± 0.2 g to T10: 13.1 ± 0.3 g, n = 14, $P < 0.0005$), propranolol + ACTH (from T0: 17.4 ± 0.4 g to T10: 12.5 ± 0.4 g n = 13, $P < 0.0005$) and propranolol + DEX (from T0: 17.2 ± 0.5 g to T10: 11.9 ± 0.6 g n = 13, $P < 0.0005$) groups.

Overall, the mean food intake for rats on saline injection and untreated ground food was 19.8 ± 0 g/rat/15-hour night. This was not significantly altered by ACTH 19.9 ± 0 g/rat/15-hour night (Figure 8.9) or DEX 19.7 ± 0 g/rat/15-hour

night (Figure 8.10). However, propranolol significantly decreased food intake in saline-, ACTH- (Figure 8.11) and DEX-treated rats (Figure 8.12) ($P' < 0.005$, each). To ensure complete propranolol intake, the amount of food provided was adjusted based on intake of the previous few days. Accounting for the inevitable nightly wastage of ground food, the mean propranolol dose consumed was 95.9, 93.5 and 95 mg/kg/day (full dose 100 mg/kg/day) (Figure 8.13).

Rats treated with both ACTH and propranolol had greater reduction in food intake compare to those on ACTH alone ($P' < 0.005$, Figure 8.11). However, there was no significant change in food intake between the DEX only group and propranolol + DEX group (Figure 8.12).

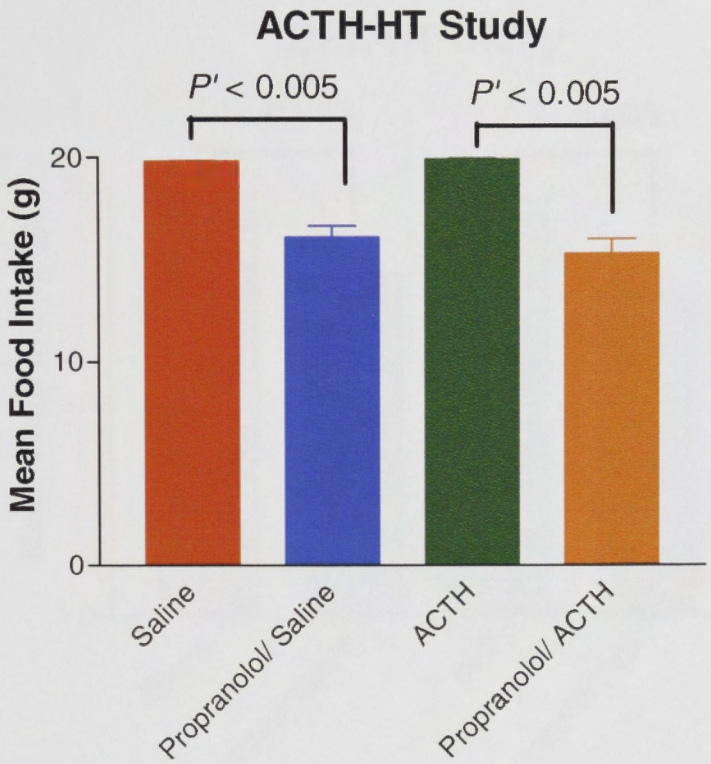

Figure 8.9: Overall mean food intake per rat per 15 hour night. Untreated food + saline, n = 14; Propranolol + saline, n = 10; Untreated food + ACTH, n = 13; Propranolol + ACTH, n = 10.

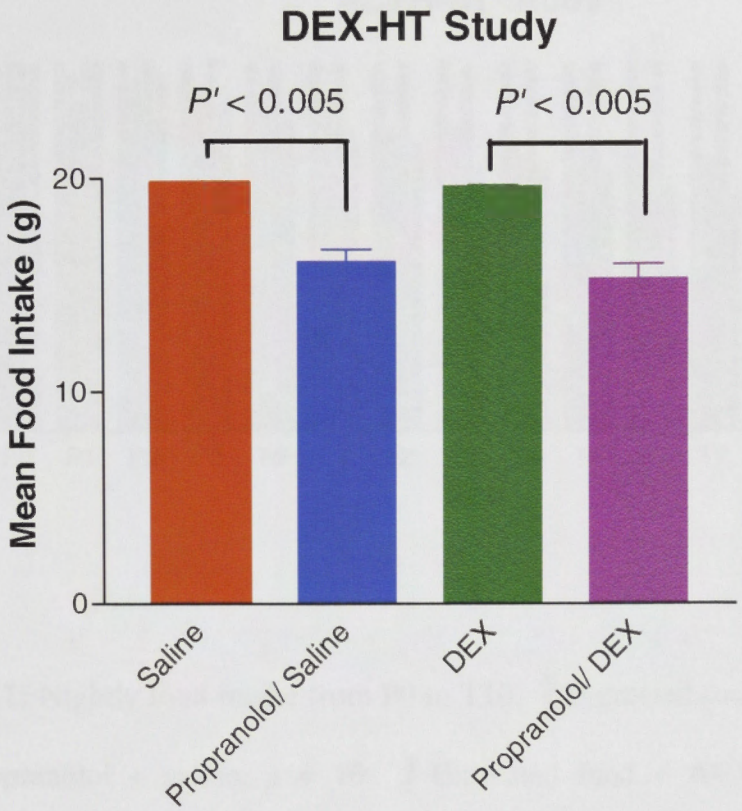

Figure 8.10: Overall mean food intake per rat per 15 hour night. Untreated food + saline, n = 14; Propranolol + saline, n = 10; Untreated food + DEX, n = 13; Propranolol + DEX, n = 10.

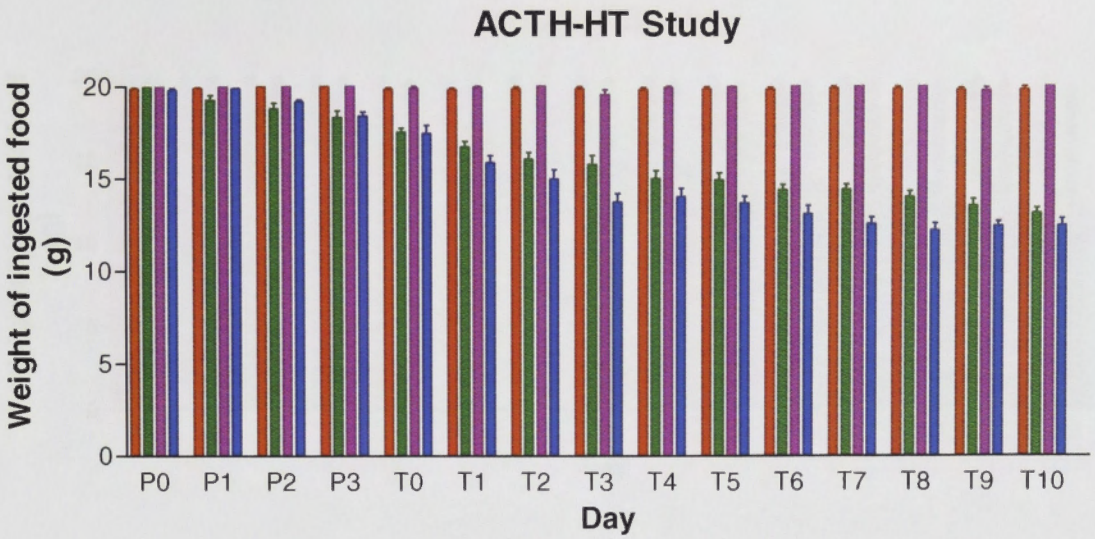

Figure 8.11: Nightly food intake from P0 to T10. Untreated food + saline, n = 14; Propranolol + saline, n = 10; Untreated food + ACTH, n = 13; Propranolol + ACTH, n = 10. $P' < 0.005$ for comparisons between the untreated food + saline group vs propranolol + saline group; untreated food + ACTH group vs propranolol + ACTH group; and propranolol + saline group vs propranolol + ACTH group using repeated measures analysis of variance.

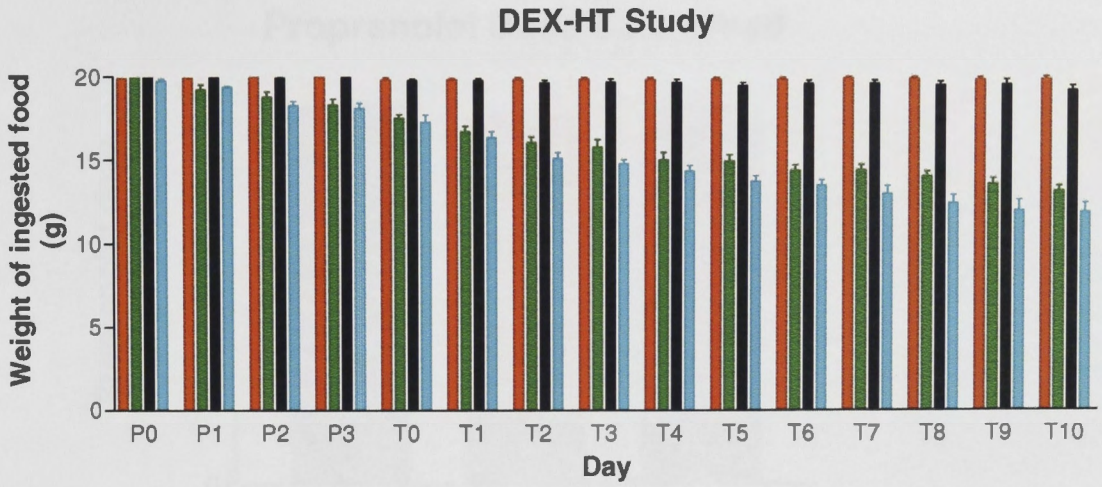

Figure 8.12: Nightly food intake from P0 to T10. ▌Untreated food + saline, n = 14; ▌ Propranolol + saline, n = 10; ▌ Untreated food + DEX, n = 13; ▌ Propranolol + DEX, n = 10. $P' < 0.005$ for comparisons between the untreated food + saline group vs propranolol + saline group; and untreated food + DEX group vs propranolol + DEX group using repeated measures analysis of variance.

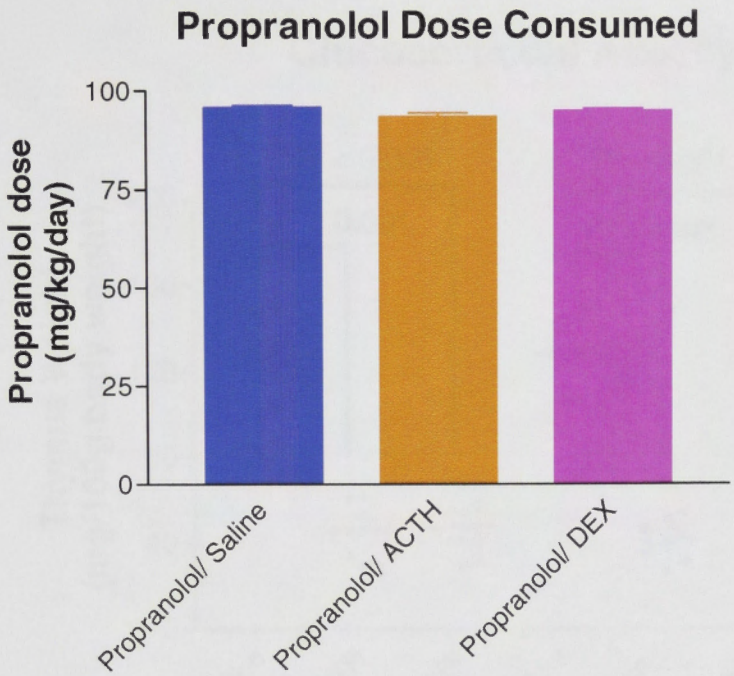

Figure 8.13: Propranolol + saline, n = 10; Propranolol + ACTH, n = 10; Propranolol + DEX, n = 10.

8.3.5 Thymus weight

Thymus weight of rats treated with ACTH and DEX was significantly lower than in those on saline injection ($P' < 0.001$). These changes were not altered by propranolol treatment. Propranolol alone did not modify thymus weight (Figure 8.14 and Table 8.1).

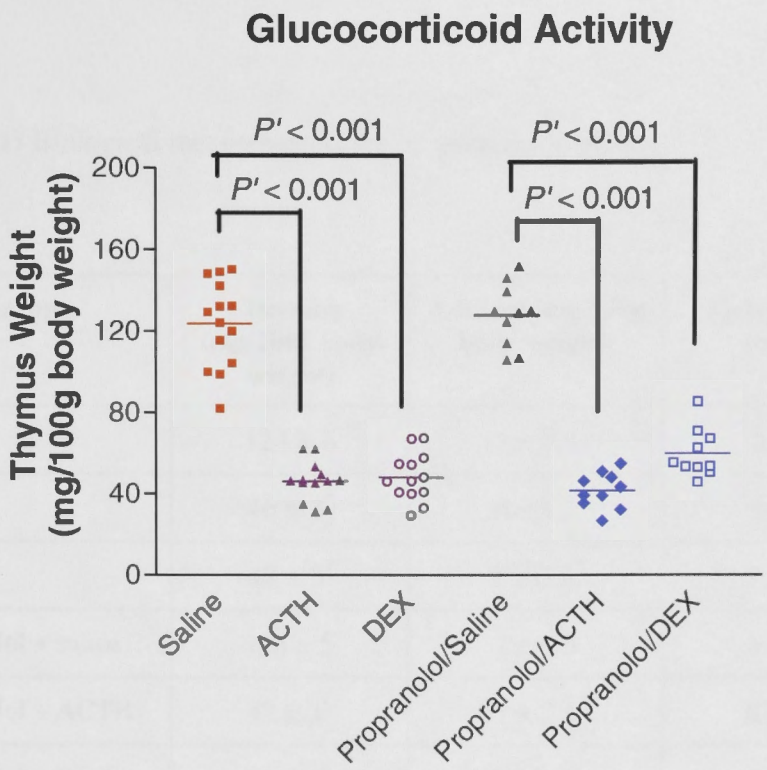

Figure 8.14: Thymus weight as an indicator of glucocorticoid activity. ■ Untreated food + saline, n = 14; ▲ Propranolol + saline, n = 10; ▼ Untreated food + ACTH, n = 13; ♦ Propranolol + ACTH, n = 10; ○ Untreated food + DEX, n = 13; □ Propranolol + DEX, n = 10.

Table 8.1: Biological measurements for propranolol studies

Groups	Thymus (mg/100g body weight)	Adrenal (mg/100g body weight)	F_2-Isoprostane (nmol/L)
Saline	124 ± 6	7 ± 0.4	5 ± 0.3
ACTH	46 ± 3*	37 ±4.2*	5 ± 0.4
DEX	48 ± 3*	5 ± 0.2*	7 ± 0.6†
Propranolol + saline	128 ± 5	7 ± 0.3	6 ± 0.2†
Propranolol + ACTH	42 ± 3§	31 ± 2.6§	8 ± 0.7#
Propranolol + DEX	60 ± 4§	5 ± 0.2§	7 ± 0.4

* $P' < 0.001$ vs saline, § $P' < 0.001$ vs propranolol ± saline, † $P' < 0.05$ vs saline, # $P' < 0.05$ vs ACTH.

8.3.6 Adrenal weight

Adrenal weight was significantly increased by ACTH treatment ($P' < 0.001$) but not by propranolol or saline. The increase in adrenal weight by ACTH was not modified by propranolol treatment (Figure 8.15a and Table 8.1).

DEX treatment significantly decreased adrenal weight ($P' < 0.001$). This reduction was not affected by propranolol treatment (Figure 8.15b and Table 8.1).

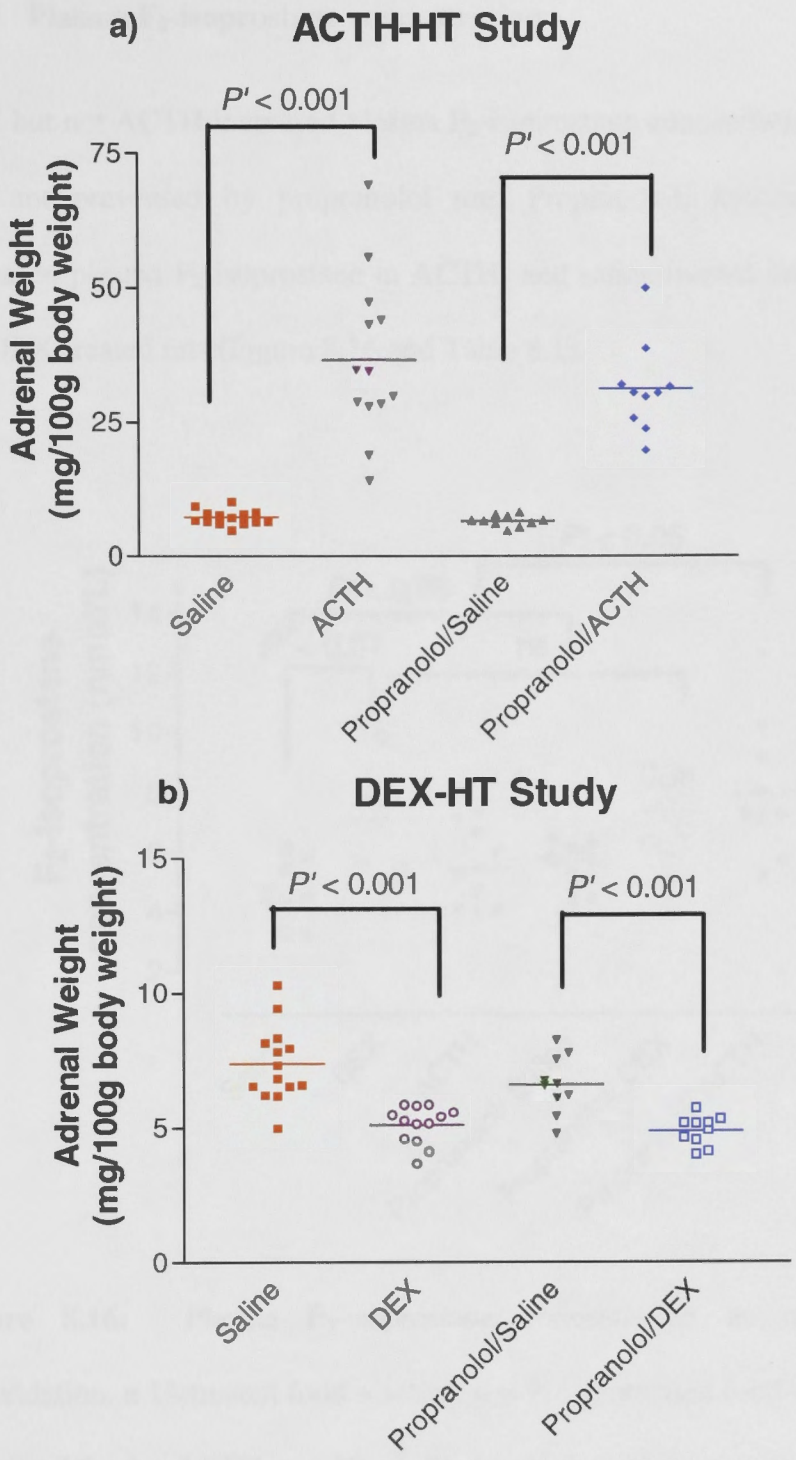

Figure 8.15: Adrenal weight as a marker of effective ACTH (**a**) and DEX (**b**) administration. ■ Untreated food + saline, n = 14; ▲ Propranolol + saline, n = 10; ▼ Untreated food + ACTH, n = 13; ♦ Propranolol + ACTH, n = 10; ○ Untreated food + DEX, n = 13; □ Propranolol + DEX, n = 10.

8.3.7 Plasma F_2-isoprostane concentration

DEX but not ACTH increased plasma F_2-isoprostane concentration. This increase was not prevented by propranolol use. Propranolol, however, significantly increased plasma F_2-isoprostane in ACTH- and saline-treated rats ($P' < 0.05$) but not DEX-treated rats (Figure 8.16 and Table 8.1).

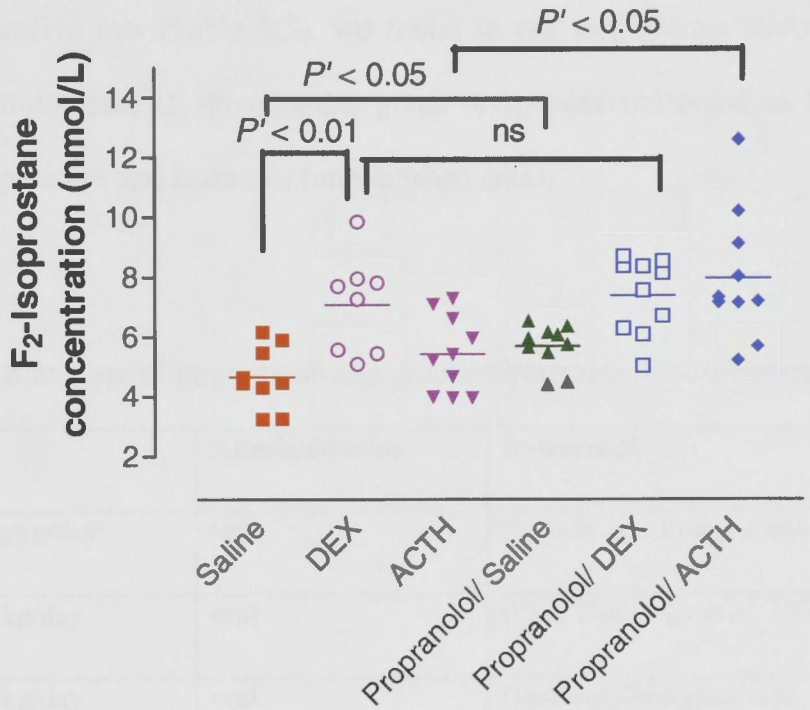

Figure 8.16: Plasma F_2-isoprostane concentration as marker of lipid peroxidation. ■ Untreated food + saline, n = 9; ○ Untreated food + DEX, n = 8; ▼ Untreated food + ACTH, n = 10; ▲ Propranolol + saline, n = 10; □ Propranolol + DEX, n = 10; ♦ Propranolol + ACTH, n = 10.

8.4 DISCUSSION

In this study, propranolol did not prevent GC-HT despite effectively inhibiting β-adrenergic receptors. The dose used (100 mg/kg/day) significantly reduced heart rate in all rats. Thus, the negative results seen in this study were not due to inadequate dosing. Although a range of propranolol dosages and regimens were effective in lowering heart rates in normal rats (Table 8.2) and blood pressure in hypertensive rats (Table 8.3), we found in our preliminary study that a lower propranolol dose at 10mg/kg/day given orally was ineffective in lowering both blood pressure and heart rate (unpublished data).

Table 8.2: Dose of propranolol that reduced heart rate in normotensive rats

Dose	Administration	References
100 mg/kg/day	oral	(Takeda and Bunag 1980)
30 mg/kg/day	oral	(Ebii, Fukunaga *et al.* 1991)
30 mg/kg/day	oral	(Igarashi, Nakajima *et al.* 1977)
30 mg/kg/day	oral	(Tsunoda, Takezawa *et al.* 2000)
5 mg/kg b.d.	intraperitoneal	(Chakrabarti and Sharma 1993)
2 mg/kg/day	subcutaneous	(Bunag 1977)

Table 8.3: Dose of propranolol that decreased heart rate in hypertensive rats

Dose	Administration	Strain	References
100 mg/kg	oral	SHR	(Kishi, Kawashima *et al.* 1985)
64 mg/kg		SHR	(Kubo, Esumi *et al.* 1977)
30 mg/kg	oral	SHR	(Antonaccio, High *et al.* 1986)
15 mg/kg	oral	SHR	(Ishihara, Chin *et al.* 1989)
5 mg/kg	intraperitoneal	Stressed-induced hypertensive rats	(Bennett and Gardiner 1979)
5 mg/kg	subcutaneous	Methylprednisolone and DOCA-hypertensive	(Burris, Waeber *et al.* 1984)
1.5 mg/L water	oral	SHR	(Owens 1987)

DOCA: deoxycorticosterone acetate, SHR: spontaneously hypertensive rat

Heart rate was used in this study as a surrogate marker of propranolol treatment efficacy as this is a parameter commonly used in the clinical setting to determine the beta blocking effect of this class of medication in humans. Propranolol level is not readily available. Furthermore, identification of a drug in the serum does not necessarily correlate with the desired clinical response. In this experiment, heart rate was assessed non-invasively using the tail cuff equipment at the time blood pressure was measured. This data was readily available from the tail cuff experiment performed to obtain the SBP. Although telemetry may be a better method to measure HR, it was not feasible in this experiment which involved only non-invasive BP monitoring.

In this study, we observed a progressive decline in heart rate in both glucocorticoid-treated and saline control rats over time throughout the entire experiment. This was expected as the rats became accustomed to the experimental procedure. As glucocorticoid (DEX, 35 μg/ 100 g body weight, orally) has been shown to reduce heart rate in male Sprague Dawley rats (Roy, De *et al.* 2009), we assessed the blood pressure changes in these groups during the period after administration of propranolol but before glucocorticoid treatment.

In this study, propranolol was added to food and was given rats overnight, when the rats were most active and awake. The amount of food provided was adjusted daily based on the weight of the animals. To ensure complete propanolol intake, the designated rats were given drug-laced food, which accounted for 90% of their food intake, at night. Each morning, the remaining food was collected and weighed. Untreated pellet food was subsequently given during the day to make up for the daily deficit.

In this study rats treated with both propranolol and either ACTH or DEX had significant body weight loss compared to control rats. This effect was not seen in the propranolol + saline treated rats. It is unclear why combination treatment with propranolol and glucocorticoid resulted in this. There is no evidence in the literature to suggest any possible interactions between propranolol and ACTH or DEX to exacerbate the catabolic effects of glucocorticoids. The reduction in food intake observed in this study could contribute to the weight loss although

reduction in food consumption was seen in all groups (ie saline, ACTH and DEX-treated groups).

The role of propranolol in reducing food intake in this study remains unclear. It is possible that propranolol affected the palatability of the ground rat food although this is unlikely to be the reason for the weight changes described above as unlimited normal pellet rat food was provided during the day to ensure that weight loss was not due to food restriction. Propranolol alone has been shown not to alter food intake in rats (Racotta and Soto-Mora 1993). However, it was shown to inhibit the hypophagic effects of the β adrenoreceptor agonists salbutamol (β1) and isoproterenol (β2) (Racotta and Soto-Mora 1993). Whether it can exert an anorexigenic effect when used in conjunction with ACTH or glucocorticoids remain unclear.

The antihypertensive effect of propranolol is likely to be related to the blockade of vasoconstriction induced by sympathetic stimulation. It has been shown that the fall in blood pressure due to propranolol was also associated with reductions in plasma renin and aldosterone concentrations (van den Meiracker, Man in't Veld *et al.* 1989). Changes in cardiac output and circulating blood volume, however, were not shown to be critical factors (van den Meiracker, Man in't Veld *et al.* 1989). Propranolol has also been reported to potentiate the effect of atrial natriuretic peptide (Yoshimoto, Naruse *et al.* 1998). The renin-angiotensin-aldosterone and atrial natriuretic peptide pathways were not tested in this study.

This study confirmed that activation of the β-adrenergic pathways is not a main mechanism of GC-HT. This is also true in other aspects of the sympathetic pathways. In one study which directly assessed the sympathetic vasomotor drive to skeletal muscle in human subjects, oral cortisol (200 mg/day, for 5 days) and DEX (3 mg/day, for 5 days) but not placebo individually increased blood pressure, and suppressed resting and stimulated muscle sympathetic activity (Macefield, Williamson *et al.* 1998). Noradrenaline spillover rate and noradrenaline uptake studies did not show any increase in sympathetic nervous activity in cortisol-induced hypertension in humans (Sudhir, Jennings *et al.* 1989). Chemical sympathectomy using 6-hydroxy dopamine did not inhibit or delay the development of ACTH-HT in rats (Li and Whitworth 1991) and sympathetic nervous activity was not increased in ACTH-HT in sheep (Spence, Mathai *et al.* 1989).

Selective inhibition of β1-adrenergic receptor with atenolol (50 mg/kg/day, orally) failed to prevent ACTH-HT in rats despite a demonstrable decrease in cardiac output (Wen, Fraser *et al.* 1999). The outcome was similar with blockade of both the β1- and β2-adrenergic receptors using propranolol, suggesting that non-selective activation of β-adrenergic receptors does not play a significant role in the development of GC-HT. Thus, the utility of β-adrenergic receptor blockers in GC-HT is limited in this form of hypertension.

As indicated earlier, propranolol is also an antioxidant via its anti-lipid peroxidation effect. Contrary to previous reports demonstrating its effectiveness

in preventing lipid peroxidation in canine sarcolemnal membranes (Mak and Weglicki 1988) and rat liver microsomes (Aruoma, Smith *et al.* 1991), propranolol was found to promote an increase in plasma F_2-isoprostane concentration in saline and ACTH-treated rats in this study (Figure 8.16). The reason for the observed discrepancy is unclear but could be due to differences in the mode of propranolol treatment (*in vitro* vs *in vivo*), target tissue of examination (heart and liver vs plasma) and assay used to evaluate lipid peroxidation (malondialdehyde and thiobarbituric vs F_2-isoprostane assays). Furthermore, there is no evidence suggesting that high dose propranolol is pro-oxidant. In the present study, there was no significant difference in the plasma F_2-isoprostane concentration in the DEX + propranolol group compared with DEX-only group (Figure 8.16). This is most likely because DEX had already resulted in raised F_2-isoprostane concentration and further increase was not apparent. With these results, it is also likely that the blood pressure lowering effect of β-adrenergic blockade was counteracted by an increase in oxidative stress in this study. Therefore, despite being known as an antioxidant, propranolol failed to prevent GC-HT.

8.5 CONCLUSION

Propranolol at 100 mg/kg/day was effective in lowering heart rate in rats. However, despite adequate treatment, propranolol was unsuccessful in preventing ACTH and DEX-HT in rats. Despite previous reports that propranolol is an antioxidant, it served as a pro-oxidant in this study.

This study, together with previous evidence that atenolol is ineffective in ACTH-HT, suggests that β-adrenoreceptor activation is not a major contributor to GC-HT in the rat and that β-adrenoreceptor blocker has a limited therapeutic role in GC-HT.

This study also showed that lipid peroxidation does not play a major role in the pathogenesis of GC-HT in rats.

CHAPTER 9

Role of 20-Hydroxyeicosatetraenoic Acid in Dexamethasone-Induced Hypertension in the Rat

9.1 INTRODUCTION

Arachidonic acid has long been known to be metabolised by cyclooxygenase and lipoxygenase to prostaglandins, prostacyclines, thromboxanes and leucotrienes. Arachidonic acid was subsequently found to be also metabolised, by cytochrome P450 enzymes to form 19- and 20-hydroxyeicosatetraenoic acids, epoxyeicosatrienoic acids and dihydroeicosatrienoic acids.

20-Hydroxyeicosatetraenoic acid (20-HETE) participates in the regulation of vascular tone in the renal, cerebral, coronary and skeletal muscle arterioles (Miyata and Roman 2005). It is a potent vasoconstrictor which can also potentiate vascular smooth muscle response to vasoconstrictor and myogenic stimuli (Miyata and Roman 2005). Furthermore, 20-HETE plays an important role in regulating renal tubular sodium reabsorption resulting in natriuretic and diurectic properties (Miyata and Roman 2005).

The interactions of NO and 20-HETE have been recognised. The catalytic activity of cytochrome P450 enzymes can be inhibited by NO or NO donors (Morgan, Ullrich *et al.* 2001). 20-HETE can be inhibited directly and functionally by NO (Alonso-Galicia, Drummond *et al.* 1997; Sun, Alonso-Galicia *et al.* 1998; Oyekan, Youseff *et al.* 1999). In addition, 20-HETE has the ability to reduce eNOS activation (Cheng, Ou *et al.* 2008) and accelerate degradation of NO by increasing NAD(P)H oxidase-related superoxide overproduction (Wang, Singh *et al.* 2006), which may further decrease the availability of NO and exacerbate

hypertension. Therefore, based on these data, 20-HETE production is likely to be increased in the presence of NO deficiency (Figure 9.1).

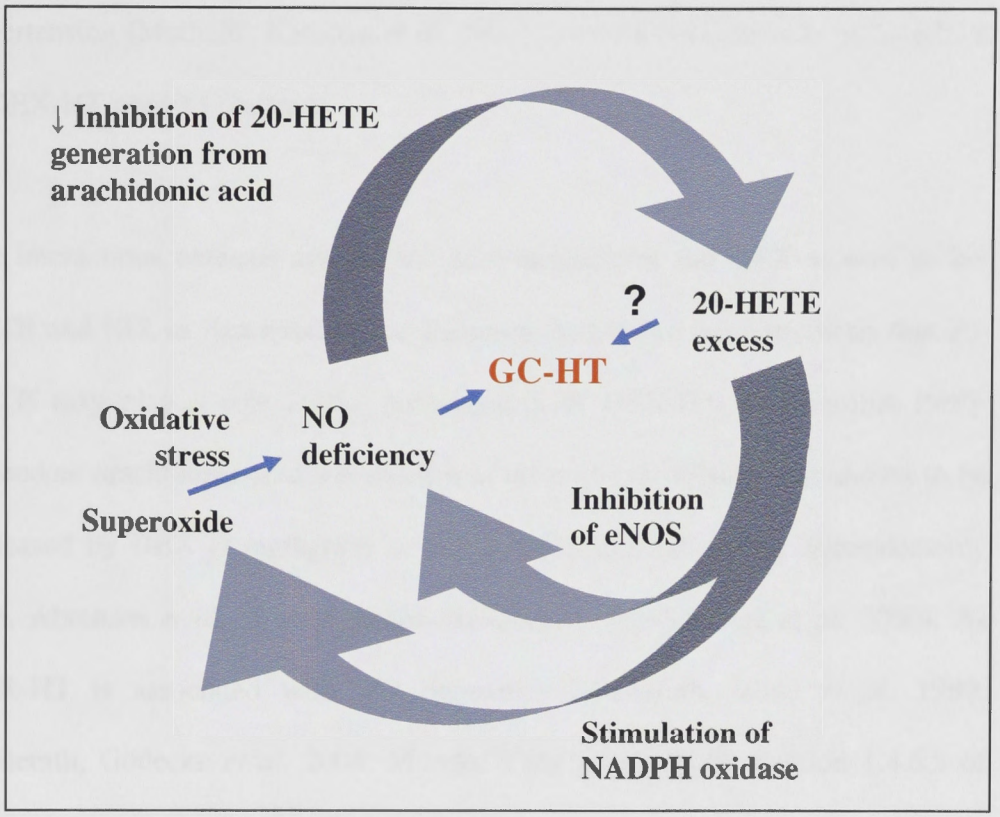

Figure 9.1: Proposed mechanism of GC-HT involving 20-HETE.

There is considerable evidence suggesting that 20-HETE plays a role in the pathogenesis of a number of experimental hypertensive models. Liu *et. al.* demonstrated that CYP4F2 transgenic mice with increased 20-HETE production have significantly higher blood pressure readings compared with wild-type controls (Liu, Zhao *et al.* 2009). They have also shown a positive correlation between blood pressure and urinary 20-HETE excretion (Liu, Zhao *et al.* 2009). Production of 20-HETE is increased in kidneys of androgen-induced hypertensive

rats (Singh, Cheng *et al.* 2007). Furthermore, chronic inhibition of 20-HETE production decreased blood pressure in rats treated with angiotensin II suggesting that 20-HETE contributes to the development of angiotensin II-induced hypertension (Muthalif, Karzoun *et al.* 2000). Nevertheless, the role of 20-HETE in DEX-HT remains unclear.

The interactions between arachidonic acid metabolism and DEX as well as 20-HETE and NO, as described in the literature, had led to our hypothesis that 20-HETE may play a role in the pathogenesis of DEX-HT. Cytochrome P450-dependent arachidonic acid metabolism in rat proximal tubules was shown to be increased by DEX (1 mg/kg/day sc for 7 days) and reduced by adrenalectomy (Lin, Abraham *et al.* 1994; Sanchez-Mendoza, Lopez-Sanchez *et al.* 2000). As DEX-HT is associated with NO deficiency (Wallerath, Witte *et al.* 1999; Wallerath, Godecke *et al.* 2004; Mondo, Yang *et al.* 2006) (Section 1.4.6.3 of Chapter 1 and Section 7.3.6 of Chapter 7), it was also important to evaluate whether excess 20-HETE availability, which is linked with NO deficiency, is a cause of DEX-HT. Despite these results, a recent study from our group showed that DEX-hypertensive rats (DEX 20 μg/kg/day, subcutaneously, for 12 days) did not have increased 20-HETE excretion (Zhang, Hu *et al.* 2008). Whilst this finding suggests the absence of 20-HETE excess in DEX-hypertensive rats, an increase in plasma and tissue 20-HETE concentrations cannot be assumed. Furthermore, the absence of an increased 20-HETE does not exclude an increase in sensitivity of the vasculature to 20-HETE. The role of 20-HETE in the

development of DEX-HT can only be assessed by evaluating the blood pressure response of DEX-hypertensive rats using a 20-HETE inhibitor.

Therefore, the aim of this study was to investigate whether renal parenchymal 20-HETE is increased by low dose DEX (10 μg/rat/day); and to investigate if the specific 20-HETE inhibitor *N*-hydroxy-*N′*-(4-butyl-2-methylphenyl) formamidine (HET0016) can reverse DEX-HT. The kidney tissue was used because of its relevance in ACTH-HT. We have previously demonstrated that urinary excretion of 20-HETE in ACTH-hypertensive rats was elevated (Zhang, Hu et al. 2008). We have also shown that ACTH increased renal vascular resistance (Wen, Fraser et al. 1998; Wen, Fraser et al. 1999). Furthermore, the rise in BP due to ACTH in rats was accompanied by reductions in iNOS and eNOS gene expression in the kidney (Lou, Wen et al. 2001).

9.2 METHODS

9.2.1 Experimental protocol

This study was approved by the Animal Experimentation Ethics Committee (J.HB. 23.06). General methods used in this study have been described in Chapter 2. After 8 days treatment with DEX, the rats were injected with HET0016 (10 mg/kg/day, in a volume of 2 mL/kg) or vehicle (2 mL/kg, 10% lecithin in saline) intraperitoneally.

HET0016 was generously donated by Taisho Pharmaceutical Co. Ltd, Saitama, Japan. HET0016, a lipid soluble powder, was prepared in a lecithin-based vehicle (10% lecithin in normal saline).

Thirty-two male Sprague Dawley rats weighing 250-300 g were divided into 4 treatment groups.

Group 1: Saline (0.1 mL/rat/day subcutaneous injection) + Vehicle (2 mL/kg, 10% lecithin in saline, intraperitoneal injection), n = 8

Group 2: Saline + HET 0016 (10 mg/kg/day, intraperitoneal injection), n = 8

Group 3: DEX (10 μg/rat/day subcutaneous injection) + Vehicle, n = 8

Group 4: DEX + HET0016, n = 8

9.2.2 Tail-cuff systolic blood pressure and body weight measurements

The animals underwent second-daily tail-cuff experiments until day T8 when SBP readings will be obtained daily. The tail-cuff experimental protocol was unlike the one described in Chapter 2. Because of the limited amount of HET0016 available to our laboratory, the duration of treatment had to be shortened. Therefore, the tail-cuff experimental protocol had to be modified to maximise the number of tail-cuff experimental days over the shortened experimental duration. This

modification to the original tail-cuff experiment highlighted in Chapter 2 is described in Figure 9.2.

Body weight was measured immediately after the tail-cuff experiments.

9.2.3 Metabolic measurements

Twenty-four hour food and water consumption and urine volume were measured on the day before the last tail-cuff blood pressure measurement (day T11) using individual metabolic cages as described in Section 2.7 of Chapter 2.

9.2.4 Thymus weight measurement

At the end of the experiment, rats were sacrificed under anaesthesia. Thymus resection and blood sampling procedures were as described in Section 2.8 of Chapter 2.

Thymus wet weight, expressed relative to body weight (grams thymus weight per 100 g body weight), was used as a marker of glucocorticoid activity.

9.2.5 Plasma nitrate and nitrite assay

Plasma NOx concentrations, measured using the Griess colorimetric reaction described in Section 2.10.1 of Chapter 2, were used as a marker of endogenous NO availability.

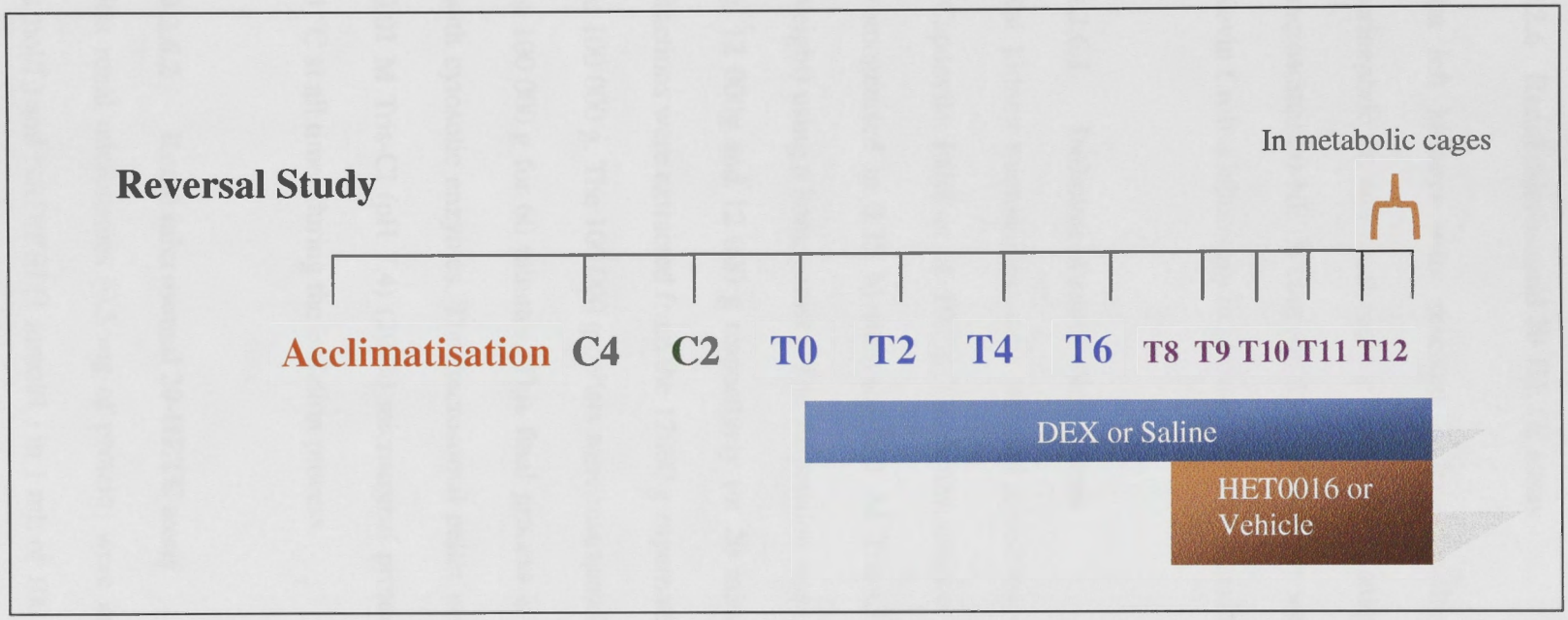

Figure 9.2: Modified tail-cuff experimental protocol. The prefix "C" denotes control days and "T" denotes treatment days.

9.2.6 Renal microsomal 20-HETE assay

Rat left kidneys were resected under anaesthesia. They were dissected free of perinephric fat and renal capsule before being snap frozen at -70 °C for assay of renal microsomal 20-HETE concentration. This assay was performed by Associate Professor Kevin Croft's laboratory in University of Western Australia.

9.2.6.1 Isolation of renal microsomes

Rat kidney microsomes were isolated according to previously published techniques (Capdevila, Falck *et al.* 1990). The frozen kidneys were thawed, weighed, minced and homogenised in 0.25 M sucrose, 0.01 M Tris-Cl (pH 7.4) (15 mL/g of wet kidney weight) using a homogeniser. The suspension was centrifuged thrice successive at 3000 g, 12 000g and 12 000 g respectively for 20 minutes each time. Finally, microsomal fractions were extracted from the 12000 g supernatants by centrifugation for 60 minutes at 100 000 g. The 100 000 g pellets were resuspended in 0.15 M KCl and re-centrifuged at 100 000 g for 60 minutes. This final process is necessary to reduce contaminations with cytosolic enzymes. The microsomal pellet was suspended in 0.25 M sucrose and 0.01 M Tris-Cl (pH 7.4) (20-30 microsomal protein/mL). The specimens were kept at 4 °C at all times during the isolation process.

9.2.6.2 Renal microsomal 20-HETE assay

Rat renal microsomes (0.5 mg of protein) were incubated with arachidonic acid (100 μmol/L) and NAD(P)H (1 mmol/L) in 1 mL of 100 mmol/L potassium phosphate buffer (pH 7.4). Reactions were started with the addition of NAD(P)H, incubated for 15

minutes at 37 °C, and then stopped with the addition of 20 μL 2N HCl. Extraction of the mixture was performed using 2 mL ethyl acetate. The extract was then evaporated under a nitrogen stream and resuspended in H_2O:acetonitrile (6:4). The reaction products were separated on an Agilent LiChrosphere C18 reversed phase column using a Hewlett-Packard series 1100 instrument (Hewlett-Packard, Waldbronn, Germany). The rate of product formation was analysed with ultraviolet detection at 200 nm. The initial mobile phase consisted of acetonitrile: water: acetic acid (40: 60: 0.1%) and a flow rate of 1 mL/min. Compounds were eluted with a linear gradient starting at 40% acetonitrile and eventually increased to 100% acetonitrile over 20 minutes. The formation of 20-HETE, expressed as nmol/min/mg protein, was determined by comparing the peak areas of individual samples with a reference 20-HETE standard curve that was run on the same day as the sample analysis (Cayman Chemicals, Ann Arbor. Michigan. USA).

9.2.7 Plasma F_2-isoprostane assay

Plasma F_2-isoprostane concentration was used as a marker of systemic lipid peroxidation. The assay technique was described in Section 2.11.3 of Chapter 2.

9.2.8 Statistical analysis

Results were expressed as mean ± SEM. Statistical analysis were as described in Section 2.12 of Chapter 2.

The plasma NOx, renal microsomal 20-HETE, plasma F_2-isoprostane results for the saline + vehicle and saline + HET0016 groups consist of pooled data from the 20-

HETE/ACTH-HT reversal and prevention studies performed by other investigators in our laboratory to increase the sample size and hence, statistical power.

9.3 RESULTS

9.3.1 Tail-cuff systolic blood pressure

SBP in the DEX + vehicle group increased significantly from 121 ± 3 on day T0 to 138 ± 2 mmHg on day T6 ($P < 0.01$). There was no significant change in SBP following treatment with the vehicle lecithin from day T8 (140 ± 3 mmHg) to T12 (140 ± 5 mmHg) in this group. Similarly, SBP in the DEX + HET0016 group increased significantly from 120 ± 4 mmHg on day T0 to 133 ± 3 mmHg on day T6 ($P < 0.0005$) but did not change significantly with the commencement of HET0016 from T8 (140 ± 3 mmHg) to T12 (138 ± 6 mmHg).There was no significant change in SBP in the saline + vehicle group from day T0 (118 ± 2 mmHg) to day T6 (120 ± 2 mmHg) and from day T8 (119 ± 1 mmHg) to day T12 (112 ± 2 mmHg). Rat receiving saline and HET0016 treatments also did not show any significant blood pressure change from day T0 (119 ± 3 mmHg) to T6 (118 ± 2 mmHg) and from day T8 (121 ± 2 mmHg) to T12 (119 ± 3 mmHg) (Figure 9.3).

Between-group comparisons showed that SBP was significantly higher in the DEX-treated groups (DEX + vehicle and DEX + HET0016) compared to the saline-treated group from day T0 to day T6 (n = 8, $P' < 0.05$ and $P' < 0.005$ respectively). Neither

HET0016 nor vehicle altered the blood pressure profiles from day T8 to T12 in all groups (Figure 9.3).

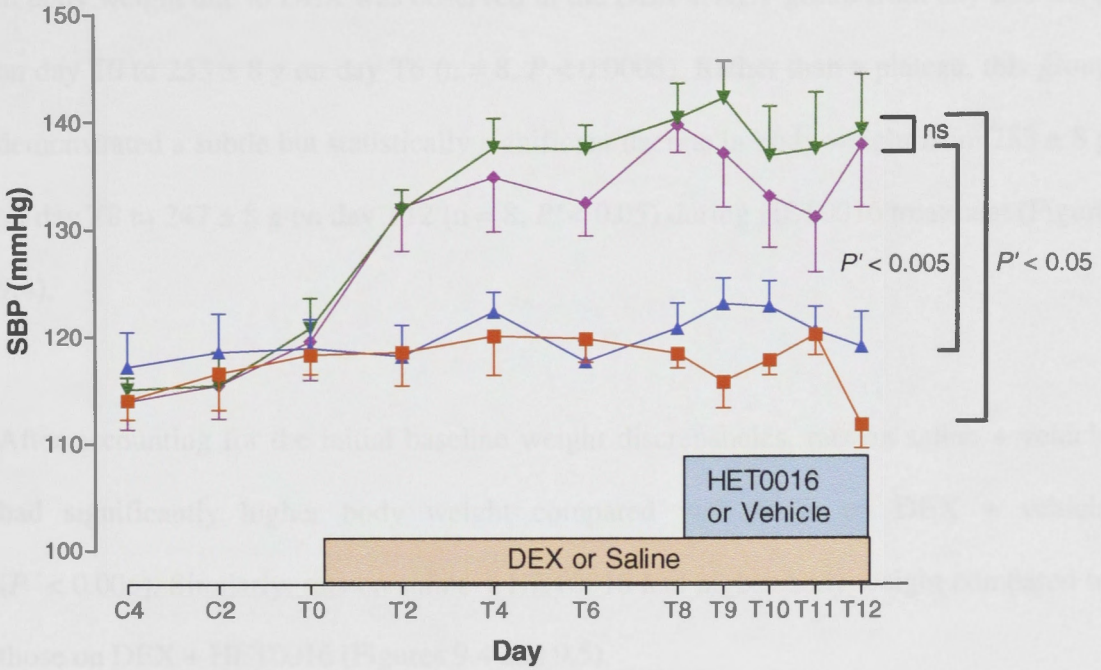

Figure 9.3: Tail-cuff systolic blood pressure. ■ Saline + Vehicle, n = 8; ▲ Saline + HET0016, n = 8; ▼ DEX + Vehicle, n = 8; ♦ DEX + HET0016, n = 8.

9.3.2 Body weight

There was an increase in body weight in the saline + vehicle-treated group from 299 ± 15 g on day T0 to 321 ± 17 g on day T6 ($P < 0.0005$). This statistically significant increase in body weight was not observed from day T8 to T12 following the commencement of lecithin (T8: 328 ± 17, T12: 335 ± 17 g, n = 6, *ns*). However, in the

DEX + vehicle group, DEX treatment resulted in a slight but significant weight loss from 278 ± 10 g on day T0 to 266 ± 9 g on day T6, n = 8, $P < 0.0005$) which plateaued from day T8 (267 ± 10 g) to T12 (264 ± 9 g, *ns*) whilst on vehicle treatment. Similar fall in body weight due to DEX was observed in the DEX + HET group from day 266 ± 9 g on day T0 to 253 ± 8 g on day T6 (n = 8, $P < 0.0005$). Rather than a plateau, this group demonstrated a subtle but statistically significant decline in body weight from 253 ± 8 g on day T8 to 247 ± 8 g on day T12 (n = 8, $P' < 0.05$) during HET0016 treatment (Figure 9.4).

After accounting for the initial baseline weight discrepancies, rats on saline + vehicle had significantly higher body weight compared with those on DEX + vehicle ($P' < 0.005$). Similarly, rats on saline + HET0016 had higher body weight compared to those on DEX + HET0016 (Figures 9.4 and 9.5).

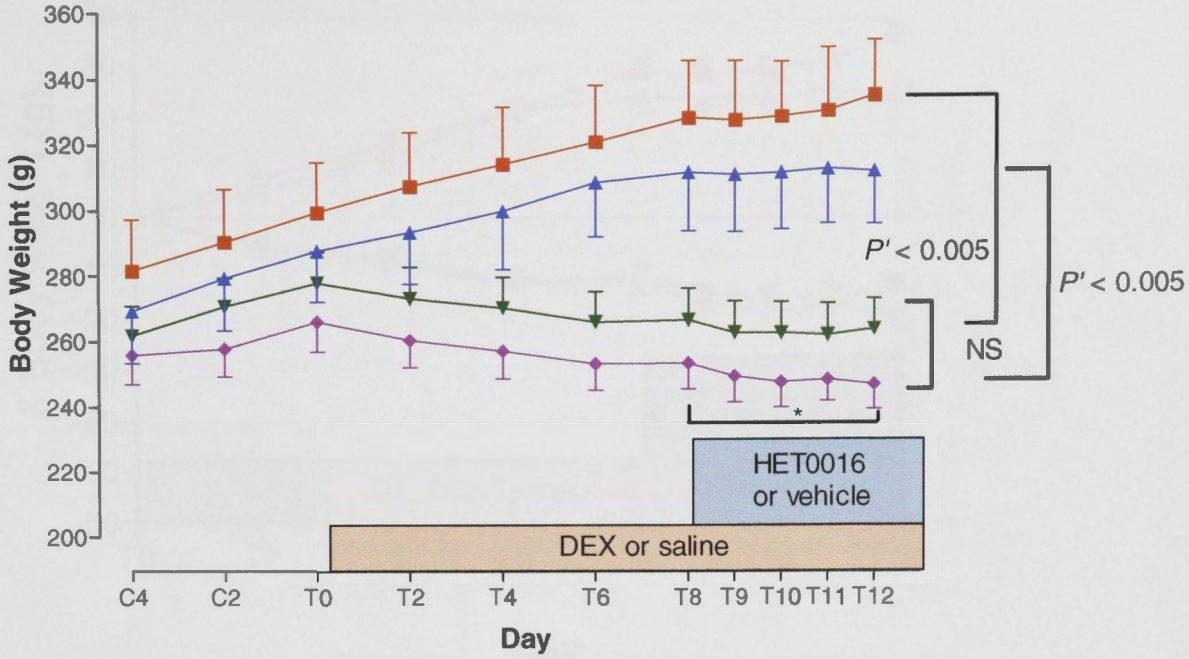

Figure 9.4: Body weight measurements. ■ Saline + Vehicle, n = 8; ▲ Saline + HET0016, n = 8; ▼ DEX + Vehicle, n = 8; ♦ DEX + HET0016, n = 8. * There was a statistically significant decline in body weight from T8 to T12 in the DEX + HET0016 group ($P' < 0.005$, one way ANOVA).

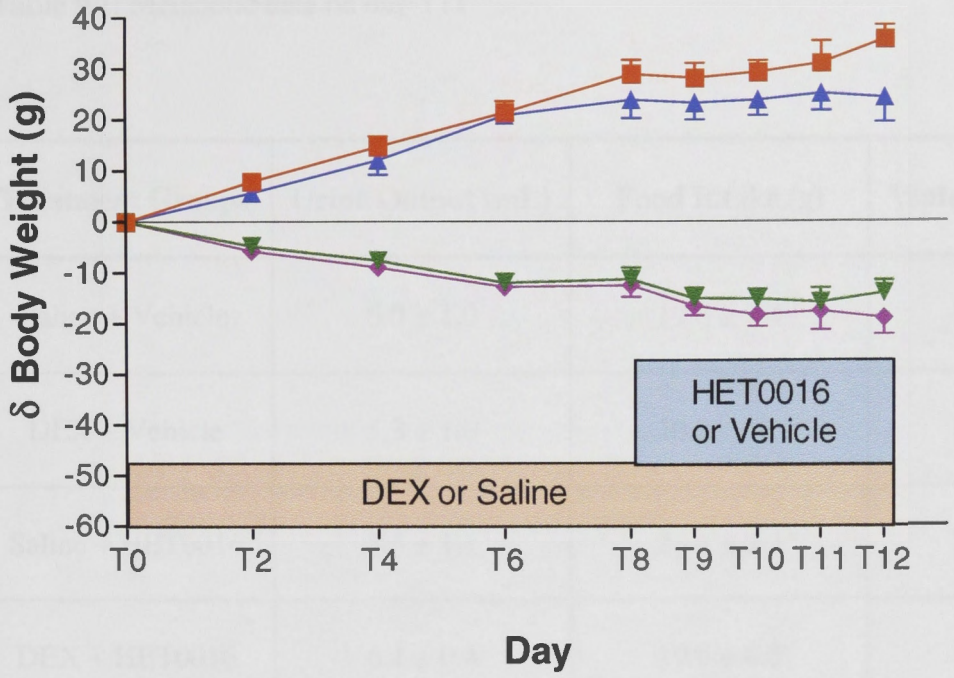

Figure 9.5: Change in body weight. ■ Saline + Vehicle, n = 8; ▲ Saline + HET0016, n = 8; ▼ DEX + Vehicle, n = 8; ♦ DEX + HET0016, n = 8.

9.3.3 Metabolic parameters

On day T11, there was no significant difference in urine output, food and water consumption in any treatment group (Table 9.1, Figures 9.6-9.8).

Table 9.1: Metabolic data on day T11.

Treatment Groups	Urine Output (mL)	Food Intake (g)	Water Intake (mL)
Saline + Vehicle	6.0 ± 1.0	19.6 ± 1.4	36.1 ± 2.2
DEX + Vehicle	5.3 ± 1.0	20.8 ± 1.1	30.1 ± 2.2
Saline + HET0016	4.3 ± 1.1	21.4 ± 2.3	33.1 ± 2.6
DEX + HET0016	6.1 ± 0.4	19.9 ± 0.5	34.8 ± 4.3

Results were expressed as mean ± SEM.

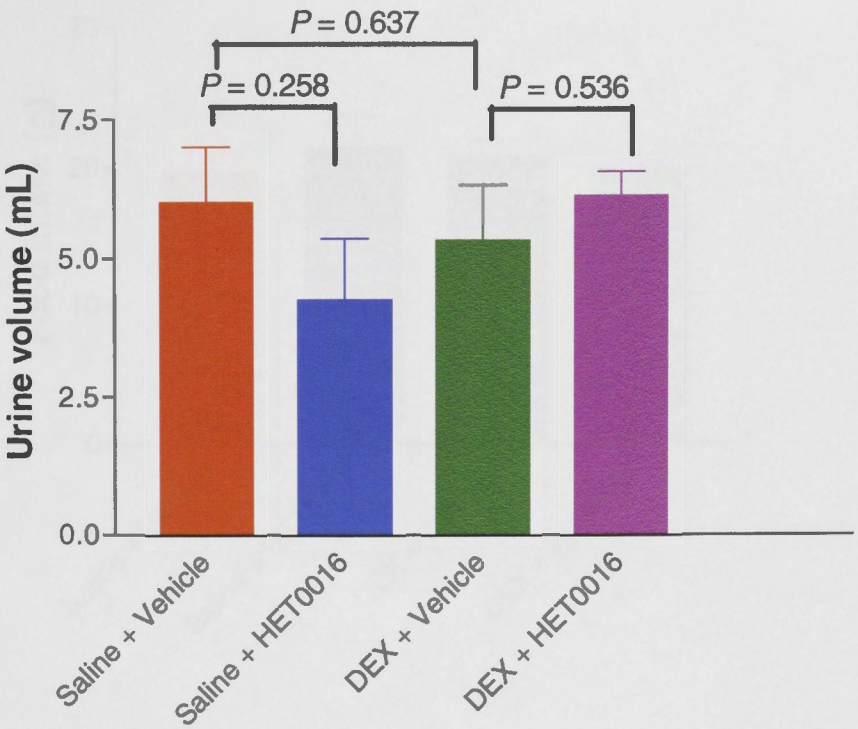

Figure 9.6: 24 hour urine volume on day T11. Saline + Vehicle, n = 8; Saline + HET0016, n = 8; DEX + Vehicle, n = 8; DEX + HET0016, n = 8.

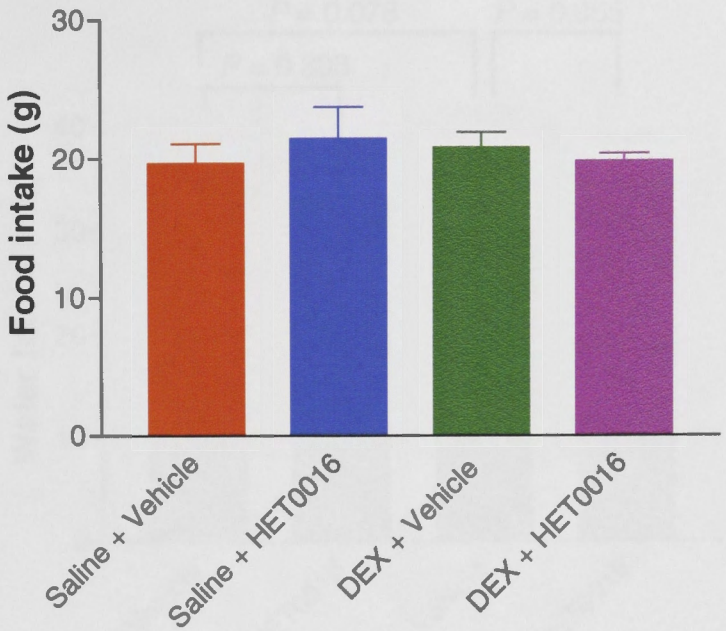

Figure 9.7: 24-hour food consumption. Saline + Vehicle, n = 8; Saline + HET0016, n = 8; DEX + Vehicle, n = 8; DEX + HET0016, n = 8.

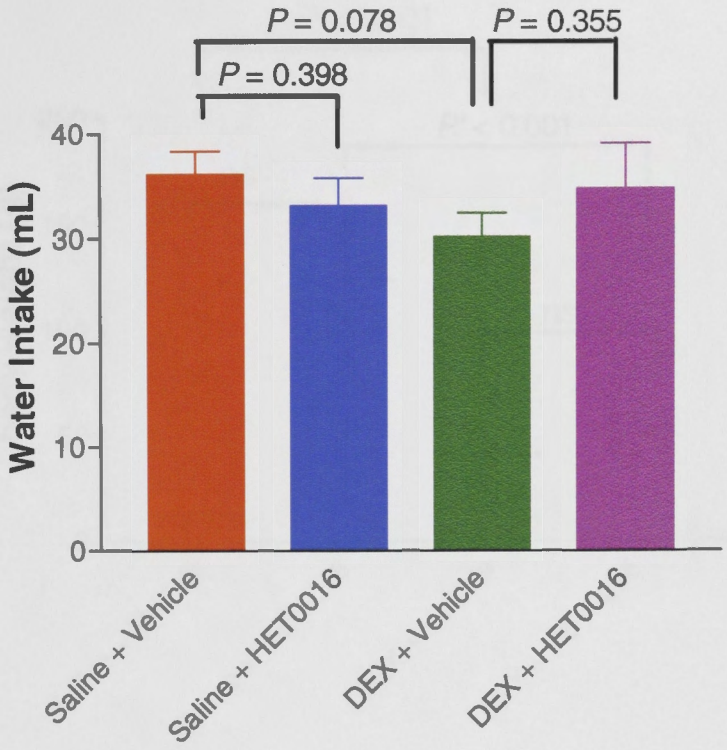

Figure 9.8: 24-hour water consumption. Saline + Vehicle, n = 8; Saline + HET0016, n = 8; DEX + Vehicle, n = 8; DEX + HET0016, n = 8.

9.3.4 Thymus weight

There was a significant decrease in thymus weight associated with DEX treatment (saline + vehicle: 119 ± 6 vs DEX + vehicle: 41 ± 6 mg/g body weight, $P' < 0.005$). This decrease was not modified by HET0016 (DEX + vehicle: 41 ± 6 vs DEX + HET0016: 51 ± 3 mg/g body weight, *ns*) (Figure 9.9).

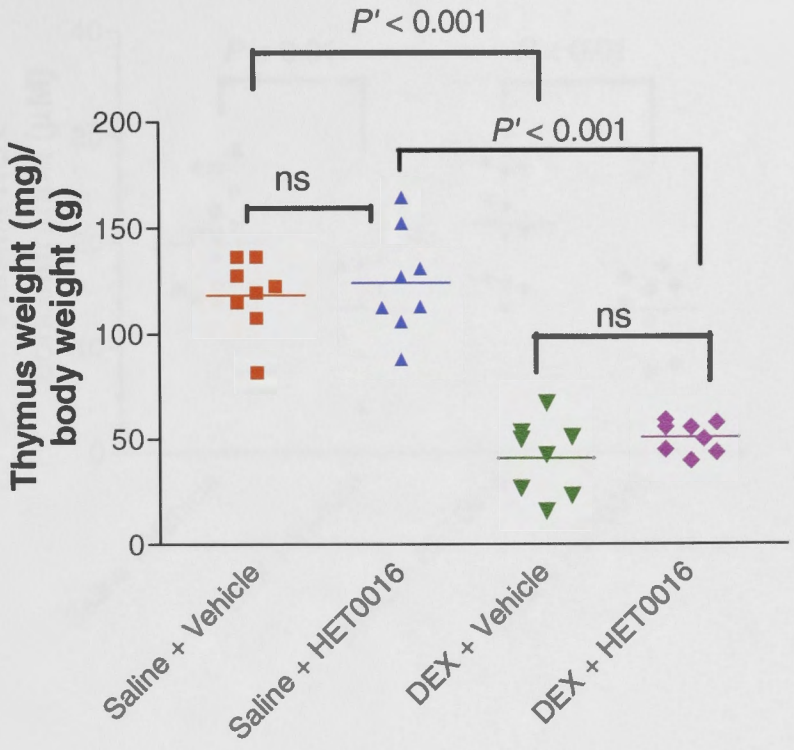

Figure 9.9: Thymus weight as marker of glucocorticoid activity. ■ Saline + Vehicle, n = 8; ▲ Saline + HET0016, n = 8; ▼ DEX + Vehicle, n = 8; ♦ DEX + HET0016, n = 8.

9.3.5 Plasma nitrate and nitrite concentration

DEX significantly decreased plasma NOx concentration from 20 ± 1 (n = 16) to 14 ± 2 μM (n = 8, $P < 0.01$) and this decrease was not reversed by HET0016 (saline + HET0016: 22 ± 2, n = 13 vs DEX + HET0016: 14 ± 1 μM, n = 8, $P < 0.01$). HET0016 did not alter plasma NOx levels in either the saline or DEX-treated groups (Figure 9.10).

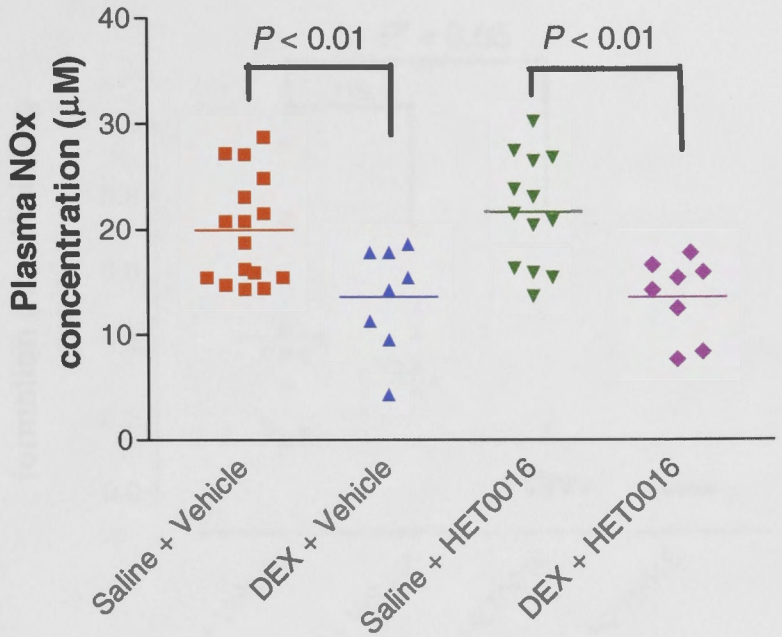

Figure 9.10: Plasma nitrate and nitrite concentrations. ■ Saline + Vehicle, n = 16; ▼ DEX + Vehicle, n = 8; ▲ Saline + HET0016, n = 13; ♦ DEX + HET0016, n = 8.

9.3.6 Renal microsomal 20-HETE concentration

DEX treatment did not alter renal microsomal 20-HETE concentration (saline + vehicle: 0.42 ± 0.07, n = 12 vs DEX + vehicle: 0.36 ± 0.03 nmol/min/mg protein, n = 6). Renal microsomal 20-HETE was significantly lower in saline + HET0016-treated rats (0.03 ± 0.02 nmol/min/mg protein, n = 8) compared to saline + vehicle-treated rats (0.42 ± 0.07 nmol/min/mg protein, n = 12, $P' < 0.05$) and was undetectable in the DEX + HET1106 group (Figure 9.11).

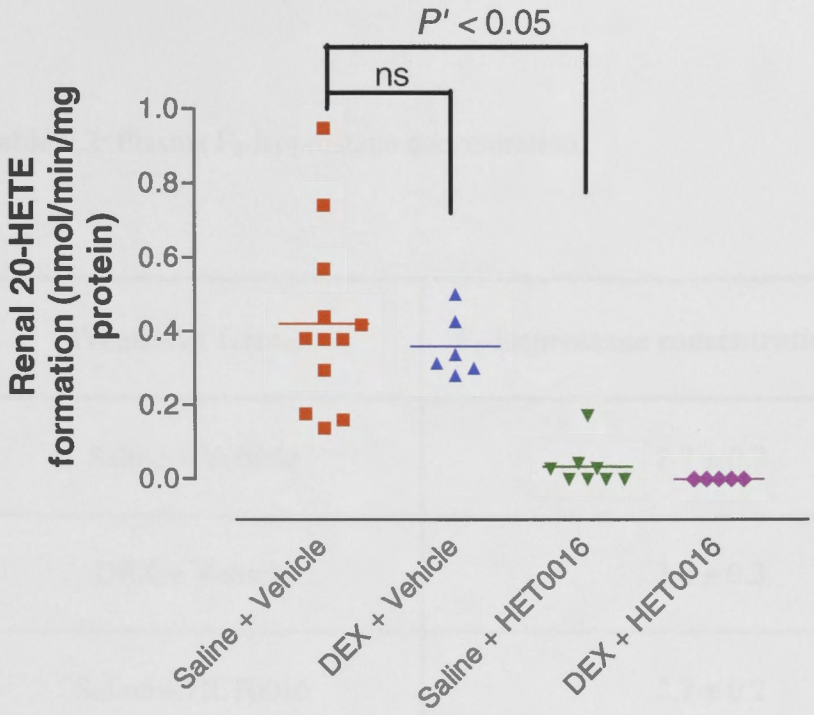

Figure 9.11: Renal microsomal 20-HETE concentration. ■ Saline + Vehicle, n = 12; ▼ DEX + Vehicle, n = 6; ▲ Saline + HET0016, n = 8; ♦ DEX + HET0016, n = 5.

9.3.7 Plasma F_2-isoprostane concentration

There was no significant difference in plasma F_2-isoprostane concentration in any of the treatment groups. There was no significant difference in plasma F_2-isoprostane concentration between saline- and DEX-treated rats. HET0016 did not alter F_2-isoprostane concentration in DEX- or saline-treated rats (Table 9.2 and Figure 9.12).

Table 9.2: Plasma F_2-isoprostane concentration

Treatment Groups	F_2-isoprostane concentration (nmol/L)
Saline + Vehicle	2.7 ± 0.2
DEX + Vehicle	3.3 ± 0.3
Saline + HET0016	2.7 ± 0.2
DEX + HET0016	2.8 ± 0.3

Results were expressed as mean ± SEM.

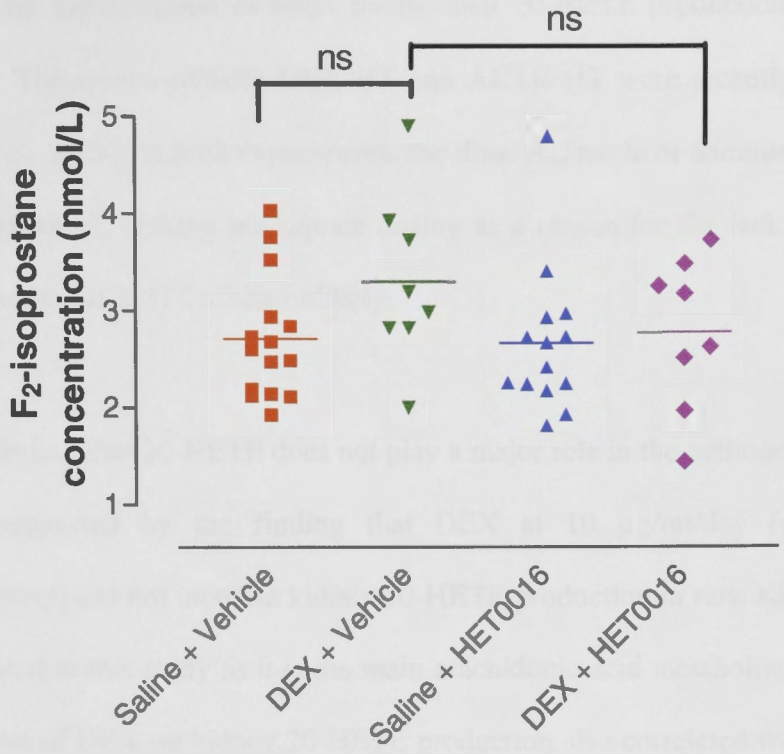

Figure 9.12: Plasma F_2-isoprostane concentration as marker of systemic oxidative stress. ■ Saline + Vehicle, n = 15; ▼ DEX + Vehicle, n = 8; ▲ Saline + HET0016, n = 14; ♦ DEX + HET0016, n = 8.

9.4 DISCUSSION

The salient finding of this study was that the 20-HETE inhibitor HET0016 was unable to reverse established hypertension due to DEX despite completely inhibiting renal microsomal 20-HETE production. This was in contrast to the rat ACTH-HT model where HET0016 was effective in preventing and reversing hypertension as well as

reversing the elevation of renal microsomal 20-HETE production (Zhang, Wu *et al.* 2009). The results of both DEX-HT and ACTH-HT were recently published (Zhang, Wu *et al.* 2009). In both experiments, the dose and mode of administration of HET0016 were identical, making inadequate dosing as a reason for the lack of antihypertensive response in DEX-HT seems unlikely.

This finding that 20-HETE does not play a major role in the pathogenesis of DEX-HT is also supported by the finding that DEX at 10 μg/rat/day (approximately 0.03 mg/kg/day) did not increase kidney 20-HETE production in rats. Kidney 20-HETE was evaluated in this study as it is the main arachidonic acid metabolite in the rat. The lack of effect of DEX on kidney 20-HETE production also correlated with the evidence that urinary excretion of 20-HETE was not increased in DEX-hypertensive rats (Zhang, Hu *et al.* 2008). These findings, however, do not completely eliminate the possibility of a role of renal 20-HETE in DEX-HT as higher DEX doses in rats (0.3-1 mg/kg/day) have been reported to result in increased renal 20-HETE production (Lin, Abraham *et al.* 1994; Sanchez-Mendoza, Lopez-Sanchez *et al.* 2000). Thus, DEX at higher doses could influence 20-HETE production and the likely effect on blood pressure regulation warrants further investigations in future studies.

As discussed in Section 1.7 of Chapter 1, there is increasing evidence implicating the role of oxidative stress and NO-redox imbalance in the pathogenesis of DEX-HT (Zhang, Croft *et al.* 2004; Hu, Zhang *et al.* 2006). The latter phenomenon is associated with NO deficiency. As in another study conducted in our laboratory (Krug, Zhang *et al.* 2008), this study once again demonstrated that DEX-hypertensive rats have lower

plasma NOx. This finding is consistent with data shown by Wallerath *et al.* that DEX resulted in downregulation of eNOS in mice (Wallerath, Witte *et al.* 1999). In this study, inhibition of 20-HETE production with HET0016 failed to restore decreased plasma NOx availability induced by DEX. This suggests that NO does not have a regulatory effect on the renal 20-HETE production in the DEX-HT model. Furthermore, it is possible that the reduction in nitric oxide due to DEX may be independent of the 20-HETE pathway.

The association of 20-HETE and oxidative stress is recognised. 20-HETE has been shown to stimulate ROS production through eNOS uncoupling (Cheng, Ou *et al.* 2008) and activation of the NAD(P)H oxidase pathway (Medhora, Chen *et al.* 2008). In this study F_2-isoprostane, a marker of systemic lipid peroxidation and oxidative stress, was not elevated by DEX treatment. This result is inconsistent with other studies (Chapters 6 and 8) in this project which showed significant a significant increase in plasma F_2-isoprostane concentration due to DEX. This may represent a false negative result due to insufficient power of the relatively small sample size to detect the difference. Pooled results from the rats treated with only saline or DEX from the different studies in this project (Chapters 6, 8 and 9) showed that DEX significantly increased plasma F_2-isoprostane concentration (Figure 11.1, Chapter 11), consistent with our findings in Chapters 6 and 8. It is also unclear if the vehicle used in this study had caused this negative result. In the absence of a change in plasma F_2-isoprostane in the DEX-only group, it is difficult to draw any conclusion about the role of HET0016 in reversing oxidative stress associated with DEX-HT.

Whether HET0016 influences the metabolic effects induced by low dose DEX (20 μg/rat) such as growth stasis, acute transient natriuresis and diuresis, as will be described in Chapter 10, was assessed in this study. In this study, HET0016 did not reverse weight loss induced by DEX. Rather, the combination of HET0016 and DEX resulted in a slight but significant weight loss from day T8-T12. This phenomenon was not seen in DEX + vehicle treated rats. Whilst 20-HETE is known to have a diuretic effect, inhibition of 20-HETE with HET0016 failed to alter urine output. Furthermore, consistent with our findings in Chapter 10, there is no significant difference in urine volume with DEX treatment on day T11. The lack of diuresis due to DEX further strengthens the notion that 20-HETE, a known diuretic, has no major influence in this hypertensive model.

There are several studies in the literature highlighting the differences between ACTH- and DEX-HT (Chapter 1). The results demonstrated in this study, which were in contrast to those observed in ACTH-HT, further support the notion that ACTH- and DEX-HT involve different pathophysiological mechanisms. HET0016 successfully reversed ACTH-HT (Zhang, Wu *et al.* 2009) but not DEX-HT as shown in this study. DEX-HT was not associated with elevated renal microsomal 20-HETE level whilst an increase was observed in ACTH-HT (Zhang, Wu *et al.* 2009). This ACTH-induced increase was reversed by HET0016 (Zhang, Wu *et al.* 2009). Furthermore, urinary 20-HETE excretion was increased in ACTH-HT but not DEX-HT (Zhang, Hu *et al.* 2008).

9.5 CONCLUSION

DEX did not increase renal microsomal 20-HETE production and specific 20-HETE inhibition with HET0016 failed to reverse DEX-HT and DEX-induced reduction in plasma NOx. These results suggest that the arachidonic acid metabolite 20-HETE does not play a significant role in the pathogenesis of DEX-HT.

CHAPTER 10

Metabolic Profiles of Dexamethasone-Induced Hypertension in Rats

10.1 INTRODUCTION

In rats, glucocorticoid excess is associated with negative sodium balance, and markedly reduced body weight secondary to skeletal muscle and fat catabolism (Tonolo, Fraser *et al.* 1988). The metabolic effects of excess glucocorticoid, which are dose-dependent, do not correlate with the hypertensive response it causes. Tonolo *et al* have demonstrated that a DEX dose as low as 1 μg/rat/day could raise blood pressure without any change in body weight in rats (Tonolo, Fraser *et al.* 1988). Most of the studies on DEX-HT in the literature described DEX doses many times higher than the dose used by our laboratory or Tonolo *et al.* (Okuno, Suzuki *et al.* 1981; Handa, Kondo *et al.* 1984; Nakamoto, Suzuki *et al.* 1991), thus introducing potential significant confounding associated with major metabolic effects. The dose used in the haemodynamic studies (Chapters 3 and 4) was 20 μg/rat/day. Although this moderately low dose was much higher than that described by Tonolo *et al.* and slightly higher than the dose used in other DEX-related studies in this research project, it was still significantly lower that other studies in the literature (Okuno, Suzuki *et al.* 1981; Handa, Kondo *et al.* 1984; Nakamoto, Suzuki *et al.* 1991).

Even though this project aims to look at the mechanisms of DEX-HT, it is still important to note the metabolic changes associated with glucocorticoid administration as these changes not only act as surrogate markers of effective glucocorticoid administration, they may also influence blood pressure and other haemodynamic parameters. For example, changes in fluid balance can alter blood

pressure regulation via the renin angiotensin system. DEX dose of 10 μg/rat/day has been previously shown to raise blood pressure without altering body weight and water intake (Hu, Zhang *et al.* 2006). It, however, increased haematocrit (Hu, Zhang *et al.* 2006).

As the doses used in the haemodynamic studies (Chapters 3 and 4) were higher than the dose reported previously from our laboratory (Hu, Zhang *et al.* 2006), additional metabolic assessments were made on the rats used in the haemodynamic study (Chapter 3) to evaluate the metabolic consequences of DEX at 20 μg/rat/day and to verify that the haemodynamic changes observed in Chapter 3 were not consequences of sodium retention and plasma volume expansion.

In this study, the following parameters were analysed:

- Food consumption
- Water consumption
- Urine volume
- Urine sodium and potassium excretion
- Urine sodium: potassium ratio
- Body weight
- Systolic blood pressure

10.2 METHODS

10.2.1 Experimental animals

This study was approved by the Animal Experimentation Ethics Committee of the Australian National University (Protocol No. J.HB.22.06). The rats were housed and acclimatised as described in Sections 2.2 and 2.3 of Chapter 2.

As the rats were treated with either saline or DEX, the treatment protocol did not include pre-treatment days. Rather, there were 8 control days before treatment with either saline or DEX was commenced on day T0.

Fifteen rats received daily injections of saline (0.2 mL/rat, sc) and 10 rats received DEX (20 μg/rat, sc) from T0-T10 using the method described in Section 2.3 in Chapter 2.

10.2.2 Tail-cuff systolic blood pressure measurements

Second-daily tail-cuff SBP measurements were performed on all rats using the method described in Section 2.5.1 in Chapter 2.

10.2.3 Metabolic parameters

As mentioned earlier, there were 8 control days before treatment with either saline or DEX was commenced. Metabolic data were recorded second-daily from C7

onwards. Following the tail-cuff SBP and body weight measurements which were performed second-daily, the rats were then housed singly in metabolic cages that allow measurements of 24-hour urine volume, food and water consumption. These data were recorded second-daily from day C7 to T9 (Figure 10.1). Measurements of urine volume and water intake were expressed as mL per 24 hours. Food intake was adjusted for spillage and measurements were expressed in grams per 24 hours.

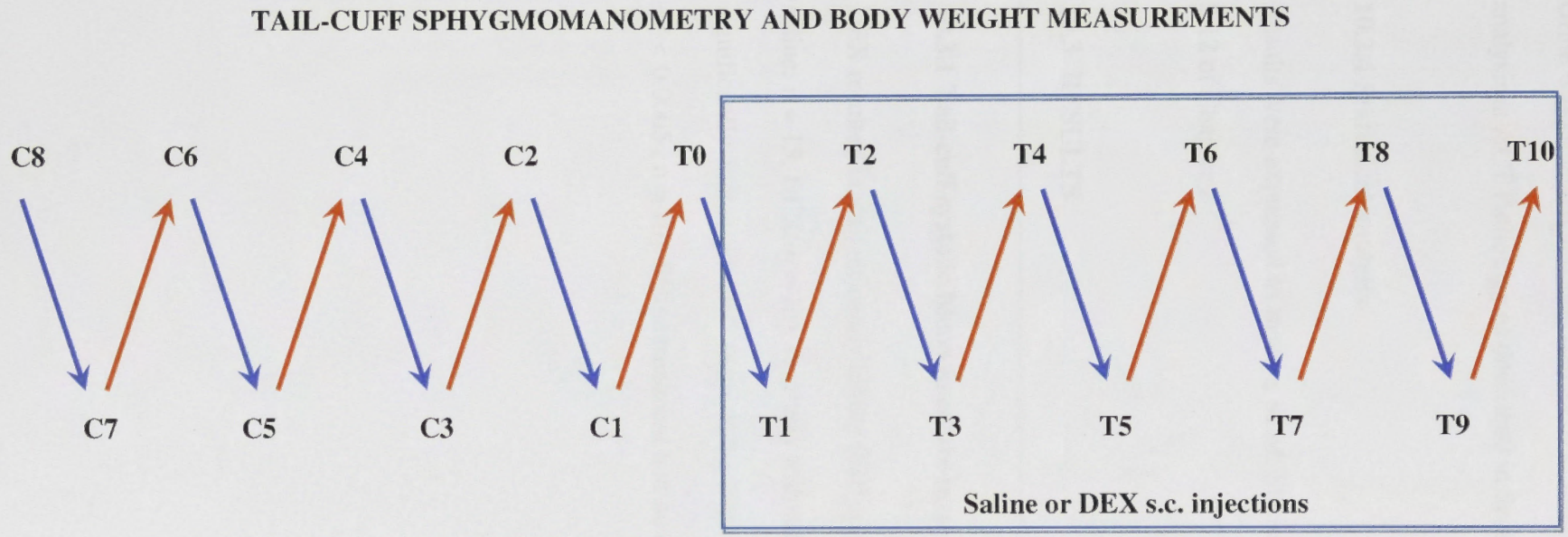

Figure 10.1: Timeline of experimental protocol. → into metabolic cages, → out of metabolic cages, C: control days, T: treatment days.

Urine was collected and stored in a -70°C freezer until sodium, potassium and creatinine analysis at ACT Pathology as described in Sections 2.10.3 and 2.10.4.

10.2.4 Statistical analysis

Results were expressed as mean ± SEM. Statistical analysis was as described in Section 2.12 of Chapter 2.

10.3 RESULTS

10.3.1 Tail-cuff systolic blood pressure measurements

DEX resulted in a significantly higher SBP compared with saline treatment ($P < 0.0005$, saline: n = 15, DEX: n = 10). Analysis within the DEX-treated group showed that DEX significantly increased SBP from 120 ± 2 on day T0 to 149 ± 6 mmHg on day T10 ($P < 0.0005$, n = 10). Saline treatment had no effect on SBP (*ns*, n = 15) (Figure 10.2).

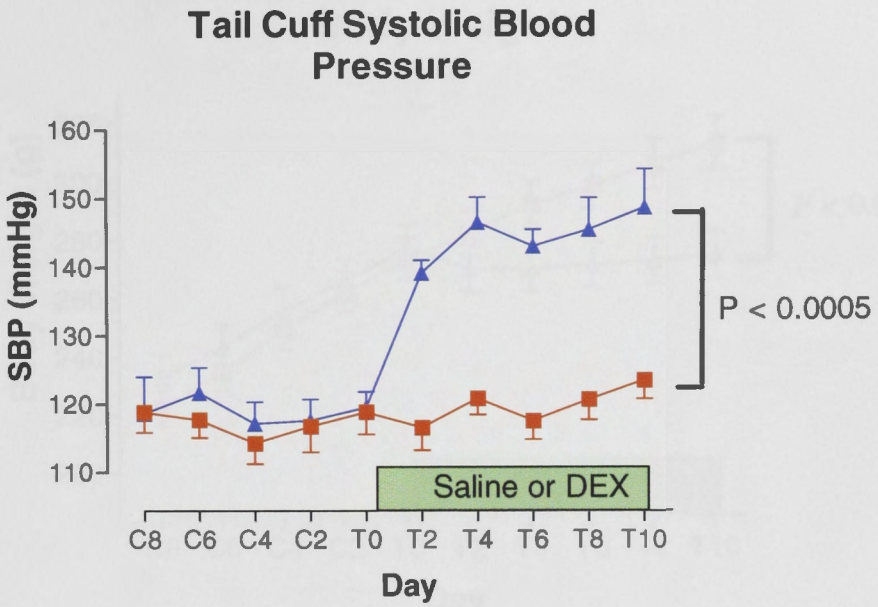

Figure 10.2: Tail-cuff systolic blood pressure. ■ Saline, n=15; ▲ DEX, n=10.

10.3.2 Body weight

DEX treatment prevented body weight gain (T0: 278 ± 8 g and T10: 275 ± 8 g, *ns*). Rats on saline treatment gained weight steadily (from T0: 274 ± 7 g to T10: 314 ± 9 g, $P < 0.0005$). Body weight was significantly lower in DEX-treated rats compared to controls ($P < 0.0005$) (Figure 10.3).

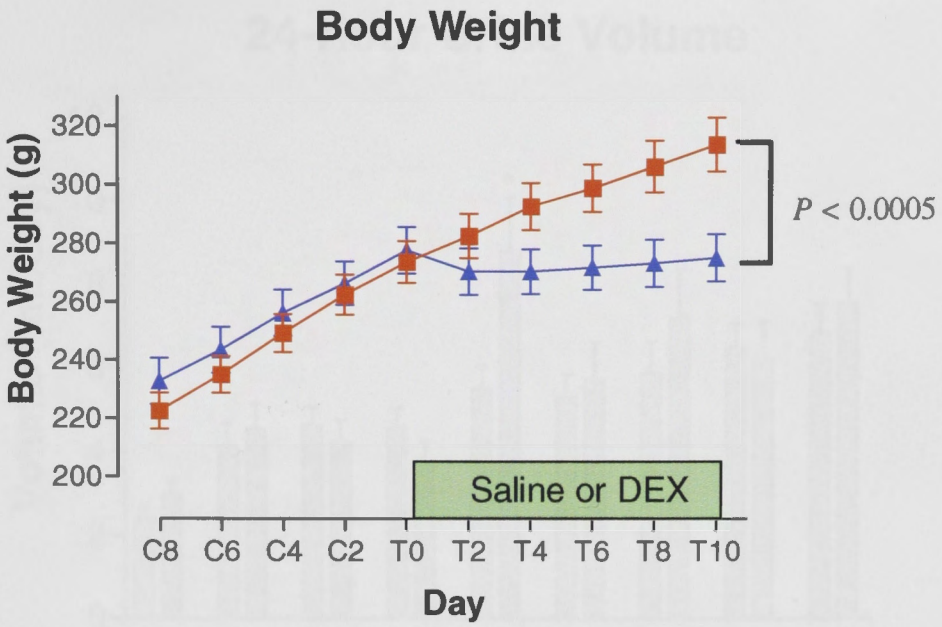

Figure 10.3: Body weight. ■ Saline, n=15; ▲ DEX, n=10.

10.3.3 Urine volume

Urine output was increased both in DEX- (from C1: 3.8 ± 0.6 mL to T9: 7.6 ± 0.9 mL, n = 10, $P < 0.005$) and saline-treated rats (from C1: 4.6 ± 0.1 mL to T9: 6.9 ± 0.7 mL, n = 15, $P < 0.01$) (Figure 10.4).

DEX resulted in a significant increase in urine volume in comparison with the saline treatment group ($P < 0.005$, saline: n = 15, DEX: n = 10) (Figure 10.4). Day to day comparisons between the saline and DEX-treated groups showed a significant increase in urine volume by DEX-treated rats on day T1 (saline: 5.5 ± 0.6 mL vs DEX: 8.8 ± 1.3 mL, $P < 0.05$), which was a day following the commencement of DEX injections (Figure 10.4).

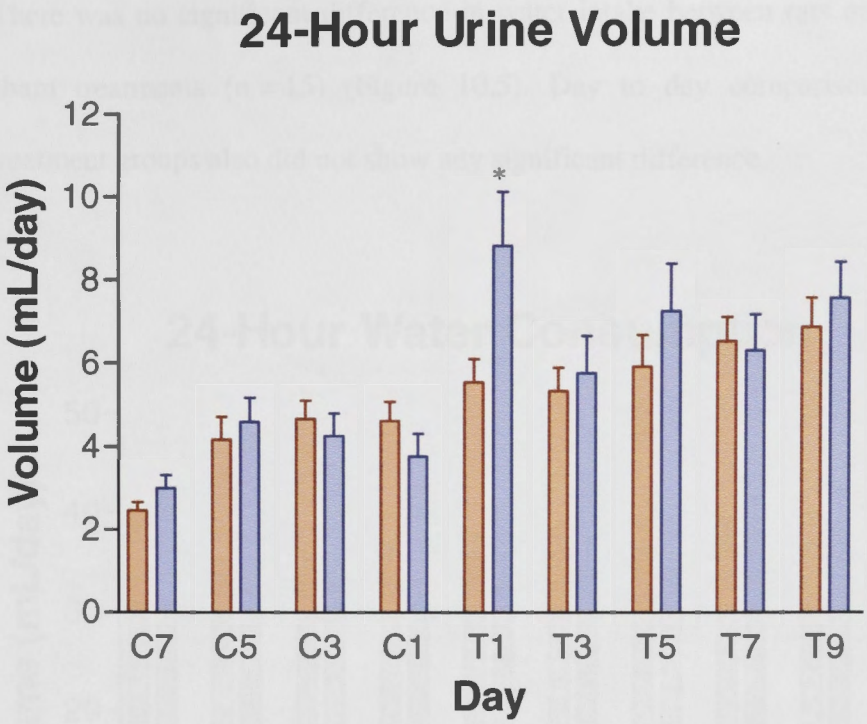

Figure 10.4: Urine volume over 24 hours. Saline, n = 15; DEX, n = 10. *$P < 0.05$ compared to control on day T1.

10.3.4 Water consumption

Analysis within the saline (n = 15) and DEX (n = 10) treatment groups did not show any difference in water consumption from day C1 (saline: 35 ± 2 mL, DEX: 31 ± 3 mL) to day T9 C1 (saline: 37 ± 3 mL, DEX: 38 ± 4 mL). In both groups, water intake per 100 g body weight was also not significantly different from day C1 (saline: 13 ± 1 mL, DEX: 11 ± 1 mL) to day T9 (saline: 12 ± 1 mL, DEX: 14 ± 2 mL).

There was no significant difference in water intake between rats on DEX (n=10) and sham treatments (n = 15) (Figure 10.5). Day to day comparisons between the 2 treatment groups also did not show any significant difference.

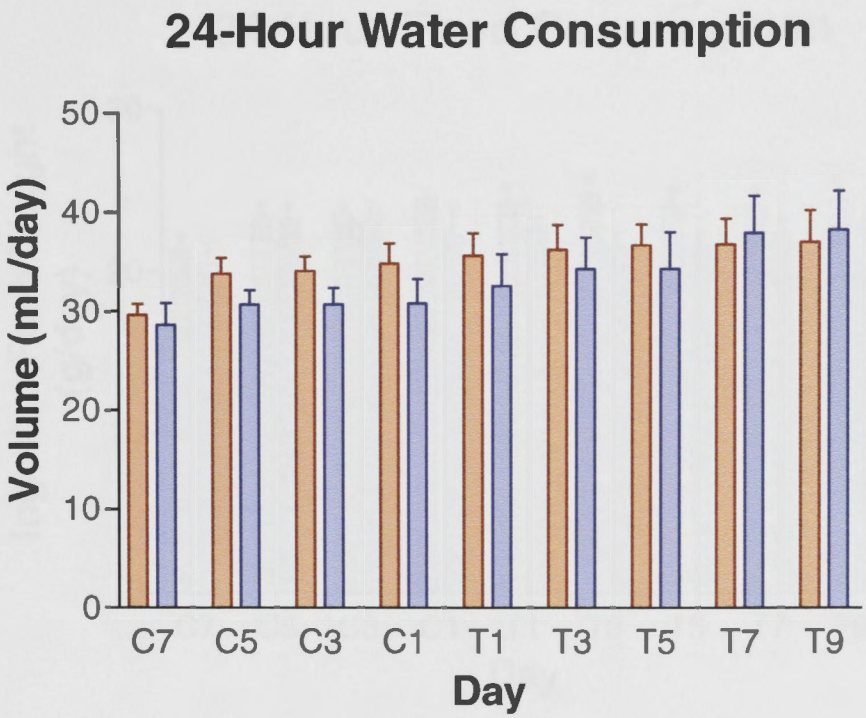

Figure 10.5: Water consumption over 24 hours. Saline, n = 15; DEX, n = 10, not significant compared with saline.

10.3.5 Food consumption

There was no significant change in food consumption within the saline (n =15) and DEX-treated groups (n = 10) from day C1 (saline: 25 ± 1 g; DEX: 22 ± 2 g) to T9 (saline: 24 ± 1 g; DEX: 23 ± 1 g) (Figure 10.6).

There was no significant difference in overall food consumption between rats on DEX (n=10) and sham treatments (n = 15). Day to day comparisons between the 2 treatment groups also did not show any significant difference (Figure 10.6).

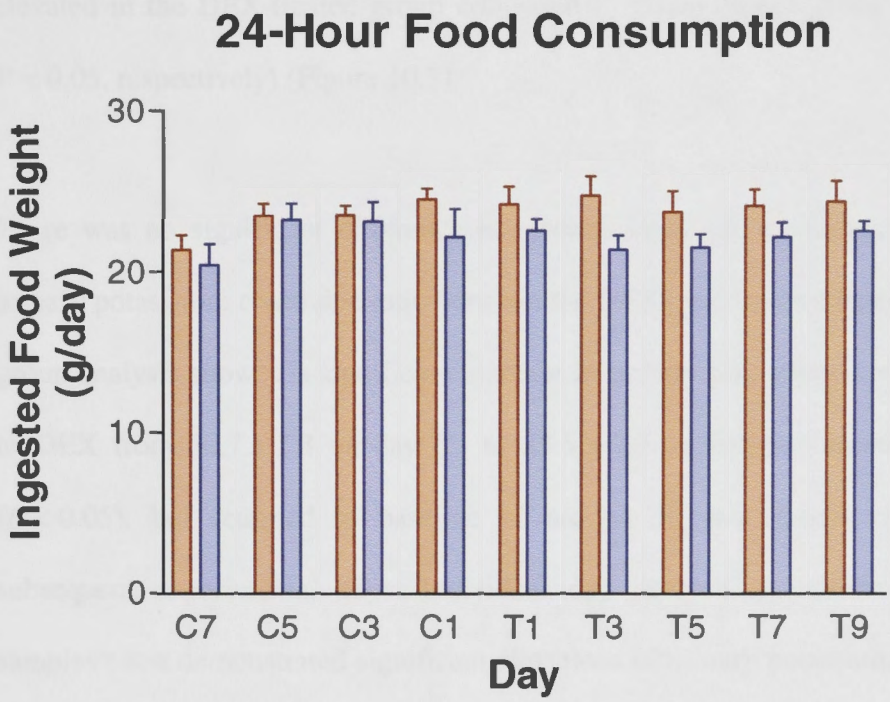

Figure 10.6: Food consumption over 24 hours. Saline, n = 15; DEX, n = 10, not significant compared with saline.

10.3.6 Urinary electrolytes

Urinary sodium excretion, as measured as urine sodium: creatinine ratio, was significantly higher in DEX-treated rats than saline-treated rats ($P < 0.0005$). Within the DEX-treated group, urine sodium: creatinine ratio was significantly increased from 23.7 ± 0.9 on day C1, a day before DEX administration; to 25.9 ± 1.0 on day T9, but

most marked on day T1, 1 day after DEX commencement, with a ratio of 37.2 ± 1.3 mmol/μmol creatinine (n = 10, $P < 0.0005$). When making comparisons between the saline- and DEX-treated groups on the individual experimental days using independent samples t-test, the sodium: creatinine ratios on days T1 and T9 were significantly elevated in the DEX-treated group compared to saline-treated group ($P < 0.0005$ and $P < 0.05$, respectively) (Figure 10.7).

There was no significant difference in urinary potassium excretion, as indicated by urinary potassium: creatinine ratio between the DEX- and saline-treated groups. Within group analysis showed a significant increase in urinary potassium: creatinine ratio due to DEX from 30.7 ± 1.3 on day C1 to 33.5 ± 0.9 mmol/μmol creatinine on day T1 ($P < 0.05$), but returned to baseline of around 30 mmol/μmol creatinine on the subsequent experimental days. Individual day analysis by means of independent samples t-test demonstrated significant elevations of urinary potassium: creatinine ratio in DEX-treated rats compared with saline-treated rats on days T1 ($P < 0.05$) and T9 ($P < 0.005$) (Figure 10.8).

Urinary sodium: potassium ratio was significantly higher in the DEX-treated group in comparison with sham treatment group (n = 10 each, $P < 0.0005$). DEX increased the sodium: potassium ratio from 0.78 ± 0.04 mmol/mmol on day C1 to 0.85 ± 0.03 mmol/mmol on day T9, but was most marked on day T1 (1.11 ± 0.03 mmol/mmol) ($P < 0.0005$). Day to day comparison using independent samples t-test showed that rats on DEX treatment on day T1 had significantly higher urine sodium: potassium ratio than those on saline treatment ($P < 0.0005$) (Figure 10.9).

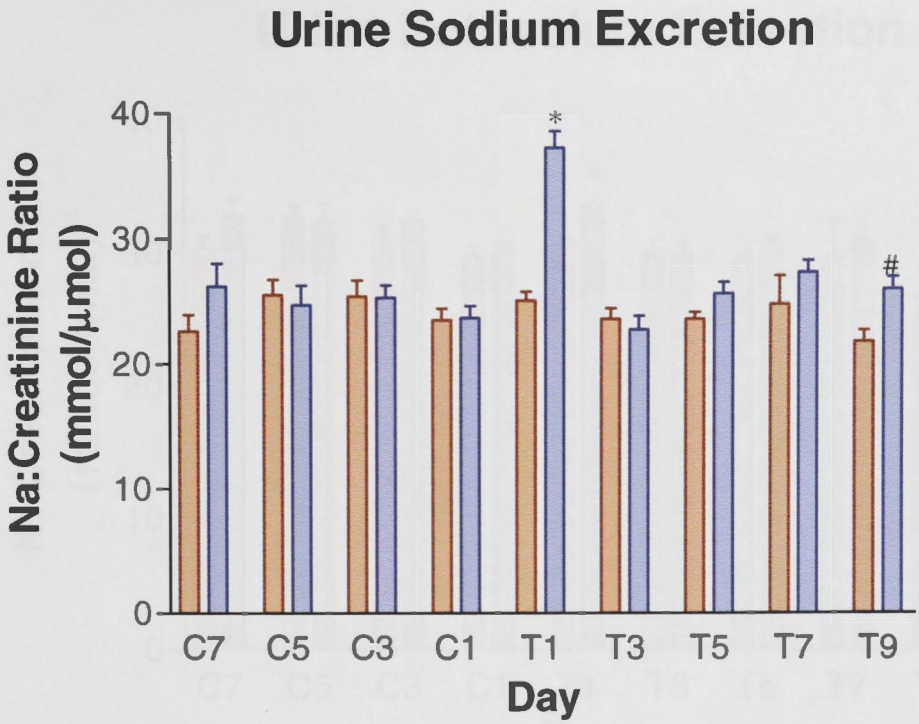

Figure 10.7: 24-hour urine sodium excretion. Saline, n = 10; DEX, n = 10. $^{*}P < 0.0005$ compared saline-treated rats on day T1; $^{\#}P < 0.05$ compared to saline-treated rats on day T9.

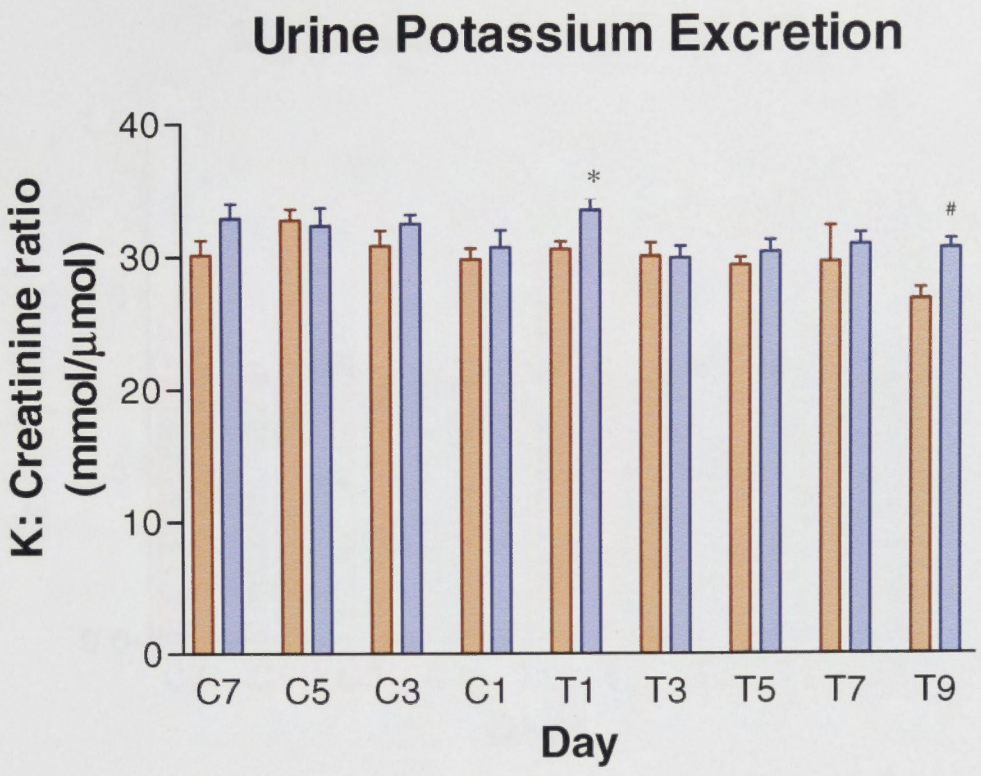

Figure 10.8: Urine potassium excretion. Saline, n = 10; DEX, n = 10. $^{*}P < 0.005$ compared to saline-treated rats on day T1; $^{\#}P < 0.05$ compared to saline-treated rats on day T9.

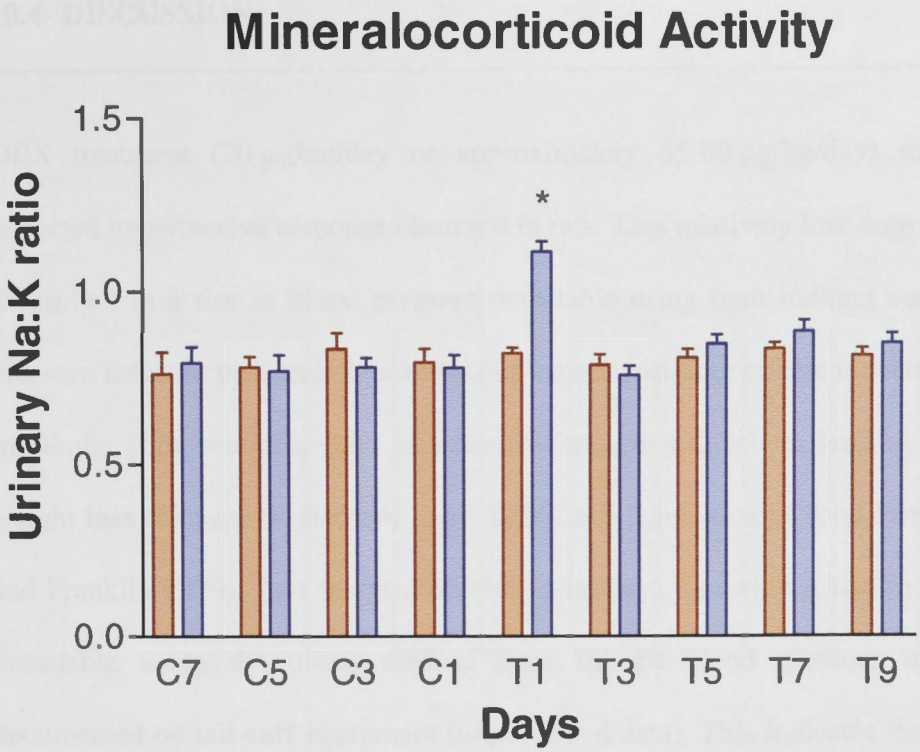

Figure 10.9: Urine sodium: potassium ratio as an index of mineralocorticoid activity. Saline, n = 10; DEX, n = 10. *$P < 0.0005$ compared to saline-treated rats on day T1.

10.4 DISCUSSION

DEX treatment (20 μg/rat/day or approximately 65-80 μg/kg/day) resulted in the expected hypertensive response observed in rats. This relatively low dose was chosen as it resulted in a rise in blood pressure detectable using both indirect and direct blood pressure measurement techniques without the confounding effects induced by profound metabolic complications, such as excessive muscle catabolism leading to precipitous weight loss (Konagaya, Bernard *et al.* 1986) and depression of food intake (Stevenson and Franklin 1970). At a lower dose (10 μg/rat/day), however, a rise in MAP was not detectable using the direct method even though blood pressure increases were documented on tail-cuff equipment (unpublished data). This indicates that a dose of 10 μg/rat/day is close to the threshold dose for a hypertensive response.

Rats on DEX treatment did not gain body weight; and had lower thymus and adrenal weights. These glucocorticoid effects in DEX-treated rats were indicative of effective administration and absorption of DEX. The observed growth stasis was not due to decreased oral food intake as there was no difference in food consumption between the DEX- and saline-treated groups. Rather, it was likely to be due to the effects of DEX on skeletal muscle mass (Konagaya, Bernard *et al.* 1986). The extent of these catabolic effects is proportional to the dose of DEX (Tonolo, Fraser *et al.* 1988; Ma, Mallidis *et al.* 2003). A significant loss of body weight due to high dose DEX administration in rats (approximately 100 μg/rat/day, in drinking water) has been reported (Handa, Kondo *et al.* 1984), but at lower doses (between 1-5 μg/day, continuous subcutaneous infusion), DEX resulted in growth stasis without inducing weight loss (Tonolo, Fraser *et al.* 1988).

DEX-induced muscle atrophy is a consequence of decreased protein synthesis and increase protein degradation (Tomas, Knowles *et al.* 1992). Tomas *et al* demonstrated that subcutaneous DEX treatment at 20 μg/rat/day resulted in progressive weight loss, increased muscle protein breakdown as assessed by urinary excretion of 3-methyl histidine and decreased protein synthesis rate (Tomas, Knowles *et al.* 1992). A number of possible explanations have been put forward to explain the effect of glucocorticoid on skeletal muscles. DEX has been implicated in dose-dependent upregulation of myostatin mRNA and protein expression *in vivo* (Ma, Mallidis *et al.* 2003). In addition, inhibition of fetal rat insulin-like growth factor-1 (a hormone responsible for stimulating protein synthesis and inhibiting protein degradation) by maternal DEX treatment has been observed (Mosier, Spencer *et al.* 1987). Co-administration of insulin-like growth factor-1 and DEX in rats prevented the catabolic effects of DEX (Tomas, Knowles *et al.* 1992). Whilst there is evidence demonstrating the role of DEX in muscle catabolism, it remains unclear if stress from growth restriction plays a role in exacerbating the hypertensive response induced by DEX.

Despite the lower DEX dose used in this project to minimise the catabolic effects of DEX, we still observed growth restriction at this dosage. This effect is unlikely to be a significant confounder in this animal model of glucocorticoid-hypertension. Zhang *et al* have previously shown that ACTH administration resulted in hypertension and weight loss (Zhang, Jang *et al.* 2003). Treatment with tempol prevented and reversed hypertension due to ACTH even though it did not prevent or reversed the observed weight loss. In another study, the administration of *N*-acetylcysteine to rats resulted in growth deceleration but did not alter blood pressure (Krug, Zhang *et al.* 2008). Rather,

it prevented hypertension in DEX-treated rats (Krug, Zhang *et al.* 2008). Thus changes in body weight do not contribute significantly to glucocorticoid-induced hypertension.

In the ACTH-hypertensive model, differences have been observed across the different species that has been studied (human, rodent, sheep and dog) (Whitworth, Zhang *et al.* 2006). The rat and human are more similar in their response to ACTH although some differences exist. The discrepancy in the effect of glucocorticoid hormones on body weight in rats and humans is obvious but the blood pressure effects are similar.

Urine output in DEX-hypertensive rats was significantly higher than control rats. This diuretic response was more pronounced on day C1, which was day 1 post commencement of DEX treatment. A lesser increase was observed on subsequent experimental days. This increase in urine output was secondary to DEX-induced natriuresis which was also more prominent on day C1. Previous studies using DEX (2.5 x 10^7 mol in drinking water) (Handa, Kondo *et al.* 1983), corticosterone (Haack, Mohring *et al.* 1977) and the glucocorticoid agonist RU 2698 (Grunfeld, Eloy *et al.* 1985) in rats, also produced diuretic and natriuretic responses. It is interesting to note that DEX treatment in the study by Handa *et al.* did not result in an acute transient increase in daily urinary sodium and water excretion observed in the present study. The different dosages used may be a contributory factor.

The mechanism of DEX-induced diuresis is unclear and is probably multifactorial. It is possible that the acute increase in urine output and sodium excretion is the renal-pressure natriuresis response consequent on the DEX-induced acute rise in blood

pressure (Hall, Mizelle *et al.* 1990; Rose and Post 2001). The observed diuresis and natriuresis can also be, in part, mediated through glucocorticoid-induced upregulation of atrial natriuretic peptide (ANP) gene expression and plasma ANP levels (Gardner, Hane *et al.* 1986). This finding was based on a higher DEX dose of 1 mg/day, administered subcutaneously in rats. This is not a universal finding as, in another study, plasma ANP concentrations in rats were decreased by DEX (Tonolo, Richards *et al.* 1989). DEX dosages may be a reason for this difference. The effective DEX dosages (1 μg/day to 10 μg/day) used in the study by Tonolo *et a.l* (Tonolo, Fraser *et al.* 1988) were significantly lower than the dose used by Gardner *et a.l* (Gardner, Hane *et al.* 1986). It also possible that ANP stimulation by the lower DEX dose used by Tonolo *et al* was unable to overcome a larger ANP suppressive response induced by systemic volume contraction due to DEX.

As mentioned earlier, urine output and urinary sodium excretion were significantly raised transiently at the early stages of DEX treatment. These were partially corrected to some extent, probably by normal renal homeostatic mechanisms in response to DEX-induced decrease in effective circulating volume. These homeostatic mechanisms include the renin-angiotensin system (RAS) and antidiuretic hormone (ADH).

The ADH acts on the renal distal convoluted tubules and collecting tubules to allow water reabsorption and, therefore, excretion of a lower volume of concentrated urine. If this mechanism is being activated, it is unlikely to provide full correction as rats treated chronically with DEX have been shown to have elevated haematocrit (Hu, Zhang *et al.* 2006). Stimulation of the RAS by volume contraction in these DEX-hypertensive rats

remains a possibility as Saruta has previously shown raised plasma renin activity in this model of hypertension (Saruta 1996).

Despite these changes, alteration to plasma volume, regulation of the RAS and ADH, these systems do not play a major role in the pathogenesis of DEX-HT as described in Sections 1.4.5.1 and 1.4.5.2 of Chapter 1.

DEX has been reported to have a very weak affinity for mineralocorticoid receptors (Grossmann, Scholz *et al.* 2004). In view of this, one would expect DEX excess to result in mineralocorticoid receptor activation. However, current evidence does not indicate the presence volume expansion in DEX-HT. In this study, serum sodium and potassium were not examined as the experimental conditions of the haemodynamic experiments on the last day (Chapter 3) would make serum electrolytes unreliable. Previous reports have shown that DEX (both at high and low doses) did not alter plasma sodium and potassium concentrations (Sinha, Rodriguez *et al.* 1981; Tonolo, Fraser *et al.* 1988). Furthermore, this study found that urine sodium: potassium ratio was significantly higher in DEX-hypertensive rats, suggesting that mineralocorticoid function was not activated in these DEX-hypertensive rats. These results further confirmed previous findings that DEX-HT is not associated with the mineralocorticoid effect of salt retention and volume expansion.

10.5 CONCLUSION

DEX at 20 μg/rat/day, given subcutaneously, effectively increased blood pressure for the haemodynamic studies without the unwanted side effects of precipitous weight loss.

The increase in blood pressure induced by DEX was not due to increased mineralocorticoid activity and plasma volume expansion. This also explained why cardiac output and stroke volume (Chapter 3) were unchanged in DEX-HT.

CHAPTER 11

Summary and Conclusion

GC-HT was previously thought to be a consequence of mineralocorticoid receptor activation resulting in salt and water retention, and hence, plasma volume expansion, increase in cardiac output and hypertension. However, studies to date in humans and experimental animals have not supported this notion. GC-HT has been shown not to be associated with plasma expansion (Whitworth, Gordon *et al.* 1989; Montrella-Waybill, Clore *et al.* 1991; Williamson, Kelly *et al.* 1996; Li, Wen *et al.* 1999).

More recent evidence now revolves around the availability of NO and interactions between NO and ROS. Studies evaluating the mechanisms of GC-HT using the ACTH-HT model, a representation of hypertension due to naturally-occuring glucocorticoid, and the DEX-HT model, that of synthetic GC-HT, have revealed differences between the two.

This project examined the mechanism of DEX-HT in rats. The haemodynamics of DEX-HT along with the role of oxidative stress and its interactions with NO were tested in this project.

11.1 HAEMODYNAMICS

The study of the haemodynamics of DEX-HT in rats revealed that DEX at 20 μg/rat/day administered subcutaneously increased blood pressure rapidly within 2 days (Chapters 3 and 4). DEX-HT in rats was characterised by increased TPR, decreased TPC but no change in CO, SV, RVR, MVR and HVR. The increase in

TPR and decrease in TPC were not due to individual changes in resistance and conductance in the mesenteric, renal and hindquarter vascular beds.

Pharmacological manipulation using the vasodilator minoxidil to test the role of TPR and TPC in the genesis of DEX-HT showed that these haemodynamic parameters are associated features of DEX-HT that are not essential for its development.

11.2 OXIDATIVE STRESS

There is a body of evidence highlighting the role of oxidative stress in DEX-HT. In this project, DEX-HT was associated with an increase in plasma F_2-isoprostane (Figure 11.1), a product of lipid peroxidation and marker of systemic oxidative stress. Treatment with the antioxidant alpha-lipoic acid prevented and partially reversed DEX-HT (Chapter 6). This finding was also consistent with previous studies using the antioxidants tempol (Zhang, Croft *et al.* 2004) and N-acetylcysteine (Krug, Zhang *et al.* 2008). Increased production of superoxide from the NAD(P)H pathway has been implicated in the pathogenesis of DEX-HT based on the prevention of DEX-HT in rats using apocynin (Hu, Zhang *et al.* 2006), a NAD(P)H oxidase inhibitor. Other sources of superoxide in the blood vessel wall have been evaluated in this project. Two main sources of superoxide, the mitochondria (Chapters 5 and 6) and the xanthine oxidase pathway (Chapter 7), were found in this project not to play significant roles in the pathogenesis of DEX-HT. Whilst there is an increase in lipid peroxidation in DEX-HT as

indicated by an increase in plasma F_2-isoprostane, inhibition of lipid peroxidation by propranolol (an antihypertensive drug known to have this effect) did not prevent DEX-HT (Chapter 8). This suggests that lipid peroxidation also does not play a major role in the development of DEX-HT.

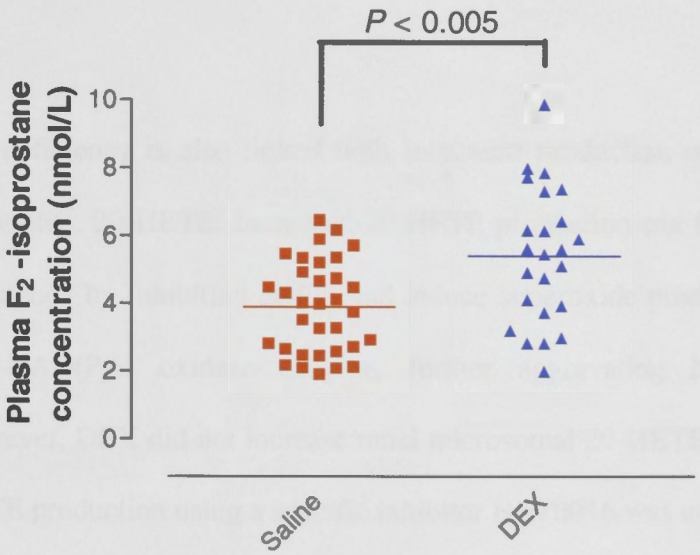

Figure 11.1: Pooled plasma F_2-isoprostane concentration results from all the relevant studies in this project. ■ Saline, 3.9 ± 0.2 nmol/L, n = 33, ▲ DEX, 5.4 ± 0.4 nmol/L, n = 24.

11.3 NITRIC OXIDE DEFICIENCY

The pathways contributing to NO deficiency have been reviewed in Chapter 1. The finding in this thesis (Chapters 7 and 9) that plasma NOx was reduced in DEX-HT is consistent with the notion that NO deficiency is implicated in DEX-HT.

NO deficiency is also linked with increased production of an arachidonic acid metabolite, 20-HETE. Increased 20-HETE production can further exacerbate NO deficiency by inhibiting eNOS and induce superoxide production by stimulating the NAD(P)H oxidase enzyme, further aggravating NO-redox imbalance. However, DEX did not increase renal microsomal 20-HETE and inhibition of 20-HETE production using a specific inhibitor HET0016 was unable to reverse DEX-HT and DEX-induced reduction in plasma NOx (Chapter 9). These data suggest that 20-HETE does not have a role in DEX-HT.

11.4 OTHER MECHANISMS

Propranolol is a common antihypertensive medication that acts via the inhibition of the β-adrenoreceptor. It failed to prevent DEX-HT despite effectively decreased HR. This study showed that β-adrenergic activation is not a main feature of DEX-HT and propranolol likely has a limited therapeutic role in DEX-HT (Chapter 8).

11.5 OTHER OBSERVATIONS

In all the studies described in this thesis, DEX at 10-20 μg/rat/day increased blood pressure, prevented growth, decreased thymus weight, and decreased adrenal weight. Food and water consumption in these rats were not altered compared to controls (Chapter 10).

In the rat, DEX at 10 μg/rat/day given subcutaneously up to 11 days has no significant effect on blood glucose concentration (Chapter 6).

On the other hand, DEX treatment (20 μg/rat/day) resulted in natriuresis and diuresis, more pronounced in the first few days following the commencement of DEX (Chapter 10). Haematocrit was not altered after 11 days of DEX treatment (20 μg/rat/day) (Chapters 3 and 4). These observations further substantiate the evidence that DEX-HT is not due to mineralocorticoid activation and plasma volume expansion.

11.6 FURTHER DIFFERENCES BETWEEN ACTH- AND DEX-HYPERTENSION IDENTIFIED IN THIS PROJECT

In addition to the differences highlighted in Chapter 1 (Section 1.9.2), further dissimilar features between ACTH- and DEX-HT have been demonstrated in this project.

11.6.1 Effects on body weight

In this project, DEX resulted in growth stasis and maintenance in body weight whilst ACTH resulted in weight loss. This discrepancy was, in part, due to the dosages used. The dose of ACTH used in this study is unlikely to produce a level of endogenous glucocorticoid that is equivalent to the dose of DEX used. Whilst the low DEX dose used resulted in growth stasis but not weight loss, higher doses have been shown previously to result in significant weight loss (Handa, Kondo et al. 1984).

11.6.2 Effects on cardiac output

ACTH-HT, which is due to overproduction of cortisol in humans and corticosterone in rats, is associated with volume expansion due to stimulation of mineralocorticoid receptors. Consequently, cardiac output is increased in this model.(Wen, Fraser *et al.* 1998; Wen, Fraser *et al.* 1999) In contrast, this phenomenon of mineralocorticoid receptor activation, plasma volume expansion and increase in CO is absent in DEX-HT as DEX is a pure glucocorticoid with negligible mineralocorticoid effect (Table 1.1).

11.6.3 Effects on plasma F_2-isoprostane concentration

In this project, DEX treatment but not ACTH increased plasma F_2-isoprostane concentration in rats. This, however, may not be a true difference as the response observed in the ACTH-treated rats was most likely influenced by the relatively

small sample size. In an analysis using pooled data from our laboratory, F_2-isoprostane concentration was increased in ACTH-hypertensive rats (Ong, Zhang et al. 2008).

11.6.4 The role of 20-HETE

Increased production of urinary 20-HETE was previously observed in ACTH-induced hypertensive but not DEX-induced hypertensive rats.(Zhang, Hu *et al.* 2008) Futhermore, the use of the 20-HETE inhibitor HET0016 successfully prevented and reversed ACTH- (Zhang, Croft *et al.* 2008) but not DEX-induced hypertension as seen in Chapter 9.

11.7 CONCLUSION AND FUTURE DIRECTIONS

In conclusion, an increase in TPR and an imbalance between NO and ROS appear to be characteristics of DEX-HT in the rat. The exact mechanism by which DEX raises blood pressure remains unclear. Further studies exploring the differences in mechanisms between naturally-occuring and synthetic glucocorticoids, as well as the relevance of oxidative stress and NO-redox imbalance in human GC-HT will be important in advancing our understanding in this form of hypertension. Whilst the antioxidants tempol, apocynin and N-acetylcysteine have been shown to be effective in preventing DEX-HT in the rat, the role of antioxidants in glucocorticoid- and DEX-HT in humans needs to be further evaluated.

Application of the currently available evidence on GC-HT to research of clinical conditions associated with raised glucocorticoid levels should also be undertaken. One important area is the study of the role of defective 11β-hydroxysteroid dehydrogenase type 2 (leading to increased cortisol half life and cortisol: cortisone ratio) in the pathogenesis of hypertension in patients with chronic kidney disease. Although chronic kidney disease has previously been shown to be associated with defective cortisol inactivation (Homma, Tanaka *et al.* 2001; N'Gankam, Uehlinger *et al.* 2002), the causal relationship between glucocorticoid and hypertension in the CKD patients needs to be established. The relationships between 1) renal function and cortisol: cortisone ratio; and 2) cortisol: cortisone ratio, blood pressure and cardiovascular risks also need further evaluation. Further studies assessing the role of nitric oxide-redox imbalance, a mechanism that has been shown to implicate GC-HT, in the CKD-associated hypertension should also be pursued.

BIBLIOGRAPHY

Adam-Vizi V. Production of reactive oxygen species in brain mitochondria: contribution by electron transport chain and non-electron transport chain sources. *Antioxid Redox Signal* 2005; **7**(9-10): 1140-1149.

Addison T. On the constitution and local effects of disease of the supra-renal capsules. *Medical Classics* 1937; **2**: 244-277.

Adrian TE, Allen JM, Bloom SR, Ghatei MA, Rossor MN, Roberts GW, Crow TJ, Tatemoto K, Polak JM. Neuropeptide Y distribution in human brain. *Nature* 1983; **306**(5943): 584-586.

Allen YS, Adrian TE, Allen JM, Tatemoto K, Crow TJ, Bloom SR, Polak JM. Neuropeptide Y distribution in the rat brain. *Science* 1983; **221**(4613): 877-879.

Alonso-Galicia M, Drummond HA, Reddy KK, Falck JR, Roman RJ. Inhibition of 20-HETE production contributes to the vascular responses to nitric oxide. *Hypertension* 1997; **29**(1): 320-325.

Amudha G, Josephine A, Sudhahar V, Varalakshmi P. Protective effect of lipoic acid on oxidative and peroxidative damage in cyclosporine A-induced renal toxicity. *Int Immunopharmacol* 2007; **7**(11): 1442-1449.

Antonaccio MJ, High J, DeForrest JM, Sybertz E. Antihypertensive effects of 12 beta adrenoceptor antagonists in conscious spontaneously hypertensive

rats: relationship to changes in plasma renin activity, heart rate and sympathetic nerve function. *J Pharmacol Exp Ther* 1986; **238**(1): 378-387.

Arimura K, Egashira K, Nakamura R, Ide T, Tsutsui H, Shimokawa H, Takeshita A. Increased inactivation of nitric oxide is involved in coronary endothelial dysfunction in heart failure. *Am J Physiol Heart Circ Physiol* 2001; **280**(1): H68-75.

Armas-Padilla MC, Armas-Hernandez MJ, Sosa-Canache B, Cammarata R, Pacheco B, Guerrero J, Carvajal AR, Hernandez-Hernandez R, Israili ZH, Valasco M. Nitric oxide and malondialdehyde in human hypertension. *Am J Ther* 2007; **14**(2): 172-176.

Aruoma OI, Smith C, Cecchini R, Evans PJ, Halliwell B. Free radical scavenging and inhibition of lipid peroxidation by β-blockers and by agents that interfere with calcium metabolism: A physiologically-significant process? *Biochem Pharmacol* 1991; **42**(4): 735-743.

Azarov I, Huang KT, Basu S, Gladwin MT, Hogg N, Kim-Shapiro DB. Nitric oxide scavenging by red blood cells as a function of hematocrit and oxygenation. *J Biol Chem* 2005; **280**(47): 39024-39032.

Ballinger SW. Mitochondrial dysfunction in cardiovascular disease. *Free Radic Biol Med* 2005; **38**(10): 1278-1295.

Bauer J. The so-called Cushing's Syndrome, its history, terminology and differential diagnosis. *Acta Med Scand* 1950; **137**(6): 411-416.

Bayir H. Reactive oxygen species. *Crit Care Med* 2005; **33**(12 (Suppl)): S498-501.

Bengele HH, McNamara ER, Alexander EA. Natriuresis after adrenal enucleation: effect of spironolactone and dexamethasone. *Am J Physiol Renal Physiol* 1977; **233**(1): F8-12.

Bengtsson SHM, Gulluyan LM, Dusting GJ, Drummond GR. Novel isoforms of NADPH oxidase in vascular physiology and pathophysiology. *Clin Exp Pharmacol Physiol* 2003; **30**(11): 849-854.

Bennett T, Gardiner SM. Prevention and reversal of isolation-induced systolic arterial hypertension in rats by treatment with beta-adrenoceptor antagonists. *Br J Pharmacol* 1979; **65**(2): 205-213.

Berry CE, Hare JM. Xanthine oxidoreductase and cardiovascular disease: molecular mechanisms and pathophysiological implications. *J Physiol* 2004; **555**(3): 589-606.

Biewenga GP, Haenen GRMM, Bast A. The pharmacology of the antioxidant lipoic acid. *Gen Pharmacol* 1997; **29**(3): 315-331.

Birmingham MK, Sar M, Stumpf WE. Dexamethasone target sites in the central nervous system and their potential relevance to mental illness. *Cell Mol Neurobiol* 1993; **13**(4): 373-386.

Borcsok I, Schairer HU, Sommer U, Wakley GK, Schneider U, Geiger F, Niethard FU, Ziegler R, Kasperk CH. Glucocorticoids regulate the expression of the human osteoblastic endothelin A receptor gene. *J Exp Med* 1998; **188**(9): 1563-1573.

Bos AF, van Asselt WA, Okken A. Dexamethasone treatment and fluid balance in preterm infants at risk for chronic lung disease. *Acta Paediatr* 2000; **89**(5): 562-565.

Bradford MM. A rapid and sensitive method for the quantitation of microgram quantities of protein utilizing the principle of protein-dye binding. *Anal Biochem* 1976; **72**: 248-254.

Brookes PS, Morse K, Ray D, Tompkins A, Young SM, Hilchey S, Salim S, Konopleva M, Andreeff M, Phipps R, Bernstein SH. The triterpenoid 2-cyano-3,12-dioxooleana-1,9-dien-28-oic acid and Its derivatives elicit human lymphoid cell apoptosis through a novel pathway involving the unregulated mitochondrial permeability transition pore. *Cancer Res* 2007; **67**(4): 1793-1802.

Brown-Sequard ME. Recherches experimentales sur le physiologie et la pathologie des capsules surrenales. *Academy of Science Paris* 1856; **43**: 422-425.

Brown MR, Fisher LA. Glucocorticoid suppression of the sympathetic nervous system and adrenal medulla. *Life Sci* 1986; **39**(11): 1003-1012.

Bunag RD. Propranolol in DOCA hypertensive rats: development of hypertension inhibited and pressor responsiveness enhanced. *Eur J Pharmacol* 1977; **43**(4): 323-331.

Burrell LM, Phillips PA, Stephenson JM, Risvanis J, Rolls KA, Johnston CI. Blood pressure-lowering effect of an orally active vasopressin V1 receptor antagonist in mineralocorticoid hypertension in the rat. *Hypertension* 1994; **23**(6 Pt 1): 737-743.

Burris JF, Waeber B, Nussberger J, Brunner HR. Enhanced acute antihypertensive effect of propranolol in the absence of circulating epinephrine in the rat. *J Cardiovasc Pharmacol* 1984; **6**(4): 697-700.

Cai H, Harrison DG. Endothelial dysfunction in cardiovascular diseases: the role of oxidant stress. *Circ Res* 2000; **87**(10): 840-844.

Çakatay U. Pro-oxidant actions of [alpha]-lipoic acid and dihydrolipoic acid. *Med Hypotheses* 2006; **66**(1): 110-117.

Campo ML, Kinnally KW, Tedeschi H. The effect of antimycin A on mouse liver inner mitochondrial membrane channel activity. *J Biol Chem* 1992; **267**(12): 8123-8127.

Capdevila JH, Falck JR, Dishman E, Karara A. Cytochrome P-450 arachidonate oxygenase. *Methods Enzymol* 1990; **187**: 385-394.

Carletti M, Cantiello M, Giantin M, Nebbia C, Cannizzo FT, Bollo E, Dacasto M. Serum antioxidant enzyme activities and oxidative stress parameters as possible biomarkers of exposure in veal calves illegally treated with dexamethasone. *Toxicol In Vitro* 2007; **21**(2): 277-283.

Chabria NL, Gaitonde BB. Effect of dexamethasone on urine output and electrolyte excretion in rats. *Arch Int Pharmacodyn Ther* 1966; **162**(2): 364-370.

Chakrabarti A, Sharma PL. A study on withdrawal related haemodynamic response in chronic propranolol treated conscious rats. *Indian J Physiol Pharmacol* 1993; **37**(3): 235-237.

Cheng J, Ou J-S, Singh H, Falck JR, Narsimhaswamy D, Pritchard KA, Jr., Schwartzman ML. 20-Hydroxyeicosatetraenoic acid causes endothelial dysfunction via eNOS uncoupling. *Am J Physiol Heart Circ Physiol* 2008; **294**(2): H1018-1026.

Codde JP, Beilin LJ. Dietary fish oil prevents dexamethasone induced hypertension in the rat. *Clin Sci (Lond)* 1985; **69**(6): 691-699.

Connell JM, Whitworth JA, Davies DL, Lever AF, Richards AM, Fraser R. Effects of ACTH and cortisol administration on blood pressure, electrolyte metabolism, atrial natriuretic peptide and renal function in normal man. *J Hypertens* 1987; **5**(4): 425-433.

Connell JM, Whitworth JA, Davies DL, Richards AM, Fraser R. Haemodynamic, hormonal and renal effects of adrenocorticotrophic hormone in sodium-restricted man. *J Hypertens* 1988; **6**(1): 17-23.

Corder R, Pralong F, Turnill D, Saudan P, Muller AF, Gaillard RC. Dexamethasone treatment increases neuropeptide Y levels in rat hypothalamic neurones. *Life Sci* 1988; **43**(23): 1879-1886.

Cordero M, De Miguel M, Moreno Fernandez A, Carmona Lopez I, Garrido Maraver J, Cotan D, Gomez Izquierdo L, Bonal P, Campa F, Bullon P, Navas P, Sanchez Alcazar J. Mitochondrial dysfunction and mitophagy activation in blood mononuclear cells of fibromyalgia patients: implications in the pathogenesis of the disease. *Arthritis Res Ther* 2010; **12**(1): R17 [Epub ahead of print].

Cosentino F, Sill JC, Katusic ZS. Role of superoxide anions in the mediation of endothelium-dependent contractions. *Hypertension* 1994; **23**(2): 229-235.

Crawford DR, Davies KJ. Adaptive response and oxidative stress. *Environ. Health Perspect.* 1994; **102 Suppl 10**: 25-28.

Cremer DR, Rabeler R, Roberts A, Lynch B. Long-term safety of α-lipoic acid (ALA) consumption: A 2-year study. *Regul Toxicol Pharmacol* 2006; **46**(3): 193-201.

Dalle-Donne I, Rossi R, Colombo R, Giustarini D, Milzani A. Biomarkers of oxidative damage in human disease. *Clin. Chem.* 2006; **52**(4): 601-623.

Dawson TL, Gores GJ, Nieminen AL, Herman B, Lemasters JJ. Mitochondria as a source of reactive oxygen species during reductive stress in rat hepatocytes. *Am J Physiol Cell Physiol* 1993; **264**(4): C961-967.

Degli Esposti M. Measuring mitochondrial reactive oxygen species. *Methods* 2002; **26**(4): 335-340.

Dhalla NS, Temsah RM, Netticadan T. Role of oxidative stress in cardiovascular diseases. *J Hypertens* 2000; **18**(6): 655-673.

Distelmaier F, Koopman WJH, Testa ER, de Jong AS, Swarts HG, Mayatepek E, Smeitink JAM, Willems PHGM. Life cell quantification of mitochondrial membrane potential at the single organelle level. *Cytometry Part A* 2008; **73A**(2): 129-138.

Dobrian AD, Schriver SD, Prewitt RL. Role of angiotensin II and free radicals in blood pressure regulation in a rat model of renal hypertension. *Hypertension* 2001; **38**(3): 361-366.

Drost CJ. Vessel diameter-dependent volume flow measurements using ultrasound. *Proc San Diego Biomed Symp* 1978; **17**: 463-485.

Du J, Daniels DH, Asbury C, Venkataraman S, Liu J, Spitz DR, Oberley LW, Cullen JJ. Mitochondrial production of reactive oxygen species mediate dicumarol-induced cytotoxicity in cancer cells. *J Biol Chem* 2006; **281**(49): 37416-37426.

Duranteau J, Chandel NS, Kulisz A, Shao Z, Schumacker PT. Intracellular signaling by reactive oxygen species during hypoxia in cardiomyocytes. *J Biol Chem* 1998; **273**(19): 11619-11624.

Dvorak K, Payne CM, Chavarria M, Ramsey L, Dvorakova B, Bernstein H, Holubec H, Sampliner RE, Guy N, Condon A, Bernstein C, Green SB, Prasad A, Garewal HS. Bile acids in combination with low pH induce oxidative stress and oxidative DNA damage: relevance to the pathogenesis of Barrettâ€™s oesophagus. *Gut* 2007; **56**(6): 763-771.

Ebii K, Fukunaga R, Taniguchi T, Fujiwara M, Nakayama S, Saitoh Y, Kimura Y. Effects of chronic administration of carteolol on beta-adrenoceptors in spontaneously hypertensive rat heart. *Jpn J Pharmacol* 1991; **56**(4): 505-512.

Echtenkamp SF, Dandridge PF. Renal actions of neuropeptide Y in the primate. *Am J Physiol Renal Physiol* 1989; **256**(4): F524-531.

Edvinsson L, Ekblad E, Hakanson R, Wahlestedt C. Neuropeptide Y potentiates the effect of various vasoconstrictor agents on rabbit blood vessels. *Br J Pharmacol* 1984; **83**(2): 519-525.

Eggena P, Barrett JD. Renin substrate release in response to perturbations of renin-angiotensin system. *Am J Physiol Endocrinol Metab* 1988; **254**(4): E389-393.

El Midaoui A, Elimadi A, Wu L, Haddad PS, de Champlain J. Lipoic acid prevents hypertension, hyperglycemia, and the increase in heart mitochondrial superoxide production. *Am J Hypertens* 2003; **16**(3): 173-179.

El Midaoui A, Wu R, de Champlain J. Prevention of hypertension, hyperglycemia and vascular oxidative stress by aspirin treatment in chronically glucose-fed rats. *J Hypertens* 2002; **20**(7): 1407-1412.

Eustachius B (1564). Opuscula Anatomica de Renum Structura, Efficio et Administratione. Venice, V. V. Lucchino.

Faggiano A, Pivonello R, Spiezia S, De Martino MC, Filippella M, Di Somma C, Lombardi G, Colao A. Cardiovascular risk factors and common carotid artery caliber and stiffness in patients with Cushing's disease during active disease and 1 year after disease remission. *J Clin Endocrinol Metab* 2003; **88**(6): 2527-2533.

Falardeau P, Martineau A. Prostaglandin I2 and glucocorticoid-induced rise in arterial pressure in the rat. *J Hypertens* 1989; **7**(8): 625-632.

Ferrario CM, Chappell MC. Angiotensin formation and degradation. In: Izzo Jr J. L., Sica D. A.,Black H. R., eds. *Hypertension Primer: the essentials of high blood pressure: basic science, population science and clinical management*. 4th ed. Philadelphia: Lippincott Williams Wilkins; 2008:52-58.

Flower RJ, Blackwell GJ. Anti-inflammatory steroids induce biosynthesis of a phospholipase A2 inhibitor which prevents prostaglandin generation. *Nature* 1979; **278**(5703): 456-459.

Fraillon D, Wynne KN, Funder JW. Further studies on neomycin and experimental hypertension. *Clin Exp Pharmacol Physiol* 1984; **11**(4): 339-341.

Fraser TB, Turner SW, Mangos GJ, Ludbrook J, Whitworth JA. Comparison of telemetric and tail-cuff blood pressure monitoring in adrenocorticotrophic hormone-treated rats. *Clin Exp Pharmacol Physiol* 2001; **28**(10): 831-835.

Fraser TB, Turner SW, Wen C, Li M, Burrell LM, Whitworth JA. Vasopressin V1a receptor antagonism does not reverse adrenocorticotrophin-induced hypertension in the rat. *Clin Exp Pharmacol Physiol* 2000; **27**(11): 866-870.

Garcia R, Debinski W, Gutkowska J, Kuchel O, Thibault G, Genest J, Cantin M. Gluco- and mineralocorticoids may regulate the natriuretic effect and the synthesis and release of atrial natriuretic factor by the rat atria in vivo. *Biochem Biophys Res Commun* 1985; **131**(2): 806-814.

Gardiner SM, Kemp PA, March JE, Bennett T. Effects of dexamethasone and SB 209670 on the regional haemodynamic responses to lipopolysaccharide in conscious rats. *Br J Pharmacol* 1996; **118**(1): 141-149.

Gardner DG, Hane S, Trachewsky D, Schenk D, Baxter JD. Atrial natriuretic peptide mRNA is regulated by glucocorticoids in vivo. *Biochem Biophys Res Commun* 1986; **139**(3): 1047-1054.

Girouard H, Chulak C, Wu L, Lejossec M, de Champlain J. N-acetylcysteine improves nitric oxide and α-adrenergic pathways in mesenteric beds of spontaneously hypertensive rats. *Am J Hypertens* 2003; **16**(7): 577-584.

Glyn J. The discovery and early use of cortisone. *J R Soc Med* 1998; **91**(10): 513-517.

Gomes A, Costa D, Lima JLFC, Fernandes E. Antioxidant activity of [beta]-blockers: An effect mediated by scavenging reactive oxygen and nitrogen species? *Bioorganic & Medicinal Chemistry* 2006; **14**(13): 4568-4577.

Graham WF, Allen KJ, Coghlan JP, Denton DA, Humphery TJ, Scoggins BA, Whitworth JA. Haemodynamic changes in ACTH-incuded hypertension in sheep. *Clin Exp Pharmacol Physiol* 1980; **7**(5): 569-572.

Grassi G, Esler M. How to assess sympathetic activity in humans. *J Hypertens* 1999; **17**(6): 719-734.

Griendling KK, Minieri CA, Ollerenshaw JD, Alexander RW. Angiotensin II stimulates NADH and NADPH oxidase activity in cultured vascular smooth muscle cells. *Circ Res* 1994; **74**(6): 1141-1148.

Groemping Y, Rittinger K. Activation and assembly of the NADPH oxidase: a structural perspective. *Biochem J* 2005; **386**(Pt 3): 401-416.

Grosser N, Schroder H. Aspirin protects endothelial cells from oxidant Damage via the nitric oxide-cGMP pathway. *Arterioscler Thromb Vasc Biol* 2003; **23**(8): 1345-1351.

Grossmann C, Scholz T, Rochel M, Bumke-Vogt C, Oelkers W, Pfeiffer AF, Diederich S, Bahr V. Transactivation via the human glucocorticoid and mineralocorticoid receptor by therapeutically used steroids in CV-1 cells: a comparison of their glucocorticoid and mineralocorticoid properties. *Eur J Endocrinol* 2004; **151**(3): 397-406.

Grunfeld JP, Eloy L, Moura AM, Ganeval D, Ramos-Frendo B, Worcel M. Effects of antiglucocorticoids on glucocorticoid hypertension in the rat. *Hypertension* 1985; **7**(2): 292-299.

Gu J, Polak JM, Adrian TE, Allen JM, Tatemoto K, Bloom SR. Neuropeptide tyrosine (NPY)--a major cardiac neuropeptide. *Lancet* 1983; **1**(8332): 1008-1010.

Guyton AC, Hall JE. The adrenocortical hormones. In: Schmitt W., Gruliow R.,Norwitz A., eds. *Textbook of medical physiology*. 10 ed. Pennsylvania: W.B. Saunders Company; 2000:869-883.

Guyton AC, Hall JE. The autonomic nervous system; and the adrenal medulla. In: Schmitt W., Gruliow R.,Norwitz A., eds. *Textbook of medical physiology*. Pennsylvania: W. B. Saunders Company; 2000:697-715.

Haack D, Mohring J, Mohring B, Petri M, Hackenthal E. Comparative study on development of corticosterone and DOCA hypertension in rats. *Am J Physiol Renal Physiol* 1977; **233**(5): F403-411.

Haas JA, Krier JD, Bolterman RJ, Juncos LA, Romero JC. Low-dose angiotensin II increases free isoprostane levels in plasma. *Hypertension* 1999; **34**(4): 983-986.

Haass M, Cheng B, Richardt G, Lang RE, Schomig A. Characterization and presynaptic modulation of stimulation-evoked exocytotic co-release of noradrenaline and neuropeptide Y in guinea pig heart. *Naunyn Schmiedebergs Arch Pharmacol* 1989; **339**(1-2): 71-78.

Hagen TM, Ingersoll RT, Lykkesfeldt J, Liu J, Wehr CM, Vinarsky V, Bartholomew JC, Ames BN. (R)-α-Lipoic acid-supplemented old rats have improved mitochondrial function, decreased oxidative damage, and increased metabolic rate. *FASEB J.* 1999; **13**(2): 411-418.

Haigh RM, Jones CT. Effect of glucocorticoids on alpha-1 adrenergic receptor-binding in rat vascular smooth muscle. *J Mol Endocrinol* 1990; **5**(1): 41-48.

Hall JE, Mizelle HL, Hildebrandt DA, Brands MW. Abnormal pressure natriuresis. A cause or a consequence of hypertension? *Hypertension* 1990; **15**(6): 547-559.

Han D, Antunes F, Canali R, Rettori D, Cadenas E. Voltage-dependent anion channels control the release of the superoxide anion from mitochondria to cytosol. *J Biol Chem* 2003; **278**(8): 5557-5563.

Handa M, Kondo K, Suzuki H, Saruta T. Urinary prostaglandin E2 and kallikrein excretion in glucocorticoid hypertension in rats. *Clin Sci (Lond)* 1983; **65**(1): 37-42.

Handa M, Kondo K, Suzuki H, Saruta T. Dexamethasone hypertension in rats: role of prostaglandins and pressor sensitivity to norepinephrine. *Hypertension* 1984; **6**(2 Pt 1): 236-241.

Harrison DG, Gongora MC, Guzik TJ, Widder J. Oxidative stress and hypertension. *J Am Soc Hypertens* 2007; **1**(1): 30-44.

Hayamizu S, Kanda K, Ohmori S, Murata Y, Seo H. Glucocorticoids potentiate the action of atrial natriuretic polypeptide in adrenalectomized rats. *Endocrinology* 1994; **135**(6): 2459-2464.

He Y. Angiotensin II receptor blockade in glucocorticoid-induced hypertension in rats. Canberra: The John Curtin School of Medical Research, The Australian National University; 2008.

Hein TW, Kuo L. LDLs impair vasomotor function of the coronary microcirculation : role of superoxide anions. *Circ Res* 1998; **83**(4): 404-414.

Heumuller S, Wind S, Barbosa-Sicard E, Schmidt HHHW, Busse R, Schroder K, Brandes RP. Apocynin is not an inhibitor of vascular NADPH oxidases but an antioxidant. *Hypertension* 2008; **51**(2): 211-217.

Hirata F, Schiffmann E, Venkatasubramanian K, Salomon D, Axelrod J. A phospholipase A2 inhibitory protein in rabbit neutrophils induced by glucocorticoids. *Proc Natl Acad Sci U S A* 1980; **77**(5): 2533-2536.

Homma M, Tanaka A, Hino K, Takamura H, Hirano T, Oka K, Kanazawa M, Miwa T, Notoya Y, Niitsuma T, Hayashi T. Assessing systemic 11β-hydroxysteroid dehydrogenase with serum cortisone/cortisol ratios in healthy subjects and patients with diabetes mellitus and chronic renal failure. *Metabolism* 2001; **50**(7): 801-804.

Hu L, Zhang Y, Lim PS, Miao Y, Tan C, McKenzie KUS, Schyvens CG, Whitworth JA. Apocynin but not L-arginine prevents and reverses dexamethasone-induced hypertension in the rat. *Am J Hypertens* 2006; **19**(4): 413-418.

Huang LQ, Whitworth JA, Chesterman CN. Effects of cyclosporin A and dexamethasone on haemostatic and vasoactive functions of vascular endothelial cells. *Blood Coagul Fibrinolysis* 1995; **6**(5): 438-445.

Huang PL, Huang Z, Mashimo H, Bloch KD, Moskowitz MA, Bevan JA, Fishman MC. Hypertension in mice lacking the gene for endothelial nitric oxide synthase. *Nature* 1995; **377**(6546): 239-242.

Humphrey TJ, Fan JS, Coghlan JP, Denton DA, Scoggins BA, Stewart KW, Whitworth JA. Inter-relationships between sodium and potassium intake and the blood pressure effects of ACTH in sheep. *J Hypertens* 1983; **1**(1): 19-26.

Igarashi T, Nakajima Y, Ohtake S. Antihypertensive effect of combined treatment with alpha- and beta-adrenergic blockers in the spontaneously hypertensive rat. *Jpn Circ J* 1977; **41**(8): 903-911.

Iijima F, Malik KU. Contribution of vasopressin in dexamethasone-induced hypertension in rats. *Hypertension* 1988; **11**(2 Pt 2): I42-46.

Intengan HD, Schiffrin EL. Structure and mechanical properties of resistance arteries in hypertension : role of adhesion molecules and extracellular matrix determinants. *Hypertension* 2000; **36**(3): 312-318.

Ishihara T, Chin WP, Yoshida Y, Sun HT, Mitomi A, Ishibashi T, Tamura K, Imai S. Effects of chronic oral administration of a new beta-blocker, bopindolol, on serum lipoprotein concentrations and blood pressure of spontaneously hypertensive rats. *Arch Int Pharmacodyn Ther* 1989; **302**: 145-157.

Iuchi T, Akaike M, Mitsui T, Ohshima Y, Shintani Y, Azuma H, Matsumoto T. Glucocorticoid excess induces superoxide production in vascular endothelial cells and elicits vascular endothelial dysfunction. *Circ Res* 2003; **92**(1): 81-87.

Janssen BJA, De Celle T, Debets JJM, Brouns AE, Callahan MF, Smith TL. Effects of anesthetics on systemic hemodynamics in mice. *Am J Physiol Heart Circ Physiol* 2004; **287**(4): H1618-1624.

Johns DG, Dorrance AM, Tramontini NL, Webb RC. Glucocorticoids inhibit tetrahydrobiopterin-dependent endothelial function. *Exp Biol Med* 2001; **226**(1): 27-31.

Kalimi M. Role of antiglucocorticoid RU 486 on dexamethasone-induced hypertension in rats. *Am J Physiol Endocrinol Metab* 1989; **256**(5): E682-685.

Kanse SM, Takahashi K, Warren JB, Ghatei M, Bloom SR. Glucocorticoids induce endothelin release from vascular smooth muscle cells but not endothelial cells. *Eur J Pharmacol* 1991; **199**(1): 99-101.

Kelly JJ, Tam SH, Williamson PM, Lawson J, Whitworth JA. The nitric oxide system and cortisol-induced hypertension in humans. *Clin Exp Pharmacol Physiol* 1998; **25**(11): 945-946.

Kennedy B, Elayan H, Ziegler MG. Glucocorticoid hypertension and nonadrenal phenylethanolamine N-methyltransferase. *Hypertension* 1993; **21**(4): 415-419.

Kennedy B, Ziegler MG. Cardiac epinephrine synthesis. Regulation by a glucocorticoid. *Circulation* 1991; **84**(2): 891-895.

Kim H, Lee JM, Park JS, Jo SA, Kim Y-O, Kim C-W, Jo I. Dexamethasone coordinately regulates angiopoietin-1 and VEGF: A mechanism of glucocorticoid-induced stabilization of blood-brain barrier. *Biochem Biophys Res Commun* 2008; **372**(1): 243-248.

Kim MS, Park JY, Namkoong C, Jang PG, Ryu JW, Song HS, Yun JY, Namgoong IS, Ha J, Park IS, Lee IK, Viollet B, Youn JH, Lee HK, Lee KU. Anti-obesity effects of alpha-lipoic acid mediated by suppression of hypothalamic AMP-activated protein kinase. *Nat Med* 2004; **10**(7): 727-733.

Kimura S, Zhang G-X, Nishiyama A, Shokoji T, Yao L, Fan Y-Y, Rahman M, Abe Y. Mitochondria-derived reactive oxygen species and vascular MAP kinases: comparison of angiotensin II and diazoxide. *Hypertension* 2005; **45**(3): 438-444.

Kishi K, Kawashima K, Sokabe H, Saito K. Chronic effects of arotinolol (S-596) in spontaneously hypertensive rats. *J Pharmacobiodyn* 1985; **8**(1): 50-55.

Knowles RG, Moncada S. Nitric oxide synthases in mammals. *Biochem J* 1994; **298 (Pt 2)**: 249-258.

Koeppen BM, Katz AI, Lindheimer MD. Effect of general anaesthesia on renal haemodynamics in the rat. *Clin Sci (Lond)* 1979; **57**(5): 469-471.

Konagaya M, Bernard PA, Max SR. Blockade of glucocorticoid receptor binding and inhibition of dexamethasone-induced muscle atrophy in the rat by RU38486, a potent glucocorticoid antagonist. *Endocrinology* 1986; **119**(1): 375-380.

Kondo-Nakamura M, Shintani-Ishida K, Uemura K, Yoshida K-i. Brief exposure to carbon monoxide preconditions cardiomyogenic cells against apoptosis in ischemia-reperfusion. *Biochem Biophys Res Commmun* 2010; **393**(3): 449-454.

Kontos HA, Wei EP, Ellis EF, Jenkins LW, Povlishock JT, Rowe GT, Hess ML. Appearance of superoxide anion radical in cerebral extracellular space during increased prostaglandin synthesis in cats. *Circ Res* 1985; **57**(1): 142-151.

Koppers AJ, De Iuliis GN, Finnie JM, McLaughlin EA, Aitken RJ. Significance of mitochondrial reactive oxygen species in the generation of oxidative stress in spermatozoa. *J Clin Endocrinol Metab* 2008; **93**(8): 3199-3207.

Krishna CM, Liebmann JE, Kaufman D, DeGraff W, Hahn SM, McMurry T, Mitchell JB, Russo A. The catecholic metal sequestering agent 1,2-dihydroxybenzene-3,5-disulfonate confers protection against oxidative cell damage. *Arch Biochem Biophys* 1992; **294**(1): 98-106.

Krug S, Zhang Y, Mori TA, Croft KD, Vickers JJ, Langton LK, Whitworth JA. N-Acetylcysteine prevents but does not reverse dexamethasone-induced hypertension. *Clin Exp Pharmacol Physiol* 2008; **35**(8): 979-981.

Kubo T, Esumi K, Ennvu K. Effect of chronic treatment with propranolol on blood pressure and cardiovascular reactivity in spontaneously hypertensive rats. *Arch Int Pharmacodyn Ther* 1977; **227**(1): 30-40.

Kumai T, Asoh K, Tateishi T, Tanaka M, Watanabe M, Shimizu H, Kobayashi S. Involvement of tyrosine hydroxylase up regulation in dexamethasone-induced hypertension of rats. *Life Sci* 2000; **67**(16): 1993-1999.

Kumar KV, Das UN. Are free radicals involved in the pathobiology of human essential hypertension? *Free Radic Res Commun* 1993; **19**(1): 59-66.

Kurland GS, Freedberg AS. The potentiating effect of ACTH and of cortisone of pressor response to intravenous infusion of L-nor-epinephrine. *Proc Soc Exp Biol Med* 1951; **78**(1): 28-31.

Kushiro T, Fujita H, Hisaki R, Asai T, Ichiyama I, Kitahara Y, Koike M, Sugiura H, Saito F, Otsuka Y, Kanmatsuse K. Oxidative stress in the Dahl salt-sensitive hypertensive rat. *Clin Exp Hypertens* 2005; **27**(1): 9 - 15.

Lachance D, Garcia R, Gutkowska J, Cantin M, Thibault G. Mechanisms of release of atrial natriuretic factor I. Effect of several agonists and steroids on its release by atrial minces. *Biochem Biophys Res Commun* 1986; **135**(3): 1090-1098.

Lassegue B, Clempus RE. Vascular NAD(P)H oxidases: specific features, expression, and regulation. *Am J Physiol Regul Integr Comp Physiol* 2003; **285**(2): R277-297.

Leenen FH, Prowse S. Time-course of changes in cardiac hypertrophy and pressor mechanisms in two-kidney, one clip hypertensive rats during treatment

with minoxidil, enalapril or after uninephrectomy. *J Hypertens* 1987; **5**(1): 73-83.

Lefer AM, Manwaring JL, Verrier RL. Effect of corticosteroids on the cardiovascular responses to angiotensin and norepinephrine. *J Pharmacol Exp Ther* 1966; **154**(1): 83-91.

Lenaz G. Role of mitochondria in oxidative stress and ageing. *Biochim Biophys Acta* 1998; **1366**(1-2): 53-67.

Lerman LO, Nath KA, Rodriguez-Porcel M, Krier JD, Schwartz RS, Napoli C, Romero JC. Increased oxidative stress in experimental renovascular hypertension. *Hypertension* 2001; **37**(2): 541-546.

Lewis GD, Campbell WB, Johnson AR. Inhibition of prostaglandin synthesis by glucocorticoids in human endothelial cells. *Endocrinology* 1986; **119**(1): 62-69.

Li M, Fraser T, Wang J, Whitworth JA. Dexamethasone-induced hypertension in the rat: effects of L-arginine. *Clin Exp Pharmacol Physiol* 1997; **24**(9-10): 730-732.

Li M, Wen C, Fraser T, Whitworth JA. Adrenocorticotrophin-induced hypertension: effects of mineralocorticoid and glucocorticoid receptor antagonism. *J Hypertens* 1999; **17**(3): 419-426.

Li M, Wen C, Martin A, Whitworth JA. Dehydroepiandrosterone does not prevent adrenocorticotrophin-induced hypertension in conscious rats. *Clin Exp Pharmacol Physiol* 1996; **23**(5): 435-437.

Li M, Whitworth JA. Role of the sympathetic nervous system in the onset of hypertension in the rat: the effect of 6-OH-dopamine. *Clin Exp Pharmacol Physiol* 1991; **18**(4): 197-204.

Lin F, Abraham NG, Schwartzman ML. Cytochrome P450 arachidonic acid omega-hydroxylation in the proximal tubule of the rat kidney. *Ann N Y Acad Sci* 1994; **744**(Cellular Generation, Transport, and Effects of Eicosanoids: Biological Roles and Pharmacological Intervention): 11-24.

Liu X, Zhao Y, Wang L, Yang X, Zheng Z, Zhang Y, Chen F, Liu H. Overexpression of cytochrome P450 4F2 in mice increases 20-hydroxyeicosatetraenoic acid production and arterial blood pressure. *Kidney Int* 2009; **75**(12): 1288-1296.

Lou Y-k, Wen C, Li M, Adams DJ, Wang M-x, Yang F, Morris BJ, Whitworth JA. Decreased renal expression of nitric oxide synthase isoforms in adrenocorticotropin-induced and corticosterone-induced hypertension. *Hypertension* 2001; **37**(4): 1164-1170.

Lund KC, Peterson LL, Wallace KB. Absence of a universal mechanism of Mitochondrial toxicity by nucleoside analogs. *Antimicrob Agents Chemother* 2007; **51**(7): 2531-2539.

Lundberg JM, Terenius L, Hokfelt T, Goldstein M. High levels of neuropeptide Y in peripheral noradrenergic neurons in various mammals including man. *Neurosci Lett* 1983; **42**(2): 167-172.

Ma K, Mallidis C, Bhasin S, Mahabadi V, Artaza J, Gonzalez-Cadavid N, Arias J, Salehian B. Glucocorticoid-induced skeletal muscle atrophy is associated with upregulation of myostatin gene expression. *Am J Physiol Endocrinol Metab* 2003; **285**(2): E363-371.

Macefield VG, Williamson PM, Wilson LR, Kelly JJ, Gandevia SC, Whitworth JA. Muscle sympathetic vasoconstrictor activity in hydrocortisone-induced hypertension in humans. *Blood Press* 1998; **7**(4): 215-222.

MacKenzie A, Martin W. Loss of endothelium-derived nitric oxide in rabbit aorta by oxidant stress: restoration by superoxide dismutase mimetics. *Br J Pharmacol* 1998; **124**(4): 719-728.

Madamanchi NR, Runge MS. Mitochondrial dysfunction in atherosclerosis. *Circ Res* 2007; **100**(4): 460-473.

Magiakou MA, Smyrnaki P, Chrousos GP. Hypertension in Cushing's syndrome. *Best Pract & Res Clin Endocrinol Metab* 2006; **20**(3): 467-482.

Mak IT, Weglicki WB. Protection by beta-blocking agents against free radical-mediated sarcolemmal lipid peroxidation. *Circ Res* 1988; **63**(1): 262-266.

Mak IT, Weglicki WB. Potent antioxidant properties of 4-hydroxyl-propranolol. *J Pharmacol Exp Ther* 2004; **308**(1): 85-90.

Mangos G, Walker B, Williamson P, Whitworth J, Kelly J. Effect of Synthetic Corticosteroids on Vascular Reactivity in the Human Forearm. *Clin Exp Hypertens* 2006; **28**(8): 707-718.

Mangos GJ, Turner SW, Fraser TB, Whitworth JA. The role of corticosterone in corticotrophin (ACTH)-induced hypertension in the rat. *J Hypertens* 2000; **18**(12): 1849-1855.

Marangon K, Devaraj S, Tirosh O, Packer L, Jialal I. Comparison of the effect of α-lipoic acid and α-tocopherol supplementation on measures of oxidative stress. *Free Radic Biol Med* 1999; **27**(9-10): 1114-1121.

Marley R, Holt S, Fernando B, arry D, Anand R, Goodier D, Davies S, Moore K. Lipoic acid prevents development of the hyperdynamic circulation in anesthetized rats with biliary cirrhosis. *Hepatology* 1999; **29**(5): 1358-1363.

Mason CS, Myers CS, Kendall EC. The chemistry of crystalline substances isolated from suprarenal gland. *J Biol Chem* 1936; **114**: 613-631.

Mattiasson G. Analysis of mitochondrial generation and release of reactive oxygen species. *Cytometry Part A* 2004; **62A**(2): 89-96.

Mattiasson G. Flow cytometric analysis of isolated liver mitochondria to detect changes relevant to cell death. *Cytometry Part A* 2004a; **60A**(2): 145-154.

Meany DL, Poe BG, Navratil M, Moraes CT, Arriaga EA. Superoxide released into the mitochondrial matrix. *Free Radic Biol Med* 2006; **41**(6): 950-959.

Medhora M, Chen Y, Gruenloh S, Harland D, Bodiga S, Zielonka J, Gebremedhin D, Gao Y, Falck JR, Anjaiah S, Jacobs ER. 20-HETE increases superoxide production and activates NAPDH oxidase in pulmonary artery endothelial cells. *Am J Physiol Lung Cell Mol Physiol* 2008; **294**(5): L902-911.

Medvei VC. The history of Cushing's disease: a controversial tale. *J R Soc Med* 1991; **84**(6): 363-366.

Mendlowitz M, Naftchi N, Weinreb HL, Gitlow SE. Effect of prednisone on digital vascular reactivity in normotensive and hypertensive subjects. *J Appl Physiol* 1961; **16**(1): 89-94.

Miao Y, Zhang Y, Lim PS, Kanjanapan Y, Mori TA, Croft KD, Earl J, Lee SY, McKenzie KU, Hu L, Whitworth JA. Folic Acid prevents and partially reverses glucocorticoid-induced hypertension in the rat. *Am J Hypertens* 2007; **20**(3): 304-310.

Mills EH, Coghlan JP, Denton DA, Spence CD, Whitworth JA, Scoggins BA. The effect of sodium depletion and potassium loading on cortisol induced hypertension in sheep. *Acta Endocrinol (Copenh)* 1986; **113**(2): 298-304.

MIMS_Online. (11 August 2008). "DBL Dexamethasone Sodium Phosphate Injection."

Mitchell BM, Dorrance AM, Webb RC. GTP cyclohydrolase 1 downregulation contributes to glucocorticoid hypertension in rats. *Hypertension* 2003; **41**(3): 669-674.

Miyata N, Roman RJ. Role of 20-hydroxyeicosatetraenoic acid (20-HETE) in vascular system. *J Smooth Muscle Res* 2005; **41**(4): 175-193.

Moini H, Packer L, Saris N-EL. Antioxidant and prooxidant activities of α-lipoic acid and dihydrolipoic acid. *Toxicol Appl Pharmacol* 2002; **182**(1): 84-90.

Mondo CK, Yang W-S, Su J-Z, Huang T-G. Atorvastatin prevented and reversed dexamethasone-induced hypertension in the rat. *Clin Exp Hypertens* 2006; **28**(5): 499-509.

Mondo CK, Yang W-S, Zhang N, Huang T-G. Anti-oxidant effects of atorvastatin in dexamethasone-induced hypertension in the rat. *Clin Exp Pharmacol Physiol* 2006a; **33**(11): 1029-1034.

Mondo CK, Zhang Y, Possamai VdM, Miao Y, Schyvens CG, McKenzie KUS, Hu L, Guo Z, Whitworth JA. N-Acetylcysteine antagonizes the development but does not reverse ACTH-induced hypertension in the rat. *Clin Exp Hypertens* 2006; **28**(2): 73 -84.

Montrella-Waybill M, Clore JN, Schoolwerth AC, Watlington CO. Evidence that high dose cortisol-induced Na+ retention in man is not mediated by the mineralocorticoid receptor. *J Clin Endocrinol Metab* 1991; **72**(5): 1060-1066.

Morgan ET, Ullrich V, Daiber A, Schmidt P, Takaya N, Shoun H, McGiff JC, Oyekan A, Hanke CJ, Campbell WB, Park C-S, Kang J-S, Yi H-G, Cha Y-N, Mansuy D, Boucher J-L. Cytochromes P450 and flavin monooxygenases-targets and sources of nitric oxide. *Drug Metab Dispos* 2001; **29**(11): 1366-1376.

Mori TA, Croft KD, Puddey IB, Beilin LJ. An improved method for the measurement of urinary and plasma F_2-isoprostanes using gas chromatography-mass spectrometry. *Anal Biochem* 1999; **268**(1): 117-125.

Morrow JD, Hill KE, Burk RF, Nammour TM, Badr KF, Roberts LJ, 2nd. A series of prostaglandin F_2-like compounds are produced in vivo in humans by a non-cyclooxygenase, free radical-catalyzed mechanism. *Proc Natl Acad Sci U S A* 1990; **87**(23): 9383-9387.

Morrow JD, Roberts LJ. The isoprostanes: Current knowledge and directions for future research. *Biochem Pharmacol* 1996; **51**(1): 1-9.

Mosier HD, Jr., Spencer EM, Dearden LC, Jansons RA. The effect of glucocorticoids on plasma insulin-like growth factor I concentration in the rat fetus. *Pediatr Res* 1987; **22**(1): 92-95.

Moura AM, Worcel M. Anti-hypertensive action of the effects of spironolactone on the permeability of smooth muscles to Na+ and Rb+. *J Physiol (Paris)* 1981; **77**(8): A2-A3.

Mukhopadhyay P, Rajesh M, Hasko G, Hawkins BJ, Madesh M, Pacher P. Simultaneous detection of apoptosis and mitochondrial superoxide production in live cells by flow cytometry and confocal microscopy. *Nat Protocols* 2007; **2**(9): 2295-2301.

Mukhopadhyay P, Rajesh M, Yoshihiro K, Hasko G, Pacher P. Simple quantitative detection of mitochondrial superoxide production in live cells. *Biochem Biophys Res Commun* 2007a; **358**(1): 203-208.

Muller FL, Liu Y, Van Remmen H. Complex III releases superoxide to both sides of the inner mitochondrial membrane. *J Biol Chem* 2004; **279**(47): 49064-49073.

Munusamy S, MacMillan-Crow LA. Mitochondrial superoxide plays a crucial role in the development of mitochondrial dysfunction during high glucose exposure in rat renal proximal tubular cells. *Free Radic Biol Med* 2009; **46**(8): 1149-1157.

Murasawa S, Matsubara H, Kizima K, Maruyama K, Mori Y, Inada M. Glucocorticoids regulate V1a vasopressin receptor expression by increasing mRNA stability in vascular smooth muscle cells. *Hypertension* 1995; **26**(4): 665-669.

Muthalif MM, Karzoun NA, Gaber L, Khandekar Z, Benter IF, Saeed AE, Parmentier J-H, Estes A, Malik KU. Angiotensin II-induced hypertension : contribution of Ras GTPase/mitogen-activated protein kinase and cytochrome P450 metabolites. *Hypertension* 2000; **36**(4): 604-609.

Myrsen-Axcrona U, Karlsson S, Sundler F, Ahren B. Dexamethasone induces neuropeptide Y (NPY) expression and impairs insulin release in the insulin-producing cell line RINm5F. Release of NPY and insulin through different pathways. *J Biol Chem* 1997; **272**(16): 10790-10796.

Myrsen U, Ahren B, Sundler F. Dexamethasone-induced neuropeptide Y expression in rat islet endocrine cells. Rapid reversibility and partial prevention by insulin. *Diabetes* 1996; **45**(10): 1306-1316.

N'Gankam V, Uehlinger D, Dick B, Frey BM, Frey FJ. Increased cortisol metabolites and reduced activity of 11β-hydroxysteroid dehydrogenase in patients on hemodialysis. *Kidney Int* 2002; **61**(5): 1859-1866.

Nabha L, Garbern JC, Buller CL, Charpie JR. Vascular oxidative stress precedes high blood pressure in spontaneously hypertensive rats. *Clin. Exp. Hypertens.* 2005; **27**(1): 71 - 82.

Nakamoto H, Suzuki H, Kageyama Y, Murakami M, Naitoh M, Saruta T. Central nervous system mediates an antihypertensive property in glucocorticoid hypertension in dogs. *J Hypertens* 1995; **13**(10): 1169-1179.

Nakamoto H, Suzuki H, Kageyama Y, Murakami M, Ohishi A, Naitoh M, Ichihara A, Saruta T. Depressor systems contribute to hypertension induced by glucocorticoid excess in dogs. *J Hypertens* 1992; **10**(6): 561-569.

Nakamoto H, Suzuki H, Kageyama Y, Ohishi A, Murakami M, Naitoh M, Saruta T. Characterization of alterations of hemodynamics and neuroendocrine hormones in dexamethasone induced hypertension in dogs. *Clin Exp Hypertens A* 1991; **13**(4): 587-606.

Nakayama K, Okamoto F, Harada Y. Antimycin A: isolation from a new Streptomyces and activity against rice plant blast fungi. *J Antibiot (Tokyo)* 1956; **9**(2): 63-66.

Nakazono K, Watanabe N, Matsuno K, Sasaki J, Sato T, Inoue M. Does superoxide underlie the pathogenesis of hypertension? *Proc Natl Acad Sci U S A* 1991; **88**(22): 10045-10048.

Nasjletti A, Erman A, Cagen LM, Baer PG. Plasma concentrations, renal excretion, and tissue release of prostaglandins in the rat with dexamethasone-induced hypertension. *Endocrinology* 1984; **114**(3): 1033-1040.

Nieman LK, Biller BMK, Findling JW, Newell-Price J, Savage MO, Stewart PM, Montori VM. The diagnosis of Cushing's syndrome: An Endocrine Society clinical practice guideline. *J Clin Endocrinol Metab* 2008; **93**(5): 1526-1540.

Nohl H, Gille L, Staniek K. Intracellular generation of reactive oxygen species by mitochondria. *Biochem Pharmacol* 2005; **69**(5): 719-723.

Okuno T, Suzuki H, Saruta T. Dexamethasone hypertension in rats. *Clin Exp Hypertens* 1981; **3**(5): 1075-1086.

Ong SLH, Zhang Y, Whitworth JA. Reactive oxygen species and glucocorticoid-induced hypertension. *Clin Exp Pharmacol Physiol* 2008; **35**(4): 477-482.

Owens GK. Influence of blood pressure on development of aortic medial smooth muscle hypertrophy in spontaneously hypertensive rats. *Hypertension* 1987; **9**(2): 178-187.

Oyekan AO, Youseff T, Fulton D, Quilley J, McGiff JC. Renal cytochrome P450 omega-hydroxylase and epoxygenase activity are differentially modified by nitric oxide and sodium chloride. *J Clin Invest* 1999; **104**(8): 1131-1137.

Pacher P, Beckman JS, Liaudet L. Nitric oxide and peroxynitrite in health and disease. *Physiol Rev* 2007; **87**(1): 315-424.

Pagano PJ, Clark JK, Cifuentes-Pagano ME, Clark SM, Callis GM, Quinn MT. Localization of a constitutively active, phagocyte-like NADPH oxidase in rabbit aortic adventitia: Enhancement by angiotensin II. *Proc Natl Acad Sci U S A* 1997; **94**(26): 14483-14488.

Pagano PJ, Ito Y, Tornheim K, Gallop PM, Tauber AI, Cohen RA. An NADPH oxidase superoxide-generating system in the rabbit aorta. *Am J Physiol* 1995; **268**(6 Pt 2): H2274-2280.

Pallotti F, Lenaz G. Isolation and subfractionation of mitochondria from animal cells and tissue culture lines. *Methods Cell Biol* 2001; **65**: 1-35.

Pamnani MB, Clough DL, Haddy FJ. Altered activity of the sodium-potassium pump in arteries of rats with steroid hypertension. *Clin Sci Mol Med Suppl* 1978; **4**: 41s-43s.

Paravicini TM, Gulluyan LM, Dusting GJ, Drummond GR. Increased NADPH oxidase activity, gp91phox expression, and endothelium-dependent vasorelaxation during neointima formation in rabbits. *Circ Res* 2002; **91**(1): 54-61.

Patrono C, FitzGerald GA. Isoprostanes: potential markers of oxidant stress in atherothrombotic disease. *Arterioscler Thromb Vasc Biol* 1997; **17**(11): 2309-2315.

Payne CM, Weber C, Crowley-Skillicorn C, Dvorak K, Bernstein H, Bernstein C, Holubec H, Dvorakova B, Garewal H. Deoxycholate induces mitochondrial oxidative stress and activates NF-{kappa}B through multiple mechanisms in HCT-116 colon epithelial cells. *Carcinogenesis* 2007; **28**(1): 215-222.

Pernow J, Lundberg JM. Modulation of noradrenaline and neuropeptide Y (NPY) release in the pig kidney in vivo: involvement of alpha 2, NPY and angiotensin II receptors. *Naunyn Schmiedebergs Arch Pharmacol* 1989; **340**(4): 379-385.

Pham N-A, Robinson BH, Hedley DW. Simultaneous detection of mitochondrial respiratory chain activity and reactive oxygen in digitonin-permeabilized cells using flow cytometry. *Cytometry* 2000; **41**(4): 245-251.

Pirpiris M, Sudhir K, Yeung S, Jennings G, Whitworth JA. Pressor responsiveness in corticosteroid-induced hypertension in humans. *Hypertension* 1992; **19**(6): 567-574.

Pirpiris M, Yeung S, Dewar E, Jennings GL, Whitworth JA. Hydrocortisone-induced hypertension in men. The role of cardiac output. *Am J Hypertens* 1993; **6**(4): 287-294.

Racotta R, Soto-Mora LM. Specificity of alpha- and beta-adrenergic inhibition of water and food intake. *Physiol Behav* 1993; **53**(2): 361-365.

Rajagopalan S, Kurz S, Munzel T, Tarpey M, Freeman BA, Griendling KK, Harrison DG. Angiotensin II-mediated hypertension in the rat increases vascular superoxide production via membrane NADH/NADPH oxidase activation . Contribution to alterations of vasomotor tone. *J Clin Invest* 1996; **97**(8): 1916-1923.

Rajashree S, Puvanakrishnan R. Dexamethasone induced alterations in the levels of proteases involved in blood pressure homeostasis and blood coagulation in rats. *Mol Cell Biochem* 1999; **197**(1-2): 203-208.

Rajesh M, Mukhopadhyay P, Batkai S, Hasko G, Liaudet L, Drel VR, Obrosova IG, Pacher P. Cannabidiol attenuates high glucose-induced endothelial cell inflammatory response and barrier disruption. *Am J Physiol Heart Circ Physiol* 2007; **293**(1): H610-619.

Ramachandran A, Levonen A-L, Brookes PS, Ceaser E, Shiva S, Barone MC, Darley-Usmar V. Mitochondria, nitric oxide, and cardiovascular dysfunction. *Free Radic Biol Med* 2002; **33**(11): 1465-1474.

Rang HP, Dale MM, Ritter JM, Flower RJ. The pituitary and the adrenal cortex. *Rang and Dale's Pharmacology*. 6 ed. Philadelphia: Churchill Livingstone Elsevier; 2007:420-436.

Rebuffat AG, Tam S, Nawrocki AR, Baker ME, Frey BM, Frey FJ, Odermatt A. The 11-ketosteroid 11-ketodexamethasone is a glucocorticoid receptor agonist. *Mol Cell Endocrinol* 2004; **214**(1-2): 27-37.

Reckelhoff JF, Zhang H, Srivastava K, Roberts LJ, II, Morrow JD, Romero JC. Subpressor doses of angiotensin II increase plasma F_2-isoprostanes in rats. *Hypertension* 2000; **35**(1): 476-479.

Rees DD, Palmer RMJ, Moncada S. Role of endothelium-derived nitric oxide in the regulation of blood pressure. *Proc Natl Acad Sci U S A* 1989; **86**(9): 3375-3378.

Reichstein T (1962). Nobel Lectures (Physiology or Medicine). Amsterdam, Elsevier.

Richter C. Do mitochondrial DNA fragments promote cancer and aging? *FEBS Letters* 1988; **241**(1-2): 1-5.

Robinson KM, Janes MS, Beckman JS. The selective detection of mitochondrial superoxide by live cell imaging. *Nat. Protocols* 2008; **3**(6): 941-947.

Robinson KM, Janes MS, Pehar M, Monette JS, Ross MF, Hagen TM, Murphy MP, Beckman JS. Selective fluorescent imaging of superoxide in vivo using ethidium-based probes. *Proc Natl Acad Sci U S A* 2006: 0601945103.

Rodriguez-Iturbe B, Sepassi L, Quiroz Y, Ni Z, Vaziri ND. Association of mitochondrial SOD deficiency with salt-sensitive hypertension and accelerated renal senescence. *J Appl Physiol* 2007; **102**(1): 255-260.

Roman RJ. P-450 metabolites of arachidonic acid in the control of cardiovascular function. *Physiol Rev* 2002; **82**(1): 131-185.

Rose BD, Post TW. Regulation of the effective circulating volume. In: Wonsciewicz M., McCullough K.,Davis K., eds. *Clinical physiology of acid base and electrolyte disorders*. 5th ed. New York: McGraw-Hill; 2001:258-284.

Ross MF, Kelso GF, Blaikie FH, James AM, Cocheme HM, Filipovska A, Da Ros T, Hurd TR, Smith RA, Murphy MP. Lipophilic triphenylphosphonium cations as tools in mitochondrial bioenergetics and free radical biology. *Biochemistry (Mosc)* 2005; **70**(2): 222-230.

Rothschild AJ, Langlais PJ, Schatzberg AF, Walsh FX, Cole JO, Bird ED. Dexamethasone increases plasma free dopamine in man. *J Psychiatr Res* 1984; **18**(3): 217-223.

Roubert P, Viossat I, Lonchampt MO, Chapelat M, Schulz J, Plas P, Gillard-Roubert V, Chabrier PE, Braquet P. Endothelin receptor regulation by endothelin synthesis in vascular smooth muscle cells: effects of dexamethasone and phosphoramidon. *J Vasc Res* 1993; **30**(3): 139-144.

Roy SG, De P, Mukherjee D, Chander V, Konar A, Bandyopadhyay D, Bandyopadhyay A. Excess of glucocorticoid induces cardiac dysfunction via activating angiotensin II pathway. *Cell Physiol Biochem* 2009; **24**(1-2): 1-10.

Ruffmann R, Wendel A. GSH rescue by N-acetylcysteine. *Klin Wochenschr* 1991; **69**(18): 857-862.

Russo-Marie F, Duval D. Dexamethasone-induced inhibition of prostaglandin production dose not result from a direct action on phospholipase activities but is mediated through a steroid-inducible factor. *Biochim Biophys Acta* 1982; **712**(1): 177-185.

Russo D, Fraser R, Kenyon CJ. Dexamethasone therapy selectively increases the sensitivity to noradrenaline of the rat mesenteric circulation. *J Hypertens Suppl* 1989; **7**(6): S126-127.

Russo D, Fraser R, Kenyon CJ. Increased sensitivity to noradrenaline in glucocorticoid-treated rats: the effects of indomethacin and desipramine. *J Hypertens* 1990; **8**(9): 827-833.

Saha DC, Saha AC, Malik G, Astiz ME, Rackow EC. Comparison of cardiovascular effects of tiletamine-zolazepam, pentobarbital, and ketamine-xylazine in male rats. *J Am Assoc Lab Anim Sci* 2007; **46**(2): 74-80.

Sakaue M, Hoffman BB. Glucocorticoids induce transcription and expression of the alpha 1B adrenergic receptor gene in DTT1 MF-2 smooth muscle cells. *J Clin Invest* 1991; **88**(2): 385-389.

Sambhi MP, Weil MH, Udhoji VN. Pressor responses to norepinephrine in humans before and after corticosteroids. *Am J Physiol* 1962; **203**(5): 961-963.

Sanchez-Mendoza A, Lopez-Sanchez P, Vazquez-Cruz B, Rios A, Martinez-Ayala S, Escalante B. Angiotensin II modulates ion transport in rat proximal tubules through CYP metabolites. *Biochem Biophys Res Commun* 2000; **272**(2): 423-430.

Sanz E, Lopez Novoa JM, Linares M, Digiuni E, Caramelo CA. Intravascular and interstitial fluid dynamics in rats treated with minoxidil. *J Cardiovasc Pharmacol* 1990; **15**(3): 485-492.

Saruta T. Mechanism of glucocorticoid-induced hypertension. *Hypertens Res* 1996; **19**(1): 1-8.

Sato A, Suzuki H, Iwaita Y, Nakazato Y, Kato H, Saruta T. Potentiation of inositol trisphosphate production by dexamethasone. *Hypertension* 1992; **19**(1): 109-115.

Sato A, Suzuki H, Nakazato Y, Shibata H, Inagami T, Saruta T. Increased expression of vascular angiotensin II type 1A receptor gene in glucocorticoid-induced hypertension. *J Hypertens* 1994; **12**(5): 511-516.

Sayre LM, Smith MA, Perry G. Chemistry and biochemistry of oxidative stress in neurodegenerative disease. *Curr Med Chem* 2001; **8**: 721-738.

Schafer SC, Wallerath T, Closs EI, Schmidt C, Schwarz PM, Forstermann U, Lehr HA. Dexamethasone suppresses eNOS and CAT-1 and induces oxidative stress in mouse resistance arterioles. *Am J Physiol Heart Circ Physiol* 2005; **288**(1): H436-444.

Schimmer BP, Parker KL. Adrenocorticotrophic hormone; adrenocortical steroids and their synthetic analogs; inhibitors of the synthesis and actions of adrenocortical hormones. In: Hardman J. G.,Limbird L. E., eds. *Goodman & Gilman's the pharmacological basis of therapeutics*. 10 ed. New York: McGraw-Hill; 2001:1649-1677.

Schmidt K, Werner ER, Mayer B, Wachter H, Kukovetz WR. Tetrahydrobiopterin-dependent formation of endothelium-derived relaxing factor (nitric oxide) in aortic endothelial cells. *Biochem J* 1992; **281** (**Pt 2**): 297-300.

Scoggins BA, Allen KJ, Coghlan JP, Denton DA, Graham WF, Humphery TJ, Whitworth JA. Haemodynamics of ACTH-induced hypertension in sheep. *Clin Sci (Lond)* 1979; **57 Suppl 5**: 333s-336s.

Sebaai N, Lesage J, Alaoui A, Dupouy JP, Deloof S. Effects of dehydration on endocrine regulation of the electrolyte and fluid balance and atrial natriuretic peptide-binding sites in perinatally malnourished adult male rats. *Eur J Endocrinol* 2002; **147**(6): 835-848.

Sellden H, Sjovall H, Ricksten SE. Sympathetic nerve activity and central haemodynamics during mechanical ventilation with positive end-expiratory pressure in rats. *Acta Physiol Scand* 1986; **127**(1): 51-60.

Shafagoj Y, Opoku J, Qureshi D, Regelson W, Kalimi M. Dehydroepiandrosterone prevents dexamethasone-induced hypertension in rats. *Am J Physiol Endocrinol Metab* 1992; **263**(2): E210-213.

Shapiro HM. Membrane potential estimation by flow cytometry. *Methods* 2000; **21**(3): 271-279.

Shapiro HM, Natale PJ, Kamentsky LA. Estimation of membrane potentials of individual lymphocytes by flow cytometry. *Proc Natl Acad Sci U S A* 1979; **76**(11): 5728-5730.

Siegal T, Soti F, Biegon A, Pop E, Brewster ME. Effect of a chemical delivery system for dexamethasone (Dex-CDS) on peritumoral edema in an experimental brain tumor model. *Pharm Res* 1997; **14**(5): 672-675.

Silvan G, Martinez-Mateos MM, Blass A, Camacho L, Gonzalez-Gil A, Garcia-Partida P, Illera JC. The effect of long-term exposure to combinations of growth promoters in Long Evans rats: Part 1: Endocrine adrenal function. *Anal Chim Acta* 2007; **586**(1-2): 246-251.

Simmons WW, Ungureanu-Longrois D, Smith GK, Smith TW, Kelly RA. Glucocorticoids regulate inducible nitric oxide synthase by inhibiting tetrahydrobiopterin synthesis and L-arginine transport. *J Biol Chem* 1996; **271**(39): 23928-23937.

Singh H, Cheng J, Deng H, Kemp R, Ishizuka T, Nasjletti A, Schwartzman ML. Vascular cytochrome P450 4A expression and 20-hydroxyeicosatetraenoic acid synthesis contribute to endothelial dysfunction in androgen-Induced hypertension. *Hypertension* 2007; **50**(1): 123-129.

Sinha SK, Rodriguez HJ, Hogan WC, Klahr S. Mechanisms of activation of renal (Na+ + K+)-ATPase in the rat Effects of acute and chronic administration of dexamethasone. *Biochim Biophys Acta* 1981; **641**(1): 20-35.

Sorescu D, Weiss D, Lassegue B, Clempus RE, Szocs K, Sorescu GP, Valppu L, Quinn MT, Lambeth JD, Vega JD, Taylor WR, Griendling KK. Superoxide production and expression of Nox family proteins in human atherosclerosis. *Circulation* 2002; **105**(12): 1429-1435.

Spence CD, Mathai M, Mills EH, Coghlan JP, Whitworth JA, Scoggins BA. Centrally mediated increased sympathetic activity is not important in the

genesis of ACTH-induced hypertension in sheep. *Clin Exp Pharmacol Physiol* 1989; **16**(7): 607-619.

Starkov AA, Fiskum G, Chinopoulos C, Lorenzo BJ, Browne SE, Patel MS, Beal MF. Mitochondrial α-ketoglutarate dehydrogenase complex generates reactive oxygen species. *J Neurosci* 2004; **24**(36): 7779-7788.

Stern N, Palant C, Ozaki L, Tuck ML. Dexamethasone enhances active cation transport in cultured aortic smooth muscle cells. *Am J Hypertens* 1994; **7**(2): 146-150.

Stevenson JA, Franklin C. Effects of ACTH and corticosteroids in the regulation of food and water intake. *Prog Brain Res* 1970; **32**: 141-152.

Stewart P. The adrenal cortex. In: Kronenberg HM M. S., Polonsky KS, Larsen PR, ed. *Williams Textbook of Endocrinology*. 11 ed. Philadelphia: Saunders Elsevier; 2008:Chapter 14.

Stewart PM, Walker BR, Holder G, O'Halloran D, Shackleton CH. 11 beta-Hydroxysteroid dehydrogenase activity in Cushing's syndrome: explaining the mineralocorticoid excess state of the ectopic adrenocorticotropin syndrome. *J Clin Endocrinol Metab* 1995; **80**(12): 3617-3620.

Stricker EM, Vagnucci AH, McDonald RH, Jr., Leenen FH. Renin and aldosterone secretions during hypovolemia in rats: relation to NaCl intake. *Am J Physiol Regul Integr Comp Physiol* 1979; **237**(1): R45-51.

Sudhir K, Jennings GL, Esler MD, Korner PI, Blomberg PA, Lambert GW, Scoggins B, Whitworth JA. Hydrocortisone-induced hypertension in man.

Pressor responsiveness and sympathetic function. *Hypertension* 1989; **13**: 416.

Sun C-W, Alonso-Galicia M, Taheri MR, Falck JR, Harder DR, Roman RJ. Nitric oxide-20–hydroxyeicosatetraenoic acid interaction in the regulation of K+ channel activity and vascular tone in renal arterioles. *Circ Res* 1998; **83**(11): 1069-1079.

Sun XM, Dinsdale D, Snowden RT, Cohen GM, Skilleter DN. Characterization of apoptosis in thymocytes isolated from dexamethasone-treated rats. *Biochemical Pharmacology* 1992; **44**(11): 2131-2137.

Sundler F, Bottcher G, Ekblad E, Hakanson R. PP, PYY and NPY. Occurrence and distrubution in the periphery. In: Colmers W.,Wahlestedt C., eds. *The biology of neuropeptide Y and related peptides*. New Jersey: Humana Press; 1993:157-196.

Suzuki H, DeLano FA, Parks DA, Jamshidi N, Granger DN, Ishii H, Suematsu M, Zweifach BW, Schmid-Schonbein GW. Xanthine oxidase activity associated with arterial blood pressure in spontaneously hypertensive rats. *Proc Natl Acad Sci U S A* 1998; **95**(8): 4754-4759.

Suzuki H, Handa M, Kondo K, Saruta T. Role of renin-angiotensin system in glucocorticoid hypertension in rats. *Am J Physiol Endocrinol Metab* 1982; **243**(1): E48-51.

Suzuki H, Swei A, Zweifach BW, Schmid-Schonbein GW. In vivo evidence for microvascular oxidative stress in spontaneously hypertensive rats: hydroethidine microfluorography. *Hypertension* 1995; **25**(5): 1083-1089.

Swei A, Lacy F, Delano FA, Parks DA, Schmid-Schonbein GW. A mechanism of oxygen free radical production in the Dahl hypertensive rat. *Microcirculation* 1999; **6**(3): 179 - 187.

Swei A, Lacy F, DeLano FA, Schmid-Schonbein GW. Oxidative stress in the Dahl hypertensive rat. *Hypertension* 1997; **30**(6): 1628-1633.

Tabarin A, Minot AP, Dallochio M, Roger P, Ducassou D. Plasma concentration of neuropeptide Y in patients with adrenal hypertension. *Regul Pept* 1992; **42**(1-2): 51-61.

Takahashi K, Suda K, Lam HC, Ghatei MA, Bloom SR. Endothelin-like immunoreactivity in rat models of diabetes mellitus. *J Endocrinol* 1991; **130**(1): 123-127.

Takeda K, Bunag RD. Chronic propranolol treatment inhibits sympathetic nerve activity and keeps blood pressure from rising in spontaneously hypertensive rats. *Hypertension* 1980; **2**(2): 228-235.

Tan C, Schyvens CG, P A, McKenzie KU, Zhang Y, Whitworth JA. The effect of adrenocorticotropic hormone treatment on nitrotyrosine levels in rat organs. *Clin Exp Pharmacol Physiol* 2005; **32**(7): A26.

Tanaka MDE, Mori MDH, Chujo MM, Yamakawa MDA, Mohammed MDMU, Shinozaki Y, Tobita MDK, Sekka MDT, Ito MDK, Nakazawa MDH. Coronary vasoconstrictive effects of neuropeptide Y and their modulation by the ATP-sensitive potassium channel in anesthetized dogs. *J Am Coll Cardiol* 1997; **29**(6): 1380-1389.

Tarpey MM, Fridovich I. Methods of detection of vascular reactive species: nitric oxide, superoxide, hydrogen peroxide, and peroxynitrite. *Circ Res* 2001; **89**(3): 224-236.

Taubert D, Berkels R, Grosser N, Schroder H, Grundemann D, Schomig E. Aspirin induces nitric oxide release from vascular endothelium: a novel mechanism of action. *Br J Pharmacol* 2004; **143**(1): 159-165.

Terzolo M, Allasino B, Bosio S, Brusa E, Daffara F, Ventura M, Aroasio E, Sacchetto G, Reimondo G, Angeli A, Camaschella C. Hyperhomocysteinemia in patients with Cushing's syndrome. *J Clin Endocrinol Metab* 2004; **89**(8): 3745-3751.

Thida M, Earl J, Zhao Y, Wang H, Tse CS, Vickers JJ, Sutton M, Ong SLH, Mori TA, Croft KD, Whitworth JA, Zhang Y. Effects of sepiapterin supplementation and NOS inhibition on glucocorticoid-induced hypertension. *Am J Hypertens* 2010; **23**(5): 569-574.

Tomas FM, Knowles SE, Owens PC, Chandler CS, Francis GL, Read LC, Ballard FJ. Insulin-like growth factor-I (IGF-I) and especially IGF-I variants are anabolic in dexamethasone-treated rats. *Biochem J* 1992; **282 (Pt 1)**(Pt 1): 91-97.

Tonolo G, Fraser R, Connell JM, Kenyon CJ. Chronic low-dose infusions of dexamethasone in rats: effects on blood pressure, body weight and plasma atrial natriuretic peptide. *J Hypertens* 1988; **6**(1): 25-31.

Tonolo G, Richards AM, Manunta P, Troffa C, Pazzola A, Madeddu P, Towrie A, Fraser R, Glorioso N. Low-dose infusion of atrial natriuretic factor in mild essential hypertension. *Circulation* 1989; **80**(4): 893-902.

Tonolo G, Soro A, Madeddu P, Troffa C, Melis MG, Patteri G, Parpaglia PP, Sabino G, Maioli M, Glorioso N. Effect of chronic intracerebroventricular dexamethasone on blood pressure in normotensive rats. *Am J Physiol Endocrinol Metab* 1993; **264**(6): E843-847.

Touyz RM, Schiffrin EL. Reactive oxygen species in vascular biology: implications in hypertension. *Histochem Cell Biol* 2004; **122**(4): 339-352.

Tretter L, Adam-Vizi V. Alpha-ketoglutarate dehydrogenase: a target and generator of oxidative stress. *Philos Trans R Soc Lond B Biol Sci* 2005; **360**(1464): 2335-2345.

Trivedi RC, Rebar L, Berta E, Stong L. New enzymatic method for serum uric acid at 500 nm. *Clin Chem* 1978; **24**(11): 1908-1911.

Tsoporis J, Fields N, Lee RM, Leenen FH. Arterial vasodilation and cardiovascular structural changes in normotensive rats. *Am J Physiol Heart Circ Physiol* 1991; **260**(6): H1944-1952.

Tsunoda M, Takezawa K, Santa T, Ina Y, Nagashima K, Ohmori K, Kobayashi S, Imai K. New approach for measurement of sympathetic nervous abnormality in conscious, spontaneously hypertensive rats. *Jpn J Pharmacol* 2000; **83**(1): 39-45.

Turner SW, Mangos GJ, Whitworth JA. Nitric oxide synthase activity in adrenocorticotrophin-induced hypertension in the rat. *Clin Exp Pharmacol Physiol* 2001; **28**(11): 881-883.

Turner SW, Wen C, Li M, Fraser TB, Whitworth JA. Adrenocorticotrophin dose-response relationships in the rat: haemodynamic, metabolic and hormonal effects. *J Hypertens* 1998; **16**(5): 593-600.

Turner SW, Wen C, Li M, Whitworth JA. L-Arginine prevents corticotropin-induced increases in blood pressure in the rat. *Hypertension* 1996; **27**(2): 184-189.

Valko M, Leibfritz D, Moncol J, Cronin MTD, Mazur M, Telser J. Free radicals and antioxidants in normal physiological functions and human disease. *Int J Biochem Cell Biol* 2007; **39**(1): 44-84.

van den Meiracker AH, Man in't Veld AJ, Boomsma F, Fischberg DJ, Molinoff PB, Schalekamp MA. Hemodynamic and beta-adrenergic receptor adaptations during long-term beta-adrenoceptor blockade. Studies with acebutolol, atenolol, pindolol, and propranolol in hypertensive patients. *Circulation* 1989; **80**(4): 903-914.

Vanasco V, Cimolai MC, Evelson P, Alvarez S. The oxidative stress and the mitochondrial dysfunction caused by endotoxemia are prevented by α-lipoic acid. *Free Radic Res* 2008; **42**(9): 815 - 823.

Vanden Hoek TL, Shao Z, Li C, Schumacker PT, Becker LB. Mitochondrial electron transport can become a significant source of oxidative Injury in cardiomyocytes. *J Mol Cell Cardiol* 1997; **29**(9): 2441-2450.

Vasquez-Vivar J, Kalyanaraman B, Martasek P, Hogg N, Masters BSS, Karoui H, Tordo P, Pritchard KA, Jr. Superoxide generation by endothelial nitric oxide synthase: The influence of cofactors. *Proc Natl Acad Sci U S A* 1998; **95**(16): 9220-9225.

Vasquez-Vivar J, Martasek P, Whitsett J, Joseph J, Kalyanaraman B. The ratio between tetrahydrobiopterin and oxidized tetrahydrobiopterin analogues controls superoxide release from endothelial nitric oxide synthase: an EPR spin trapping study. *Biochem J* 2002; **362**(Pt 3): 733-739.

Vaziri ND, Wang XQ, Oveisi F, Rad B. Induction of oxidative stress by glutathione depletion causes severe hypertension in normal rats. *Hypertension* 2000; **36**(1): 142-146.

Wakabayashi Y, Yamada E, Yoshida T, Takahashi H. Deficiency of endogenous arginine synthesis provokes hypertension by exhausting substrate arginine for nitric oxide synthesis. *Biochem Biophys Res Commun* 1994; **205**(2): 1391-1398.

Walker BR, Best R, Shackleton CHL, Padfield PL, Edwards CRW. Increased vasoconstrictor sensitivity to glucocorticoids in essential hypertension. *Hypertension* 1996; **27**(2): 190-196.

Wallerath T, Godecke A, Molojavyi A, Li H, Schrader J, Forstermann U. Dexamethasone lacks effect on blood pressure in mice with a disrupted endothelial NO synthase gene. *Nitric Oxide* 2004; **10**(1): 36-41.

Wallerath T, Witte K, Schafer SC, Schwarz PM, Prellwitz W, Wohlfart P, Kleinert H, Lehr H-A, Lemmer B, Forstermann U. Down-regulation of the expression of endothelial NO synthase is likely to contribute to glucocorticoid-mediated hypertension. *Proc Natl Acad Sci U S A* 1999; **96**(23): 13357-13362.

Wallwork CJ, Parks DA, Schmid-Schonbein GW. Xanthine oxidase activity in the dexamethasone-induced hypertensive rat. *Microvasc. Res.* 2003; **66**(1): 30-37.

Wang HD, Pagano PJ, Du Y, Cayatte AJ, Quinn MT, Brecher P, Cohen RA. Superoxide anion from the adventitia of the rat thoracic aorta inactivates nitric oxide. *Circ Res* 1998; **82**(7): 810-818.

Wang J-S, Singh H, Zhang F, Ishizuka T, Deng H, Kemp R, Wolin MS, Hintze TH, Abraham NG, Nasjletti A, Laniado-Schwartzman M. Endothelial dysfunction and hypertension in rats transduced with CYP4A2 adenovirus. *Circ Res* 2006; **98**(7): 962-969.

Wang L-L, Ou C-C, Chan JYH. Receptor-independent activation of GABAergic neurotransmission and receptor-dependent nontranscriptional activation of phosphatidylinositol 3-kinase/protein kinase Akt pathway in short-term cardiovascular actions of dexamethasone at the nucleus tractus solitarii of the rat. *Mol Pharmacol* 2005; **67**(2): 489-498.

Wassmann S, Wassmann K, Nickenig G. Modulation of oxidant and antioxidant enzyme expression and function in vascular cells. *Hypertension* 2004; **44**(4): 381-386.

Watanabe T, Noshiro T, Akama H, Kusakari T, Shibukawa S, Miura W, Abe K, Miura Y. Effect of dexamethasone on plasma free dopamine: dopaminergic modulation in hypertensive patients. *Hypertens Res* 1995; **18** (Suppl 1): S197-198.

Wen C, Fraser T, Li M, Turner SW, Whitworth JA. Haemodynamic mechanisms of corticotropin (ACTH)-induced hypertension in the rat. *J Hypertens* 1999; **17**(12 Pt 1): 1715-1723.

Wen C, Fraser T, Li M, Whitworth JA. Hemodynamic profile of corticotropin-induced hypertension in the rat. *J Hypertens* 1998; **16**(2): 187-194.

Wen C, Li M, Fraser T, Wang J, Turner SW, Whitworth JA. L-Arginine partially reverses established adrenocorticotrophin-induced hypertension and nitric oxide deficiency in the rat. *Blood Press* 2000; **9**(5): 298-304.

Wen C, Li M, Whitworth JA. Validation of transonic small animal flowmeter for measurement of cardiac output and regional blood flow in the rat. *J Cardiovasc Pharmacol* 1996; **27**(4): 482-486.

Wen C, Li M, Whitworth JA. Role of nitric oxide in adrenocorticotrophin-induced hypertension: L-arginine effects reversed by N-nitro-L-arginine. *Clin Exp Pharmacol Physiol* 2000a; **27**(11): 887-890.

Whitworth JA. Adrenocorticotrophin and steroid-induced hypertension in humans. *Kidney Int Suppl* 1992; **37**: S34-37.

Whitworth JA, Coghlan JP, Denton DA, Graham WF, Humphery TJ, Scoggins BA. Comparison of the effects of 'glucocorticoid' and 'mineralocortocoid' infusions on blood pressure in sheep. *Clin Exp Hypertens* 1979; **1**(5): 649-663.

Whitworth JA, Gordon D, Andrews J, Scoggins BA. The hypertensive effect of synthetic glucocorticoids in man: role of sodium and volume. *J Hypertens* 1989; **7**(7): 537-549.

Whitworth JA, Saines D, Scoggins BA. Blood pressure and metabolic effects of cortisol and deoxycorticosterone in man. *Clin Exp Hypertens A* 1984; **6**(4): 795-809.

Whitworth JA, Saines D, Scoggins BA. Potentiation of ACTH hypertension in man with salt loading. *Clin Exp Pharmacol Physiol* 1985; **12**(3): 239-243.

Whitworth JA, Schyvens CG, Zhang Y, Mangos GJ, Kelly JJ. Glucocorticoid-induced hypertension: from mouse to man. *Clin Exp Pharmacol Physiol* 2001; **28**(12): 993-996.

Whitworth JA, Zhang Y, Mangos G, Kelly JJ. Species variability in cardiovascular research: The example of adrenocorticotrophin-induced hypertension. *Clin Exp Pharmacol Physiol* 2006; **33**(9): 887-891.

Wilding JP, Gilbey SG, Lambert PD, Ghatei MA, Bloom SR. Increases in neuropeptide Y content and gene expression in the hypothalamus of rats treated with dexamethasone are prevented by insulin. *Neuroendocrinology* 1993; **57**(4): 581-587.

Williamson PM, Kelly JJ, Whitworth JA. Dose-response relationships and mineralocorticoid activity in cortisol-induced hypertension in humans. *J Hypertens* 1996; **14 Suppl.**(5): S37-41.

Wintour EM, Alcorn D, McFarlane A, Moritz K, Potocnik SJ, Tangalakis K. Effect of maternal glucocorticoid treatment on fetal fluids in sheep at 0.4 gestation. *Am J Physiol Regul Integr Comp Physiol* 1994; **266**(4): R1174-1181.

Wong DL, Siddall B, Wang W. Hormonal control of rat adrenal phenylethanolamine N-methyltransferase. Enzyme activity, the final critical pathway. *Neuropsychopharmacology* 1995; **13**(3): 223-234.

Wu R, Millette E, Wu L, de Champlain J. Enhanced superoxide anion formation in vascular tissues from spontaneously hypertensive and desoxycorticosterone acetate-salt hypertensive rats. *J Hypertens* 2001; **19**(4): 741-748.

Yoshimoto T, Naruse M, Irie K, Tanabe A, Seki T, Tanaka M, Imaki T, Naruse K, Muraki T, Matsuda Y, Demura H. Beta-adrenoceptor antagonist propranolol potentiates hypotensive action of natriuretic peptides. *Eur J Pharmacol* 1998; **351**(1): 61-66.

Zavitsanou K, Nguyen V, Greguric I, Chapman J, Ballantyne P, Katsifis A. Detection of apoptotic cell death in the thymus of dexamethasone treated rats using [123I]Annexin V and in situ oligonucleotide ligation. *J Mol Histol* 2007; **38**(4): 313-319.

Zhang L, Fujii S, Igarashi J, Kosaka H. Effects of thiol antioxidant on reduced nicotinamide adenine dinucleotide phosphate oxidase in hypertensive Dahl salt-sensitive rats. *Free Radic Biol Med* 2004; **37**(11): 1813-1820.

Zhang Y, Chan MMK, Andrews MC, Mori TA, Croft KD, McKenzie KUS, Schyvens CG, Whitworth JA. Apocynin but not allopurinol prevents and reverses adrenocorticotropic hormone-induced hypertension in the rat. *Am J Hypertens* 2005; **18**(7): 910-916.

Zhang Y, Croft KD, Mori TA, Schyvens CG, McKenzie KUS, Whitworth JA. The antioxidant tempol prevents and partially reverses dexamethasone-induced hypertension in the rat. *Am J Hypertens* 2004; **17**(3): 260-265.

Zhang Y, Croft KD, Veckers JJ, Ong SLH, Mori TA, Whitworth JA. HET0016, a 20-hydroxyeicosatetraenoic acid inhibitor, prevents and reverses adrenocorticotrophic hormone-induced hypertension. *Journal of Hypertension* 2008; **26**: S76-S76.

Zhang Y, Hu L, Mori TA, Barden A, Croft KD, Whitworth JA. Arachidonic acid metabolism in glucocorticoid-induced hypertension. *Clin Exp Pharmacol Physiol* 2008; **35**(5-6): 557-562.

Zhang Y, Jang R, Mori TA, Croft KD, Schyvens CG, McKenzie KU, Whitworth JA. The anti-oxidant Tempol reverses and partially prevents adrenocorticotrophic hormone-induced hypertension in the rat. *J Hypertens* 2003; **21**(8): 1513-1518.

Zhang Y, Miao Y, Whitworth JA. Aspirin prevents and partially reverses adrenocorticotropic hormone-induced hypertension in the rat. *Am J Hypertens* 2007; **20**(11): 1222-1228.

Zhang Y, Pang T, Earl J, Schyvens CG, McKenzie KU, Whitworth JA. Role of tetrahydrobiopterin in adrenocorticotropic hormone-induced hypertension in the rat. *Clin Exp Hypertens* 2004; **26**(3): 231-241.

Zhang Y, Soboloff J, Zhu Z, Berger SA. Inhibition of Ca2+ influx is required for mitochondrial reactive oxygen species-induced endoplasmic reticulum Ca2+ depletion and cell death in leukemia cells. *Mol Pharmacol* 2006; **70**(4): 1424-1434.

Zhang Y, Wu JHY, Vickers JJ, Ong SLH, Temple SEL, Mori TA, Croft KD, Whitworth JA. The role of 20-hydroxyeicosatetraenoic acid in glucocorticoid-induced hypertension. *J Hypertens* 2009; **27**(8): 1609-1616.